Application and Substrate Scope Expansion of a Unique Borylative Migration Transformation

by

Samantha Kwok

A thesis submitted to the in partial fulfillment of the requirements for the degree of

Master in Science

Department of Chemistry
University of Alberta

Abstract

A unique borylative migration of heterocyclic enol perfluorosulfonates has been developed to access six-membered heterocyclic α-substituted allylboronates in a stereoselective and efficient manner. The synthetic utility of the allylboronate intermediates was demonstrated by a highly diastereoselective aldehyde allylboration, an enantioselective and regiodivergent Suzuki-Miyaura cross coupling and the efficient synthesis of all four stereoisomers of mefloquine. Although the mechanism of this transformation is unknown (and is currently being studied), the utility of this method still needs to be explored further.

First, the application of this process towards the synthesis of all four stereoisomers of Vacquinol-1; a potential therapeutic agent for the brain cancer glioblastoma multiforme, will be described. Identified in 2014, the tested compounds were a mixture of stereoisomers. The synthetic strategy presented herein provides an efficient route to access each stereoisomer of Vacquinol-1 for the independent biological study of each compound. Moreover, analogs of Vacquinol-1 are readily accessible with the presented method. Next, efforts to expand the substrate scope of this transformation to five- and seven- membered heterocyclic substrates is disclosed. Efforts on the optimization of the amine base, chiral ligand and solvent to render the transformation enantioselective are presented.

Preface

Some of the research conducted for this thesis forms part of a research collaboration with Dr. Roseline Godbout from the Department of Oncology at the University of Alberta. The data concluding analysis in chapter 2 are my original work. No part of this thesis has been previously published.

Acknowledgement

I would like to thank my supervisor, Professor Dennis G. Hall, for his support and guidance throughout my graduate studies. I would also like to extend my appreciation towards the Hall Group members, past and present, for their support and encouragement. A special thanks to Ed Fu for his assistance. I need to also express my immense gratitude to my lab mates Xiaobin Mo, Dr. Sergiy Vshyvenko, Helen Clement, Dr. Tristan Verdelet and Dr. Ho-Yan Sun, for their camaraderie and continual support.

I would also like to mention and thank the amazing support staff employed at the Department of Chemistry at the University of Alberta. Specifically, the NMR Spectroscopy; a special thanks to Dr. Mark Miskolzie, the Mass Spectrometry and the Analytical and Instrumentation Laboratory whose services for the data collection were indispensable and essential for the work presented in this thesis. In addition, I would like to express my gratitude to the support staff from the chemical store and receiving; Ryan Lewis, Bernie Hippel, Matthew Kingston and Andrew Yeung, and the administrative staff, in particular I would like to thank Anita Weiler and Lynne Lechelt.

Next, a great big thank you to my colleagues and friends Amy Norquay, Dr. Roger Ashmus, Randy Sanichar and Tom Scully for the insightful conversations, culinary adventures and laughs through the good times and the bad. Another special thank you to Dr. Hayley Wan and Nada Djokic for providing nutritional supplement and their wholehearted support and friendship. A very special thanks must go to Ryan Sweeney for being my partner in crime and my rock during the trial and

tribulations of my studies. I also need to thank my friends outside of the department, Garreth Murphy and Hailey Dolihan for their unrelenting faith and unquestioning support.

Last, but certainly not least, I need to thank my parents, Dr. Henrianna Y. Pang and Dr. Yan C. Kwok for their unconditional love and support. I cannot express the depth of my gratitude and appreciation for everything my parents have done for me.

Table of Contents

List of Figures

List of Schemes

List of Tables

List of Abbreviations

Å	Ångström
Ac	acetyl
Ar	aryl
aq	aqueous
ATP	adenosine triphosphate
BBB	blood brain barrier
BINOL	1,1'-Bi-2-naphthol
Bn	benzyl
Boc	*tert*-butoxycarbonyl
*n*Bu	normal (primary) butyl
°C	Degree Celsius
calcd	calculated
cat.	catalytic
cm^{-1}	wavenumber
CPME	cyclopentyl methyl ether
Cr	chromium
Cy	cyclohexyl
d	doublet
DBU	1,8-diazabicyclo[5.4.0]undec-7-ene
DCM	dichloromethane or methylene chloride
DIPEA	*N,N*-diisopropylethylamine or Hünig's base

DMA	*N,N*-dimethylaniline of $PhNMe_2$
DMF	dimethylformamide
DMSO	dimethylsulfoxide
DPEPhos	Bis[(2-diphenylphosphino)phenyl] ether
DTP	Developmental Therapeutics Program (National Cancer Institue Division of Cancer Treatment & Diagnosis)
ee	enantiomeric excess
EDCI	1-ethyl-3-(3-dimethylaminopropyl)carbodiimide
EI	electron impact
equiv	equivalents
ESI	electrospray ionization
Et_2O	diethyl ether
g	gram/grams
GBM	glioblastoma multiforme
h	hour/hours
HOBt	hydroxybenzotriazole
HPLC	high-performance liquid chromatography
HRMS	high-resolution mass spectrometry
Hünig's base	*N,N*-diisopropylethylamine
Hz	hertz
IBX	2-iodoxybenzoic acid
ipc	isopinocampheyl
IR	infrared

J	coupling constant (in NMR spectrometry)
L	liter/liters
LDA	lithium diisopropylamide
LiHMDS	lithium hexamethyldisilazide
µ	micro
µwave	microwave
m	multiplet; milli
M	molar
MDR	multi-drug resistance
Mes	mesityl
MHz	megahertz
min	minute/minutes
mol	mole/moles
m.s.	molecular sieves
MTBE	methyl *tert*-butyl ether
MTS	[3-(4,5-dimethylthiazol-2-yl)-5-(3-carboxymethoxyphenyl)-2-(4-sulfophenyl)-2H-tetrazolium]
NIH	National Institutes of Heath
2-Naph	2-naphthalene
Nf	nonaflate or nonafluorobutanesulfonyl
NfF	perfluorobutanesulfonyl fluoride or 1,1,2,2,3,3,4,4,4-nonafluorobutane-1-sulfonyl fluoride
NMR	nuclear magnetic resonance

Pd	palladium
PCC	pyridinium chlorochromate
Pgp	plasma membrane glycoprotein
Ph	phenyl
pin	pinacol
i-Pr	*iso*-propyl
Py	pyridine
q	quartet
R	generic alkyl group (unless otherwise specified)
Rh	rhodium
rt	room temperature
s	singlet
SAR	structure activity relationship
sat.	saturated
t	tertiary
T	triplet
(+) TANIAPHOS	(R)-(+)-[(R)-2-diphenylphosphinoferrocenyl](*N,N*-dimethylamino)(2-diphenylphosphinophenyl)methane
(-) TANIAPHOS	(S)-(-)-[(S)-2-diphenylphosphinoferrocenyl](*N,N*-dimethylamino)(2-diphenylphosphinophenyl)methane
TBS	*tert*-butyldimethylsilyl
TBSOTf	*tert*-butyldimethylsilyl trifluoromethanesulfonate
Tf	trifluoromethanesulfonyl

TFA	trifluoroacetic acid
THF	tetrahydrofuran
TLC	thin-layer chromatography
TMRE	tetramethylrhodamine ethyl ester
TMS	trimethylsilyl
XPhos	2-dicyclohexylphosphino-2′,4′,6′-triisopropylbiphenyl

Chapter 1. Thesis Introduction

1.1 Catalysis in Organic Chemistry

Perhaps one of the greatest enduring challenges for an organic chemist is the ability to access complex and useful molecules in an atom-economical and selective manner. One way this challenge has been addressed is the development of catalytic, and subsequently enantioselective, methods. The term catalyst was first introduced by Berzelius in 1836, and defined by Ostwald in 1894, as a substance that increases the rate of a chemical transformation without itself being consumed.[1] The role of a catalyst is to lower the energy of the transition states during a reaction and thus increase the rate and efficiency of the transformation. The catalyst should also be regenerated, and as a result a substoichiometric amount of is necessary.

Several modes of catalysis have been developed which include, but are not limited to, acid catalysis, organocatalysis, photoredox catalysis and transition-metal catalysis. Metal-catalyzed cross-coupling reactions was notably recognized in 2010 with the Nobel Prize in Chemistry being awarded to Dr. Richard Heck, Dr. Ei-ichi Negishi and Dr. Akira Suzuki for their work.[2] In many cases, a catalyzed reaction is achieved under milder conditions and with a higher tolerance for different functional groups. Catalysis has become an indispensable addition to the toolbox of a synthetic chemist.

1.2 Importance of Enantioselective Methods

We live in a world where chirality is a vital component of life. A molecule is chiral if its two mirror images are non-superimposable; the two different "images" are called enantiomers. There are several examples where enantiomers can exhibit different properties in a wide range of areas of research, such as pharmacology.[3,4,5] One infamous example of the striking difference in the biological properties of two enantiomers is the drug thalidomide (Scheme 1-1). Thalidomide was marketed as a racemate under several different names world wide. In the UK and Australia, it was called Distaval, while it was distributed under the name Softenon in Europe and Contergan in Germany. Prescribed as a treatment for morning sickness to pregnant women, one enantiomer exhibited the desired effects while the other tragically caused teratogenic effects.[6]

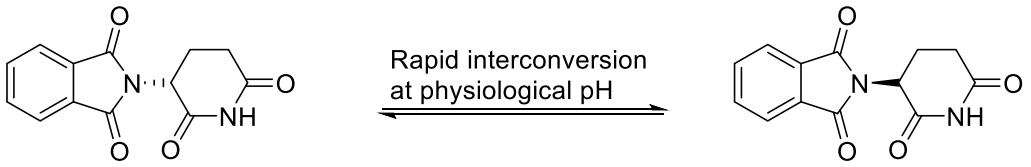

R(+)-thalidomide
(sedative)

S(–)-thalidomide
(teratogenic)

Scheme 1-1: The two enantiomers of thalidomide (and their drastically different effects) which can rapidly interconvert in the body resulting in an equal concentration of both.

Considering the example illustrated in Scheme 1-1, there is a significant demand for methods that selectively forms one enantiomer over the other. In the pharmaceutical industry it is now crucial that if a molecule is chiral the enantiomers are independently prepared and studied.

1.3 Enantioselective Catalysis

Significant progress has been made towards developing methods that are catalytic and enantioselective. These methods must exhibit high chemo- and regio-selectivity, in addition to high efficiency to ensure enantioselectivity. In enantioselective reactions, stereodifferentiation can be achieved by enzyme catalysis (there are several elegant examples in literature of asymmetric desymmetrization using enzyme catalysis[7,8]), organo-catalysis or transition-metal catalysis (the use of a chiral ligand complexed to a metal center). One of the challenges in developing catalytic enantioselective methods is promoting a significant rate difference between the catalyzed and non-catalyzed pathways for enantioselectivity to occur.

Chemists have met this challenge with great success and to highlight the importance of enantioselective catalytic methods, the 2001 Nobel Prize in Chemistry was awarded to William S. Knowles and Ryoji Noyori for their work on "chirally catalysed hydrogenation reactions" and K. Barry Sharpless "for his work on chirally catalysed oxidation reactions".

1.4 Chiral Allylboronates

An area of research that has undergone extensive study is the transformation of simple building blocks, generally achiral molecules, into enantioenriched complex molecules. A particularly useful strategy is to access a chiral synthetic building block that can demonstrate versatile and facile chemical transformations. One such class of compounds is allylboronates. Allylic boronate reagents have demonstrated tremendous utility in organic synthesis for the allylation of carbonyl

compounds[9] and in transition-metal catalyzed cross-coupling[10] transformations. Specifically, the use of allylboronates for carbonyl allylation is very rarely rivalled due to the high regio- and stereo-selectivity exhibited by these reagents. The high level of selectivity is due to the stability of the allylic boronate; i.e. metallotropic rearrangements and *E/Z* isomerization are essentially supressed, and the highly constrained conformation of the six-membered ring transition state promotes strong differentiation in the stereoselection process (Scheme 1-2).[11]

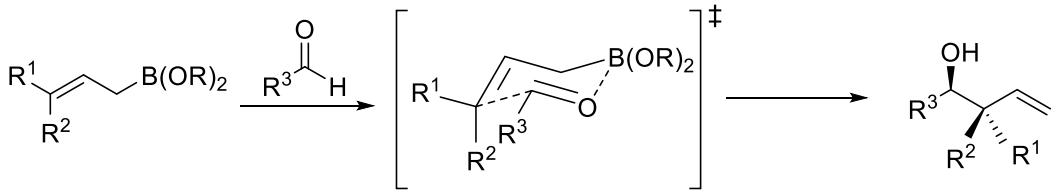

Scheme 1-2: Carbonyl allylation mechanism with an allyl organoboron reagent. Selectivity arises from a tight chairlike Zimmerman-Traxler transition state.

Additionally, the chiral allylboronate building blocks for cross-coupling reactions present an interesting point of divergence since there are two sites for the Pd-catalyzed cross-coupling transformation to occur (Scheme 1-3). The α-product is formed as a result of the cross-coupling event occurring at the carbon that once bore the boron functional group. In contrast, the γ-product is formed as a result of a distal cross-coupling event.

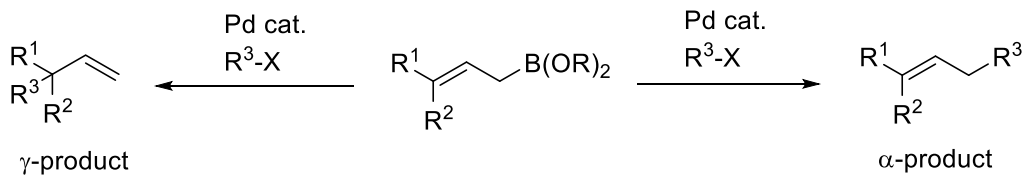

Scheme 1-3: Regio-divergent cross-coupling of a generic allyl boron reagent to the synthesis of either the α-product or γ-product.

The efforts of Miyaura[12,13] and Szabó[14] have resulted in highly selective methods for the γ- coupled product. In 2012, Organ and co-workers published their seminal work in the development of a method for the selective formation of the α-product.[15] Furthermore, allylboronate building blocks are advantageous in transition-metal catalyzed cross-coupling transformations because if the allylboronate is chiral, the chiral information may be retained and therefore efficiently translated to the cross-coupling product. In 2013, the Crudden group published their work on an enantiospecific and regioselective cross-coupling reaction of secondary allylic boronic esters.[10] Of note, chiral allylic boron reagents can be divided into two types; "B-chiral" and "C-chiral" allylic boron reagents.[16] This topic is discussed in the next section.

1.5 "B-chiral" Allylic Boronate Reagents

"B-chiral" compounds bear the chirality on a covalently bonded chiral auxiliary attached to the boron atom. Although these reagents are widely used in carbonyl additions, one significant disadvantage is that the chiral auxiliary must be used in stoichiometric quantities. Some notable examples are the chiral allylboronates developed by Hoffmann[17], Corey[18], Brown[19] and Roush[20] (Figure 1-1). Subsequently, our group discovered Lewis and Brønsted acid catalyzed manifolds

that were developed into catalytic enantioselective aldehyde allylboration methods using achiral allylboronates.[21,22,23]

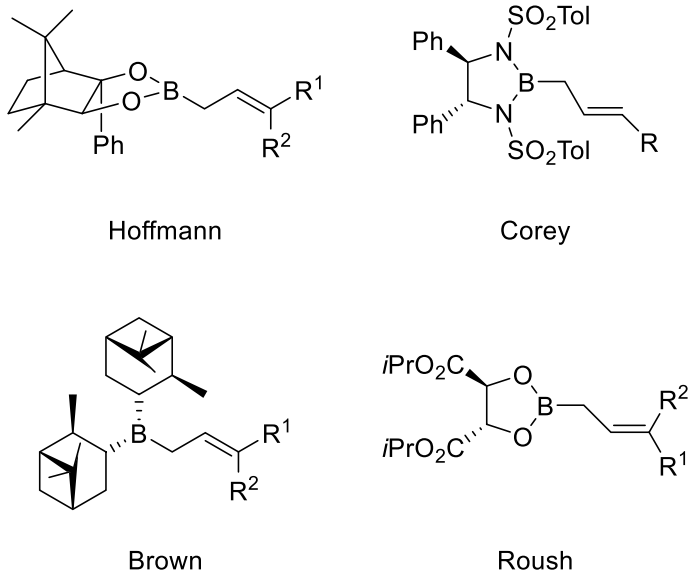

Figure 1-1: Selected examples of "B-chiral" allyl boron reagents.

In the context of this thesis, two accounts on the use and synthesis of cyclic "B-chiral" allylic reagents should be mentioned. First, a report by Brown and co-workers demonstrated the hydroboration of cyclohexadiene with a pinene-derived borane and subsequent aldehyde allylboration to provide cyclic exo-homoallylic alcohols (1-(2-cyclohexenyl)-1-alkanols) in good yield with excellent diastereoselectivity and enantioselectivity (Scheme 1-4).[24] A subsequent account in 1991 by the same laboratory showed the application of this transformation to seven- and eight- membered rings. However, after the allylboration, an increase in ring size provided a significantly lowered yield and racemization of the cyclic borane occurred at ambient temperature.[25] Additional disadvantages of this transformation are; allylic dialkylboranes are

sensitive to air, moisture and temperature and in pure form or solutions of high concentration these reagents are known to be pyrophoric.[26]

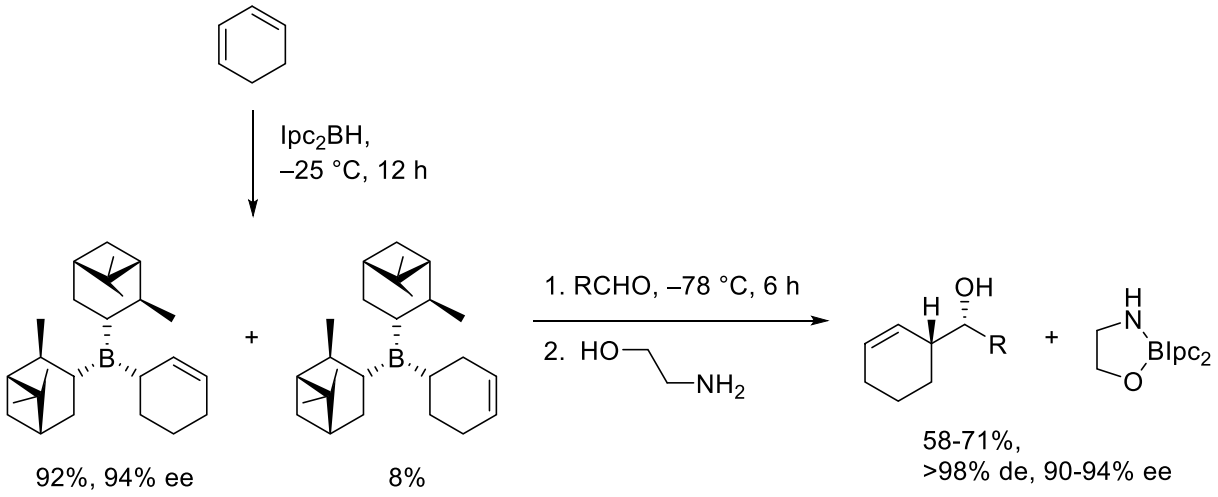

Scheme 1-4: Synthesis of "B-chiral" cyclic allylic boron reagent and subsequent aldehyde allylboration by Brown and co-workers.

The second example of "B-chiral" cyclic allylic boron reagent is from Lallemand and co-workers. In 1996, the Lallemand group demonstrated that chiral allylic boronates could be formed via [4+2] cycloaddition with a tartrate derived 1,3-dienylboronate (Scheme 1-5). The endo cycloadduct was preferentially formed and, as previously mentioned, was sensitive to air and moisture therefore the subsequent aldehyde allylboration was performed without purification of the chiral allyl boronate.[27] The overall transformation yielded the silyl-protected homoallylic alcohol in 49% yield, 9:1 diastereomeric ratio (or 80% diastereomeric excess) and 70% enantiomeric excess.

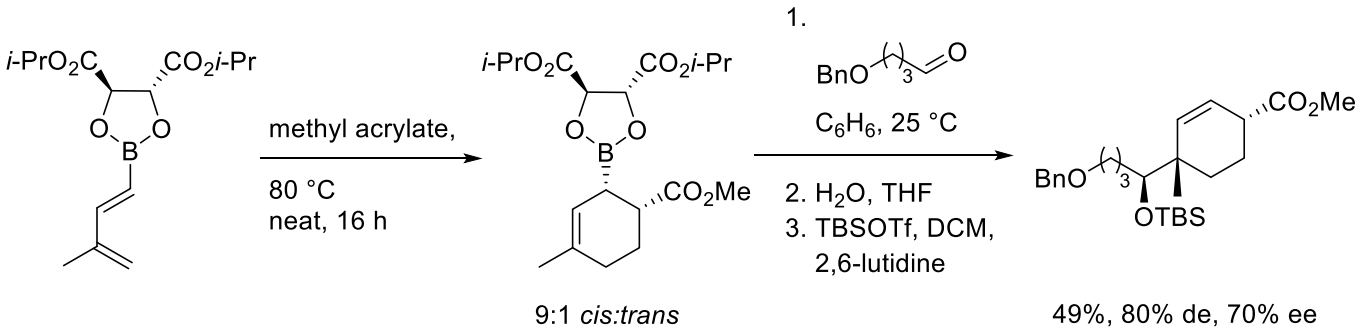

Scheme 1-5: Synthesis of "B-chiral" cyclic allylic boron reagent and subsequent aldehyde allylboration by Lallemand and co-workers.

1.6 "C-chiral" Allylic Boronate Reagents

In contrast to "B-chiral" allylic boron compounds, "C-chiral" reagents bear the chirality on the α-carbon of the "allyl" unit, or directly adjacent carbon, to the boron atom. Thus, these reagents are also known as chiral α-substituted allylboronates. Hoffmann and co-workers showed that enantioenriched chiral α-substituted allylboronates provide high chirality transfer during aldehyde allylboration. [28,29,30,31] Furthermore, the use of cyclic chiral α-substituted allylboronates is desirable because of the high diastereoselectivity generally observed for aldehyde allylboration.

Notable syntheses of cyclic chiral α-substituted allylboronates include the work of Ito and co-workers, who demonstrated that a silyl-boronate reagent could add stereospecifically to cyclohexadiene in the presence of a nickel catalyst.[32] This process was improved upon by Moberg and co-workers who attempted to render the transformation enantioselective through the use of a chiral ligand: successfully establishing a system using a BINOL-based phophoramidite ligand and platinum (II) complex.[33,34] The development of heterocyclic allylic boron reagents is of great

interest because these synthetic intermediates are often exploited for the synthesis of motifs present in biologically active compounds. In this regard, an approach that uses an aza [4+2] cycloaddition[35] was developed to provide a piperidyl allylic boronate. However, this transformation requires the use of a stoichiometric amount of chiral auxiliary. The corresponding hetero Diels-Alder reaction to provide the pyranyl allylic boronate is achieved through the use of Jacobsen's chiral salen chromium (III) complex (Scheme 1-6).[36,37,38] The synthesis of the chiral pyranyl- allylboronate via hetero Diels-Alder suffers from a disadvantage; namely, the residual acetal unit which may be undesirable. As such, synthetic methods to access chiral piperidinyl- and pyranyl- allylic boronates require significant improvements.

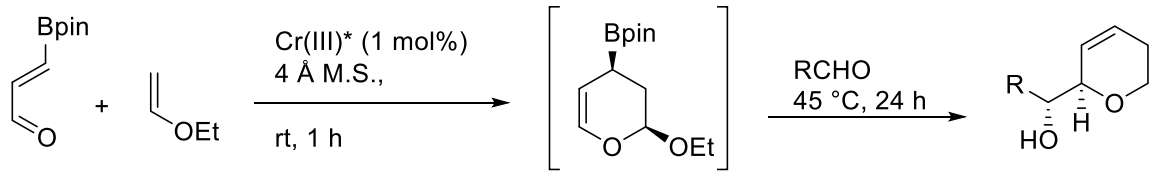

Scheme 1-6: Enantioselective hetero Diels-Alder reaction using Jacobsen's chiral salen chromium complex for the synthesis of a chiral pyranyl allylboronate followed by the aldehyde allylboration.

1.7 Catalytic Enantioselective of Heterocyclic Allylic Boronate Formation

In 2009, our group reported the optimization and utility of a unique palladium catalyzed borylative migration method to access enantiomerically enriched heterocyclic allylic boronates (Scheme 1-7).[39] Observed by Masuda in 2000, the allylic boronate was considered an undesirable major product from the borylation of alkenyl triflates.[40] The competing pathway of allylic boronate

formation was surprising and provided the pyranyl-allylic boronate as the major product. In contrast, the cyclohexenyl-allylic boronate was the minor product under the same conditions.[40]

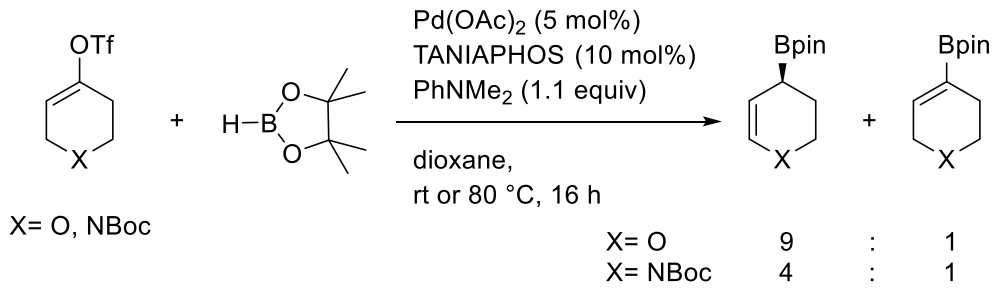

Scheme 1-7: Catalytic enantioselective piperidinyl- and pyranyl-chiral allylic boronate preparation by a unique borylative migration transformation.

Intrigued by the unexpected transformation and encouraged by the potential to easily access heterocyclic allylic boronates, this reaction was fervently studied by our group. Several obstacles where subdued, namely; suppressing the formation of the alkenyl boronate and optimizing the enantioselectivity. The parameters of this transformation were carefully examined, specifically the solvent, temperature, palladium catalyst source, chiral ligand and base were optimized. It was demonstrated that the nature of the base has a determining influence on the enantioselectivity of this borylative migration transformation.[39]

This seminal work provided an efficient method to access pyranyl- and piperidinyl-chiral allylic boronate building blocks. However, the conditions in the procedure reported in 2009 were optimized for the pyranyl substrate. Although, acceptable for the pyranyl substrates, the parameters for the piperidinyl substrate warranted further investigation. Thus, in 2016,[41] the reaction parameters were fine-tuned for the piperidinyl substrate and notably the conditions provided

improved yields and enantiomeric excess (Scheme 1-8). Additionally, the improved parameters render this transformation more accessible to industrial scale.

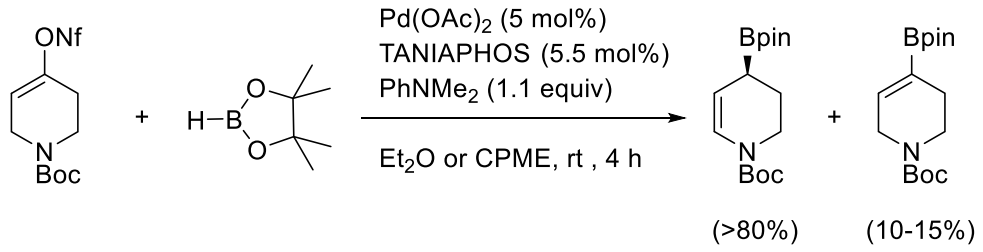

Scheme 1-8: Optimized conditions for the synthesis of the piperidinyl- chiral allylic boronate.

Specifically, the reaction substrate was modified to the *N*-Boc-protected alkenyl nonaflate from the corresponding alkenyl triflate. This change presented significant advantages in that the preparation of the nonaflate is higher-yielding, more cost-effective and provides a more facile purification. Second, the use of dioxane as solvent was re-examined and it was determined that the more environmentally friendly ethereal solvent cyclopentyl methyl ether and less peroxide forming prone solvent diethyl ether were both appropriate. Lastly, exploration of the catalyst loading and ligand ratio and concentration revealed that reduction of the catalyst loading to 3 mol%, ligand loading to 3.3% provided the desired allylic boronate.

1.8 Synthetic Utility of Pyranyl- and Piperidinyl- Chiral Allylic Boronates

Thus far, the pyranyl- and piperidinyl- chiral allylic boronate building blocks have proven to be of indispensable synthetic utility in two ways. First, through the diastereoselective allylboration of the allylic boronates with aldehyde electrophiles (Scheme 1-9).[39] This method efficiently provides

α-hydroxyalkyl heterocycles containing two contiguous stereogenic centres in a "one-pot" manner. This synthetic method was demonstrated to be effective in preparing functionalized pyran and piperidine scaffolds from a simple achiral starting material, the one-pot transformation efficiently introduced complexity in an enantio- and diastereo- selective manner.

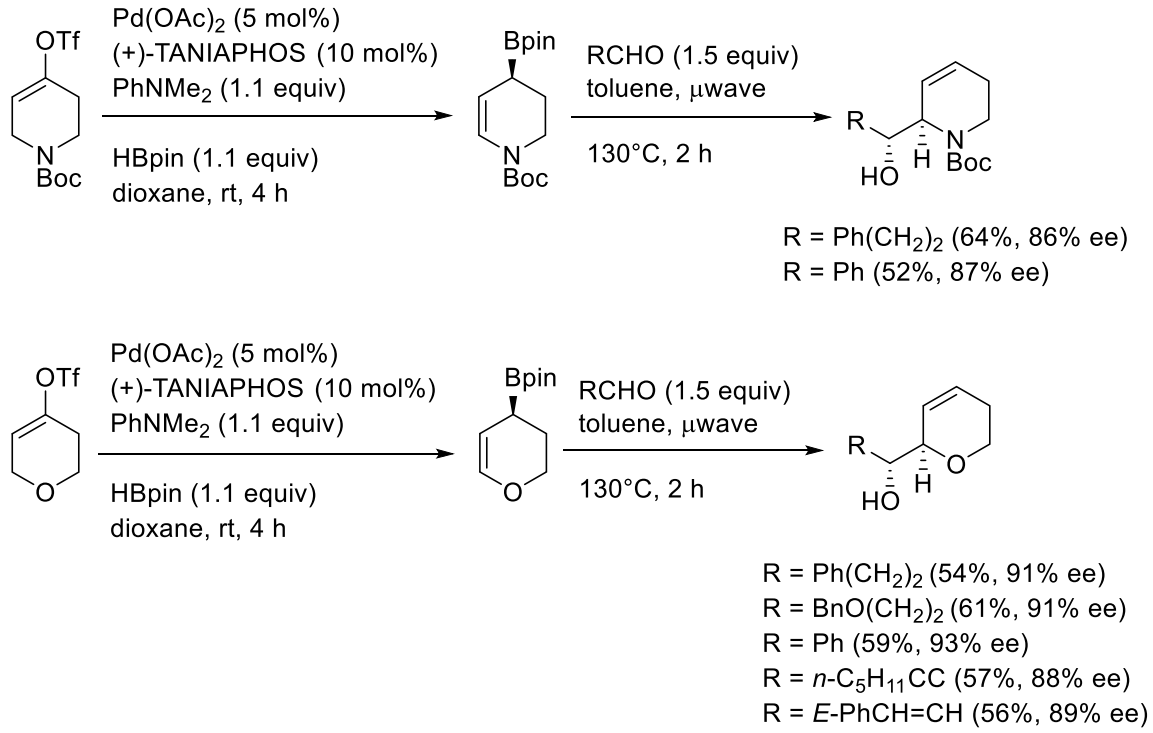

Scheme 1-9: Aldehyde allylboration substrate scope of piperidinyl- and pyranyl- allylic boronate.

Furthermore, the scope of the allylboration with the piperidinyl allylic boronate was expanded (Scheme 1-10), after subsequent exploration of the optimized parameters, to include hetero-

aromatic aldehydes and substituted aryl rings. A multi-gram synthesis was also achieved to illustrate the scalability of this transformation.[41]

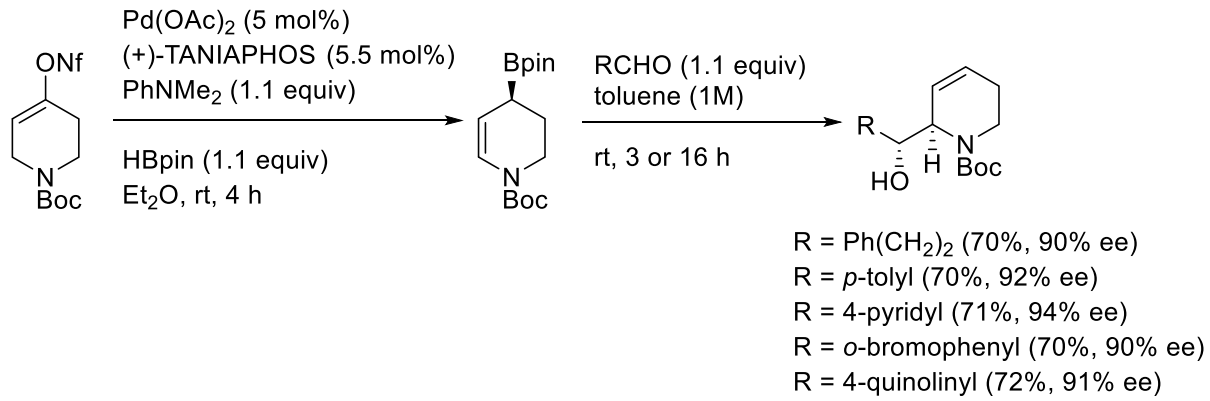

Scheme 1-10: Aldehyde allylboration substrate scope of piperidinyl- allylic boronate after careful optimization of reaction parameters.

The synthetic utility of the allylic boronates was more recently demonstrated through the regiodivergent and enantioselective Suzuki-Miyaura cross-coupling reaction (Scheme 1-11).[42] Our group reported a remarkably stereoselective sp^2-sp^3 cross-coupling, while elegantly addressing the additional challenge of regioselectivity. The process displayed an extremely selective and efficient way to access 2- or 4- substituted arylpyrans and arylpiperidines. These structural scaffolds are present in many privileged compounds that exhibit a wide range of biological properties.

For example, Hall and co-workers demonstrated the application of this regiodivergent and enantioselective method towards the preparation of a natural product and an advanced synthetic drug intermediate, namely, (+)-anabasine (nicotinic acetylcholine receptor agonist) and the two-step precursor to (+)-paroxetine (serotonin reuptake inhibitor, antidepressant drug) respectively.[42] A previously reported synthesis provided the Boc-protected (+)-anabasine in a 51% yield and

90:10 er.[43] In contrast, our group's method provides a significantly more desirable overall yield of 63% and 95:5 er to the same compound.[42] Furthermore, previous syntheses of the advanced intermediate to (+)-paroxetine only afforded the intermediate at 36% yield over 7 steps (er was not reported).[44] Our synthetic route is not only more industry friendly, it is able to access the same compound in 6 steps with an overall yield of 25% and 95.4: 4.5 er.[42]

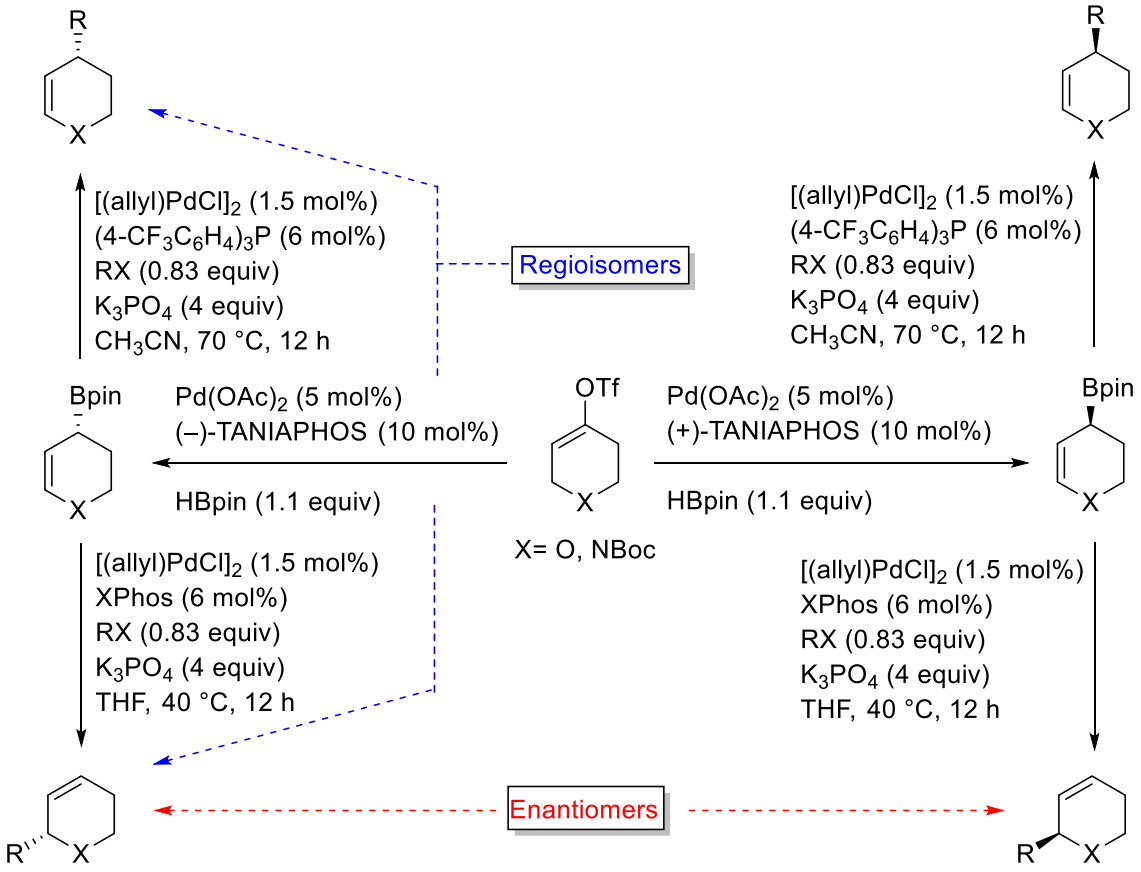

Scheme 1-11: Regioselective and enantiospecific Suzuki-Miyaura cross-coupling of pyranyl- and piperidinyl- allylic boronates.

The regioselectivity of this transformation relies on the mechanistic nature of the transmetallation step and whether it occurs with or without allylic rearrangement.[42] Thus, the ligand plays a critical role and it was demonstrated that the use of a strong σ-donor phosphine ligand provided

functionalization at the position adjacent to the heteroatom. In contrast, electron deficient phosphine ligands provided site selectivity at the most distal site from the heteroatom. It is worthy to note, that the chiral information from the allylic boronate intermediate is nearly or completely retained and overall stereorentention was observed. The stereoretention is due to a stereoretentive transmetallation followed by a stereoretentive reductive elimination.[45,46]

1.9 Application of the Catalytic Enantioselective Borylative Migration Towards the Synthesis of Mefloquine

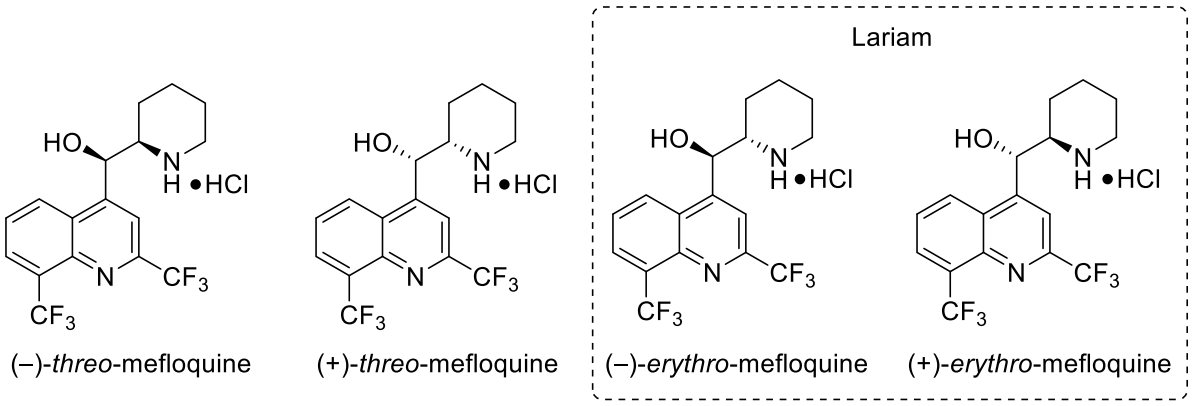

Figure 1-2: Four stereoisomers of mefloquine.

With such a powerful synthetic method in hand, our group turned towards applying the borylative migration of enol perfluorosulfonates towards the synthesis of other pharmaceutically important compounds. Structurally, the anti-malarial drug mefloquine lends itself perfectly to the application of the synthetic method (Figure 1-2).[47] Marketed under the name Lariam, mefloquine may exist as four stereoisomers. Studies have shown that the (+)-*erythro*- and *threo*-mefloquine stereoisomers are active against the *Plasmodium* parasite, however the (−) -*erythro*-mefloquine stereoisomer

causes psychotropic side effects.[48] Previously reported enantioselective syntheses of mefloquine include the synthesis of (+)-*erythro* mefloquine by Roche in 1993 that took advantage of a Rh-catalyzed enantioselective hydrogenation.[49] Later, in 2008, Xie and co-workers used an organocatalytic aldol addition[50] for the synthesis of (+)-*erythro* mefloquine, and more recently in 2011, Coltart and co-workers published their efforts towards the same compound using an asymmetric Darzens reaction.[51]

Considering the lack of synthetic routes toward the *threo*- mefloquine stereoisomer, a unified synthetic strategy with the unique borylative migration transformation at its core was devised and executed by our group in 2013.[47] Both *erythro*-mefloquine enantiomers were accessed over 4 steps while both *threo*- mefloquine enantiomers were obtained after 2 steps. In addition, the synthetic route proved to be scalable since the transformation was achieved at gram scale, and subsequently may prove applicable to industrial scale. Moreover, with this seminal work we provide the first chemical proof to lay rest to the controversy that surrounded the assignment of the absolute stereochemistry of mefloquine.

1.10 Expansion of the Catalytic Enantioselective Borylative Migration Towards the Selective Synthesis of Vacquinol-1 and Vacquinol-15 Stereoisomers

In 2014, a Swedish group published their findings that a certain class of small organic molecules, called vacquinols, induced cell death in glioblastoma cells. Glioblastoma multiforme is an extremely aggressive form of brain cancer. It is essentially incurable with only 3-5% of patients surviving longer than 3 years after surgical removal of the cancerous growth with concomitant

chemotherapy and radiotherapy.[52] Many cancer therapies are developed with the aid of decoding the genetic information from the cancer cells. However, identification of a therapeutic target for the treatment of glioblastoma has been prevented by the genetic complexity that has been observed. In addition, for the treatment of brain cancer the therapeutic agent must be able to cross the blood brain barrier (BBB). This account identified two potential therapeutic compounds, Vacquinol-1 and Vacquinol-15 (Figure 1-3).

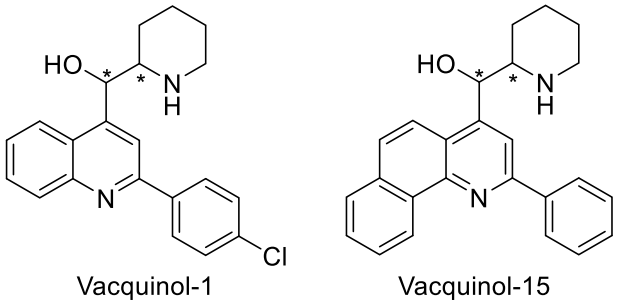

Figure 1-3: Top candidates for the treatment of glioblastoma, screened from a series of 21 vacquinol compounds.

Of interest, Ernfors and co-workers provided evidence to support that the mechanism of action of these compounds is not by the traditional pathway of apoptosis (cell death) induction or autophagy-associated cell death. Several established apoptotic cell markers were probed and shown to not have been affected by the vacquinol compounds. Namely; Vacquinol-1 had no effect on the enzymatic activity of Caspase-3 and Caspase-7 at any concentration or time point, accumulation of tetramethylrhodamine ethyl ester (TMRE) (during disruption of active mitochondria, TMRE is accumulated in the mitochondria and endoplasmic reticulum)[53] was largely unaffected and cytosolic calcium flux was also not affected. To determine if the mechanism of action of Vacquinol-1 was via autophagic programmed cell death (autophagy is the process by which a cell

undergoes partial self-digestion)[54], the treated cells were observed under high magnification. Autophagic cell death is mainly a morphologic definition. However, Ernfors and co-workers observed a morphological change that was indicative of the over production of vacuoles and not autophagic cell death. Vacuoles are membrane-bound organelles that act as dynamic storage units to help maintain hydrostatic pressure and pH, isolate and export waste or harmful products and store water or macromolecules. Additional imaging experiments confirmed the induction of endocytic activity and excessive vacuole formation by Vacquinol-1 that caused cell death.

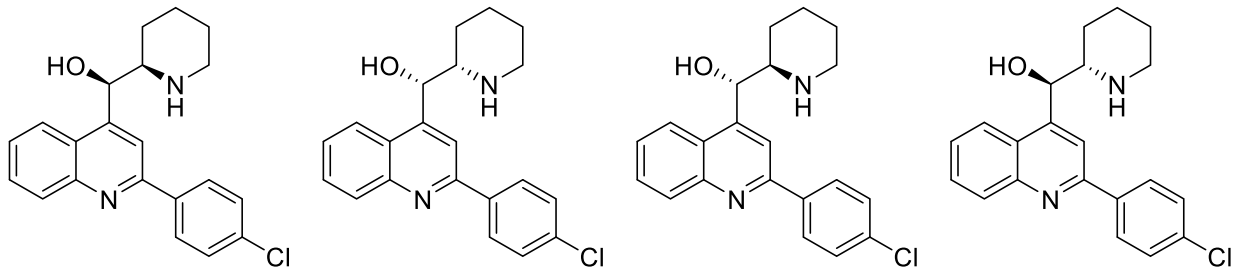

Figure 1-4: Four stereoisomers of Vacquinol-1.

Similar to mefloquine, the vacquinol compounds can exist as four diastereomers and the α-hydroxyalkyl piperidyl backbone fits perfectly with the borylative migration, with subsequent allylboration, chemistry (Figure 1-4). However, unlike mefloquine where studies have been conducted on each stereoisomer, the biological experiments that have been conducted by Ernfors and co-workers used an undefined mixture of all four stereoisomers of the vacquinol compounds. Therefore, it is of great interest to selectively synthesize each stereoisomer and determine the efficacy against glioblastoma cells. This would require a thorough study of both the synthetic chemistry and biological assays. Ultimately, identification of the most effective stereoisomer

would lead to a comprehensive structure-activity relationship (SAR) study and would facilitate the development of a more effective therapeutic by focusing on modifying the optimal stereoisomer.

1.11 Application of the Catalytic Enantioselective Borylative Migration Towards the Synthesis of Pyrrolidinyl- and Tetrahydrofuryl- Chiral Allylic Boronates

Application of this unique borylative migration to access other heterocyclic scaffolds has yet to be explored. To the best of our knowledge the synthesis of pyrrolidinyl- and tetrahydrofuryl- allylic boronates has yet to be accomplished (Scheme 1-12).

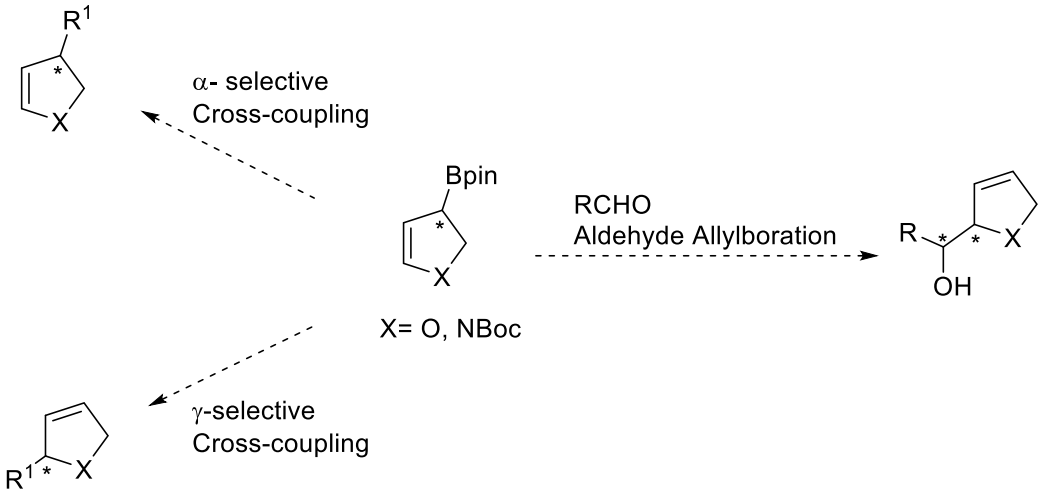

Scheme 1-12: Potential synthetic applications of pyrrolidinyl- and tetrahydrofuryl-allylic boronates, prepared by catalytic enantioselective borylative migration.

This underexplored area of research is limiting the synthetic access of a potentially powerful building block. Considering the precedence of the six-membered heterocyclic allylic boronate and the synthetic utility of this building block, synthesis of the five-membered heterocyclic allylic boronates could become another indispensable tool to an organic chemist. Additionally, expanding

the scope of this transformation to include acyclic substrates and the seven-membered heterocyclic series would potentially afford a diverse range of synthetic building blocks.

1.12 Thesis Objectives

As described in Section 1.7, the catalytic and enantioselective synthesis of pyranyl- and piperidyl-allylic boronate was realized through a unique borylative migration sequence. The synthetic power of this intermediate was demonstrated by the highly diastereoselective allylboration to access α-hydroxyalkyl heterocyclic units as well as the enantiospecific and regiodivergent Suzuki-Miyaura cross-coupling transformation. The utility of the piperidyl allylic boronate intermediate was further demonstrated in the synthesis of all four stereoisomers of mefloquine. The synthetic utility of the borylative migration transformation has not been fully explored. In the context of this thesis, applying this special piece of chemistry to efficiently synthesize potentially life-saving therapeutics to combat brain cancer and expanding the substrate scope of this transformation to access new synthetic building blocks will be described.

In Chapter 2, the synthetic strategy that was used in the synthesis of all four diastereomers of mefloquine will be applied towards the synthesis of Vacquinol-1 and Vacquinol-15. Structurally very similar to mefloquine, the vacquinol compounds lend themselves perfectly to the application of the borylative migration transformation. Furthermore, the synthetic strategy provides efficient access to intermediates that can be easily functionalized to provide a series of analogs. Namely, synthesis of the aldehyde partner (which is a strategic point to install different functional groups on the aryl substituent) will be described, access to all four stereoisomers of the vacquinol

compounds and their analogs, as well as biological results in collaboration with Dr. Roseline Godbout from the Cross Cancer Institute will be disclosed.

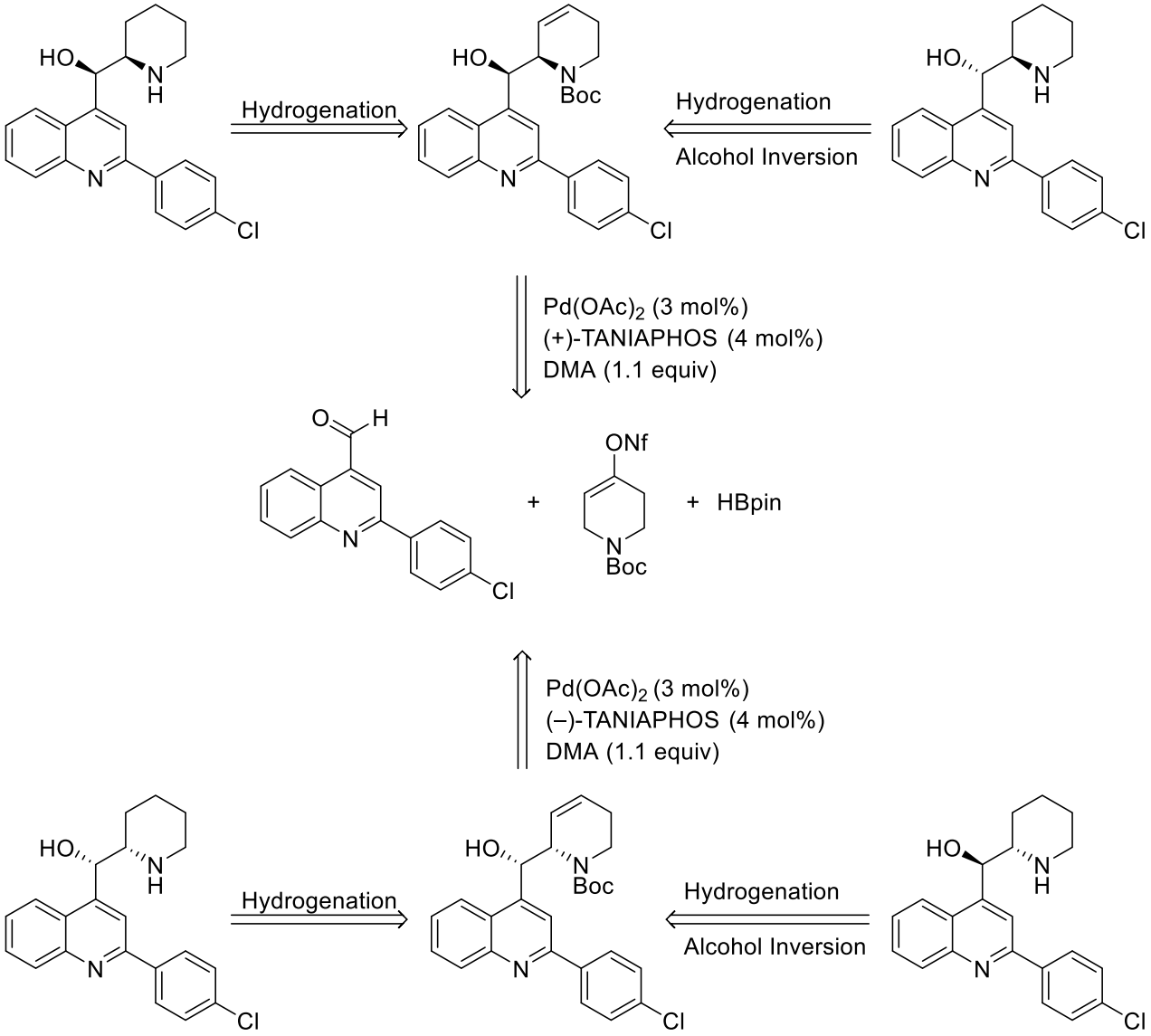

Scheme 1-13: Unified retrosynthetic scheme to access all four stereoisomers of Vacquinol-1.

In Chapter 3, efforts towards expanding the scope of the unique borylative migration will be discussed. Specifically, the challenges in obtaining the prerequisite achiral starting material for the synthesis of tetrahydrofuryl- and pyrrolidinyl- allylic boronates and a brief study on the influence of the leaving group on the achiral starting material will be detailed. Furthermore, variations of the borylative migration conditions for the generation of the pyrrolidinyl allylic boronate will also be described.

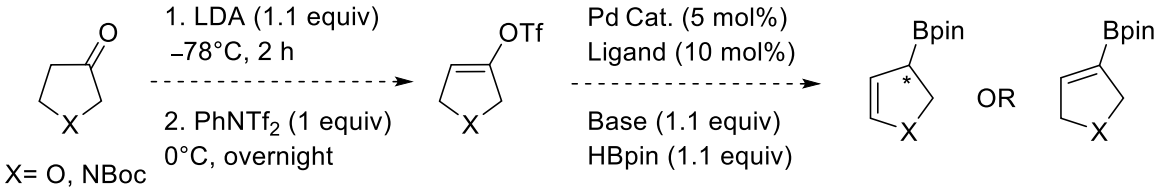

Scheme 1-14: Synthetic route towards accessing tetrahydrofuryl- and pyrrolidinyl- allylic boronate building blocks.

1.13 References

(1) Hartwig, J. *Organotransition Metal Chemistry: From Bonding to Catalysis*; University Science Books, **2009**.

(2) All Nobel Prizes in Chemistry http://www.nobelprize.org/nobel_prizes/chemistry/laureates/.

(3) Dougherty, D. A., Anslyn, E. V. In *Modern Physical Organic Chemistry*; University Science Books, **2004**; pp 333–340.

(4) Pirkle, W.H., Pochapsky, T. C. *Chem. Rev.* **1989**, *89*, 347–362.

(5) Itsuno, S. *Prog. Polym. Sci* **2005**, *30*, 540–558.

(6) Vargesson, N. *Birth Defects Res. (Part C)* **2015**, *105*, 140–156.

(7) Candy, M.; Audran, G.; Bienaymé, H.; Bressy, C.; Pons, J.-M. *Org. Lett.* **2009**, *11* (21), 4950–4953.

(8) Patel, R. N. *ACS Catal.* **2011**, *1* (9), 1056–1074.

(9) Lachance, H.; Hall, D. G. *Allylboration of Carbonyl Compounds*; John Wiley & Sons, Inc., **2009**.

(10) Chausset-Boissarie, L.; Ghozati, K.; LaBine, E.; Chen, J. L.-Y.; Aggarwal, V. K.; Crudden, C. M. *Chem. – A Eur. J.* **2013**, *19* (52), 17698–17701.

(11) Raducan, M.; Alam, R.; Szabó, K. J. *Angew. Chem. Int. Ed.* **2012**, *51*, 13050–13053.

(12) Yamamoto, Y.; Takada, S.; Miyaura, N. *Chem. Lett.* **2006**, *35* (7), 704–705.

(13) Yamamoto, Y.; Takada, S.; Miyaura, N. *Chem. Lett.* **2006**, *35* (7), 1368–1369.

(14) Sebelius, S.; Olsson, V. J.; Wallner, O. A.; Szabó, K. J. *J. Am. Chem. Soc.* **2006**, *128* (25), 8150–8151.

(15) Farmer, J. L.; Hunter, H. N.; Organ, M. G. *J. Am. Chem. Soc.* **2012**, *134* (42), 17470–17473.

(16) Elford, T. G.; Hall, D. G. *Boronic Acids*; Wiley-VCH Verlag GmbH & Co. KGaA, **2011**; *73*, 393–425.

(17) Herold, T.; Hoffmann, R. W. *Angew. Chem. Int. Ed.* **1978**, *17* (10), 768–769.

(18) Corey, E. J.; Yu, C. M.; Kim, S. S. *J. Am. Chem. Soc.* **1989**, *111* (14), 5495–5496.

(19) Brown, H. C.; Jadhav, P. K.; Bhat, K. S. *J. Am. Chem. Soc.* **1985**, *107* (8), 2564–2565.

(20) Roush, W. R.; Walts, A. E.; Hoong, L. K. *J. Am. Chem. Soc.* **1985**, *107* (26), 8186–8190.

(21) Rauniyar, V.; Hall, D. G. *Angew. Chem. Int. Ed.* **2006**, *45* (15), 2426–2428.

(22) Carosi, L.; Lachance, H.; Hall, D. G. *Tetrahedron Lett.* **2005**, *46* (52), 8981–8985.

(23) Peng, F.; Hall, D. G. *J. Am. Chem. Soc.* **2007**, *129* (11), 3070–3071.

(24) Brown, H. C.; Jadhav, P. K. *J. Am. Chem. Soc.* **1985**, *10*, 2564–2565.

(25) Brown, H.C., Bhat, K.S., Jadhav, P. K. *J. Chem. Soc. Transac* **1991**, *11*, 2633–2638.

(26) Atkins, W. J.; Burkhardt, E. R.; Matos, K. *Org. Process Res. Dev.* **2006**, *10* (6), 1292–1295.

(27) Renard, P.-Y., Lallemand, J.-Y. *Tetrahedron: Asymmetry* **1996**, *7* (9), 2523–2524.

(28) Hoffmann, R. W.; Dresely, S. *Angew. Chem. Int. Ed.* **1986**, *25* (2), 189.

(29) Hoffmann, R. W.; Dresely, S.; Hoffmann, R. W.; Dresely, S. *Chem. Ber.* **1989**, *122*, 903–

909.

(30) Hoffmann, R.W., Landmann, B. *Tetrahedron Lett.* **1983**, *24* (31), 3209–3212.

(31) Hoffmann, R. W.; Landmann, B. *Chem. Ber.* **1986**, *119* (3), 1039–1053.

(32) Suginome, M.; Ito, Y. *J. Organomet. Chem.* **2003**, *680* (1-2), 43–50.

(33) Durieux, G.; Gerdin, M.; Moberg, C.; Jutand, A. *Eur. J. Inorg. Chem.* **2008**, *27*, 4236–4241.

(34) Gerdin, M.; Penhoat, M.; Zalubovskis, R.; Pétermann, C.; Moberg, C. *J. Organomet. Chem.* **2008**, *693* (23), 3519–3526.

(35) Tailor, J.; Hall, D. G. *Org. Lett.* **2000**, *2* (23), 3715–3718.

(36) Deligny, M.; Carreaux, F.; Carboni, B. *Synlett* **2005**, *9*, 1462–1464.

(37) Gademann, K.; Chavez, D. E.; Jacobsen, E. N. *Angew. Chem. Int. Ed.* **2002**, *41* (16), 3059–3061.

(38) Gao, X.; Hall, D. G. *J. Am. Chem. Soc.* **2005**, *127* (6), 1628–1629.

(39) Lessard, S.; Peng, F.; Hall, D. G. *J. Am. Chem. Soc.* **2009**, *131* (28), 9612–9613.

(40) Murata, M.; Oyama, T.; Watanabe, S.; Masuda, Y. *Synthesis.* **2000**, *6*, 778–780.

(41) Kim, Y.-R.; Hall, D. G. *Org. Biomol. Chem.* **2016**, *14*, 4739–4748.

(42) Ding, J.; Rybak, T.; Hall, D. G. *Nat. Commun.* **2014**, *5*, 1–9.

(43) Beng, T. K.; Gawley, R. E. *Org. Lett.* **2011**, *8*, 11–14.

(44) Amat, M.; Bosch, J.; Hidalgo, J.; Cantó, M.; Perez, M.; Llor, N.; Molins, E.; Miravitlles, C.; Orozco, M.; Luque, J. *J. Org. Chem.* **2000**, *65* (10), 3074–3084.

(45) Matos, K.; Soderquist, J. A. *J. Org. Chem.* **1998**, *63*, 461–470.

(46) Ridgway, B. H.; Woerpel, K. A. *J. Org. Chem.* **1998**, *63* (3), 458–460.

(47) Ding, J.; Hall, D. G. *Angew. Chem. Int. Ed.* **2013**, *52* (31), 8069–8073.

(48) Karle, J. M., Olmeda, R., Gerena, L., Milhous, W. K. *Exp. Parasitol.* **1993**, *76*, 345–351.

(49) Roche, F.H.-L., Brober, E., Hofneinz, W., Meili, A. Eur. Pat. 553778, 1993.

(50) Xie, Z.X., Zhang, L.Z., Ren, X.J., Tang, S.Y., Li, Y. *Chinese J. Chem.* **2008**, *26*, 1272–1276.

(51) Knight, J. D.; Sauer, S. J.; Coltart, D. M. *Org. Lett.* **2011**, *13* (12), 3118–3121.

(52) Kitambi, S. S.; Toledo, E. M.; Usoskin, D.; Wee, S.; Harisankar, A.; Svensson, R.; Sigmundsson, K.; Kalderén, C.; Niklasson, M.; Kundu, S.; Aranda, S.; Westermark, B.; Uhrbom, L.; Andäng, M.; Damberg, P.; Nelander, S.; Arenas, E.; Artursson, P.; Walfridsson, J.; Forsberg Nilsson, K.; Hammarström, L. G. J.; Ernfors, P. *Cell* **2014**, *157* (2), 313–328.

(53) Galluzzi, L.; Zamzami, N.; La, T. De; Rouge, M.; Lemaire, C.; Brenner, C.; Kroemer, G. *Apoptosis* **2007**, *12*, 803–813.

(54) Tsujimoto, Y.; Shimizu, S. *Cell Death Differ.* **2005**, *12*, 1528–1534.

Chapter 2. Application of the Unique Borylative Migration of Enol Perfluorosulfonates towards the Synthesis of Therapeutic Agents

2.1 Introduction

Cancer is a class of disease that is characterized by uncontrolled cell growth. In the context of this thesis, brain cancer is the focal point. These cancers can exist in a variety of forms, such as astrocytoma, lymphoma and meningioma. With over 120 different types of brain tumours, effective treatment is complicated and requires a combination of surgical treatment, chemotherapy and radiotherapy. An exceptionally aggressive type of tumour is called glioblastoma multiforme (GBM). GBM has the highest number of cases of all malignant tumours.[1] Malignant tumours consist of cells that grow and divide uncontrollably and can invade neighbouring tissue. In contrast, benign tumours are formed from cells that lack the ability to metastasize and are unable to invade neighbouring tissues.

GBM normally arise from astrocytes (the star-shaped cells that make up the supportive tissue of the brain) and the tumour is usually highly heterogeneous (a variety of cell types are present). These tumours are highly cancerous since the cells are able to reproduce rapidly. Rapid cell growth is supported by a large network of blood vessels that support cell growth by providing abundant supplies of oxygen and nutrients. Additionally, GBM tumours exhibit a diverse genetic make-up where several genetic alterations promote enhanced survival and invasion properties as well as increased cell proliferation.[2] As such, GBM is essentially incurable. Only 3-5% of patients survive longer than 3 years even after surgical tumour resection (physical removal) with concomitant chemotherapy and radiotherapy.[2]

2.2 Challenges for the Treatment of Glioblastoma Multiforme

As challenging as it is to effectively treat cancer, the successful treatment of glioblastoma multiforme tumours must overcome several additional obstacles. Namely, the therapeutic compound must be able to cross the blood brain barrier (BBB) and the diversity in genetic make-up of the tumour limits the use of therapeutics that target specific biochemical pathways. First, the blood brain barrier is a highly selective and active interface that lines the blood vessels in the brain and spinal cord.[3] The main function of the BBB is to block the passage of toxic and harmful molecules through several defense mechanisms; such as, an enzymatic barrier, immunological barrier and highly efficient efflux transport systems.[4] In effect, the blood brain barrier renders the glioblastoma tumours highly resistant to multiple drugs. One way this challenge has been addressed is the development of polymeric nanoparticles, liposomes and lipid nanocarriers for drug delivery.[3]

Second, therapeutics are often developed with the aid of genetic and molecular studies to determine the genes, pathways and proteins involved in the proliferation of the tumour and thus provide a target to neutralize the functional advantage of the cancerous cells. However, due to the complexity and diversity of glioblastoma genetics, this strategy has been greatly hindered. Within the tumour there is a highly diverse range of environments surrounding the cancerous cells. For example, some regions are hypoxic (a condition whereby an insufficient amount of oxygen is present), while other regions are normoxic (a sufficient supply of oxygen is available); some regions are proliferative and others are quiescent (a state of dormancy or inactivity); and some regions of the tumour are

highly vascularized (surrounded by blood vessels) or not.[5] Additionally, the increased rate of proliferation of cancerous cells can increase the possibility of these cells to develop additional mutations that increase drug resistance. Of note, a recent review described the molecular mechanisms underlying the resistance of glioblastoma multiforme cancerous cells to the predominant chemotherapeutic agent temozolomide.[6] Temozolomide is usually applied in combination with radiotherapy and is an alkylating agent. This review summarized the evidence of various molecular mechanisms and concluded that the main mechanisms of resistance are linked to systems of DNA repair, control of cellular propagation and ABC (ATP-binding cassette) transporters.[6]

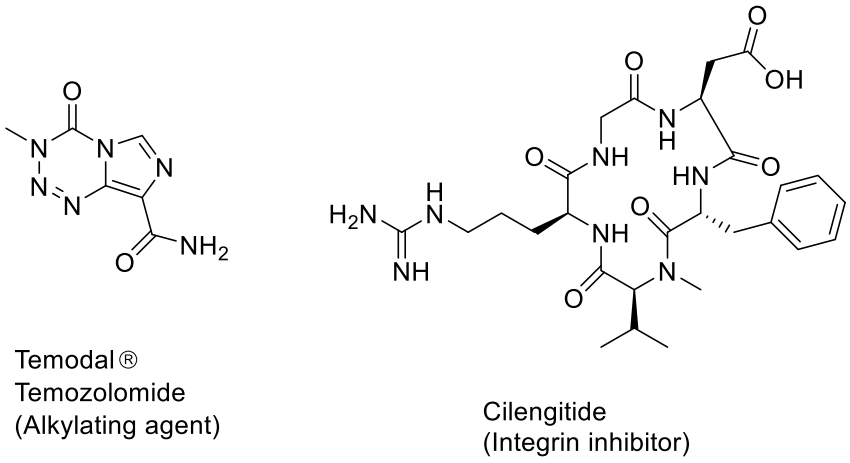

Figure 2-1: Structure of temozolomide (the predominante chemotherapeutic agent) and cilengitide (a chemotherapeutic agent under study).

2.3 Current Treatments for Glioblastoma Multiforme Therapeutic

Currently, there are no truly effective treatment for GBM. A surgical cure is not possible for GBM because despite extensive surgical tumour resection, the infiltrating tumour cells have been found

far removed from the gross macroscopic disease.[5] The current standard of care entails the maximal safe resection of the tumour followed by six weeks of radiation with concurrent daily treatment of temozolomide chemotherapy. Subsequently, six months of adjuvant treatment with temozolomide concludes the first-line of treatment of GBM.[5] Although several clinical trials are currently underway to establish a targeted form of treatment; for example, one such clinical study attempted to target the angiogenic (angiogenesis is the process by which new blood vessels form from pre-existing vessels) phenotype of this disease by treatment with bevacizumab (immunoglobulin G1, anti-human vascular endothelial growth factor) and cilengitide, there has been little to no success. Moreover, recurrence of GBM typically occurs within six to nine months of initial diagnosis and treatment. Salvage therapy, if effective at all, is only able to control the growth of the cancerous cells for another four to six months.

Considering the overall failure of new therapeutics and approaches focused on neutralizing the anomalies of the cancerous cells by targeting specific biochemical pathways, Ernfors and co-workers[2] hypothesized that an overall unique cellular property could be exploited. In 2014, this Swedish group published their findings of a class of small molecules that was effective against glioblastoma multiforme. These compounds were selected from a screening of 1 364 compounds from the NIH diversity set II and were given the name vacquinols due to the quinoline-alcohol scaffold.[2] Of note, one compound from this study exhibited high efficacy against GBM, namely, Vacquinol-1. After a brief structure activity relationship study was conducted another highly effective compound, Vacquinol-15, was identified.

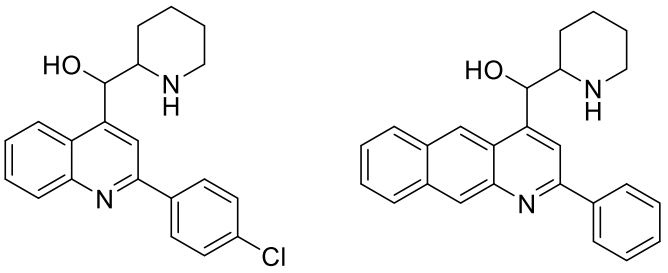

Vacquinol-1 Vacquinol-15

Figure 2-2: Structure of two potentially new chemotherapeutic agents against glioblastoma multiforme, Vacquinol-1 and Vacquinol-15.

Initial cytotoxicity studies revealed that Vacquinol-1 selectively targets glioblastoma multiforme cancerous cells. Vacquinol-1 did not affect fibroblasts (cells that make up the connective tissues and is responsible for making the extracellular matrix and collagen), mouse embryonic stem cells or osteosarcoma (cancerous bone) cells when mixed in co-cultures with GBM cells. Furthermore, this compound was ineffective against bladder, prostate, breast and neuroblastoma cancer cell lines. Moreover, Vacquinol-1 exhibited a median IC_{50} (inhibition concentration of 50%) of 2.36 μM (24 h) compared to temozolomide (the standard chemotherapeutic), which exhibits an IC_{50} of 139 μM (48 h; employed as a positive control). Of note, Vacquinol-15 demonstrated poor selectivity and therefore subsequent biological assays were only conducted with Vacquinol-1.

2.4 Induction of Cancerous Cell Death by Vacquinol-1: Investigation of the Biochemical Pathway and Attenuation of Tumor Growth *In Vivo*

To probe and investigate the mechanism of cell death induction, Ernfors and co-workers studied several established apoptotic pathways as well as non-apoptotic autophagy-associated cell death

markers. First, the enzymatic activity of Caspase-3 and Caspase-7 was measured. Both Caspase-3 and Caspase-7 are "effector" caspases that play an active role in a protease cascade that initiates and sustains the apoptotic pathway.[7] Vacquinol-1 had no effect on caspase activity at any concentration (5-30 μM) or time point (5-600 min). Additionally, disruption of active mitochondria was probed by determining the accumulation of tetramethylrhodamine ethyl ester (TMRE) (TMRE accumulates in the mitochondria and endoplasmic reticulum when active mitochondria is disrupted)[8] in the mitochondria and determining the cytosolic calcium flux (abnormal Ca^{2+} influx, efflux and compartmentalization all attribute to inducing apoptotic pathways)[9]. Vacquinol-1 did not affect either of these processes. The above results indicate that Vacquinol-1 induced cell death occurs via a non-apoptotic mechanism.

Additionally, autophagy is a general term for the degradation of cytoplasmic components within lysosomes (lysosomes are organelles within the cytoplasm that contain degradative enzymes enclosed in a membrane).[10] Within healthy cells, autophagy is a process by which a cell can compensate when it is in a state of depleted amino acids, eliminate cytoplasmic content that may be harmful to the cell and/or organelles that are in excess or not required. When a cell undergoes autophagic-induced cell death, these events are observable by the morphological changes that the cell undertakes. Live imaging of Vacquinol-1 treated GBM cells revealed rapid formation of intracellular vacuoles and membrane invaginations. Vacuole size and numbers increased over time leading to displacement of the cytoplasm and eventually cell death by cell lysis (also known as cell rupture). Additional immunofluorescent studies revealed that excessive macropinocytosis (form of endocytosis for non-selective uptake of extracellular molecules) initiated by Vacquinol-1, led to catastrophic vacuolization and resulted in necrotic-like cell death. Of note, the activity of

Vacquinol-1 is dependent on MKK4 (mitogen-activated protein kinase kinase 4 is a member of a family of enzymes that respond to external stimuli and permit enzymatic amplification).[11] When MKK4 was disrupted the cancerous cells exhibited resistance to cell death. In summary, these observations provide evidence that the mechanism of action of Vacquinol-1 is to induce GBM cells to over produce vacuoles which ultimately leads to cell death by rupture.

Lastly, *in vivo* studies were conducted to determine the viability of Vacquinol-1 as a therapeutic agent against GBM.[2] A zebrafish xenograft glioblastoma model and a mouse model for human GBM were both treated with Vacquinol-1 and exhibited attenuation of tumour growth. Taking into account these encouraging results the bioavailability of Vacquinol-1 was investigated by oral and intravenous administration. Intravenous administration indicated rapid tissue distribution of Vacquinol-1 and the compound exhibited good stability with very low systemic plasma clearance. Additional *in vivo* studies with a GBM mouse model examined, by MRI, the progression of tumor growth with treatment of Vacquinol-1. It was observed that the treated mice exhibited normal brain morphology, brain weight and an enhanced survival rate. In contrast, the brains of non-treated mice displayed hemorrhage, areas of necrosis and increased brain weight. These findings suggest that Vacquinol-1 induces cell death selectively in cancerous cells, as well as inhibits the migration of the tumour to surrounding tissues. In summary, Vacquinol-1 shows remarkable promise to become an effective therapeutic agent against glioblastoma multiforme.

2.5 Vacquinol-1: Synthesis and Identification of the Active Stereoisomer

As described in the previous sections, Vacquinol-1 is a promising lead compound for treatment of GBM. However, the set of compounds that were studied by Ernfors and co-workers was a complex mixture of four possible stereoisomers.[2] With the current stringent standards for the development of a new therapeutic agent, it is insufficient and negligent to advance a mixture of four stereoisomers. Therefore, there is a dearth of evidence for the efficacy of each stereoisomer. Furthermore, it is well established that enantiomers may exhibit vastly different biological effects. One likely reason that a mixture of stereoisomers was tested is the lack of an efficient and enantioselective synthetic method to access all stereoisomers independently.

The synthetic route employed by Ernfors and co-workers is illustrated in Scheme 2-1.[2] To summarize, the target compound was synthesized as a mixture of stereoisomers; starting from isatin **2.11**, over 7 steps were required with an overall yield of 0.8 % yield. Of note, methyl 6-benzamidohexanoate had to be synthesized over two steps and required the use of the coupling reagents, EDCI (1-ethyl-3-(3-dimethylaminopropyl)carbodiimide) and HOBt (1-hydroxybenzotriazole). The authors report that they separated the protecting-group free piperidinyl-amine stereoisomers by chiral HPLC (high performance liquid chromatography) and performed preliminary biological assays with each enantioenriched stereoisomer. They found that three of the four stereoisomers exhibited very similar biological effects, however, they did not disclose or identify these stereoisomers. Of note, determining the absolute configuration and separating the protecting group free piperidinyl-amine is no trivial task and the authors do not describe a method that could assess the absolute configuration of their tested compounds.

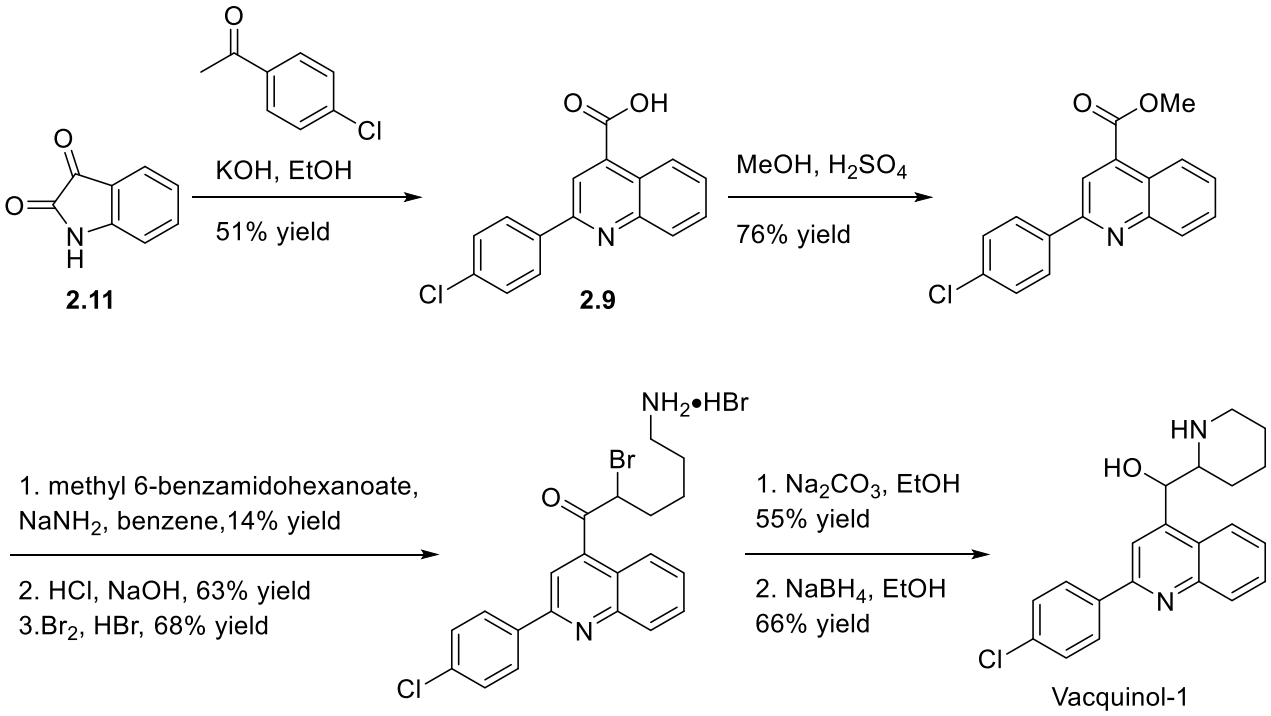

Scheme 2-1: Synthetic route performed by Ernfors and co-workers to access Vacquinol-1.

Structurally, the vacquinol compounds feature an α-hydroxyalkyl piperidine with two contiguous stereogenic centers (therefore, these compounds may exist as four stereoisomers). This part of the molecule lends itself to the borylative migration with subsequent aldehyde allylboration transformation described in Chapter 1. Therefore, the unique chemical transformation developed in our laboratory, provides a method that can efficiently synthesize all four enantioenriched stereoisomers of Vacquinol-1 and Vacquinol-15. With each stereoisomer in hand, a much needed study of the bioactivity of each stereoisomer can be performed and the identification of the most bioactive stereoisomers can be determined.

2.6 Unified Synthetic Strategy Towards all Four Stereoisomers of Vacquinol Compounds

Considering the precedence and success of the synthesis of all four stereoisomers of mefloquine reported by our group in 2013,[12] a unified synthetic strategy towards all four stereoisomers of Vacquinol-1 is illustrated in Scheme 2-2. At the core of the synthetic strategy is the unique borylative migration chemistry and subsequent aldehyde allylboration. As shown, **2.2** can be prepared from the key dehydro-intermediate **2.5** through hydrogenation and inversion of the alcohol (with subsequent deprotection of the piperidinyl amine). Its diastereomer **2.1** is obtained directly after hydrogenation and deprotection; without the alcohol inversion. Likewise, the two other stereoisomers **2.3** and **2.4** could be accessed from **2.6** using (-)-TANIAPHOS.

In contrast to the synthetic route used by Ernfors and co-workers, the proposed synthetic strategy is convergent and able to selectively access each stereoisomer independently. This strategy employs two parallel synthetic routes; one to access the aldehyde (illustrated by Scheme 2-4) and the other route is to access the enantioenriched allylic-boronate intermediate **2.19** and **2.20** (illustrated by Schemes 2-7 and 2-8). From this point of convergence, Vacquinol-1 stereoisomers **2.1** and **2.3** can be accessed in three steps, while Vacquinol-1 stereoisomers **2.2** and **2.4** can be accessed in five steps. In addition, this proposed synthetic route is significantly more atom-economical than what was reported by Ernfors and co-workers,[2] since the use if EDCI and HOBt is not required.

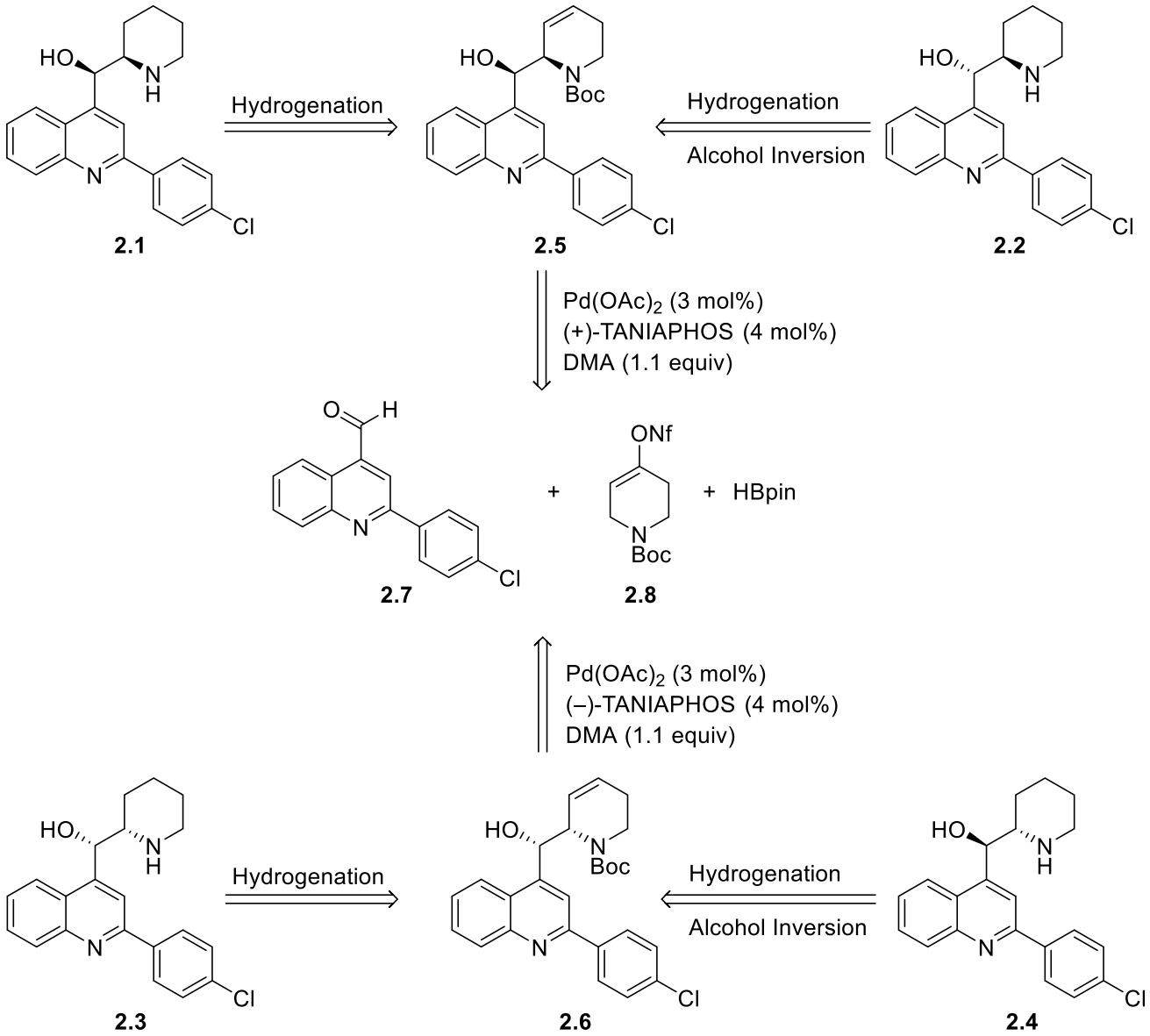

Scheme 2-2: Unified retrosynthetic strategy for all four Vacquinol-1 stereoisomers.

2.7 Synthesis of all Four Stereoisomers of Vacquinol-1

To begin the synthesis, access to all necessary components illustrated in Scheme 2-2 was achieved following literature precedence. Alkenyl nonaflate **2.8** was readily synthesized in gram scale as previously described (illustrated in Scheme 2-3).[13]

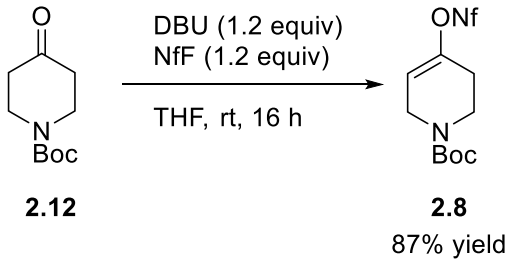

2.12 **2.8**
87% yield

Scheme 2-3: Synthesis of alkenyl nonaflate **2.8**; Nf = $CF_2CF_2CF_2CF_3$

Although **2.9** is commercially available, the aldehyde coupling partner **2.7** for Vacquinol-1 was synthesized in gram scale as described in Scheme 2-4. Of note, the synthesis of **2.9** from **2.10** and **2.11**, proceeds by the Pfitzinger reaction.[14]

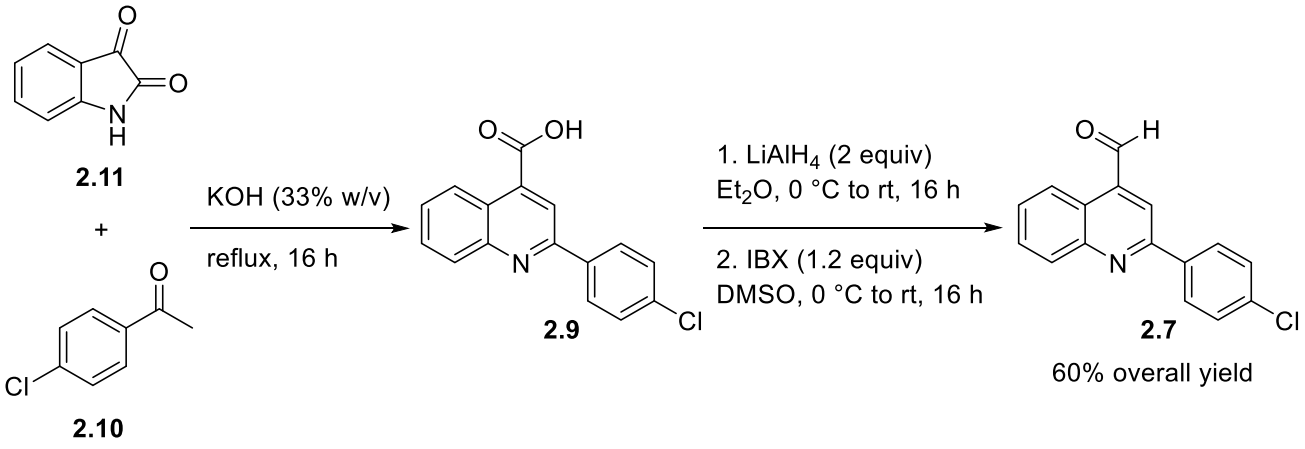

Scheme 2-4: Synthesis of aldehyde **2.7**.

Traditionally, two possible isomers can form during the Pfitzinger reaction, as depicted in Scheme 2-5. In general, the larger substituent of **2.13** would end up *meta* to the carboxylic acid, presumably due to steric control,[15] to afford **2.14**. In contrast, the other possible isomer would feature the larger substituent *ortho* to the carboxylic acid.

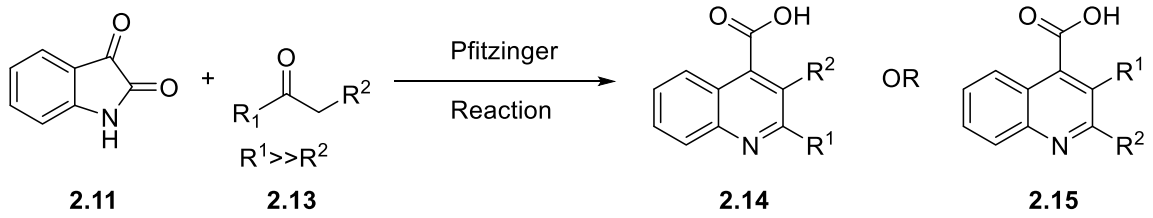

Scheme 2-5: General reaction scheme of the Pfitzinger reaction.

Fortuitously, in accessing **2.9**, the issue of regioselectivity is not of concern. Considering the proposed mechanism, (Scheme 2-6) formation of the enamine **2.18**, after condensation of **2.13** to **2.16**, can solely occur at the α-carbon with acidic hydrogens. As illustrated in Scheme 2-4, the identity of ketone **2.13** (Scheme 2-6) is compound **2.10** for the synthesis of **2.9**. It is evident that there is only one possible site for deprotonation. Furthermore, the geometry of enamine **2.18** does not influence the conformation of the final product due to the subsequent dehydration and aromatization steps.

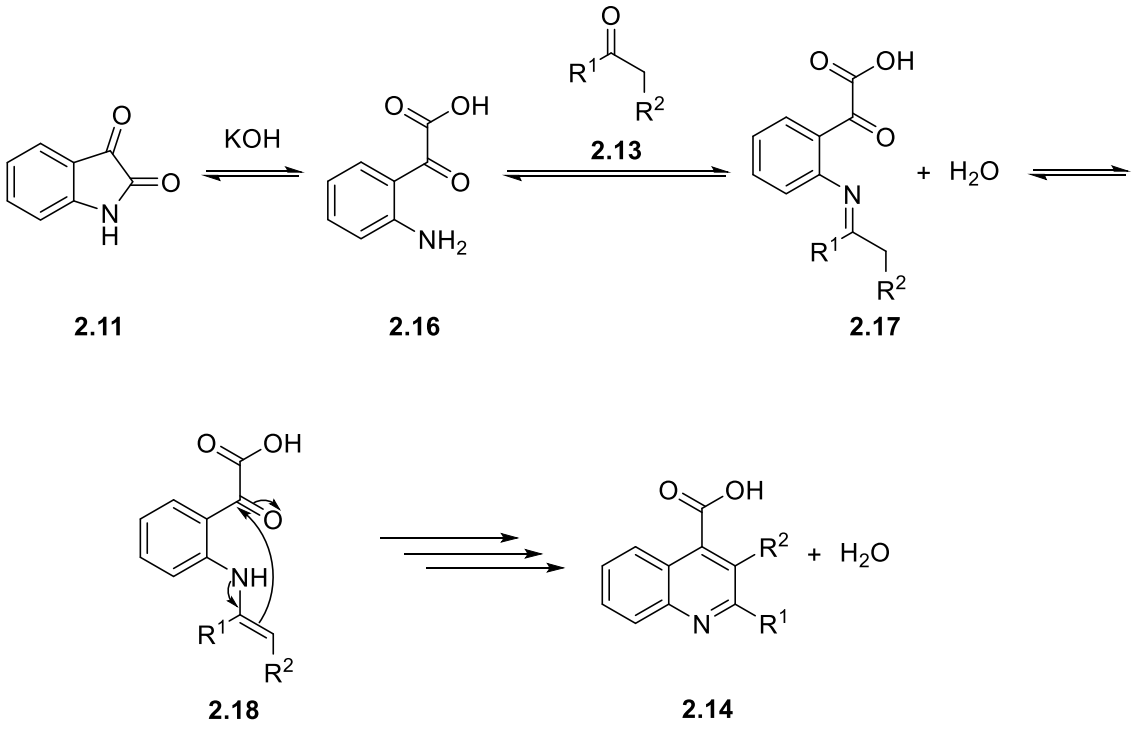

Scheme 2-6: Proposed mechanism of the Pfitzinger reaction.

With all the components in hand, synthesis of enantiomers **2.5** and **2.6** was achieved with good overall yield and enantioselectivity without purification of the borylative migration intermediate **2.19** and **2.20**, when (+)-TANIAPHOS and (-)-TANIAPHOS were employed respectively. The chiral allylic boronate was subjected to the thermal aldehyde allylboration with aldehyde **2.7**, after a quick filtration and solvent change, using a microwave reactor.

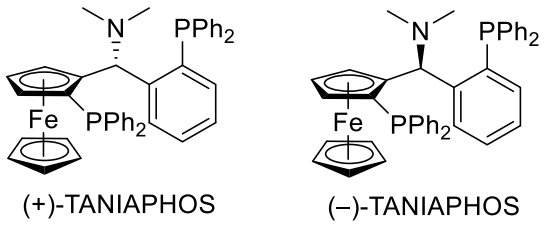

Figure 2-3: Structure of TANIAPHOS ligand.

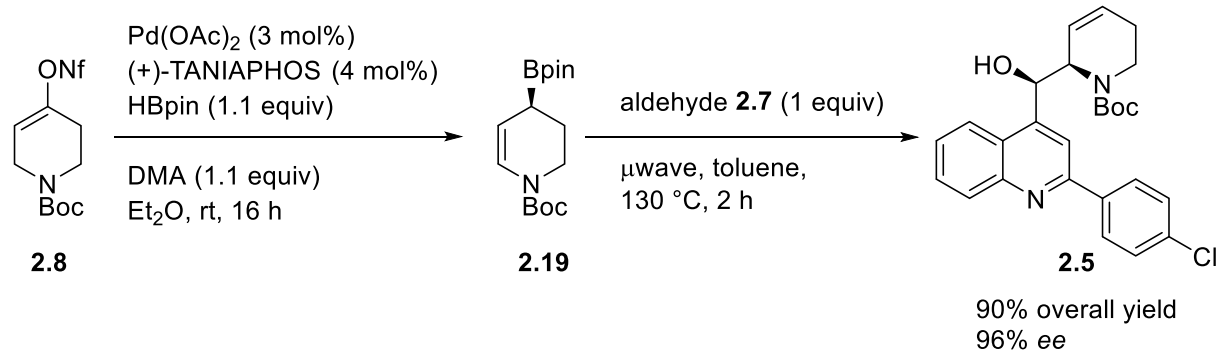

Scheme 2-7: Synthesis of **2.5**, an advanced intermediate of Vacquinol-1.

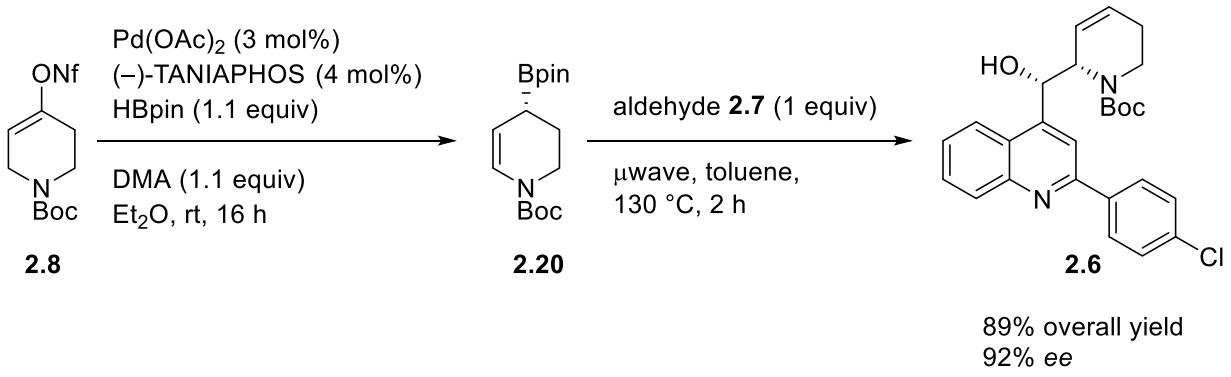

Scheme 2-8: Synthesis of **2.6**, an advanced intermediate of Vacquinol-1.

Of note, it is imperative that *N,N*-dimethylaniline (DMA), diethyl ether and pinacolborane are purified via distillation before use. Substrate **2.8** and aldehyde **2.7** must be purified via flash column chromatography before use and care must be taken to store palladium (II) acetate catalyst under argon.

2.8 Optimization of the Hydrogenation Conditions

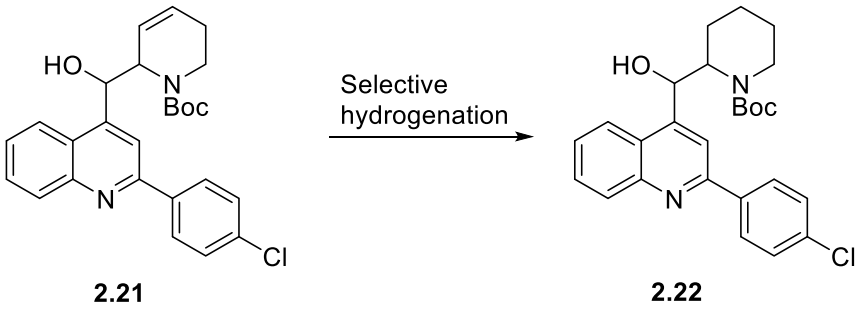

2.21 **2.22**

Scheme 2-9: General scheme for the reduction of the endocyclic alkene featured in **2.21**.

Surprisingly, the transformation illustrated by Scheme 2-9 required several attempts. One foreseeable challenge of chemoselectivity is the undesired reduction of the quinoline moiety in the presence of the endocyclic alkene of the dehydropiperidine ring. However, considering the reactivity of an isolated double bond in contrast to the aromatic quinoline system, the reduction is not expected to be problematic. Several hydrogenation conditions were investigated.

2.81 Homogeneous Catalytic Hydrogenation Conditions

The first variations of hydrogenation conditions that were investigated were based upon the precedence from the synthesis of mefloquine.[12] Crabtree's catalyst has been observed to coordinate to alcohols to deliver the catalyst and thereby provide an efficient reduction of the alkene (this is often used to provide diastereoselective reduction).[16] In addition, reactions conditions were chosen based on literature precedence.[12]

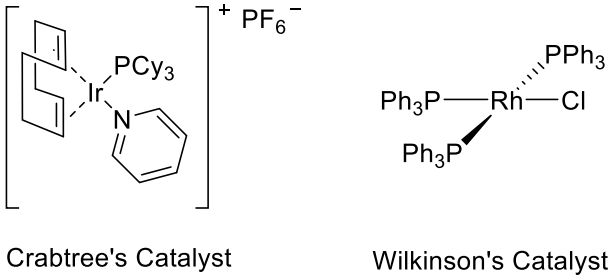

Crabtree's Catalyst Wilkinson's Catalyst

Figure 2-4: Structure of Crabtree's and Wilkinson's Catalyst.

Alternatively, Wilkinson's catalyst is another reliable catalyst for the hydrogenation of alkenes to alkanes. As summarized in Table 2-1 and Table 2-2, these homogeneous hydrogenation systems did not promote the desired transformation. With the interest of full disclosure, considerably mild hydrogenation conditions were the focus of this exploration to avoid over reduction of the advanced intermediate **2.21**.

Table 2-1: Evaluation of the reaction conditions using Wilkinson's catalyst.

Entry	Catalyst Loading	Hydrogen Pressure	Time	Solvent	Result
1	5 mol%	1 atm**	16 h	THF	Recovered S.M.*
2	5 mol%	1 atm**	96 h	THF	Recovered S.M.*
3	7.5 mol%	40 psi	120 h	THF	Recovered S.M.*
4	10 mol%	55 psi	120 h	THF	Recovered S.M.*

* Determined by ^{1}H NMR after filtering the reaction mixture through a short silica plug

**1 atm = 14.6959 psi

Table 2-2: Evaluation of the reaction conditions using Crabtree's catalyst.

Entry	Catalyst Loading	Hydrogen Pressure	Time	Solvent	Result
1	4 mol%	1 atm**	16 h	DCM	Recovered S.M.*
2	4 mol%	1 atm**	48 h	DCM	Recovered S.M.*
3	5 mol%	1 atm**	16 h	DCM	Recovered S.M.*
4	5 mol%	1 atm**	96 h	DCM	Recovered S.M.*
5	7.5 mol%	40 psi	120 h	DCM	Recovered S.M.*
6	7.5 mol%	50 psi	120 h	DCM	Recovered S.M.*
7	10 mol%	40 psi	120 h	DCM	Recovered S.M.*
8	10 mol%	50 psi	120 h	DCM	Recovered S.M.*

* Determined by ^{1}H NMR after filtering the reaction mixture through a short silica plug

**1 atm = 14.6959 psi

2.82 Heterogeneous Catalytic Hydrogenation Condition

The next hydrogenation conditions to be explored employed the use of heterogeneous catalyst systems. After several endeavors, Adam's catalyst (PtO_2) afforded the desired transformation in near quantitative yield. After deprotection of **2.22**, compounds **2.1** and **2.3** were obtained in good yield without enantiomeric erosion (Scheme 2-2).

Table 2-3: Evaluation of the reaction conditions using Pd/C as catalyst.

Entry	Catalyst Loading	Hydrogen Pressure	Time	Solvent	Result
1	5 mol%	1 atm**	16 h	EtOAc	Recovered S.M.*
2	5 mol%	1 atm**	96 h	EtOAc	Recovered S.M.*
3	7.5 mol%	40 psi	120 h	EtOAc	Recovered S.M.*
4	10 mol%	55 psi	120 h	EtOAc	Recovered S.M.*

* Determined by ^{1}H NMR after filtering the reaction mixture through a Celite® 545 plug

**1 atm = 14.6959 psi

Table 2-4: Evaluation of the reaction conditions using $Pd(OH)_2$ as catalyst.

Entry	Catalyst Loading	Hydrogen Pressure	Time	Solvent	Result
1	10 mol%	1 atm**	16 h	EtOH	Recovered S.M.*
2	5 mol%	40 psi	96 h	EtOH	Recovered S.M.*
3	7.5 mol%	40 psi	120 h	EtOH	Recovered S.M.*
4	10 mol%	55 psi	120 h	EtOH	Recovered S.M.*

* Determined by ^{1}H NMR after filtering the reaction mixture through a Celite® 545 plug

**1 atm = 14.6959 psi

Table 2-5: Evaluation of the reaction conditions using Adam's catalyst.

Entry	Catalyst Loading	Hydrogen Pressure	Time	Solvent	Result
1	5 mol%	1 atm**	16 h	EtOAc	Recovered S.M.*
2	10 mol%	1 atm**	16 h	EtOAc	**2.22** quant.*
3	20 mol%	1 atm**	16 h	EtOAc	**2.22** quant.*
4	40 mol%	1 atm**	16 h	EtOAc	**2.22** quant.*

* Determined by ^{1}H NMR after filtering the reaction mixture through a Celite® 545 plug

**1 atm = 14.6959 psi

Table 2-6: Evaluation of the other hydrogenation systems.

Entry	Catalyst	Catalyst Loading	Hydrogen	Time	Solvent	Result
1	Rh/activated alumina	10 mol%	50 psi	120 h	EtOH	Recovered S.M.*
2	n/a	1 equiv	H_2NNH_2	16 h, reflux	EtOH	Decomposition

* Determined by ^{1}H NMR after filtering the reaction mixture through a Celite® 545 plug

2.9 Inversion of the Stereogenic Secondary Alcohol Centre

Concurrent with the investigations into reducing the endocyclic alkene, epimerization of the benzylic alcohol containing stereogenic centre was achieved. Considering the efforts conducted during the synthesis of mefloquine, and in the interest of time, exploration of this transformation was limited to the protocol that was successful to avoid unnecessary decomposition and waste of the starting material. Therefore, a straightforward oxidation followed by diastereoselective reduction was performed to obtain **2.24** and the enantiomeric partner **2.26** (Scheme 2-10 and 2-11).

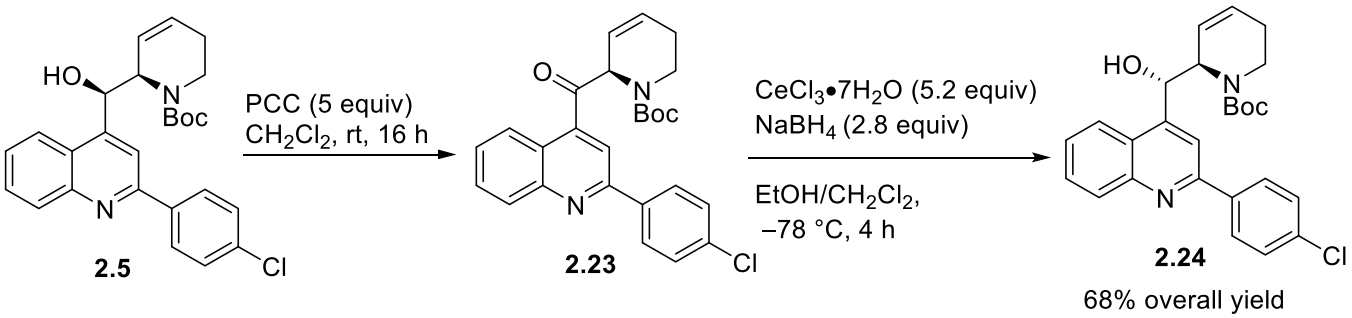

Scheme 2-10: Inversion of the stereogenic alcohol centre to obtain **2.24**.

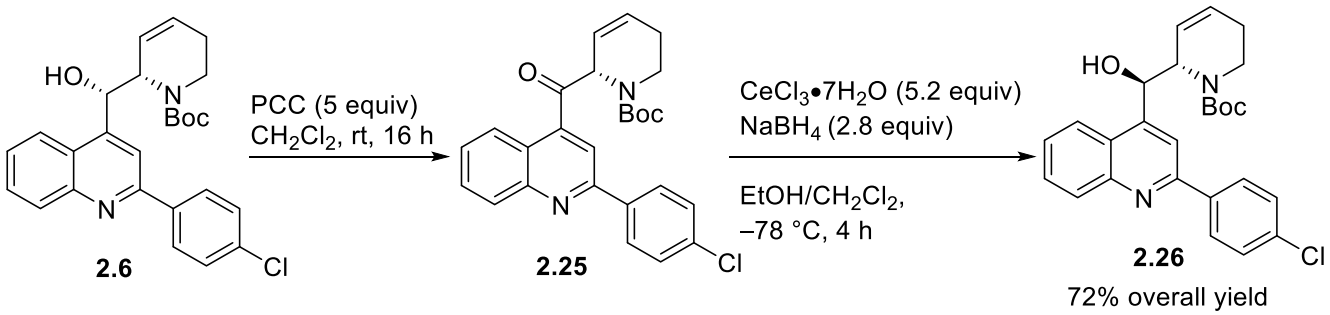

Scheme 2-11: Inversion of the stereogenic alcohol centre to obtain **2.26**.

Additionally, following hydrogenation and deprotection compounds **2.2** and **2.4** were obtained (Scheme 2-12 and Scheme 2-13). Enantiomeric erosion was not observed after hydrogenation nor epimerization of the benzylic centre, this will be discussed in the next section. To summarize, for the Vacquinol-1 stereoisomer **2.1** the overall yield is 88%, for the Vacquinol-1 stereoisomer **2.2** the overall yield is 61%, for the Vacquinol-1 stereoisomer **2.3** the overall yield is 86%, and for the Vacquinol-1 stereoisomer **2.4** the overall yield is 64%. With all four enantioenriched stereoisomers of Vacquinol-1 and the corresponding unsaturated analogs in hand, investigation into the biological effects of these compounds would be performed in partnership with Dr. Roseline Godbout at the Cross Cancer Institute.

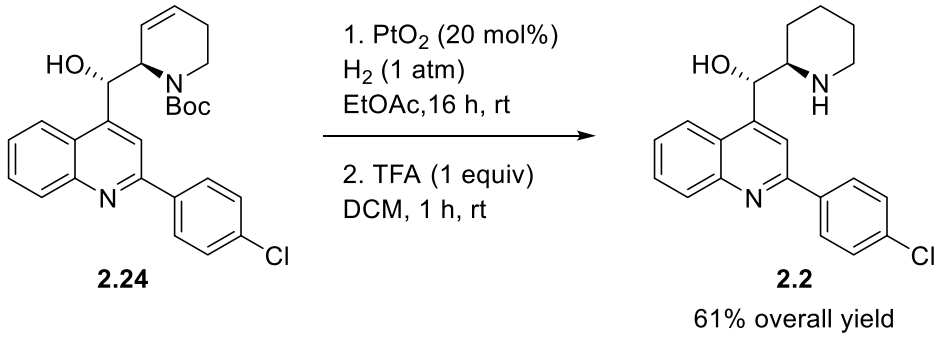

Scheme 2-12: Hydrogenation and deprotection of **2.24** to afford **2.2**.

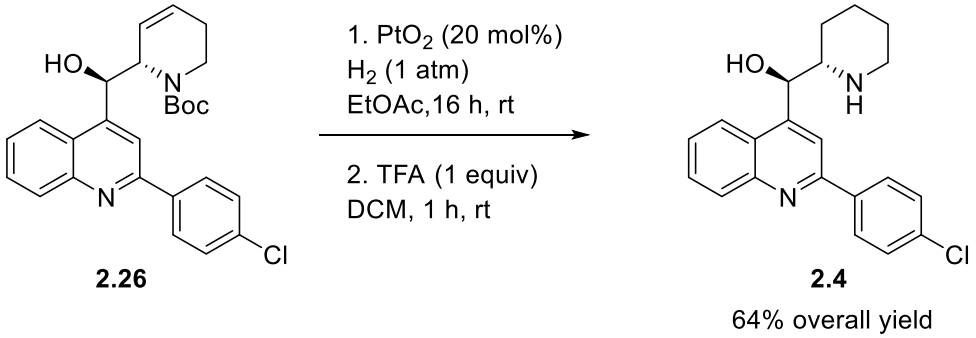

Scheme 2-13: Hydrogenation and deprotection of **2.26** to afford **2.4**.

2.10 Examination of the Separation of All Four Stereoisomers of Vacquinol-1

However, before any biological assays may be conducted the assessment of the stereochemistry must be performed. Delving into the Supplementary Information of the account by Ernfors and co-workers to ascertain the HPLC conditions for the separation of all four stereoisomers of Vacquinol-1 revealed inadequate evidence that the stereoisomers were separated. Indeed, efforts to separate protecting-group free Vacquinol-1 failed. However, separation of the *tert*-butyloxycarbonyl (Boc) protected variants was achieved and thus confirmed that all four stereoisomers were synthesized via a co-injection experiment (illustrated by Figure 2-5). Credit for determining the HPLC

conditions and performing the experiments must be attributed to Ed Fu. It is worthy to note that throughout the synthetic route undesired epimerization of both stereocenters does not occur. Careful consideration of the HPLC spectra (Figure 2-5) and additional co-injection experiments supports this observation.

2.11 Biological Assays

In collaboration with Dr. Roseline Godbout from the Department of Oncology in the Faculty of Medicine and Dentistry at the University of Alberta, the efficacy of each enantioenriched stereoisomer of Vacquinol-1 and one series of analogues (illustrated in Figure 2-6) was investigated. The initial biological assays that were conducted probed the efficacy of these compounds to induce cell death.

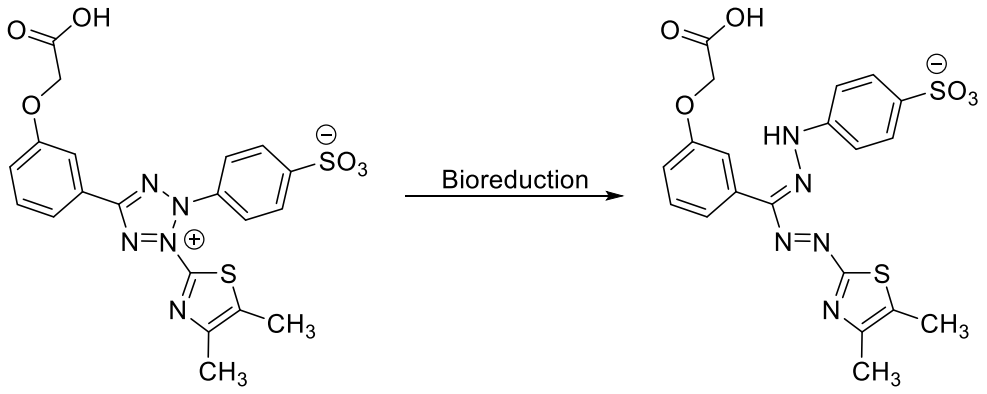

Scheme 2-14: Structure of MTS and formation of formazan *via* bioreduction of viable cells.

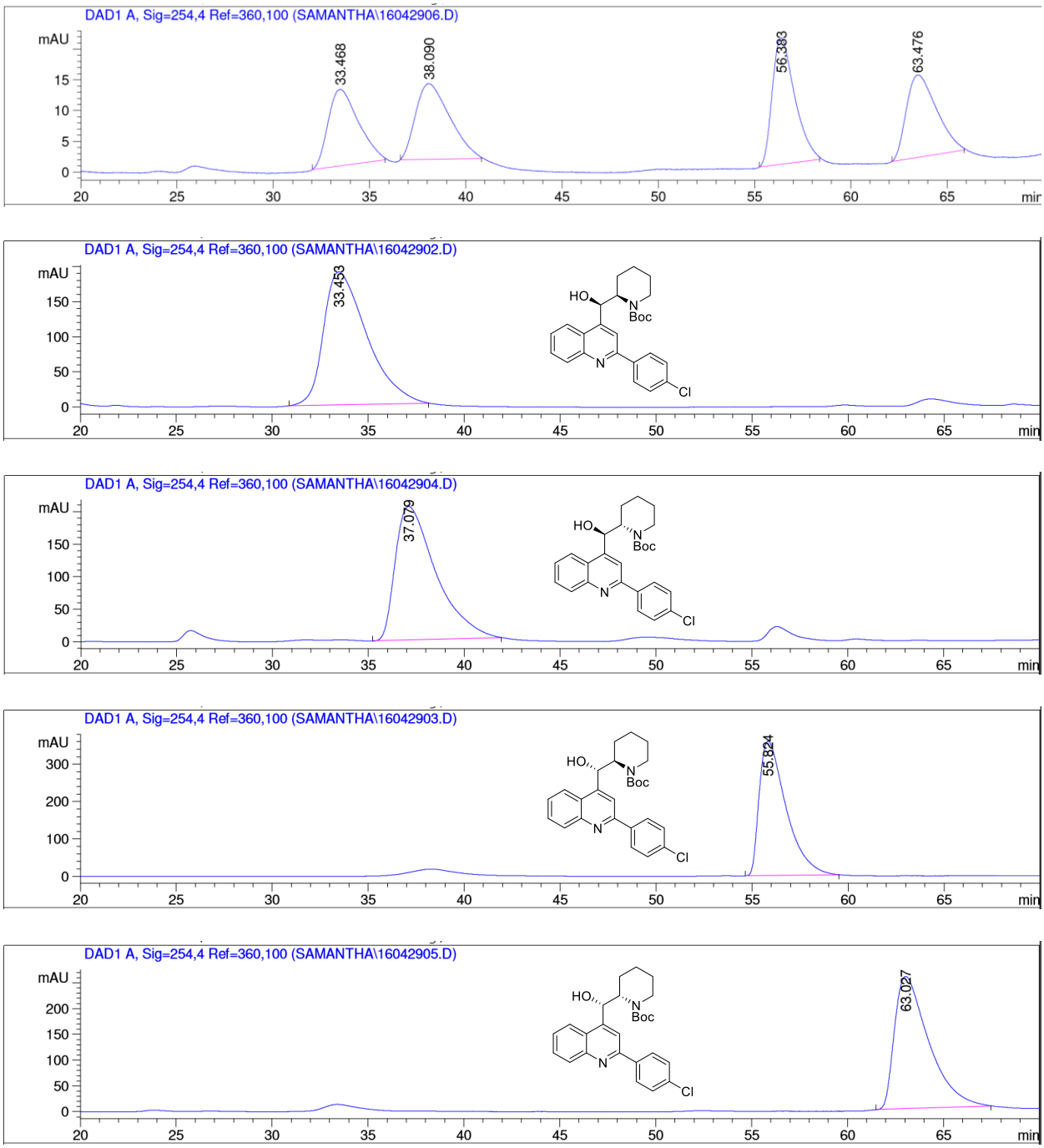

Figure 2-5: HPLC spectra sketches, co-injection experiment with all four stereoisomers is shown in the top spectrum.

Briefly, the assay used to determine the number of viable cells after treatment is a colourimetric method developed and manufactured by Promega. The CellTiter 96® AQ_{ueous} Non-Radioactive Cell Proliferation Assay relies on the ability of viable cells to reduce the chromophore MTS ([3-(4,5-dimethylthiazol-2-yl)-5-(3-carboxymethoxyphenyl)-2-(4-sulfophenyl)-2H-tetrazolium] to formazan (Scheme 2-14). The absorbance of formazan is measured at 490 nm and the quantity of formazan is directly proportional to the number of living cells. Of note, the original publication measured ATP levels to assay cell viability.[2]

Furthermore, it is insufficient in the development of a therapeutic agent against glioblastoma multiforme to test a compound's efficacy solely for cell death induction. Another important parameter is the inhibition of cell migration. GBM is considered one of the most aggressive cancers because the cancerous cells are exceptionally pervasive. As such the collaborators are equipped to conduct two assays that investigate the inhibitory effects of Vacquinol-1 on cell migration. Namely, the "scratch" test and migration assay. Briefly, the scratch test involves growing the cells in a monolayer at the bottom of a 12-well plate. A scratch is made in the center of the well and the cells are washed with buffer to remove any cellular debris. The cells are then imaged using a digital imaging microscope (Axiovert 200M, Zeiss) to observe them as they migrate to fill in the "scratched" area. The percentage of cell migration can be quantified in this manner.

Moreover, directional cell migration can be measured using the Transwell migration assay, which is also known as the Boyden chamber assay. This assay consists of a cylindrical cell culture insert nested inside the well of a cell culture plate. The insert contains a membrane at the bottom with a

defined pore size. The membrane of these inserts are often coated with a component that facilitates adherence and migration. Cells are then seeded in the top of the insert, while serum is placed in the well below. The cells are allowed to migrate and after a certain time point the cells are stained and counted to determine the percentage of cells that were able to traverse past the insert.

2.12 Biological Results

Initial screening of the eight enantioenriched compounds depicted in Figure 2-6 (all compounds were further purified by preparative HPLC), provided some very promising results.

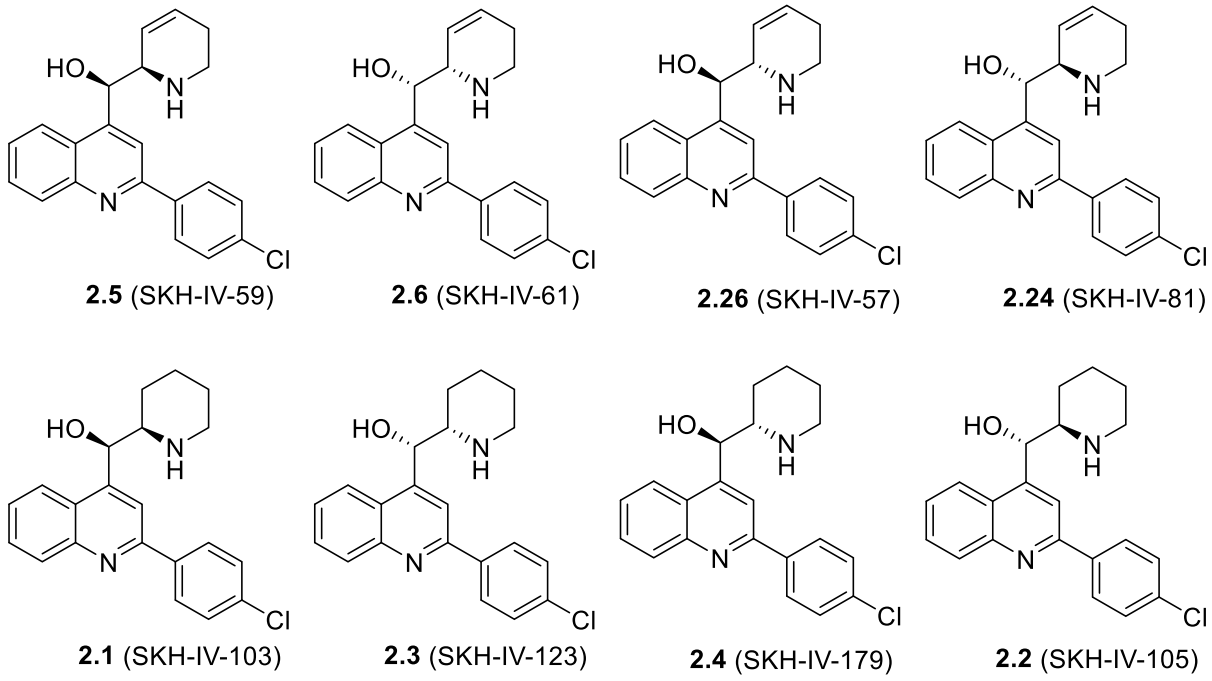

Figure 2-6: Structure of tested compounds and legend for Figure 2-7 and Figure 2-8.

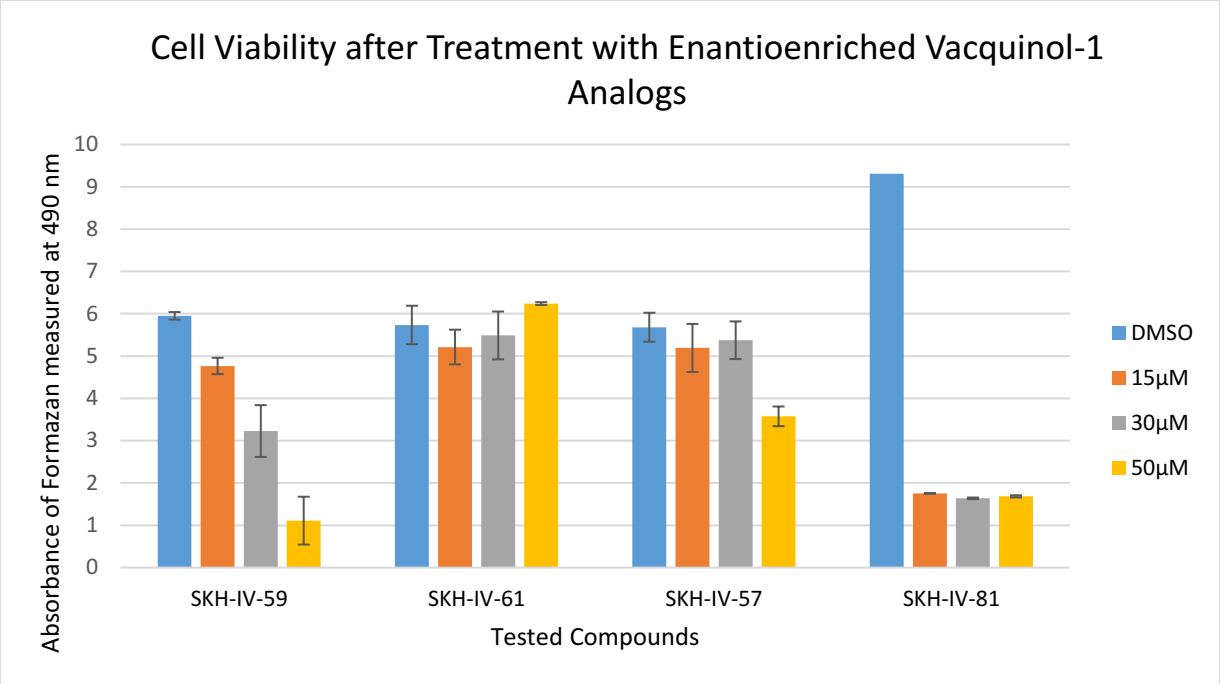

Figure 2-7: MTS cell viability assay to determine the efficacy of enantioenriched stereoisomers of Vacquinol-1 analogs.

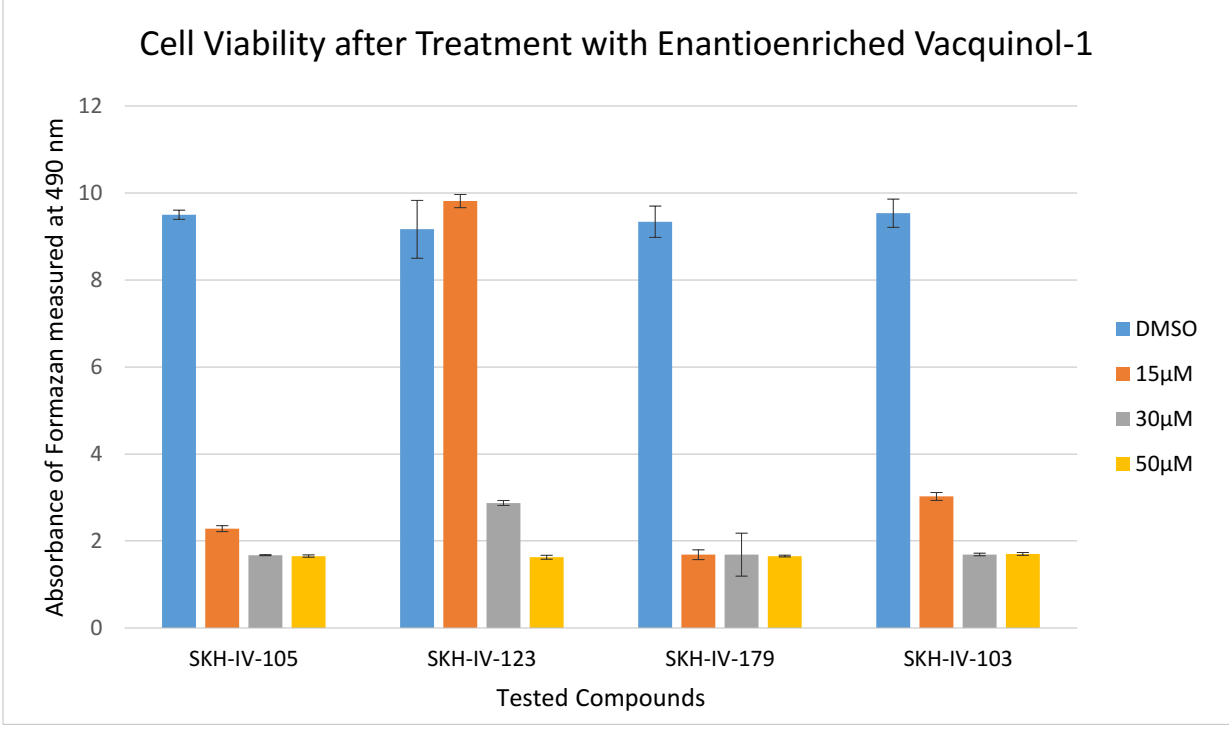

Figure 2-8: MTS cell viability assay to determine the efficacy of enantioenriched stereoisomers of Vacquinol-1.

Employing the CellTiter 96® AQ_{ueous} Non-Radioactive Cell Proliferation Assay described above, the following results (illustrated in Figures 2-6 and 2-7) employing a model cell line for GBM were obtained. The biological experiments were performed by Saket Jain and is gratefully acknowledged.

In summary, it is apparent that the saturation of the endocyclic alkene significantly improves the efficacy of Vacquinol-1; as shown by the contrasting efficacy between SKH-IV-57 and SKH-IV-179. However, **2.24** (SKH-IV-81) appears to be an exception to this general observation. Surprisingly, the enantiomeric pairs SKH-IV-179 and SKH-IV-105 appear to have very similar efficacy. Perhaps what is important for the landscape of the piperidine moiety, in relation to the efficacy of the molecule, is the anti relationship between the hydroxyl and amine functionalities. Currently, investigations into a suitable concentration to assay the efficacy of these compounds to inhibit cancerous cell migration and subsequently appraise these inhibitory effects, as well as, an extensive study to determine the IC_{50} are ongoing. It is also worthy to note that the efficacy of these compounds will be evaluated using a model cell line as well as several patient cell lines in collaboration with Dr. Godbout.

2.13 Synthesis of Vacquinol-1 Analogs

It is important to note the synthetic strategy features key-steps where derivatizations can be introduced for the synthesis of potentially more potent analogues. To illustrate one point of divergence, a small library of compounds was synthesized where the aryl-group of the aldehyde

coupling partner featured different functional groups. From readily available acetophenone derivatives the corresponding aldehydes were synthesized as illustrated in Scheme 2-15.[14]

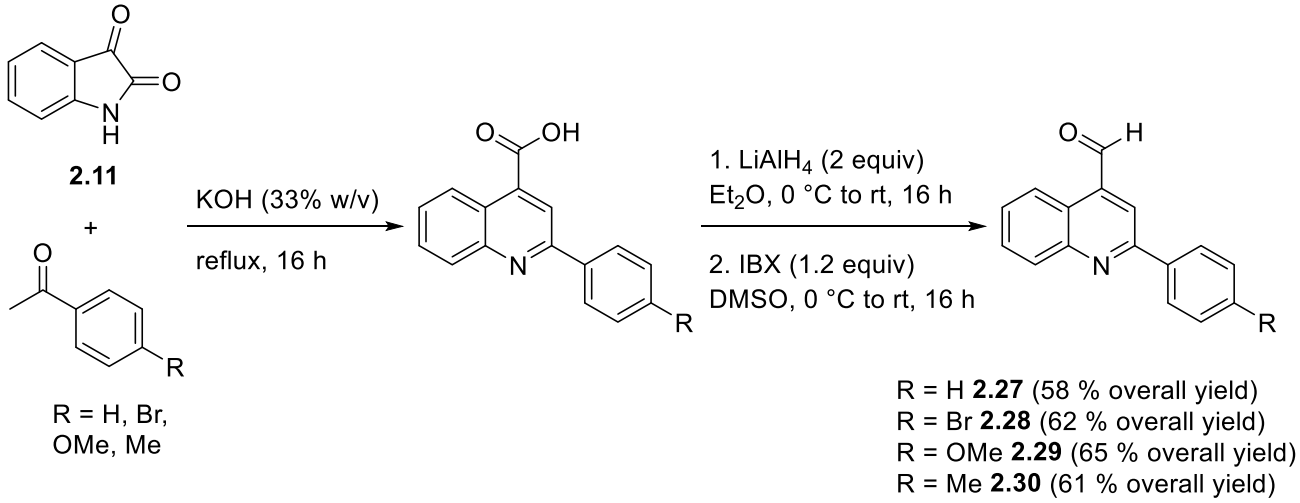

Scheme 2-15: Synthesis of aldehyde partner for the synthesis of Vacquinol-1 analogs.

The prepared aldehydes were then subjected to allylboration with enantioenriched allylic boronate **2.19** and **2.20** and after subsequent hydrogenation of the endocyclic alkene and deprotection the compounds illustrated in Figure 2-9 were synthesized in a highly efficient manner. Additionally, the endocyclic alkene provides a very useful facilely manipulated synthetic functional group. One can imagine using this synthetic handle to access a variety of analogs.

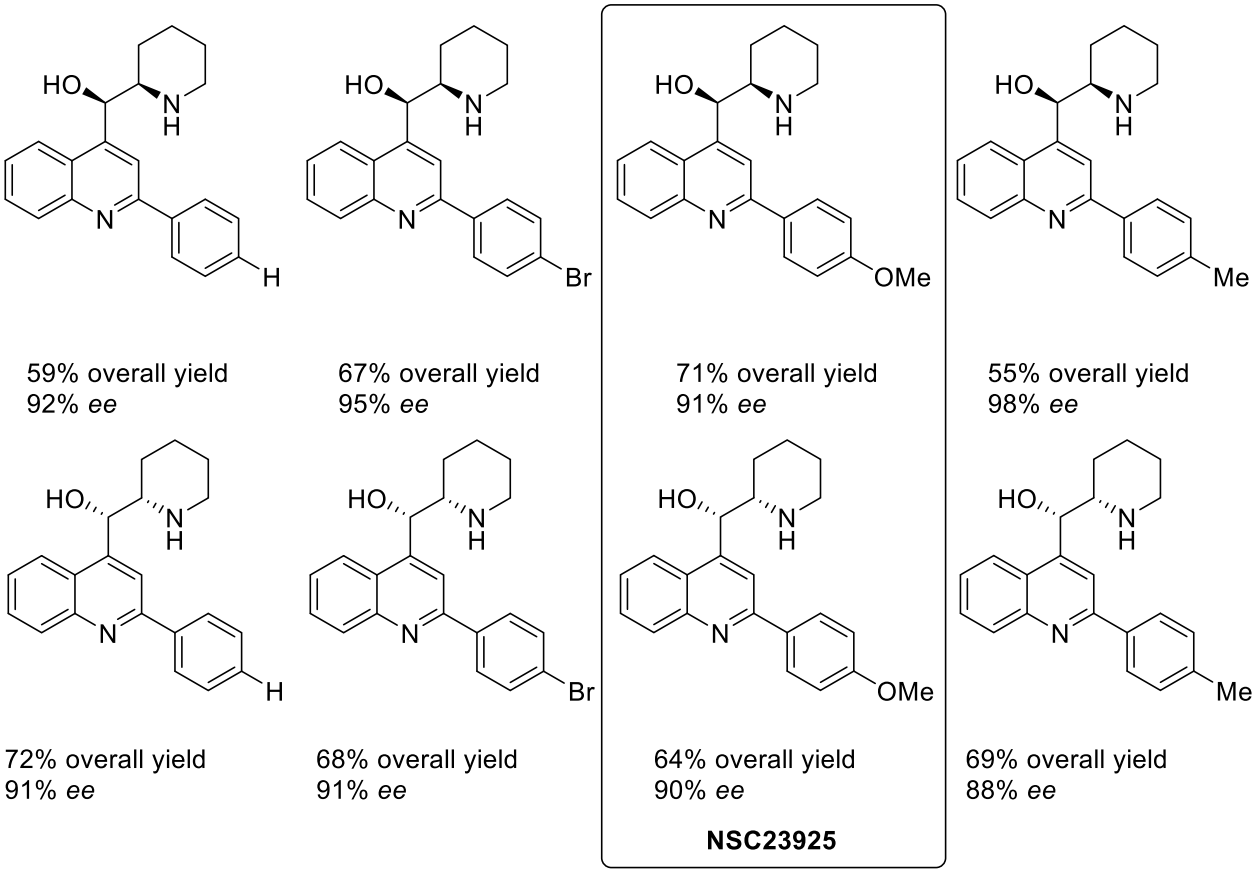

Figure 2-9: Series of Vacquinol-1 analogs.

Of interest, the analog with the *p*-methoxy substituted aryl moiety (NSC23925); recall, Vacquinol-1 features a *p*-chloro substituted aryl moiety, has been previously described in a study that investigated the efficacy of compounds to reverse multidrug resistance (MDR) in cancer therapy.[17] In 2011, Hornicek and co-workers studied the efficacy of a series of compounds to interact with plasma membrane glycoprotein (Pgp) and thereby block drug efflux to reverse the MDR phenotype expressed by cancerous cells. Pgp is a member of the ATP binding cassette superfamily of transporter proteins that act in an energy-dependent manner to actively pump therapeutic agents out of the cell. In their report, Harnicek and co-workers synthesized NSC23925 as a mixture of

stereoisomers; via a synthetic route that is reminiscent of the one used by Ernfors and co-workers, and then painstakingly separated all four stereoisomers. In their account, it was emphasized that the separation of the protecting-group free piperidinyl-amine failed and only after protection with di-*tert*-butyl dicarbonate were they able to separate all four stereoisomers. This observation parallels the results for separating all four stereoisomers of Vacquinol-1 as described in Section 2.10. Moreover, the authors were able to identify one stereoisomer as a potent and selective modulator of Pgp-mediated MDR.

2.14 Synthetic Investigations of Vacquinol-15

With a solid synthetic strategy, efforts towards the synthesis of Vacquinol-15 are described. Of note, the *in vitro* and *in vivo* studies was not conducted with Vacquinol-15 because this compound exhibited significant undesirable side- effects. Even though Vacquinol-15 was determined to have an IC_{50} of 0.39 ± 0.73 μM; in contrast to the measured IC_{50} of Vacquinol-1 of 3.14 ± 1.23 μM, when mixed cell cultures were treated with Vacquinol-15 the assay revealed that Vacquinol-15 caused cell death non-specifically.[2] To elaborate, healthy cells also underwent necrotic-like cell death. In this case, studying the biological effects of each enantioenriched stereoisomer is very important.

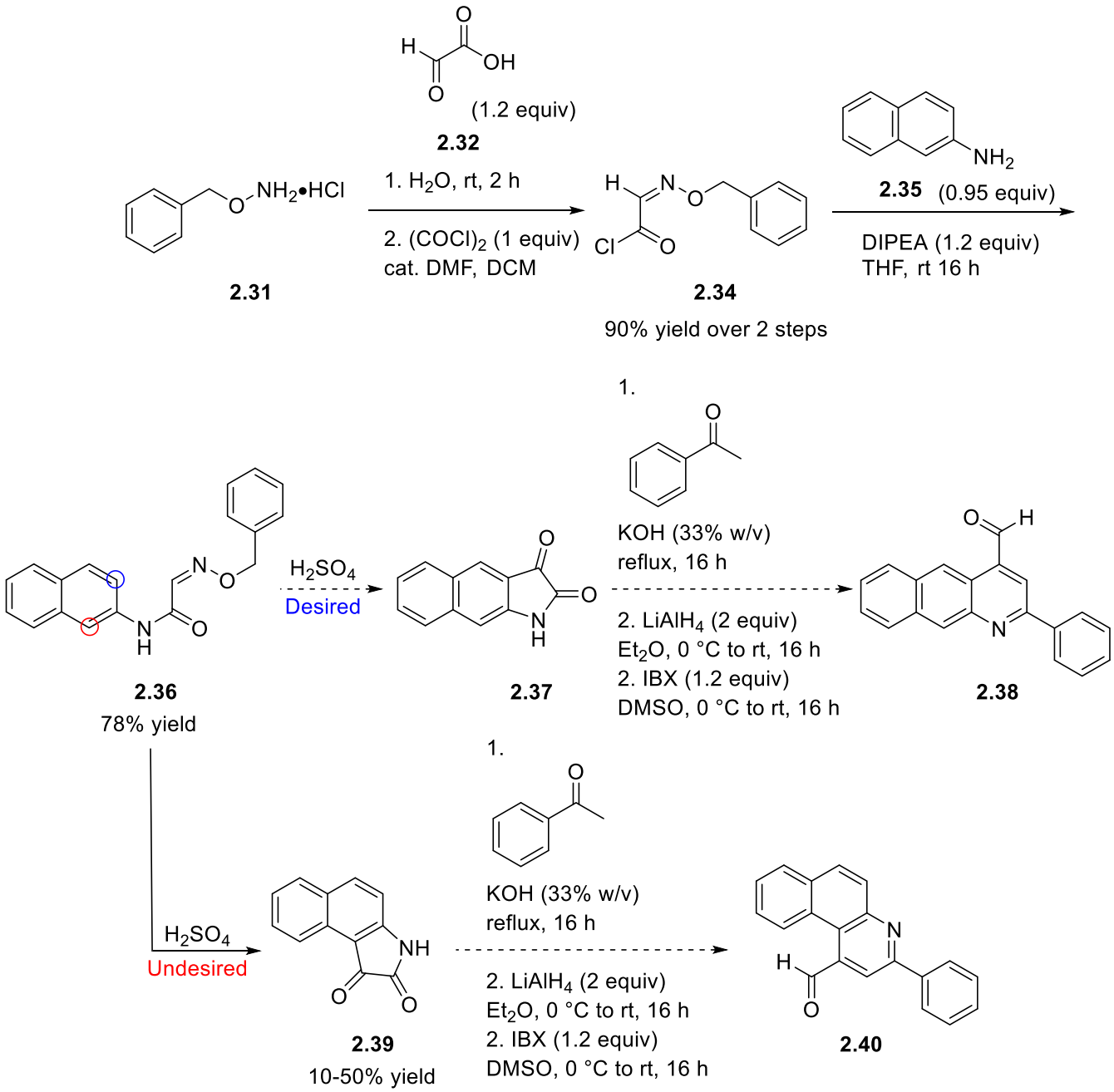

Scheme 2-16: Synthetic route towards aldehyde coupling partner **2.38**.

The first challenge encountered during the efforts towards synthesizing all four stereoisomers of Vacquinol-15 began with the synthesis of the aldehyde coupling partner. Adapted from the reported synthesis[2] it was determined that the desired cyclized product **2.37**, a linear isatin, was

not obtained. Digging deeper into the literature, the cited synthetic route used chemistry developed in 1951 by Staehelin.[18] Regrettably, it was not until after months of effort to reproduce the work from 1951 that several reports that refuted the report by Staehelin was unearthed. A German group in 1956,[19] a Russian group in 1987,[20] and more recently a Ukrainian group in 2006,[21] showed that the synthetic method from 1951 provides the bent isatin **2.39** (Scheme 2-16). Using NMR, it was confirmed that the isatin product formed is indeed **2.39**. The coupling constants of the protons are inconsistent with the proposed linear isatin structure. Taking this into consideration, the revised structure of Vacquinol-15 is proposed as illustrated in Figure 2-10.

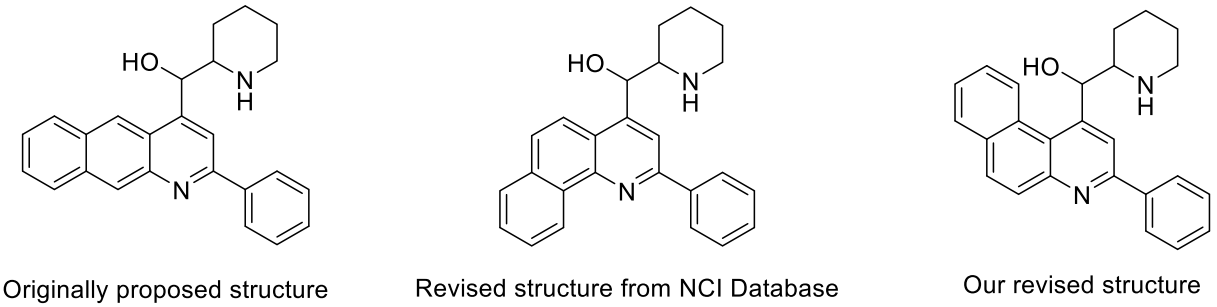

Figure 2-10: Possible structures of Vacquinol-15.

Subsequently, a sample of Vacquinol-15 from the National Cancer Institute Division of Cancer Treatment & Diagnosis, Developmental Therapeutics Program (DTP) was requested. The DTP maintains a repository of synthetic compounds and pure natural products that are available for non-clinical research. When the synthetic investigation towards Vacquinol-15 began, the DTP database was consulted and the originally proposed structure was depicted as shown in Figure 2-10. However, during a more recent inquiry the DTP depository updated the structure of Vacquinol-15. No explanation or statements from the original authors was found. Current efforts to obtain a

crystal structure from the sample received have thus far, unfortunately, been futile. As such, this endeavor has not been abandoned since the correct structural assignment is crucial for future enterprises.

It should be noted, that the revised structure of Vacquinol-15 reveals the fact that 1-napthylamine **2.41** is the desired building towards the synthesis of the aldehyde coupling partner **2.44** (Scheme 2-17). Contrary to 2-napthylamine **2.35** from the original synthetic plan (Scheme 2-16). Additionally, using 1-napthylamine **2.41**, eliminates the problem of regioselectivity for the ring closing and isatin forming step (Scheme 2-17).

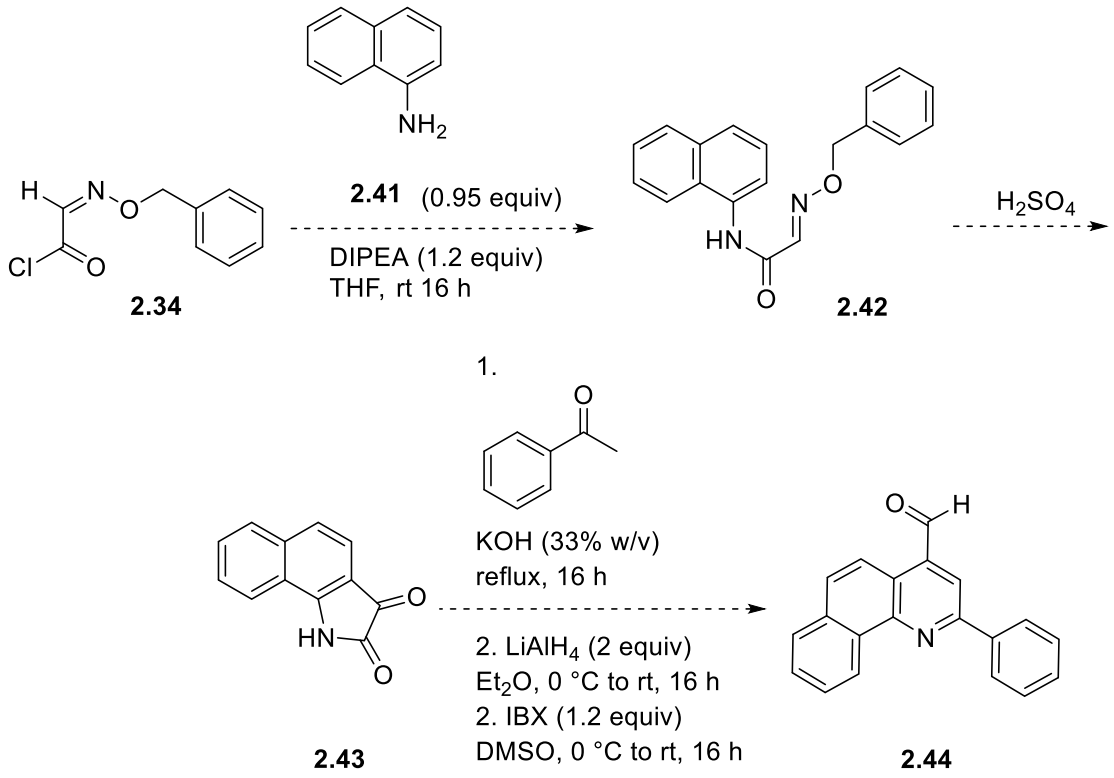

Scheme 2-17: Synthetic plan to access the aldehyde partner **2.44** for the synthesis of Vacquinol-15 (revised structure).

2.15 Summary

In summary, all four enantioenriched stereoisomers of Vacquinol-1 have been synthesized along with a set of dehydro-analogs (as illustrated in Figure 2-6). Biological testing of these compounds to determine the efficacy to induce cell death and inhibit cell migration are currently under investigation. Additionally, a set of eight analogs of Vacquinol-1 was readily synthesized to demonstrate the versatility of the convergent synthetic strategy. Moreover, this research deserves further consideration; specifically, utilizing the endocyclic alkene as a synthetic handle to further functionalize the piperidine moiety with the motivation to find a potential therapeutic agent for glioblastoma multiforme. Lastly, with the revised structure of Vacquinol-15 the issue of regioselectivity for the synthesis of the aldehyde allylboration partner is no longer of concern and moving forward, accessing all four stereoisomers of Vacquinol-15 can be readily achieved.

2.16 Experimental Procedure

2.16.1 General Information

Unless otherwise indicated, all reactions were performed under a nitrogen atmosphere using glassware that was washed thoroughly with water and acetone and flame-dried *in vacuo* prior to use. Toluene, tetrahydrofuran and dichloromethane were used directly from a mBraun Solvent Purification System. Diethyl ether was distilled over sodium/benzophenone ketyl. *N,N*-Dimethylaniline was purchased from Sigma Aldrich and distilled over sodium hydroxide prior to use. 1-Boc-piperidone (reagent grade, 98%) and perfluorobutanesulfonyl fluoride (reagent grade, 96%); Adam's Catalyst (regent grade, >99%) palladium (II) acetate (reagent grade, >99%), (+) and (-)- TANIAPHOS (reagent grade, >97%), were respectively purchased from Combi-Blocks Inc. and Strem Chemical Inc.; and used without further purification. Pinacolborane (reagent grade, >97%) was purchased from Oakwood Chemicals and was purified by distillation. Flash chromatography was performed on ultra pure silica gel 230-400 mesh. Nuclear magnetic resonance (NMR) spectra were recorded on Agilent/Varian DD2-400, INOVA-400, INOVA-500 or VNMRS-500 MHz instruments. ^{1}H NMR data are presented as follows: chemical shift in ppm downfield from tetramethylsilane (multiplicity, coupling constant, integration). High resolution mass spectra were recorded by the University of Alberta Mass Spectrometry Services Laboratory using either electron impact (EI) or electrospray (ESI) ionization techniques. Infrared spectra (performed on a Nicolet Magna-IR 750 instrument equipped with a Nic-Plan microscope) and optical rotations (performed using a Perkin-Elmer 241 polarimeter) were recorded by the University of Alberta Analytical and Instrumentation Laboratory. The enantiomeric excess for chiral compounds were determined using a HPLC Agilent instrument with a Chiralcel-OD column. Specific conditions indicated in individual compound procedures.

2.16.2 Procedure and Spectral Data for the Alkenyl Nonaflate

***Tert*-Butyl-4-(nonafluorobutylsulfonyloxy)-5,6-dihydropyridine-1(2H)-carboxylate (2.8):**

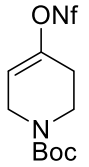

1-Boc-4-piperidone (2.0 g, 10 mmol, 1.0 equiv) was dissolved in 50 ml THF in a pre-dried 100 mL round bottom flask under a nitrogen atmosphere. The solution was cooled to 0 °C, then DBU (1.8 mL, 12 mmol, 1.2 equiv) was added dropwise, followed by the dropwise addition of perfluorobutanesulfonyl fluoride (2.2 mL, 12 mmol, 1.2 equiv) at 0 °C. The reaction was allowed to slowly warm to rt with stirring overnight. The reaction was quenched with a saturated aqueous solution of sodium bicarbonate and the aqueous layer was extracted three times with dichloromethane. The combined organic layer was washed with water, brine, dried (Na_2SO_4), filtered, then the solvent was removed under reduced pressure. The residue was purified by flash column chromatography (20% diethyl ether/hexanes) to afford **2.8** as a light yellow oil in 87% yield (4.2 g). Spectral data correspond to that reported.[22] ^{1}H NMR (400 MHz, Chloroform-*d*) δ 5.78 (app s, 1 H), 4.07 – 4.02 (m, 2 H), 3.63 (app t, J = 5.6 Hz, 2H), 2.45 (app s, 2 H), 1.48 (s, 9 H).

2.16.3 General Procedure for the Synthesis of Optically Enriched α-hydroxyalkyl dehydropiperidinyl Vacquinol-1 and Vacquinol-1 Analog Intermediates

A flame dried round bottom flask was charged with palladium (II) acetate (1.4 mg, 6.2 µmol, 0.03 equiv) and TANIAPHOS (5.8 mg, 8.3 µmol, 0.04 equiv). The flask was evacuated and backfilled with argon three times. The catalyst and ligand were dissolved in 2 ml of freshly distilled ether and allowed to stir at room temperature for one hour. *N,N*-dimethylaniline (30 µl, 0.23 mmol, 1.1 equiv), pinacolborane (35 µl, 0.23 mmol, 1.1 equiv) and the alkenyl nonaflate **2.8** (100 mg, 0.20 mmol, 1 equiv) were added respectively. The resulting reaction mixture was allowed to stir for 16 hours at room temperature. The solvent was removed by reduced pressure and the resulting residue was quickly filtered through a silica plug (100% ether). Once again the solvent was removed by reduced pressure and the crude allylboronate was dissolved in 2 mL toluene. Aldehyde (0.23 mmol, 1.1 equiv) was added and the reaction was heated at 130°C for 2 hours in a Biotage™ microwave oven. The reaction mixture was cooled to rt and the solvent was removed by reduced pressure and purified as described below.

***tert*-Butyl 2-(4-chlorophenyl)-α-(2*R*)-2-5,6-dihydropyridinyl-, (α*R*)- 4-quinolinemethanol-1(2H)-carboxylate (2.5):**

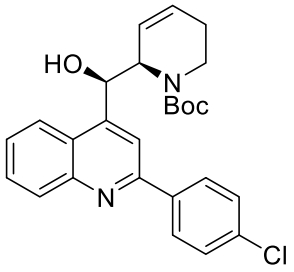

Flash chromatography (gradient 10% to 25% ethyl acetate/pentanes) afforded a yellow solid (84 mg, 90% yield). ^{1}H NMR (400 MHz, $CDCl_3$) rotamers are present: δ 8.25 – 8.02 (m, 5 H), 7.73 (app t, *J* = 7.2 Hz, 1 H), 7.58 – 7.46 (m, 3 H), 5.81 (app. s, 1 H), 5.59 (br m, 1 H), 5.11 – 4.82 (br m, 1 H), 4.38 (br m, 1 H), 3.10 – 2.62 (br m, 2 H), 2.33 – 1.88 (br m, 2 H), 1.24 (s, 9 H). ^{13}C NMR (126 MHz, $CDCl_3$) rotamers are present: δ 194.0, 168.9, 141.4, 135.6, 132.7, 131.3, 129.6, 129.1, 1289.0, 127.9, 126.4, 117.3, 94.4, 83.4, 83.0, 75.2, 28.4, 28.1, 27.9, 24.8, 24.7, 24.6, 24.1. IR ($CHCl_3$ cast film, cm^{-1}): 3411, 2976, 1694, 1427, 1163, 1013, 802. HRMS (ESI) for $(M+H)^+$ $C_{26}H_{28}ClN_2O_3$: calcd. 451.1783; found 451.1780; $[\alpha]_D^{20}$: + 63.4° (c= 1.13, $CHCl_3$). Chiralcel OD, 20 °C, 5 % *iso*-propanol/hexanes, 0.5 mL/min., UV detection at 210 nm, retention times: minor enantiomer 32.8 min.; major enantiomer 20.9 min.; 94% ee.

***tert*-Butyl 2-(4-chlorophenyl)-α-(2*S*)-2-5,6-dihydropyridinyl-, (α*S*)- 4-quinolinemethanol-1(2H)-carboxylate (2.6):**

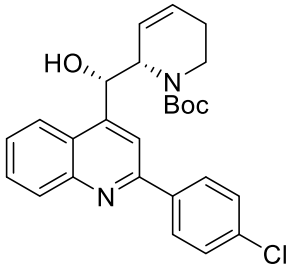

Flash chromatography (gradient 10% to 25% ethyl acetate/pentanes) afforded a yellow solid (83 mg, 89% yield). ^{1}H NMR (400 MHz, $CDCl_3$) rotamers are present: δ 8.22 – 8.05 (m, 5 H), 7.72 (app. t, *J* = 6.8 Hz, 1 H), 7.56 – 7.45 (m, 3 H), 6.11 – 5.75 (br m, 1 H), 5.60 (app. d, *J* = 8.8 Hz, 1 H), 4.86 (br m, 1 H), 4.46 (br m, 1 H), 3.22 – 2.65 (br m, 2 H), 2.33 – 1.87 (br m, 2 H), 1.24 (s, 9 H). ^{13}C NMR (126 MHz, $CDCl_3$) rotamers are present: δ 194.0, 168.9, 141.4, 135.6, 132.7, 131.3,

129.6, 129.1, 1289.0, 127.9, 126.4, 117.3, 94.4, 83.4, 83.0, 75.2, 28.4, 28.1, 27.9, 24.8, 24.7, 24.6, 24.1. IR ($CHCl_3$ cast film, cm^{-1}): 3411, 2931, 1694, 1391, 1271, 1013, 852. HRMS (ESI) for $(M+H)^+$ $C_{26}H_{28}ClN_2O_3$: calcd. 451.1783; found 451.1786; $[\alpha]_D^{20}$:− 63.4° (c= 1.36, $CHCl_3$). Chiralcel OD, 20 °C, 5 % *iso*-propanol/hexanes, 0.5 mL/min., UV detection at 210 nm, retention times: minor enantiomer 20.9 min.; major enantiomer 32.8 min.; 96% ee.

***tert*-Butyl 2-(-phenyl)-α-(2*R*)-2-5,6-dihydropyridinyl-, (α*R*)- 4-quinolinemethanol- 1(2H)-carboxylate:**

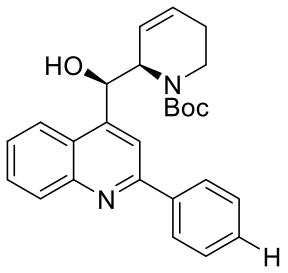

Flash chromatography (gradient 10% to 25% ethyl acetate/pentanes) afforded a yellow solid (53 mg, 61% yield). ^1H NMR (400 MHz, $CDCl_3$) rotamers are present: δ 8.23 – 7.91 (m, 4 H), 7.68 (m, 1 H), 7.51 – 7.38 (m, 4 H), 6.03 – 5.71 (m, 1 H), 5.63 – 5.38 (m, 1 H), 5.18 (m, 0.5 H), 4.98 – 4.73 (m, 1 H), 4.29 – 4.14 (m, 0.5 H), 4.05 – 3.91 (m, 0.5 H), 3.16 – 2.97 (m, 0.6 H), 2.88 – 2.72 (m, 0.5 H), 2.26 – 2.05 (m, 1 H), 1.99 – 1.83 (m, 1 H), 1.20 (s, 9 H). ^{13}C NMR (126 MHz, $CDCl_3$) rotamers are present: δ 157.3, 154.6, 148.5, 130.7, 130.6, 129.3, 129.3, 128.8, 127.7, 127.6, 126.1, 125.4, 124.6, 124.3, 123.4, 117.5, 83.3, 83.1, 75.1, 28.5, 28.1, 27.9, 24.9, 24.7, 24.6, 24.6, 24.4. IR ($CHCl_3$ cast film, cm^{-1}): 3423, 2978, 1677, 1475, 1367, 1167, 760. HRMS (ESI) for $(M+H)^+$ $C_{26}H_{29}N_2O_3$: calcd. 417.2173; found 417.2178; $[\alpha]_D^{20}$: +6.5° (c= 1.23, $CHCl_3$). Chiralcel OD,

20 °C, 5 % *iso*-propanol/hexanes, 0.5 mL/min., UV detection at 254 nm, retention times: minor enantiomer 46.8 min.; major enantiomer 21.6 min.; 92% ee.

***tert*-Butyl 2-(4-bromophenyl)-α-(2*R*)-2-5,6-dihydropyridinyl-, (α*R*)- 4-quinolinemethanol-1(2H)-carboxylate:**

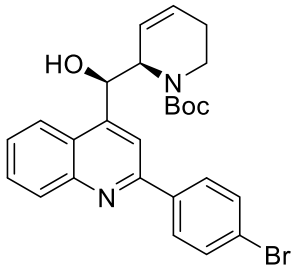

Flash chromatography (gradient 10% to 25% ethyl acetate/pentanes) afforded a yellow solid (72 mg, 70% yield). ^{1}H NMR (400 MHz, $CDCl_3$) rotamers are present: δ 8.16 (m, 1 H), 8.07 – 7.86 (m, 4 H), 7.69 (m, 1 H), 7.59 (m, 2 H), 7.47 (m, 1 H), 6.14 – 5.70 (m, 1 H), 5.65 – 5.40 (m, 1 H), 5.21 – 4.69 (m, 1 H), 4.23 – 4.19 (m, 0.5 H), 4.05 – 3.90 (m, 0.5 H), 3.18 – 2.73 (m, 1 H), 2.15 (m, 1 H), 1.99 – 1.83 (m, 1 H), 1.20 (s, 9 H). ^{13}C NMR (126 MHz, $CDCl_3$) rotamers are present: δ 148.5, 138.6, 138.4, 131.9, 130.7, 130.6, 130.5, 129.5, 129.3, 129.2, 128.0, 126.4, 124.0, 117.0, 83.3, 83.1, 75.1, 38.5, 29.7, 28.4, 28.5, 28.3, 28.1, 27.9, 25.0, 24.7, 24.6, 24.5, 24.4. IR ($CHCl_3$ cast film, cm^{-1}): 3424, 2978, 1677, 1598, 1421, 1167, 801. HRMS (ESI) for $(M+H)^+$ $C_{26}H_{28}BrN_2O_3$: calcd. 495.1278; found 495.1275 $[\alpha]_D^{20}$: +67.2° (c= 1.24, $CHCl_3$). Chiralcel OD, 20 °C, 5 % *iso*-propanol/hexanes, 0.5 mL/min., UV detection at 254 nm, retention times: minor enantiomer 31.3 min.; major enantiomer 20.4 min.; 95% ee.

***tert*-Butyl 2-(4-methylphenyl)-α-(2*R*)-2-5,6-dihydropyridinyl-, (α*R*)- 4-quinolinemethanol-1(2H)-carboxylate:**

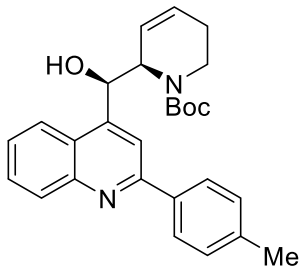

Flash chromatography (gradient 10% to 25% ethyl acetate/pentanes) afforded a yellow solid (52 mg, 58% yield). ^{1}H NMR (400 MHz, $CDCl_3$) rotamers are present: δ 8.21 – 8.13 (m, 1 H), 8.09 – 7.79 (m, 4 H), 7.67 (m, 1 H), 7.44 (m, 1 H), 7.27 – 7.25 (m, 2 H), 6.03 – 5.68 (m, 1 H), 5.64 – 5.36 (m, 1 H), 5.15 (m, 0.5 H), 5.00 – 4.70 (m, 1 H), 4.58 – 4.55 (m, 0.4 H), 4.20 (m, 0.4 H), 4.06 – 3.95 (m, 0.5 H), 3.72 – 3.57 (m, 0.3 H), 3.07 – 2.92 (m, 0.4 H), 2.92 – 2.76 (m, 0.5 H), 2.40 (m, 3 H), 2.14 (m, 1 H), 1.98 – 1.84 (m, 1 H), 1.24 (s, 9 H). ^{13}C NMR (126 MHz, $CDCl_3$) rotamers are present: δ 148.5, 147.5, 139.4, 136.9, 136.9, 136.8, 130.6, 129.5, 129.2, 127.8, 127.6, 127.5, 125.9, 125.7, 125.0, 124.7, 123.4, 117.4, 83.3, 83.1, 75.1, 72.7, 58.3, 57.1, 38.5, 28.5, 28.1, 28.0, 24.9, 24.7, 24.6, 24.6, 24.4, 24.1, 21.4. IR ($CHCl_3$ cast film, cm^{-1}): 3420, 2978, 1676, 1600, 1422, 1168, 803. HRMS (ESI) for $(M+H)^+$ $C_{27}H_{31}N_2O_3$: calcd. 431.2329; found 431.2332. $[\alpha]_D^{20}$: +56.7° (c= 1.66, $CHCl_3$). Chiralcel OD, 20 °C, 5 % *iso*-propanol/hexanes, 0.5 mL/min., UV detection at 254 nm, retention times: minor enantiomer 39.6 min.; major enantiomer 19.8 min.; 98% ee.

***tert*-Butyl 2-(4-methoxyphenyl)-α-(2*R*)-2-5,6-dihydropyridinyl-, (α*R*)- 4-quinolinemethanol-1(2H)-carboxylate:**

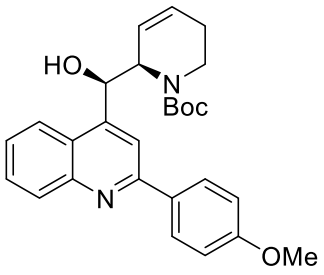

Flash chromatography (gradient 10% to 25% ethyl acetate/pentanes) afforded a yellow solid (70 mg, 75% yield). ^{1}H NMR (400 MHz, $CDCl_3$) rotamers are present: δ 8.18 – 7.88 (m, 5 H), 7.65 (m, 1 H), 7.42 (m, 1 H), 6.99 (m, 2 H), 6.03 – 5.69 (m, 1 H), 5.62 – 5.34 (m, 1 H), 5.24 – 4.98 (m, 0.3 H), 4.97 – 4.69 (m, 0.7 H), 4.20 (m, 0.4 H), 4.04 – 3.90 (m, 0.3 H), 3.85 (s, 3H), 3.15 – 2.93 (m, 0.4 H), 2.89 – 2.71 (m, 0.3 H), 2.26 – 2.03 (m, 1 H), 1.98 – 1.80 (m, 1 H), 1.20 (s, 9 H). ^{13}C NMR (126 MHz, $CDCl_3$) rotamers are present: δ 160.8, 148.5, 132.3, 132.3, 132.2, 130.4, 130.3, 129.1, 129.0, 127.8, 125.8, 117.0, 114.2, 83.3, 83.1, 75.0, 72.6, 72.5, 55.4, 29.7, 28.5, 28.1, 28.0, 24.9, 24.7, 24.6, 24.6, 24.4. IR ($CHCl_3$ cast film, cm^{-1}): 3427, 2977, 1684, 1601, 1424, 1174, 763. HRMS (ESI) for $(M+H)^+$ $C_{27}H_{31}N_2O_4$: calcd. 447.2278; found 447.2282. $[\alpha]_D^{20}$: +59.8° (c= 1.44, $CHCl_3$). Chiralcel OD, 20 °C, 5 % *iso*-propanol/hexanes, 0.5 mL/min., UV detection at 254 nm, retention times: minor enantiomer 33.4 min.; major enantiomer 18.8 min.; 91% ee.

***tert*-Butyl 2-(-phenyl)-α-(2*S*)-2-5,6-dihydropyridinyl-, (α*S*)- 4-quinolinemethanol- 1(2H)-carboxylate:**

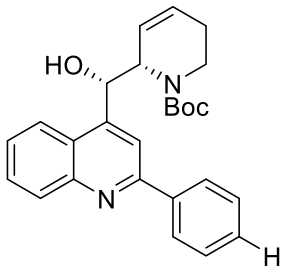

Flash chromatography (gradient 10% to 25% ethyl acetate/pentanes) afforded a yellow solid (65 mg, 75% yield). ^{1}H NMR (400 MHz, $CDCl_3$) rotamers are present: δ 8.24 – 7.92 (m, 4 H), 7.70 (m, 1 H), 7.51 – 7.38 (m, 4 H), 6.03 – 5.71 (m, 1 H), 5.63 – 5.38 (m, 1 H), 5.19 (m, 0.5 H), 4.98 – 4.73 (m, 1 H), 4.29 – 4.14 (m, 0.5 H), 4.04 – 3.91 (m, 0.5 H), 3.16 – 2.96 (m, 0.6 H), 2.88 – 2.72 (m, 0.5 H), 2.26 – 2.05 (m, 1 H), 1.99 – 1.83 (m, 1 H), 1.18 (s, 9 H). ^{13}C NMR (126 MHz, $CDCl_3$) rotamers are present: δ 157.3, 154.6, 148.5, 130.7, 130.6, 129.3, 129.3, 128.8, 127.7, 127.6, 126.1, 125.4, 124.6, 124.3, 123.4, 117.5, 83.3, 83.1, 75.1, 28.5, 28.1, 27.9, 24.9, 24.7, 24.6, 24.6, 24.4. IR ($CHCl_3$ cast film, cm^{-1}): 3423, 2978, 1676, 1475, 1367, 1167, 762. HRMS (ESI) for $(M+H)^+$ $C_{26}H_{29}N_2O_3$: calcd. 417.2173; found 417.2177; $[\alpha]_D^{20}$:−62.5° (c= 1.26, $CHCl_3$). Chiralcel OD, 20 °C, 5 % *iso*-propanol/hexanes, 0.5 mL/min., UV detection at 254 nm, retention times: minor enantiomer 21.2 min.; major enantiomer 44.4 min.; 91% ee.

***tert*-Butyl 2-(4-bromophenyl)-α-(2*S*)-2-5,6-dihydropyridinyl-, (α*S*)- 4-quinolinemethanol-1(2H)-carboxylate:**

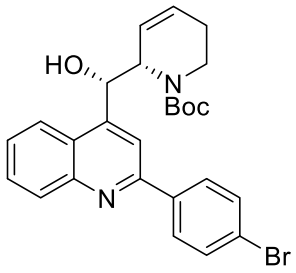

Flash chromatography (gradient 10% to 25% ethyl acetate/pentanes) afforded a yellow solid (75 mg, 71% yield). ^{1}H NMR (400 MHz, $CDCl_3$) rotamers are present: δ 8.18 (m, 1 H), 8.07 – 7.86 (m, 4 H), 7.69 (m, 1 H), 7.59 (m, 2 H), 7.46 (m, 1 H), 6.14 – 5.70 (m, 1 H), 5.65 – 5.40 (m, 1 H), 5.20 – 4.67 (m, 1 H), 4.23 – 4.19 (m, 0.5 H), 4.03 – 3.88 (m, 0.5 H), 3.18 – 2.73 (m, 1 H), 2.15 (m, 1 H), 1.99 – 1.83 (m, 1 H), 1.20 (s, 9 H). ^{13}C NMR (126 MHz, $CDCl_3$) rotamers are present: δ 148.5, 138.6, 138.4, 131.9, 130.7, 130.6, 130.5, 129.5, 129.3, 129.2, 128.0, 126.4, 124.0, 116.9, 83.3, 83.1, 75.1, 38.5, 29.7, 28.5, 28.5, 28.3, 28.1, 27.9, 24.9, 24.7, 24.6, 24.5, 24.4. IR ($CHCl_3$ cast film, cm^{-1}): 3424, 2978, 1677, 1598, 1421, 1167, 801. HRMS (ESI) for $(M+H)^+$ $C_{26}H_{28}BrN_2O_3$: calcd. 495.1278; found 495.1276. $[\alpha]_D^{20}$:−64.2° (c= 1.21, $CHCl_3$). Chiralcel OD, 20 °C, 5 % *iso*-propanol/hexanes, 0.5 mL/min., UV detection at 254 nm, retention times: minor enantiomer 22.6 min.; major enantiomer 33.2 min.; 90% ee.

***tert*-Butyl 2-(4-methylphenyl)-α-(2*S*)-2-5,6-dihydropyridinyl-, (α*S*)- 4-quinolinemethanol-1(2H)-carboxylate:**

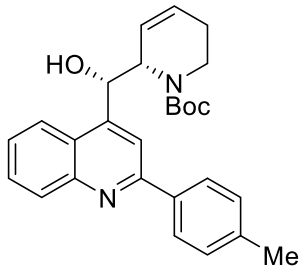

Flash chromatography (gradient 10% to 25% ethyl acetate/pentanes) afforded a yellow solid (64 mg, 71% yield). ^{1}H NMR (400 MHz, $CDCl_3$) rotamers are present: δ 8.18 – 8.10 (m, 1 H), 8.09 – 7.79 (m, 4 H), 7.67 (m, 1 H), 7.44 (m, 1 H), 7.27 – 7.25 (m, 2 H), 6.03 – 5.68 (m, 1 H), 5.64 – 5.36 (m, 1 H), 5.15 (m, 0.5 H), 5.00 – 4.70 (m, 1 H), 4.58 – 4.55 (m, 0.4 H), 4.18 (m, 0.4 H), 4.06 – 3.95 (m, 0.5 H), 3.72 – 3.55 (m, 0.3 H), 3.07 – 2.92 (m, 0.4 H), 2.92 – 2.76 (m, 0.5 H), 2.40 (m, 3 H), 2.14 (m, 1 H), 1.98 – 1.84 (m, 1 H), 1.22 (s, 9 H). ^{13}C NMR (126 MHz, $CDCl_3$) rotamers are present: δ 148.5, 147.5, 139.4, 136.9, 136.9, 136.8, 130.6, 129.5, 129.2, 127.8, 127.6, 127.5, 125.9, 125.7, 125.0, 124.7, 123.4, 117.4, 83.3, 83.1, 75.1, 72.7, 58.3, 57.1, 38.5, 28.5, 28.1, 28.0, 24.9, 24.7, 24.6, 24.6, 24.4, 24.1, 21.4. IR ($CHCl_3$ cast film, cm^{-1}): 3422, 2978, 1676, 1599, 1422, 1168, 801. HRMS (ESI) for $(M+H)^+$ $C_{27}H_{31}N_2O_3$: calcd. 431.2329; found 431.2330. $[\alpha]_D^{20}$:−54.7° (c= 1.65, $CHCl_3$). Chiralcel OD, 20 °C, 5 % *iso*-propanol/hexanes, 0.5 mL/min., UV detection at 254 nm, retention times: minor enantiomer 19.8 min.; major enantiomer 39.6 min.; 91% ee.

***tert*-Butyl 2-(4-methoxyphenyl)-α-(2*S*)-2-5,6-dihydropyridinyl-, (α*S*)- 4-quinolinemethanol-1(2H)-carboxylate:**

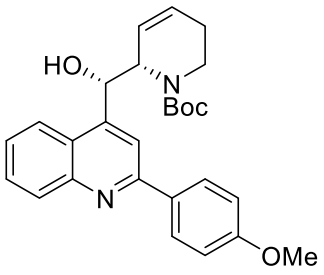

Flash chromatography (gradient 10% to 25% ethyl acetate/pentanes) afforded a yellow solid (62 mg, 67% yield). ^{1}H NMR (400 MHz, $CDCl_3$) rotamers are present: δ 8.18 – 7.88 (m, 5 H), 7.65 (m, 1 H), 7.40 (m, 1 H), 6.99 (m, 2 H), 6.03 – 5.70 (m, 1 H), 5.62 – 5.34 (m, 1 H), 5.24 – 4.98 (m, 0.3 H), 4.97 – 4.69 (m, 0.7 H), 4.20 (m, 0.4 H), 4.04 – 3.90 (m, 0.3 H), 3.85 (s, 3H), 3.15 – 2.93 (m, 0.4 H), 2.89 – 2.71 (m, 0.3 H), 2.26 – 2.01 (m, 1 H), 1.98 – 1.80 (m, 1 H), 1.20 (s, 9 H). ^{13}C NMR (126 MHz, $CDCl_3$) rotamers are present: δ 160.8, 148.5, 132.3, 132.3, 132.2, 130.4, 130.3, 129.0, 128.9, 127.8, 125.8, 117.0, 114.2, 83.3, 83.1, 75.0, 72.6, 72.5, 55.4, 29.7, 28.5, 28.1, 28.0, 24.9, 24.7, 24.6, 24.6, 24.4. IR ($CHCl_3$ cast film, cm^{-1}): 3427, 2977, 1684, 1601, 1424, 1174, 763. HRMS (ESI) for $(M+H)^+$ $C_{27}H_{31}N_2O_4$: calcd. 447.2278; found 447.2280. $[\alpha]_D^{20}$:−58.8° (c= 1.34, $CHCl_3$). Chiralcel OD, 20 °C, 5 % *iso*-propanol/hexanes, 0.5 mL/min., UV detection at 254 nm, retention times: minor enantiomer 18.8 min.; major enantiomer 33.4 min.; 88% ee.

2.16.4 General Procedure for the Hydrogenation of the Endocyclic Alkene

Dihydropyridinyl intermediate (20 mg, 4.4 μmol, 1 equiv) and Adam's Catalyst (1.0 mg, 0.004 mmol, 0.1 equiv) was dissolved in 1 ml of ethyl acetate. A balloon of hydrogen gas was applied and the reaction mixture was allowed to stir at rt for 16 h. Upon complete consumption of starting material, monitored by TLC, the reaction mixture was filtered through a Celite™ plug (100% ethyl acetate). The solvent was removed by reduced pressure.

***tert*-Butyl 2-(4-chlorophenyl)-α-(2*R*)-2-piperinyl-, (α*R*)- 4-quinolinemethanol- 1(2H)-carboxylate:**

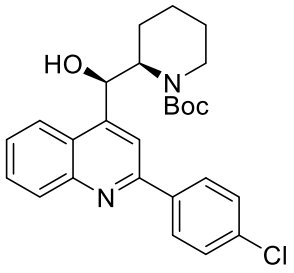

The title compound was obtained in quantitative yield as a yellow solid (20 mg). ^{1}H NMR (400 MHz, $CDCl_3$) rotomers are present: δ 8.24 (m, 1 H), 8.17 (m, 1 H), 8.11 – 8.00 (m, 3 H), 7.71 (m, 1 H), 7.59 – 7.48 (m, 1 H), 7.48 – 7.41 (app d of AA'BB', 2 H), 5.71 – 5.47 (m, 1 H), 4.79 – 4.58 (m, 1 H), 3.23 – 2.89 (m, 2 H), 1.75 – 1.64 (m, 6 H). ^{13}C NMR (101 MHz, $CDCl_3$): δ 170.6, 156.5, 148.3, 139.0, 136.1, 130.1, 129.0, 128.8, 126.9, 125.6, 124.8, 59.9, 27.9, 24.4, 20.8, 20.5, 19.3, 13.7. IR ($CHCl_3$ cast film, cm^{-1}): 3392, 2934, 1672, 1603, 1520, 1203, 834. HRMS (ESI) for $(M+H)^+$ $C_{26}H_{30}ClN_2O_3$: calcd. 453.1939; found 453.1939.

***tert*-Butyl 2-(4-chlorophenyl)-α-(2*S*)-2-piperinyl-, (α*S*)- 4-quinolinemethanol- 1(2H)-carboxylate:**

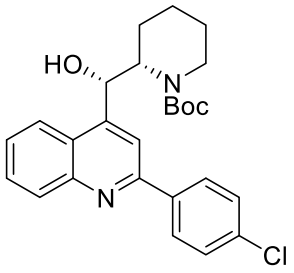

The title compound was obtained in quantitative yield as a yellow solid (20 mg). ^{1}H NMR (400 MHz, $CDCl_3$) rotomers are present: δ 8.24 (m, 1 H), 8.17 (m, 1 H), 8.11 – 8.00 (m, 3 H), 7.71 (m, 1 H), 7.59 – 7.48 (m, 1 H), 7.48 – 7.41 (app d of AA'BB', 2 H), 5.71 – 5.47 (m, 1 H), 4.79 – 4.58 (m, 1 H), 3.23 – 2.89 (m, 2 H), 1.75 – 1.64 (m, 6 H). ^{13}C NMR (101 MHz, $CDCl_3$) δ 170.6, 156.5, 148.3, 139.0, 136.1, 130.1, 129.0, 128.8, 126.9, 125.5, 124.78, 59.9, 41.0, 27.9, 24.4, 20.8, 20.5, 19.3, 13.7. IR ($CHCl_3$ cast film, cm^{-1}): 3394, 2924, 1672, 1603, 1420, 1203, 834. HRMS (ESI) for $(M+H)^+$ $C_{26}H_{30}ClN_2O_3$: calcd. 453.1939; found 453.1933.

2.16.5 General Procedure for the Epimerization of the Benzylic Centre

A flame dried round bottom flask was charged with PCC (240 mg, 5 equiv, 1.1 mmol) which was dissolved in 10 ml DCM. Dihydropyridinyl intermediate (100 mg, 1 equiv, 0.22 mmol) was added as a solution in DCM (0.66 M) and the reaction was allowed to stir at rt overnight. The solvent was removed by reduced pressure and the residue was passed through a Celite™ plug (50% diethyl ether/hexanes). The solvent was removed under reduced pressure to afford the ketone. The ketone was used without further purification and immediately after isolation to reduce undesired epimerization. Ketone was dissolved in 15 ml DCM and added to a flame dried flask containing a

solution of $CeCl_3 \cdot 7H_2O$ (414 mg, 5 equiv, 1.1 mmol) in anhydrous ethanol (0.73 M). The reaction mixture was cooled to −78 °C. One third of a solution of sodium borohydride (25 mg, 3 equiv, 0.67 mmol) in anhydrous ethanol (0.87 M) was added dropwise to the reaction mixture. Another third of the solution of sodium borohydride was added dropwise to the reaction mixture at −78 °C after 1 h and after 2 h respectively. After another 20 min, the reaction was quenched with water and allowed to warm to rt. The aqueous layer was extracted three times (10 mL) with ethyl acetate. The combined organic layer was washed with water, brine, dried (Na_2SO_4), filtered then concentrated to dryness by reduced pressure.

***tert*-Butyl 2-(4-chlorophenyl)-α-(2*R*)-2-5,6-dihydropyridinyl-, (α*S*)- 4-quinolinemethanol-1(2H)-carboxylate (2.24):**

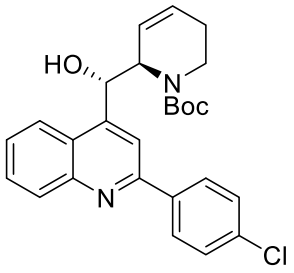

Flash column chromatography (14% ethyl acetate/pentanes) afforded a yellow solid (67 mg, 68% yield) ^{1}H NMR (400 MHz, $CDCl_3$): δ 8.17 (d, J = 8.4 Hz, 1 H), 8.14 – 8.07 (m, 2 × 1 H overlapping), 7.98 (s, 1 H), 7.72 (ddd, J = 8.3, 6.9, 1.1 Hz, 2 H), 7.61 – 7.52 (m, 1 H), 7.46 (dd, J = 8.9, 2.2 Hz, 2 H), 6.05 – 5.95 (m, 1 H), 5.81 (s, 1 H), 5.39 (d, J = 8.0 Hz, 1 H), 4.88 (s, 1 H), 4.31 – 4.22 (m, 1 H), 2.12 (m, 1 H), 1.99 (m, 1 H), 1.50 (s, 9 H). ^{13}C NMR (101 MHz, $CDCl_3$) rotomers present: δ 192.2, 155.6, 154.7, 148.9, 137.3, 136.64, 136.3, 135.9, 123.0, 129.7, 128.7, 128.6, 128.4, 128.1, 123.6, 122.8, 122.4, 62.0, 61.1, 39.0, 27.9, 27.5, 24.2, 24.2. IR ($CHCl_3$ cast film, cm^{-1}): 3295, 2957,

1672, 1503, 1202, 1136, 834. HRMS (ESI) for $(M+H)^+$ $C_{26}H_{28}ClN_2O_3$: calcd. 451.1783; found 451.1778.

***tert*-Butyl 2-(4-chlorophenyl)-α-(2*S*)-2-5,6-dihydropyridinyl-, (α*R*)- 4-quinolinemethanol-1(2H)-carboxylate (2.26):**

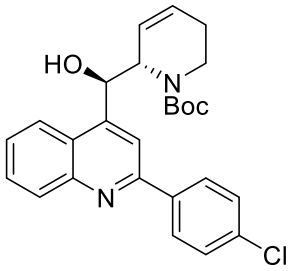

Flash column chromatography (14% ethyl acetate/pentanes) afforded a yellow solid (73 mg, 72% yield) ^{1}H NMR (400 MHz, $CDCl_3$): δ 8.17 (d, J = 8.4 Hz, 1 H), 8.14 – 8.07 (m, 2 × 1 H overlapping), 7.98 (s, 1 H), 7.72 (ddd, J = 8.3, 6.9, 1.1 Hz, 2 H), 7.61 – 7.52 (m, 1 H), 7.46 (dd, J = 8.9, 2.2 Hz, 2 H), 6.05 – 5.95 (m, 1 H), 5.81 (s, 1 H), 5.39 (d, J = 8.0 Hz, 1 H), 4.88 (s, 1 H), 4.31 – 4.22 (m, 1 H), 2.12 (m, 1 H), 1.99 (m, 1 H), 1.50 (s, 9 H). ^{13}C NMR (101 MHz, $CDCl_3$) rotomers present: δ 192.2, 155.5, 154.7, 148.9, 137.3, 136.64, 136.3, 135.8, 123.0, 129.7, 128.7, 128.6, 128.4, 128.1, 123.6, 122.8, 122.5, 62.0, 61.1, 39.0, 27.9, 27.5, 24.3, 24.2. IR ($CHCl_3$ cast film, cm^{-1}): 3295, 2866, 1673, 1419, 1205, 1136, 804. HRMS (ESI) for $(M+H)^+$ $C_{26}H_{28}ClN_2O_3$: calcd. 451.1783; found 451.1782.

2.16.6 General Procedure for the Deprotection of the tert-Butyloxycarbonyl Protecting Group

Tert-Butyloxycarbonyl protected intermediate (15 mg, 1 equiv) was dissolved in 2 mL DCM, stirring at rt. 300 µl of trifluoroacetic acid was added dropwise and the reaction mixture was stirred at rt for one hour. The mixture was quenched with the careful addition of a saturated aqueous solution of sodium bicarbonate. The aqueous layer was extracted three times (2 mL) with dichloromethane. The combined organic layer was washed with water, brine, dried (Na_2SO_4), filtered then concentrated to dryness by reduced pressure.

2-(4-Chlorophenyl)-α-(2*R*)-2-5,6-dihydropyridinyl-, (α*R*)- 4-quinolinemethanol:

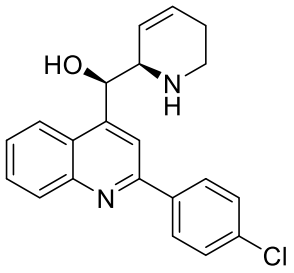

The title compound was obtained in near quantitative yield (11 mg, 95% yield). ^{1}H NMR (500 MHz, $CDCl_3$): δ 8.22 – 8.19 (m, 1H), 8.15 (app d of AA'BB', 2H), 8.06 (s, 1H), 7.97 (d, *J* = 8.3 Hz, 1H), 7.74 (ddd, *J* = 8.2, 6.9, 1.1 Hz, 1H), 7.54 (ddd, *J* = 8.2, 6.9, 1.2 Hz, 1H), 7.51 – 7.46 (app d of AA'BB', 2H), 6.01 – 5.95 (m, 1H), 5.57 – 5.51 (m, 1H), 5.37 (d, *J* = 5.2 Hz, 1H), 3.72 – 3.67 (m, 1H), 3.08 (dt, *J* = 10.6, 5.1 Hz, 1H), 2.91 (ddd, *J* = 12.3, 7.5, 4.7 Hz, 1H), 2.27 – 2.19 (m, 1H), 2.07 – 2.00 (m, 1H). ^{13}C NMR (126 MHz, $CDCl_3$): δ 155.7, 148.5, 148.4, 138.0, 135.6, 130.6, 129.5, 129.0, 128.9, 126.8, 126.4, 124.9, 123.0, 116.0, 77.31, 70.6, 58.5, 40.3, 25.2. IR ($CHCl_3$

cast film, cm^{-1}): 3319, 2954, 1672, 1596, 1092, 834, 759. HRMS (ESI) for $(M+H)^+$ $C_{21}H_{20}ClN_2O$: calcd. 351.1259; found 351.1259.

2-(4-Chlorophenyl)-α-(2*S*)-2-5,6-dihydropyridinyl-, (α*S*)- 4-quinolinemethanol:

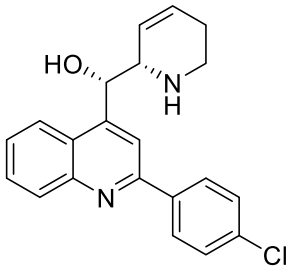

The title compound was obtained in near quantitative yield (12 mg, 97% yield). ^{1}H NMR (500 MHz, $CDCl_3$): δ 8.22 – 8.19 (m, 1H), 8.15 (app d of AA'BB', 2H), 8.06 (s, 1H), 7.97 (d, *J* = 8.3 Hz, 1H), 7.74 (ddd, *J* = 8.2, 6.9, 1.1 Hz, 1H), 7.54 (ddd, *J* = 8.2, 6.9, 1.2 Hz, 1H), 7.51 – 7.46 (app d of AA'BB', 2H), 6.01 – 5.95 (m, 1H), 5.57 – 5.51 (m, 1H), 5.37 (d, *J* = 5.2 Hz, 1H), 3.72 – 3.67 (m, 1H), 3.08 (dt, *J* = 10.6, 5.1 Hz, 1H), 2.91 (ddd, *J* = 12.3, 7.5, 4.7 Hz, 1H), 2.27 – 2.19 (m, 1H), 2.07 – 2.00 (m, 1H). ^{13}C NMR (126 MHz, $CDCl_3$): δ 155.7, 148.5, 148.4, 138.0, 135.6, 130.6, 129.5, 129.0, 128.9, 126.8, 126.4, 124.9, 123.0, 116.0, 77.31, 70.6, 58.5, 40.3, 25.2. IR ($CHCl_3$ cast film, cm^{-1}): 3319, 2954, 1672, 1596, 1092, 834, 759. HRMS (ESI) for $(M+H)^+$ $C_{21}H_{20}ClN_2O$: calcd. 351.1259; found 351.1258.

2-(4-Chlorophenyl)-α-(2*R*)-2-5,6-dihydropyridinyl-, (α*S*)- 4-quinolinemethanol:

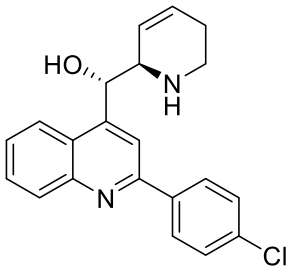

The title compound was obtained in near quantitative yield (12 mg, 97% yield). ^{1}H NMR (400 MHz, $CDCl_3$): δ 8.16 (d, *J* = 8.5 Hz, 1 H), 8.14 – 8.07 (m, 2 H), 7.97 (s, 1 H), 7.72 (ddd, *J* = 8.3, 6.9, 1.2 Hz, 1 H), 7.61 – 7.50 (m, 2 H), 7.49 – 7.42 (m, 2 H), 6.04 – 5.94 (m, 1 H), 5.80 (m, 1 H), 5.45 – 5.29 (m, 1 H), 4.96 – 4.79 (m, 1 H), 2.21 – 1.89 (m, 4 H). ^{13}C NMR (126 MHz, $CDCl_3$): δ 156.0, 148.0, 146.9, 137.9, 135.6, 130.2, 129.7, 128.9, 128.8, 126.6, 124.7, 122.6, 115.6, 61.7, 38.9, 30.6, 29.7, 29.0, 24.0. IR ($CHCl_3$ cast film, cm^{-1}): 3319, 2954, 1672, 1596, 1092, 834, 759. HRMS (ESI) for $(M+H)^+$ $C_{21}H_{20}ClN_2O$: calcd. 351.1259; found 351.1260.

2-(4-Chlorophenyl)-α-(2*S*)-2-5,6-dihydropyridinyl-, (α*R*)- 4-quinolinemethanol:

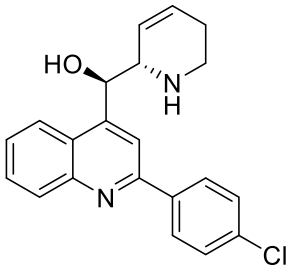

The title compound was obtained in near quantitative yield (11 mg, 95% yield). ^{1}H NMR (400 MHz, $CDCl_3$): δ 8.16 (d, *J* = 8.5 Hz, 1 H), 8.14 – 8.07 (m, 2 H), 7.97 (s, 1 H), 7.72 (ddd, *J* = 8.3, 6.9, 1.2 Hz, 1 H), 7.61 – 7.50 (m, 2 H), 7.49 – 7.42 (m, 2 H), 6.04 – 5.94 (m, 1 H), 5.80 (m, 1 H),

5.45 – 5.29 (m, 1 H), 4.96 – 4.79 (m, 1 H), 2.21 – 1.89 (m, 4 H). ^{13}C NMR (126 MHz, $CDCl_3$): δ 156.0, 148.0, 146.9, 137.9, 135.5, 130.2, 129.7, 129.0, 128.8, 126.7, 124.7, 122.6, 115.6, 61.7, 38.9, 30.7, 29.7, 29.0, 24.0. IR ($CHCl_3$ cast film, cm^{-1}): 3319, 2954, 1672, 1596, 1092, 834, 759. HRMS (ESI) for $(M+H)^+$ $C_{21}H_{20}ClN_2O$: calcd. 351.1259; found 351.1258.

2-(4-Chlorophenyl)-α-(2*R*)-2-piperidinyl-, (α*R*)- 4-quinolinemethanol (2.1):

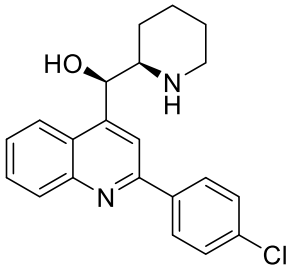

The title compound was obtained in near quantitative yield (11 mg, 94% yield). ^{1}H NMR (400 MHz, $CDCl_3$): δ 8.20 – 8.16 (m, 1 H), 8.16 – 8.11 (app d of AA'BB', 2 H), 8.04 – 7.98 (m, 1 × 1 H overlapping), 7.75 – 7.69 (m, 1 H), 7.52 (ddd, *J* = 8.2, 6.9, 1.2 Hz, 1 H), 7.49 – 7.44 (app d of AA'BB', 2 H), 5.38 (d, *J* = 5.6 Hz, 1 H), 3.18 (d, *J* = 11.2 Hz, 1 H), 3.05 – 2.97 (m, 1 H), 2.62 (td, *J* = 12.2, 2.6 Hz, 1 H), 1.83 – 1.72 (m, 1 H), 1.68 – 1.42 (m, 4 H). ^{13}C NMR (101 MHz, $CDCl_3$): δ 170.6, 155.3, 148.2, 137.3, 135.1, 130.2, 129.1, 128.5, 128.3, 126.0, 124.9, 122.7, 116.7, 59.9, 41.0, 27.9, 24.3, 20.5, 19.4, 13.7. IR ($CHCl_3$ cast film, cm^{-1}): 3394, 2956, 1777, 1732, 1671, 1203, 834. HRMS (ESI) for $(M+H)^+$ $C_{21}H_{22}ClN_2O$: calcd. 353.1415; found 353.1414.

2-(4-Chlorophenyl)-α-(2*S*)-2-piperidinyl-, (α*S*)- 4-quinolinemethanol (2.3):

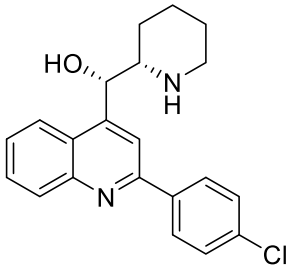

The title compound was obtained in near quantitative yield (12 mg, 98% yield). ^{1}H NMR (400 MHz, $CDCl_3$): δ 8.20 – 8.16 (m, 1 H), 8.15 – 8.10 (app d of AA'BB', 2 H), 8.04 – 7.98 (m, 1 × 1 H overlapping), 7.75 – 7.69 (m, 1 H), 7.52 (ddd, *J* = 8.2, 6.9, 1.2 Hz, 1 H), 7.49 – 7.44 (app d of AA'BB', 2 H), 5.38 (d, *J* = 5.6 Hz, 1 H), 3.18 (d, *J* = 11.2 Hz, 1 H), 3.05 – 2.97 (m, 1 H), 2.62 (td, *J* = 12.2, 2.6 Hz, 1 H), 1.83 – 1.72 (m, 1 H), 1.68 – 1.42 (m, 4 H). ^{13}C NMR (101 MHz, $CDCl_3$): δ 170.6, 155.3, 148.2, 137.3, 135.1, 130.2, 129.1, 128.5, 128.3, 126.0, 124.9, 122.7, 116.7, 59.9, 41.0, 27.9, 24.3, 20.5, 19.4, 13.6. IR ($CHCl_3$ cast film, cm^{-1}): 3394, 2923, 1732, 1420, 1203, 1014, 721. HRMS (ESI) for $(M+H)^+$ $C_{21}H_{22}ClN_2O$: calcd. 353.1415; found 353.1413.

2-(4-Chlorophenyl)-α-(2*R*)-2-piperidinyl-, (α*S*)- 4-quinolinemethanol (2.2):

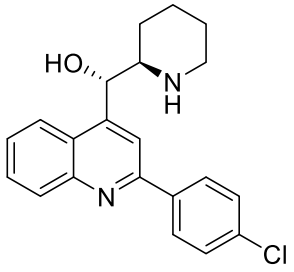

The title compound was obtained in near quantitative yield (12 mg, 98% yield). ^{1}H NMR (500 MHz, $CDCl_3$): δ 8.16 – 8.05 (m, 5 H), 7.67 (t, *J* = 7.6 Hz, 1 H), 7.51 – 7.43 (m, 2 × 1 H overlapping),

6.05 (s, 1 H), 3.50 (d, J = 13.1 Hz, 1 H), 3.36 (d, J = 12.0 Hz, 1 H), 3.03 – 2.89 (m, 1 H), 1.80 – 1.68 (m, 6H). ^{13}C NMR (125 MHz, $CDCl_3$): δ 155.6, 148.2, 146.0, 137.9, 135.7, 130.6, 129.5, 129.0, 128.8, 126.8, 124.1, 122.5, 116.0, 60.2, 45.8, 24.0, 23.5, 22.6. IR ($CHCl_3$ cast film, cm^{-1}): 3394, 2956, 1777, 1671, 1203, 1098, 834. HRMS (ESI) for $(M+H)^+$ $C_{21}H_{22}ClN_2O$: calcd. 353.1415; found 353.1416.

2-(4-Chlorophenyl)-α-(2*S*)-2-piperidinyl-, (α*R*)- 4-quinolinemethanol (2.4):

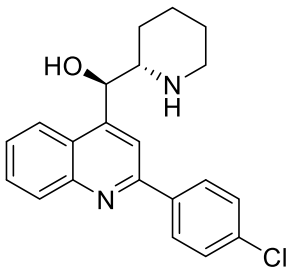

The title compound was obtained in near quantitative yield (11 mg, 95% yield). ^{1}H NMR (500 MHz, $CDCl_3$): δ 8.17 – 8.06 (m, 5 H), 7.67 (t, J = 7.6 Hz, 1 H), 7.51 – 7.43 (m, 2 × 1 H overlapping), 6.05 (s, 1 H), 3.50 (d, J = 13.1 Hz, 1 H), 3.36 (d, J = 12.0 Hz, 1 H), 3.03 – 2.89 (m, 1 H), 1.81 – 1.68 (m, 6H). ^{13}C NMR (125 MHz, $CDCl_3$): δ 155.6, 148.2, 146.0, 137.9, 135.7, 130.6, 129.5, 128.9, 128.8, 126.8, 124.1, 122.6, 116.0, 60.2, 45.8, 24.1, 23.5, 22.6. IR ($CHCl_3$ cast film, cm^{-1}): 3394, 2923, 1732, 1420, 1203, 1098, 834. HRMS (ESI) for $(M+H)^+$ $C_{21}H_{22}ClN_2O$: calcd. 353.1415; found 353.1414.

2-(Phenyl)-α-(2*R*)-2-piperidinyl-, (α*R*)- 4-quinolinemethanol:

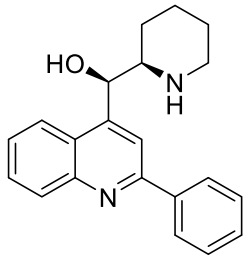

The title compound was obtained in near quantitative yield (11 mg, 96% yield). ^{1}H NMR (500 MHz, $CDCl_3$): δ 8.24 – 8.15 (m, 2 × 1 H overlapping), 8.03 (s, 1 H), 7.98 (d, *J* = 8.3 Hz, 1 H), 7.74 – 7.71 (m, 1 H), 7.56 – 7.45 (m, 3 H), 5.34 (d, *J* = 5.7 Hz, 1 H), 3.18 (d, *J* = 12.5 Hz, 1H), 3.05 – 2.98 (m, 1 H), 2.63 (td, *J* = 12.5, 2.5 Hz, 1 H), 1.83 – 1.72 (m, 1 H), 1.67 – 1.43 (m, 5 H). ^{13}C NMR (126 MHz, $CDCl_3$): δ 157.0, 148.5, 148.2, 139.5, 130.6, 129.4, 129.4, 128.8, 127.6, 126.3, 125.0, 123.0, 116.5, 72.2, 61.6, 46.0, 29.7, 28.6, 25.2, 24.9, 23.8. IR ($CHCl_3$ cast film, cm^{-1}): 3318, 2933, 1673, 1597, 1181, 758, 696. HRMS (ESI) for $(M+H)^+$ $C_{21}H_{23}N_2O$: calcd. 319.1805; found 319.1803.

2-(4-Bromophenyl)-α-(2*R*)-2-piperidinyl-, (α*R*)- 4-quinolinemethanol:

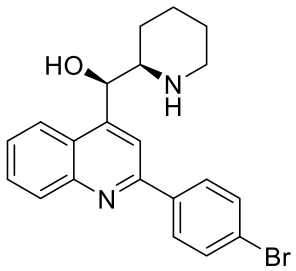

The title compound was obtained in near quantitative yield (12 mg, 98% yield). ^{1}H NMR (500 MHz, $CDCl_3$): δ 8.20 – 8.15 (m, 1 H), 8.05 – 8.03 (m, 2 H), 7.99 – 7.93 (app d of AA'BB', 2 H), 7.73 – 7.71 (m, 1 H), 7.64 – 7.62 (app d of AA'BB', 2 H), 7.55 – 7.47 (m, 1 H), 5.32 (d, *J* = 4.0 Hz, 1 H), 3.18 (d, *J* = 14.4 Hz, 1 H), 3.03 – 2.95 (m, 1 H), 2.68 – 2.57 (m, 1 H), 1.82 – 1.71 (m, 1 H), 1.67 – 1.40 (m, 4 H). ^{13}C NMR (126 MHz, $CDCl_3$): δ 155.7, 148.5, 148.4, 138.2, 131.9, 130.6, 129.6, 129.1, 128.8, 127.6, 126.5, 125.0, 124.1, 123.0, 116.0, 72.1, 61.7, 46.0, 29.7, 28.6, 25.2, 24.9, 23.8. IR ($CHCl_3$ cast film, cm^{-1}): 3066, 2935, 1673, 1596, 1201, 832, 758. HRMS (ESI) for $(M+H)^+$ $C_{21}H_{22}BrN_2O$: calcd. 397.0910; found 397.0912.

2-(4-Methoxyphenyl)-α-(2*R*)-2-piperidinyl-, (α*R*)- 4-quinolinemethanol:

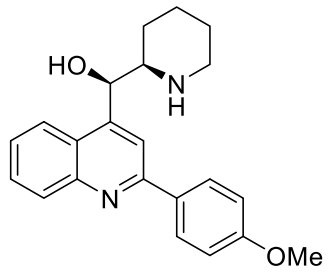

The title compound was obtained in near quantitative yield (12 mg, 97% yield). ^{1}H NMR (500 MHz, $CDCl_3$): δ 8.19 – 8.16 (m, 3 H), 8.00 (s, 1 H), 7.95 (dd, *J* = 8.6, 6.2 Hz, 1 H), 7.74 – 7.68 (m, 1 H), 7.51 – 7.48 (m, 1 H), 7.08 – 7.02 (app d of AA'BB', 2 H), 5.30 (d, *J* = 5.4 Hz, 1 H), 3.91 (s, 3 H), 3.20 – 3.10 (m, 1 H), 3.03 – 2.95 (m, 1 H), 2.61 (td, *J* = 12.5, 3.2 Hz, 1 H), 1.92 – 1.75 (m, 2 H), 1.67 – 1.41 (m, 5 H). ^{13}C NMR (126 MHz, $CDCl_3$): δ 160.9, 156.5, 148.6, 148.1, 132.1, 130.4, 129.3, 128.9, 128.1, 125.9, 124.7, 122.9, 115.9, 114.2, 72.3, 61.4, 55.4, 46.1, 29.7, 28.9, 25.4, 24.8, 24.0. IR ($CHCl_3$ cast film, cm^{-1}): 3067, 2936, 1673, 1599, 1251, 1175, 756. HRMS (ESI) for $(M+H)^+$ $C_{22}H_{25}N_2O_2$: calcd. 349.1911; found 349.1911.

2-(4-Methylphenyl)-α-(2*R*)-2-piperidinyl-, (α*R*)- 4-quinolinemethanol:

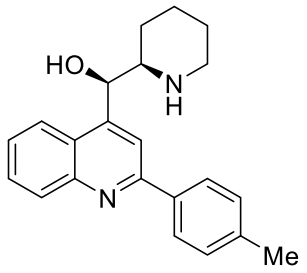

The title compound was obtained in near quantitative yield (12 mg, 98% yield). ^{1}H NMR (500 MHz, $CDCl_3$): δ 8.21 – 8.16 (m, 1 H), 8.06 – 8.04 (app d of AA'BB', 2 H), 7.96 (d, *J* = 16.7 Hz, 1 H), 7.70 (ddd, *J* = 8.3, 6.9, 1.2 Hz, 1 H), 7.48 (ddd, *J* = 8.2, 6.9, 1.1 Hz, 1 H), 7.32 – 7.31 (app d of AA'BB', 2 H), 5.31 (d, *J* = 3.2 Hz, 1 H), 3.23 – 3.15 (m, 1 H), 3.01 (ddd, *J* = 11.0, 6.5, 2.8 Hz, 1 H), 2.63 (td, *J* = 11.9, 2.6 Hz, 1 H), 2.44 (s, 3 H), 1.80 – 1.71 (m, 1 H), 1.67 – 1.40 (m, 5 H). ^{13}C NMR (126 MHz, $CDCl_3$): δ 156.9, 148.5, 147.9, 139.5, 136.6, 130.4, 129.6, 129.3, 127.4, 126.1, 124.9, 123.0, 116.4, 72.1, 61.7, 46.0, 28.5, 25.1, 23.8, 21.4. IR ($CHCl_3$ cast film, cm^{-1}): 3311, 2936, 1673, 1597, 1184, 823, 759. HRMS (ESI) for $(M+H)^+$ $C_{22}H_{25}N_2O_2$: calcd. 333.1961; found 333.1959.

2-(Phenyl)-α-(2*S*)-2-piperidinyl-, (α*S*)- 4-quinolinemethanol:

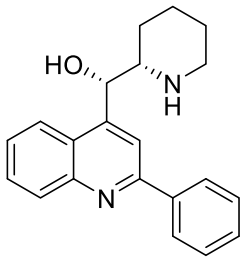

The title compound was obtained in near quantitative yield (11 mg, 96% yield). ^{1}H NMR (498 MHz, Chloroform-*d*) δ 8.24 – 8.15 (m, 2 × 1 H overlapping), 8.02 (s, 1 H), 7.99 (d, *J* = 8.3 Hz, 1 H), 7.74 – 7.71 (m, 1 H), 7.56 – 7.45 (m, 3 H), 5.36 (d, *J* = 5.7 Hz, 1 H), 3.18 (d, *J* = 12.5 Hz, 1H), 3.04 – 2.99 (m, 1 H), 2.63 (td, *J* = 12.5, 2.5 Hz, 1 H), 1.83 – 1.72 (m, 1 H), 1.65 – 1.41 (m, 5 H). ^{13}C NMR (126 MHz, cdcl$_3$) δ 157.0, 148.5, 148.2, 139.6, 130.6, 129.4, 129.4, 129.0, 127.6, 126.3, 125.0, 122.9, 116.5, 72.2, 61.6, 46.0, 30.0, 28.6, 25.2, 24.8, 23.8. IR ($CHCl_3$ cast film, cm^{-1}): 3063, 2933, 1673, 1597, 1201, 758, 721. HRMS (ESI) for $(M+H)^+$ $C_{21}H_{23}N_2O$: calcd. 319.1805; found 319.1803.

2-(4-Bromophenyl)-α-(2*S*)-2-piperidinyl-, (α*S*)- 4-quinolinemethanol:

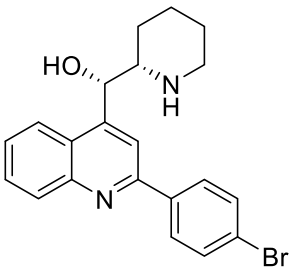

The title compound was obtained in near quantitative yield (12 mg, 98% yield). ^{1}H NMR (498 MHz, $CDCl_3$) δ 8.20 – 8.15 (m, 1 H), 8.06 – 8.02 (m, 2 H), 7.99 – 7.93 (app d of AA'BB', 2 H), 7.73 – 7.71 (m, 1 H), 7.64 – 7.62 (app d of AA'BB', 2 H), 7.55 – 7.47 (m, 1 H), 5.32 (d, *J* = 4.0

Hz, 1 H), 3.18 (d, *J* = 14.4 Hz, 1 H), 3.03 – 2.95 (m, 1 H), 2.68 – 2.57 (m, 1 H), 1.82 – 1.71 (m, 1 H), 1.67 – 1.40 (m, 4 H). ^{13}C NMR (126 MHz, $CDCl_3$): δ 155.7, 148.5, 148.4, 138.2, 131.9, 130.6, 129.6, 129.1, 128.8, 127.6, 126.5, 125.0, 124.1, 123.0, 116.0, 72.1, 61.7, 46.0, 29.7, 28.6, 25.2, 24.9, 23.8. IR ($CHCl_3$ cast film, cm^{-1}): 3310, 2935, 1673, 1596, 1201, 862, 758. HRMS (ESI) for $(M+H)^+$ $C_{21}H_{22}BrN_2O$: calcd. 397.0911; found 397.0913.

2-(4-Methoxyphenyl)-α-(2*S*)-2-piperidinyl-, (α*S*)- 4-quinolinemethanol:

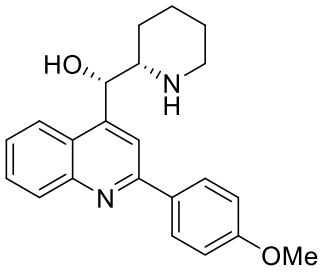

The title compound was obtained in near quantitative yield (12 mg, 97% yield). ^{1}H NMR (500 MHz, $CDCl_3$): δ 8.18 – 8.15 (m, 3 H), 8.00 (s, 1 H), 7.95 (dd, *J* = 8.6, 6.2 Hz, 1 H), 7.74 – 7.68 (m, 1 H), 7.52 – 7.49 (m, 1 H), 7.08 – 7.02 (app d of AA'BB', 2 H), 5.30 (d, *J* = 5.4 Hz, 1 H), 3.91 (s, 3 H), 3.20 – 3.10 (m, 1 H), 3.03 – 2.95 (m, 1 H), 2.63 (td, *J* = 12.5, 3.2 Hz, 1 H), 1.92 – 1.75 (m, 2 H), 1.67 – 1.41 (m, 5 H). ^{13}C NMR (126 MHz, $CDCl_3$): δ 160.9, 156.5, 148.6, 148.0, 132.1, 130.4, 129.3, 129.0, 128.1, 125.9, 124.7, 122.9, 115.8, 114.2, 72.3, 61.4, 55.4, 46.2, 29.6, 28.9, 25.4, 24.8, 24.0. IR ($CHCl_3$ cast film, cm^{-1}): 3067, 2936, 1673, 1599, 1251, 1175, 756. HRMS (ESI) for $(M+H)^+$ $C_{22}H_{25}N_2O_2$: calcd. 349.1911; found 349.1912.

2-(4-Methylphenyl)-α-(2*S*)-2-piperidinyl-, (α*S*)- 4-quinolinemethanol:

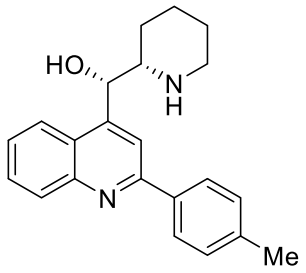

The title compound was obtained in near quantitative yield (12 mg, 98% yield). ^{1}H NMR (500 MHz, $CDCl_3$): δ 8.21 – 8.16 (m, 1 H), 8.06 – 8.04 (app d of AA'BB', 2 H), 7.96 (d, *J* = 16.7 Hz, 1 H), 7.70 (ddd, *J* = 8.3, 6.9, 1.2 Hz, 1 H), 7.47 (ddd, *J* = 8.2, 6.9, 1.1 Hz, 1 H), 7.32 – 7.31 (app d of AA'BB', 2 H), 5.32 (d, *J* = 3.2 Hz, 1 H), 3.24 – 3.14 (m, 1 H), 3.01 (ddd, *J* = 11.0, 6.5, 2.8 Hz, 1 H), 2.63 (td, *J* = 11.9, 2.6 Hz, 1 H), 2.44 (s, 3 H), 1.80 – 1.71 (m, 1 H), 1.67 – 1.40 (m, 5 H). ^{13}C NMR (126 MHz, $CDCl_3$): δ 156.9, 148.5, 147.9, 139.6, 136.6, 130.4, 129.6, 129.3, 127.4, 126.0, 124.9, 123.0, 116.4, 72.0, 61.7, 46.0, 28.5, 25.1, 23.9, 21.4. IR ($CHCl_3$ cast film, cm^{-1}): 3311, 2936, 1673, 1597, 1201, 823, 759. HRMS (ESI) for $(M+H)^+$ $C_{22}H_{25}N_2O_2$: calcd. 333.1961; found 333.1960.

2.16.7 General Procedure for the synthesis of the aldehyde coupling partner

Isatin (1 g, 6.8 mmol, 1 equiv) was dissolved 33% w/v aqueous KOH solution. Acetophenone (6.8 mmol, 1 equiv) was added and the reaction mixture was gently heated to reflux. The reaction was refluxed for 16 h. After the reaction time, the mixture was cooled to rt then transferred to an Erlenmeyer flask and subsequently cooled to 0 °C. Carefully, the reaction mixture was acidified with dropwise addition of conc. HCl and provided the carboxylic acid product as a yellow solid after collection by vacuum filtration. The carboxylic acid (1 g, 1 equiv) was dissolved in 50 ml of diethyl ether and cooled to 0 °C. Lithium aluminum hydride (1.2 equiv) was added portion-wise

at 0 °C and the reaction mixture was allowed to warm to rt, while stirring, overnight. The Feiser work-up was used to isolate the reduced product after removal of the organic solvent by reduced pressure. The alcohol was used without further purification. The alcohol (1 equiv) was dissolved in 10 ml dimethyl sulfoxide (dried over molecular sieves). IBX (2 equiv) was added to the reaction mixture at rt and the reaction was allowed to stir overnight at rt. The reaction mixture was quenched with diH_2O. The aqueous layer was extracted three times with ethyl acetate and the combined organic layer was washed with 1M NaOH, water and brine. The organic layer was then dried with sodium sulfate and the solvent was removed by reduced pressure.

2-(4-Chlorophenyl)-4-quinolinecarboxylic acid:

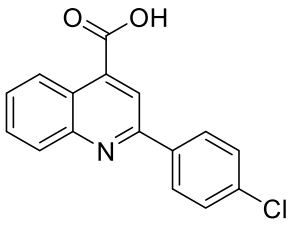

A yellow solid was obtained in near quantitative yield (1.9 g). Spectral data correspond to that reported.[23] ^{1}H NMR (400 MHz, DMSO-d_6): δ 9.03 (dd, J = 8.2, 1.5 Hz, 1 H), 8.43 – 8.38 (app d of AA'BB', 2 H), 8.21 (dd, J = 8.8, 0.9 Hz, 1 H), 7.88 (ddd, J = 8.4, 6.9, 1.4 Hz, 1 H), 7.75 (ddd, J = 8.3, 6.9, 1.3 Hz, 1 H), 7.63 – 7.58 (app d of AA'BB', 2 H).

2-(Phenyl)-4-quinolinecarboxylic acid:

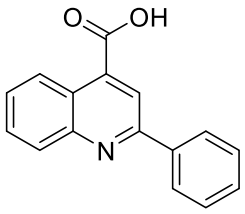

A yellow solid was obtained in near quantitative yield (1.7 g). Spectral data correspond to that reported.[23] ^{1}H NMR (400 MHz, DMSO-d_6): δ 8.65 – 8.58 (m, 1 H), 8.43 (s, 1 H), 8.26 (app d of AA'BB', 2 H), 8.18 – 8.12 (m, 1 H), 7.83 (ddd, J = 8.4, 6.9, 1.4 Hz, 1 H), 7.68 (ddd, J = 8.3, 6.9, 1.3 Hz, 1 H), 7.60 – 7.47 (m, 2 H).

2-(4-Bromophenyl)-4-quinolinecarboxylic acid:

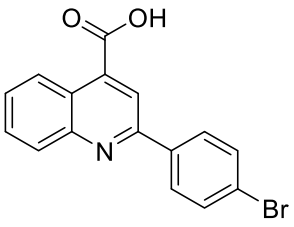

A yellow solid was obtained in near quantitative yield (2.2 g). Spectral data correspond to that reported.[24] ^{1}H NMR (400 MHz, DMSO-d_6): δ 8.62 – 8.56 (m, 1 H), 8.42 (s, 1 H), 8.25 – 8.19 (app d of AA'BB', 2 H), 8.13 (d, J = 8.4 Hz, 1 H), 7.83 (ddd, J = 8.4, 7.0, 1.3 Hz, 1 H), 7.76 – 7.71 (app d of AA'BB', 2 H), 7.68 (ddd, J = 8.3, 6.9, 1.2 Hz, 1 H).

2-(4-Methylphenyl)-4-quinolinecarboxylic acid:

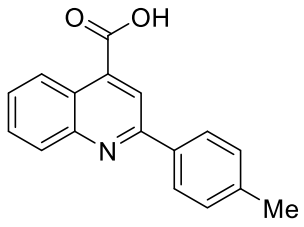

A yellow solid was obtained in near quantitative yield (1.8 g). Spectral data correspond to that reported.[23] ^{1}H NMR (400 MHz, DMSO-d_6): δ 8.63 – 8.57 (m, 1 H), 8.41 (s, 1 H), 8.16 (m, 2 × 1 H overlapping), 7.82 (ddd, J = 8.4, 6.9, 1.4 Hz, 1 H), 7.67 (ddd, J = 8.3, 6.9, 1.2 Hz, 1 H), 7.36 (app d of AA'BB', J = 8.0 Hz, 2 H), 2.37 (s, 3 H).

2-(4-Methoxyphenyl)-4-quinolinecarboxylic acid:

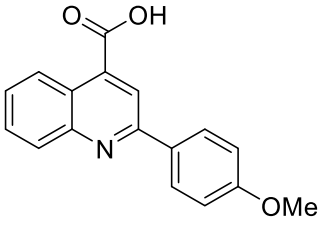

A yellow solid was obtained in near quantitative yield (1.9 g). Spectral data correspond to that reported.[25] ^{1}H NMR (400 MHz, DMSO-d_6): δ 8.60 – 8.54 (m, 1 H), 8.39 (s, 1 H), 8.28 – 8.20 (app d of AA'BB', 2 H), 8.14 (d, J = 8.3 Hz, 1 H), 7.82 (ddd, J = 8.3, 7.0, 1.2 Hz, 1 H), 7.65 (ddd, J = 8.2, 6.9, 1.2 Hz, 1 H), 7.13 – 7.06 (app d of AA'BB', 2 H), 3.82 (s, 3 H).

2-(4-Chlorophenyl)- 4-quinolinecarboxaldehyde (2.7):

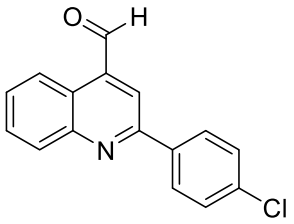

A yellow solid was obtained (570 mg, 60% overall yield). Spectral data correspond to that reported.[26] ^{1}H NMR (400 MHz, Acetone-d_6): δ 10.63 (s, 1 H), 9.03 (dd, J = 8.2, 1.5 Hz, 1 H), 8.43 – 8.38 (app d of AA'BB', 2 H), 8.21 (dd, J = 8.8, 0.9 Hz, 1 H), 7.88 (ddd, J = 8.4, 6.9, 1.4 Hz, 1 H), 7.75 (ddd, J = 8.3, 6.9, 1.3 Hz, 1 H), 7.63 – 7.58 (app d of AA'BB', 2 H).

2-Phenyl-4-quinolinecarboxaldehyde (2.27):

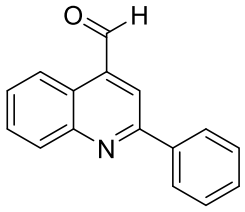

A yellow solid was obtained (550 mg, 58% overall yield). Spectral data correspond to that reported.[26] ^{1}H NMR (500 MHz, $CDCl_3$): δ 10.59 (s, 1 H), 9.00 (d, J = 8.5 Hz, 1 H), 8.31 – 8.21 (m, 4 H), 7.86 – 7.80 (m, 1 H), 7.73 – 7.68 (m, 1 H), 7.58 (m, 2 H), 7.54 (m, 1 H). ^{13}C NMR (126 MHz, $CDCl_3$): δ 193.0, 157.4, 149.4, 138.4, 137.7, 130.3, 130.3, 130.0, 129.1, 128.9, 127.4, 124.2, 124.0, 122.9. HRMS (EI) for $(M)^{+\bullet}$ $C_{16}H_{11}NO$: calcd. 233.0841; found 233.0841.

2-(4-Bromophenyl)-4-quinolinecarboxaldehyde (2.28):

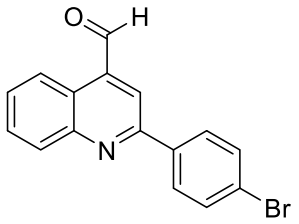

A yellow solid was obtained (590 mg, 62% overall yield). ^{1}H NMR (500 MHz, $CDCl_3$): δ 10.50 (s, 1 H), 8.89 (d, *J* = 9.1 Hz, 1 H), 8.19 (d, *J* = 8.4 Hz, 1 H), 8.10 (s, 1 H), 8.07 – 8.02 (m, 2 H), 7.81 – 7.75 (m, 1 H), 7.69 – 7.59 (m, 3 H). ^{13}C NMR (126 MHz, $CDCl_3$): δ 192.6, 155.8, 149.3, 137.7, 137.1, 132.1, 130.4, 130.2, 129.1, 128.8, 124.7, 124.1, 123.1, 122.9. IR ($CHCl_3$ cast film, cm^{-1}): 2978, 2744, 2719, 1703, 1455, 1072, 758. HRMS (EI) for $(M)^{+\bullet}$ $C_{16}H_{10}NO^{81}Br$: calcd. 312.9925; found 312.9921.

2-(4-Methylphenyl)-4-quinolinecarboxaldehyde (2.30):

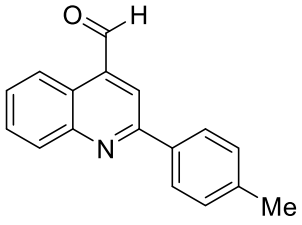

A yellow solid was obtained (570 mg, 61% overall yield). ^{1}H NMR (500 MHz, $CDCl_3$): δ 10.53 (s, 1 H), 8.97 – 8.94 (m, 1 H), 8.26 – 8.23 (m, 1 H), 8.20 (s, 1 H), 8.12 (m, 2 H), 7.80 (ddd, *J* = 8.4, 6.9, 1.4 Hz, 1 H), 7.66 (ddd, *J* = 8.3, 6.9, 1.3 Hz, 1 H), 7.35 (m, 2 H), 2.45 (s, 3 H). ^{13}C NMR (126 MHz, $CDCl_3$): δ 193.0, 157.2, 149.4, 140.2, 137.6, 135.6, 130.2, 130.1, 129.8, 128.6, 127.3, 124.2, 124.0, 122.7, 28.5. IR ($CHCl_3$ cast film, cm^{-1}): 2977, 2740, 2714, 1703, 1419, 1239, 763. HRMS (EI) for $(M)^{+\bullet}$ $C_{17}H_{13}NO$: calcd. 247.0997; found 247.0997.

2-(4-Methoxyphenyl)-4-quinolinecarboxaldehyde (2.29):

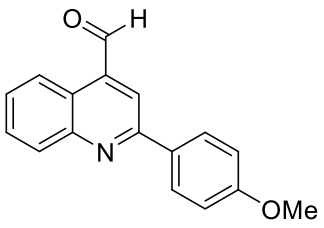

A yellow solid was obtained (610 mg, 65% overall yield). Spectral data correspond to that reported.[26] ^{1}H NMR (500 MHz, $CDCl_3$): δ 10.50 (s, 1 H), 8.92 (d, *J* = 8.4 Hz, 1 H), 8.20 (t, *J* = 8.1 Hz, 1 H), 8.18 – 8.15 (m, 2 H), 8.13 (s, 1 H), 7.82 – 7.74 (m, 1 H), 7.64 (ddd, *J* = 8.2, 7.0, 1.1 Hz, 1 H), 7.08 – 7.02 (m, 2 H), 3.89 (s, 3 H). ^{13}C NMR (126 MHz, $CDCl_3$): δ 193.0, 161.3, 156.8, 149.3, 137.5, 130.9, 130.2, 130.0, 128.8, 128.4, 124.1, 123.7, 122.5, 114.4, 55.4. HRMS (EI) for $(M)^{+\bullet}$ $C_{17}H_{13}NO_2$: calcd. 263.0946; found 263.0942.

2-[(Phenylmethoxy)imino]-acetic acid (2.33):

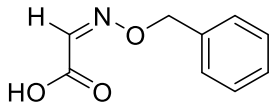

O-benzylhydroxylamine hydrochloride (1.6 g, 10.5 mmol, 1 equiv) and glyoxylic acid (0.92 g, 12.8 mmol, 1.2 equiv)) were dissolved in 100 ml diH_2O. The reaction was stirred at rt for 2 h. A white powder was obtained after filtration (1.8 g, quant. yield). Spectra data correspond to that reported.[27] ^{1}H NMR (400 MHz, $CDCl_3$): δ 7.54 (s, 1 H), 7.40-7.36 (m, 5 H), 5.31 (s, 2 H).

2-[(Benzyloxy)imino]-acetyl chloride (2.34):

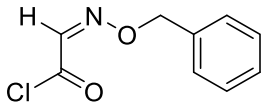

2-[(Phenylmethoxy)imino]-acetic acid (1.8 g, 10.5 mmol 1 equiv) was dissolved in 60 ml DCM with one drop of DMF. Oxalyl chloride (1.1 ml, 12.8 mmol, 1.2 equiv) was added dropwise to the reaction mixture at rt. The reaction was stirred for 1 hr at rt. The solvent was removed by reduced pressure to obtain a yellow oil (1.8 g, 90% yield). Spectra data correspond to that reported.[27] ^{1}H NMR (400 MHz, $CDCl_3$): δ 7.54 (s, 1 H), 7.40-7.36 (m, 5 H), 5.31 (s, 2 H).

***N*-2-Napthyl-2-[(phenylmethoxy)imino]- acetamide (2.36):**

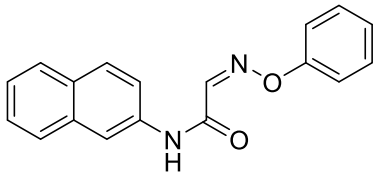

2-Naphthylamine (2.3 g, 10.5 mmol, 1 equiv) was dissolved in a solution of 50 ml DCM with *N,N*-diisopropylethylamine (2.2 ml, 12.6 mmol, 1.2 equiv). The reaction mixture was cooled to 0 °C. 2-[(Benzyloxy)imino]-acetyl chloride (2.1 g, 10.5 mmol, 1 equiv) was diluted with 50 ml of DCM and was added dropwise to the reaction mixture at 0 °C. The reaction was allowed to stir overnight and gradually warm to rt. The reaction was quenched with 1 M HCl and the aqueous layer was extracted with DCM (2x). The combined organic phase was washed with brine, dried (Na_2SO_4), filtered and concentrated to dryness to obtain the title compound (2.5 g, 78% yield). ^{1}H NMR (400

MHz, $CDCl_3$): δ 8.38 (s, 1H), 8.26 (d, *J* = 1.9 Hz, 1H), 7.81 (t, *J* = 8.9 Hz, 4H), 7.62 (s, 1H), 7.54 (dd, *J* = 8.8, 2.2 Hz, 1H), 7.50 – 7.45 (m, 1H), 7.45 – 7.35 (m, 8H), 5.30 (s, 3H).

1*H*-Benz[*e*]indole-1,2(3*H*)-dione (2.39):

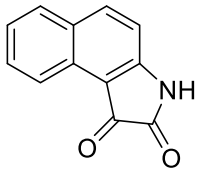

N-2-Napthyl-2-[(phenylmethoxy)imino]- acetamide **2.36** (710 mg, 2.3 mmol, 1 equiv) was treated with conc. H_2SO_4 (2.4 ml), and gently heated to 50 °C in an open flask. The reaction was heated at 50 °C for 1 h. The reaction was then heated to 70 °C for an additional 10 min. The reaction mixture was cooled to rt then transferred to an Erlenmeyer flask containing ice. The brown precipitate was collected *via* vacuum filtration to afford **2.39** as a brown solid (52 mg, 10% yield). Spectral data correspond to that reported.[21] ^{1}H NMR (400 MHz, $CDCl_3$): δ 8.51 (d, *J* = 8.4 Hz, 1 H), 8.23 (d, *J* = 8.4 Hz, 1 H), 7.89 (d, *J* = 8.0 Hz), 7.66 (app. ddd, *J* = 9.6, 7.2, 1.6 Hz, 1 H) 7.42 (app. ddd, *J* = 9.4, 7.2, 1.2 Hz, 1 H), 7.27 (d, *J* = 8.4 Hz).

2.17 References

(1) Brain Tumor Statistics http://www.abta.org/about-us/news/brain-tumor-statistics/ (accessed Apr 21, 2016).

(2) Kitambi, S. S.; Toledo, E. M.; Usoskin, D.; Wee, S.; Harisankar, A.; Svensson, R.; Sigmundsson, K.; Kalderén, C.; Niklasson, M.; Kundu, S.; Aranda, S.; Westermark, B.; Uhrbom, L.; Andäng, M.; Damberg, P.; Nelander, S.; Arenas, E.; Artursson, P.; Walfridsson, J.; Forsberg Nilsson, K.; Hammarström, L. G. J.; Ernfors, P. *Cell* **2014**, *157*, 313–328.

(3) Karim, R.; Palazzo, C.; Evrard, B.; Piel, G. *J. Control. Release* **2016**, *227*, 23–37.

(4) Hawkins, B. T.; Davis, T. P. *Pharmacol. Rev.* **2005**, *57*, 173–185.

(5) Prados, M. D.; Byron, S. A.; Tran, N. L.; Phillips, J. J.; Molinaro, A. M.; Ligon, K. L.; Wen, P. Y.; Kuhn, J. G.; Mellinghoff, I. K.; De Groot, J. F.; Colman, H.; Cloughesy, T. F.; Chang, S. M.; Ryken, T. C.; Tembe, W. D.; Kiefer, J. A.; Berens, M. E.; Craig, D. W.; Carpten, J. D.; Trent, J. M. *Neuro. Oncol.* **2015**, *17*, 1051–1063.

(6) Stavrovskaya, A. A.; Shushanov, S. S.; Rybalkina, E. Y. *Biochem.* **2016**, *81*, 91-100.

(7) Eguchi, Y.; Srinivasan, A.; Tomaselli, K. J.; Shimizu, S.; Tsujimoto, Y. *Cancer Res.* **1999**, *59*, 2174–2181.

(8) Galluzzi, L.; Zamzami, N.; La, T. De; Rouge, M.; Lemaire, C.; Brenner, C.; Kroemer, G. *Apoptosis* **2007**, *13*, 803–813.

(9) Orrenius, S.; Zhivotovsky, B.; Nicotera, P. *Nat. Rev. Mol. Cell Biol.* **2003**, *4*, 552–565.

(10) Mizushima, N. *Genes Dev.* **2007**, *21*, 2861–2873.

(11) Cuenda, A. *Int. J. Biochem. Cell Biol.* **2000**, *32*, 581–587.

(12) Ding, J.; Hall, D. G. *Angew. Chem. Int. Ed.* **2013**, *52*, 8069–8073.

(13) Kim, Y.-R.; Hall, D. G. *Org. Biomol. Chem.* **2016**, *14*, 4739–4748.

(14) Calaway, P.K., Henze, H. R. *J. Am. Chem. Soc.* **1939**, *61*, 1355–1358.

(15) Buu-Hoï N.P., Royer R., Xuong, N. D. *J. Org. Chem* **1953**, *18*, 1209–1224.

(16) Hegedus, L. S. *Transition metals in the synthesis of complex organic molecules*, 3rd ed.; Söderberg, B. C. G., Ed.; University Science Books: Sausalito, Calif., **2010**.

(17) Duan, Z.; Li, X.; Huang, H.; Yuan, W.; Zheng, S.-L.; Liu, X.; Zhang, Z.; Choy, E.; Harmon, D.; Mankin, H.; Hornicek, F. *J. Med. Chem.* **2012**, *55*, 3113–3121.

(18) Staehelin, A. *Comptes rendus Hebd. des séances l ' Académie des Sci. Série B* **1972**, *275*, 262–264.

(19) Cassebaum, H.; Modest, J.; Bergmann, F.; Smuszkovicz, J. *Dehydrasemodelle auf Chinon- und Isatin-Basis,* **1957**, *4207*, 138–139.

(20) Garalene, V.N., Stakyavichus, A.P., Mazhilis, L. Yu., Sapragonene, M.S., Risyalis, S.P., Terentyev, P.B., Rotchka, V.-S. M. In *Search of New Medecines*; 1986; pp 1305–1308.

(21) Karpenko, A. S.; Shibinskaya, M. O.; Zholobak, N. M.; Olevinskaya, Z. M.; Lyakhov, S. A.; Litvinova, L. A.; Spivak, M. Y.; Andronati, S. A. *Pharm. Chem. J.* **2006**, *40*, 595–602.

(22) Chang, D.; Gu, Y.; Shen, Q. *Chem. Eur. J.* **2015**, *21*, 6074–6078.

(23) Holla, B. S.; Poojary, K. N.; Poojary, B.; Bhat, K. S.; Kumari, N. S. *Indian J. Chem., Sec B,* **2005**, *44*, 2114–2119.

(24) Qin, J.; Li, F.; Xue, L.; Lei, N.; Ren, Q.; Wang, D.; Zhu, H. *Acta. Chim. Slov.* **2014**, 170–176.

(25) Wang, L. M.; Hu, L.; Chen, H. J.; Sui, Y. Y.; Shen, W. *J. Fluor. Chem.* **2009**, *130*, 406–409.

(26) Molina, P., Alajarin, M., Sanchez-Andrada, P. *Synthesis (Stuttg).* **1993**, 225–228.

(27) Klein, L. L.; Tufano, M. D. *Tetrahedron Lett.* **2013**, *54*, 1008–1011.

Chapter 3. Expansion of the Unique Borylative Migration to Five-membered Heterocycles

3.1 Introduction

As an organic chemist, to create and develop a synthetic method that can transform a diverse range of substrates with exceptional control is, for some, the penultimate achievement. The ability to transform an existing functional group or install a new functional group with chemo-, regio- and perhaps enantio- or diastereo- selectivity is not trivial. This challenge has resulted in a tremendous cumulative effort by chemists to develop methods that can manipulate molecules and achieve the desired connection or disconnections.

Often times, method development is driven by the need for synthetic methods to access a specific scaffold that is present in biologically active and medicinally important molecules. One such class of pervasive molecular skeletons are oxygen or nitrogen containing six- and five-membered rings. One notable class of tetrahydrofuran structure-based natural products are the annonaceous acetogenins. These compounds are isolated from *Asimina triloba,* also known as paw paw; which is a plant indigenous to the Eastern, Southern, and Midwestern United States that can produce edible fruit similar to a banana.[1] These compounds are potent inhibitors of adenosine triphosphate (ATP) production and have antitumor, pesticidal, antimalarial, antiviral and antimicrobial effects.[2] Select examples are illustrated in Figure 3-1. Notably, asimicin, bullatacin and trilobacin have all been synthesized in the laboratory.[3,4]

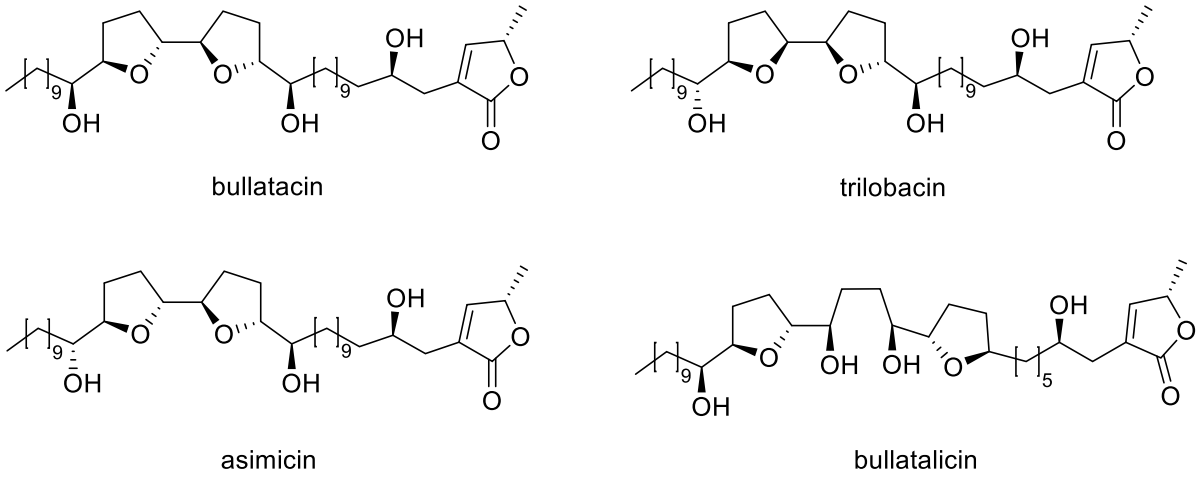

Figure 3-1: Structures of a select few compounds from the annonaceous acetogenin family of bioactive molecules.

In this chapter, efforts towards application and expansion of the unique borylative migration of enol perfluorosulfonates to access tetrahydrofuryl- and pyrrolidinyl- chiral allylic boronate building blocks will be described.

3.2 Catalytic Enantioselective Synthesis of Pyranyl- and Piperidinyl- Chiral Allylic Boronate and the Proposed Mechanism of the Borylative Migration

As previously described in Chapter 1, synthesis of the pyranyl- and piperidinyl- chiral allylic boronate was carefully optimized to provide a highly efficient and enantioselective transformation.[5,6] After careful study of the catalyst and catalyst loading, chiral ligand and chiral ligand loading, amine base, solvent, concentration and temperature; a set of conditions for the pyranyl- chiral allylic boronate and another set of conditions for the piperidinyl- chiral allylic boronate were established. [5,6] Additionally, the synthetic utility and versatility of these chiral allylic boronate intermediates was demonstrated by the highly diastereoselective aldehyde allylboration[6] which was ultimately critical to the unified synthesis of all for diastereomers of mefloquine.[7]

Furthermore, these six-membered heterocyclic allylic boronate intermediates can be transformed via ligand controlled regioselective and enantioselective Suzuki-Miyaura cross-coupling.[8]

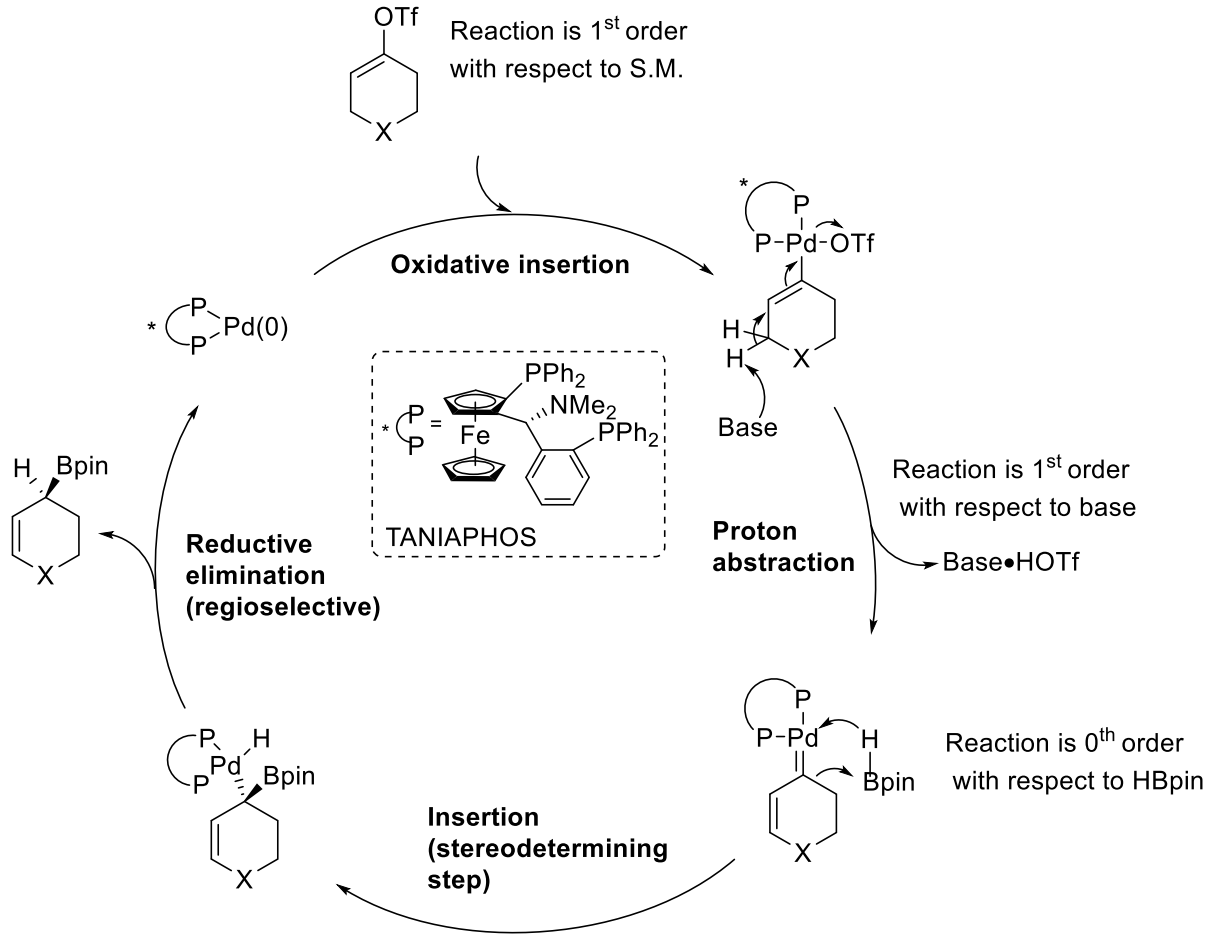

Scheme 3-1: Proposed catalytic cycle of the borylative migration transformation.

Of note, the mechanism for this powerful method is currently being investigated both experimentally and computationally, in collaboration with Professor Claude Legault (Université de Sherbrooke). The currently proposed mechanism is illustrated in Scheme 3-1.

3.3 Synthetic Strategies Towards Tetrahydrofuryl- Scaffolds

Synthetic strategies to form these scaffolds with control of the substituent pattern and stereoselectivity are of great interest. Several synthetic methods have been developed and the synthesis of substituted tetrahydrofurans is achievable by a diverse range of mechanisms; for example, intramolecular acetalization, electrocyclic cycloaddition, radical cyclization, Lewis acid catalyzed and transition metal catalyzed cyclization. A selection of recent reports will be briefly summarized to provide an overview.

In 1993, Klang and co-workers reported a general synthesis of tetrahydrofuryl ethers that took advantage of the equilibrium between 4-hydroxybutanal and its cyclic hemi-acetal tautomer 2-hydroxytetrahydrofuran (Scheme 3-2).[9] Subsequent treatment with a primary or secondary alcohol in the presence of catalytic sulphuric acid afforded the tetrahydrofuryl ether. Although this early method is very atom economical, it offers no stereoselectivity and only substitution at the α-carbon with a very limited substituent scope.

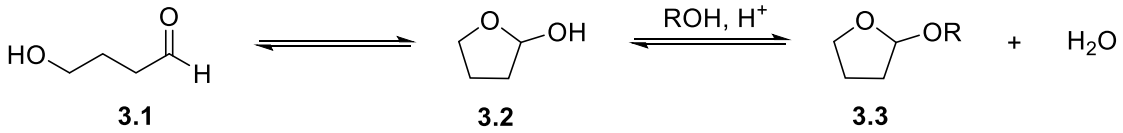

Scheme 3-2: Formation of tetrahydrofuryl ethers by Klang and co-workers.

Notably, in 2014 the Sun group reported the catalytic enantioselective desymmetrization of a prochiral 1,3-diol tethered to an acetal (Scheme 3-3). Compound **3.4** undergoes an intramolecular mono-transacetalization to cyclize and form a cyclic acetal that can readily provide substituted tetrahydrofurans (upon reduction of the cyclic acetal **3.5**).[10] The nature of the substituent R ranged

from *ortho*-, *para*- bromo-substituted benzyl moieties, thiophenyl, indole, cyclohexyl and di- or tri- methoxy-substituted benzyl groups. Notably, this method provides an all carbon substituted quaternary stereocenter at the remote δ-carbon to the acetal group.

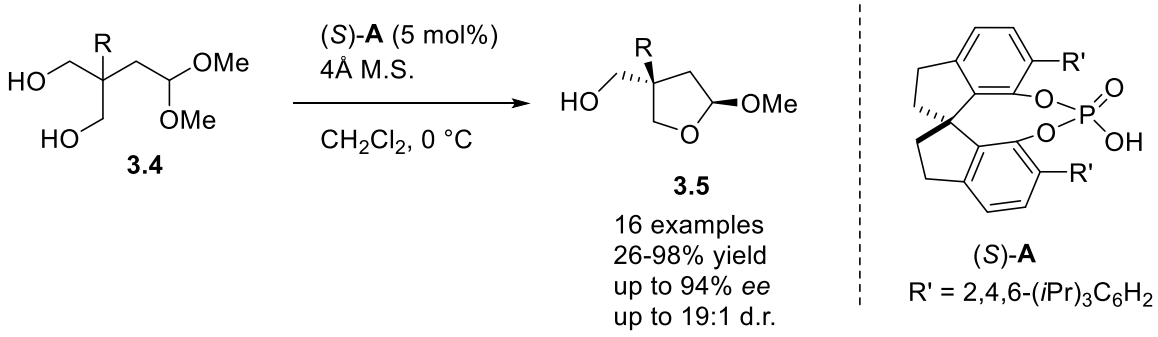

Scheme 3-3: Synthesis of δ-substituted tetrahydrofuran by Sun and co-workers.

Moreover, Fox and co-workers reported a highly diastereo- and regio- selective multicomponent cycloaddition (Scheme 3-4).[11] Treatment of **3.7** with catalytic dirhodium tetrapivalate and aldehyde **3.6** produces the reactive carbonyl ylide that participates in a [3+2] cycloaddition with alkyne **3.8** as the exogenous alkene dipolarophile. Although this method is quite tolerant to a range of substrates, it is not enantioselective.

More recently, the Feng group published their efforts in developing a catalytic asymmetric [3+2] cycloaddition of heterosubstituted alkenes with oxiranes (Scheme 3-5).[12] Oxiranes, with the correct substituents, exhibit efficient and selective C-C bond cleavage to provide an atom-economical substrate for the generation of carbonyl ylides.

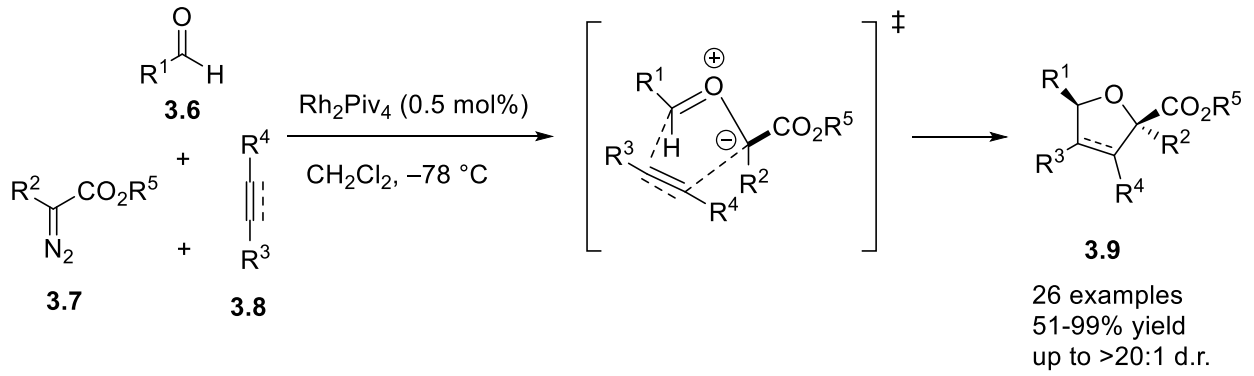

Scheme 3-4: Synthesis of substituted tetrahydrofurans via [3+2] cycloaddition by Fox and co-workers.

With the use of an optimized chiral *N,N'*-dioxide-Ni(II) catalyst system, Feng and co-workers were able to synthesize twenty-seven examples of chiral substituted tetrahydrofurans in up to 99% yield, 92:8 d.r. and 99% ee. The scope of the heterosubstituted alkenyl dipolarophile **3.10** included cyclic vinyl ethers and vinyl thiirane.

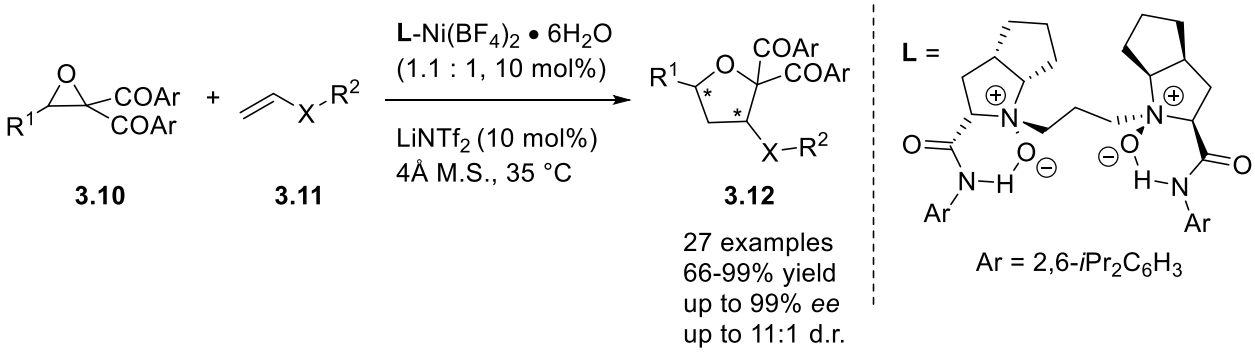

Scheme 3-5: Synthesis of substituted tetrahydrofurans via oxirane cleavage and subsequent [3+2] cycloaddition by Feng and co-workers.

An alternative strategy to accessing substituted tetrahydrofuran scaffolds is through the use of radical transformations. In 2013, Nicewicz and co-workers investigated the synthesis of substituted

tetrahydrofurans by catalytic polar-radical-crossover cycloaddition of alkene **3.14** and allylic alcohol **3.13** (Scheme 3-6).[13] Of interest, the mechanism of the catalytic cycle entails the single-electron oxidation of the alkene to provide the corresponding radical cation. Subsequently, the allylic alcohol adds with anti-Markovnikov selectivity and the intermediate would be poised to undergo a 5-*exo* radical cyclization with the pendent alkene. Ultimately, these conditions could provide the substituted tetrahydrofuran scaffold under mild conditions, however with only moderate diastereoselectivity, limited functional group compatibility and considerably long reaction times.

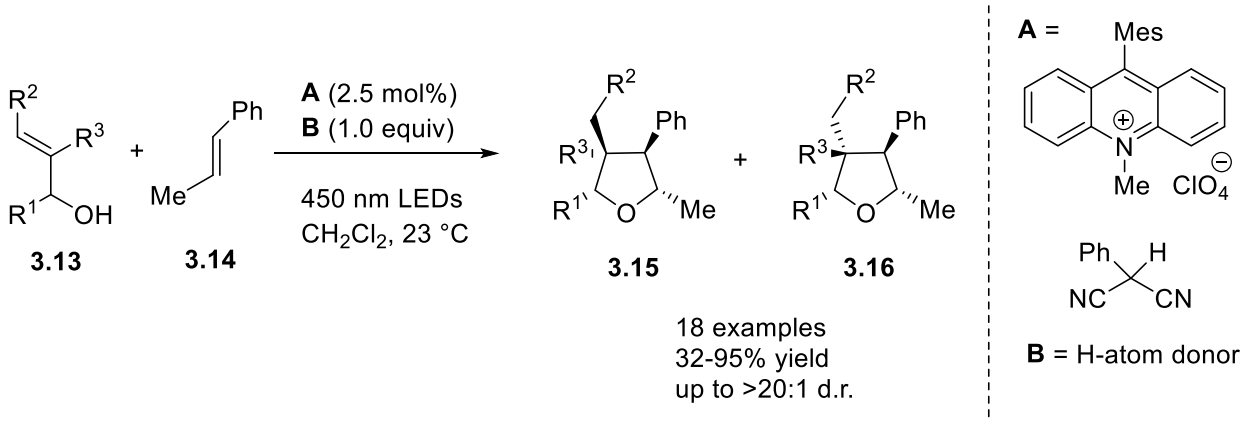

Scheme 3-6: Synthesis of substituted tetrahydrofurans via polar-radical-crossover cycloaddition by Nicewicz and co-workers.

Furthermore, the preparation of substituted tetrahydrofurans can also be achieved through a Lewis acid catalyzed cyclization reaction. The Cheng Group in 2001 published their efforts in assembling tetrahydrofurans from aldehydes and homo-allylic alcohols using the Lewis acid $In(OTf)_3$ (Scheme 3-7).[14] Their investigations revealed that increasing the temperature from 0 to 40 °C would provide

the thermodynamic isomer **3.18** over the kinetic product **3.19**. Thus, this method provided a divergent pathway to two differently substituted tetrahydrofuran cores.

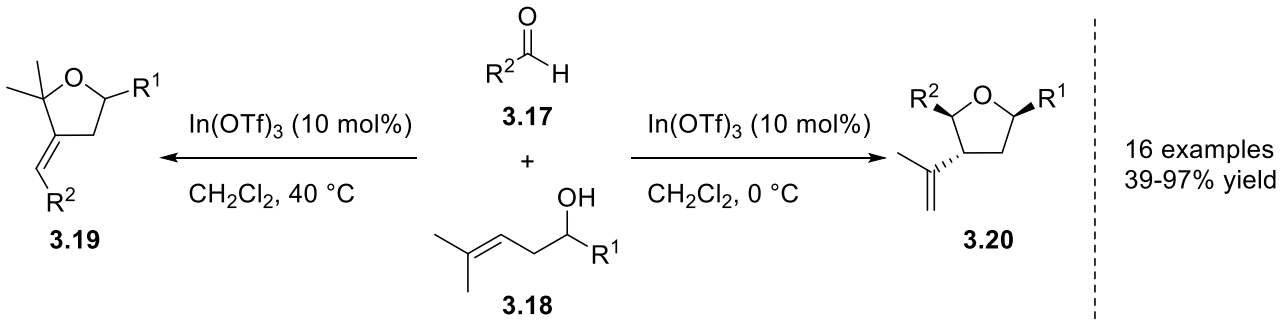

Scheme 3-7: Synthesis of substituted tetrahydrofurans via Lewis Acid catalyzed cyclization by Cheng and co-workers.

More recently, the Saikia Group in 2014 reported their method for the stereoselective synthesis of *cis*-2,5-tetrahydrofurans using a Lewis acid catalyzed Prins cyclization reaction (Scheme 3-8).[15] These authors observed good diastereoselectivity and the substrate scope of this transformation was tolerant of a decent range of functional group. However, the inherent disadvantage of this method is that the substrate must be set-up to undergo the specific cascade reaction. Additionally, the progression towards enantiospecific conditions is not trivial.

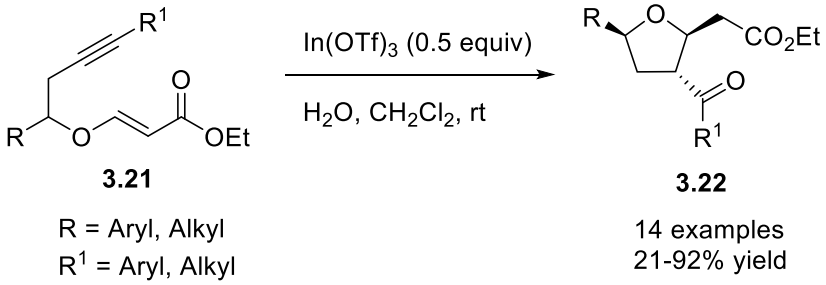

Scheme 3-8: Synthesis of substituted tetrahydrofuran via Lewis Acid catalyzed Prins cyclization by Saikia and co-workers.

Furthermore, in 2007 Hall and co-workers published a method to access all-cis trisubstituted tetrahydrofurans and 1,1,2,4-tetrasubstituted tetrahydrofurans in very high diastereo- and enantio-selectivity (Scheme 3-9).[16] One step preparation of **3.23** with subsequent allylation affords intermediate **3.25**; condensation with an aldehyde or ketone provides enantiomerically enriched trisubstituted and tetrasubstituted tetrahyrdofurans respectively.

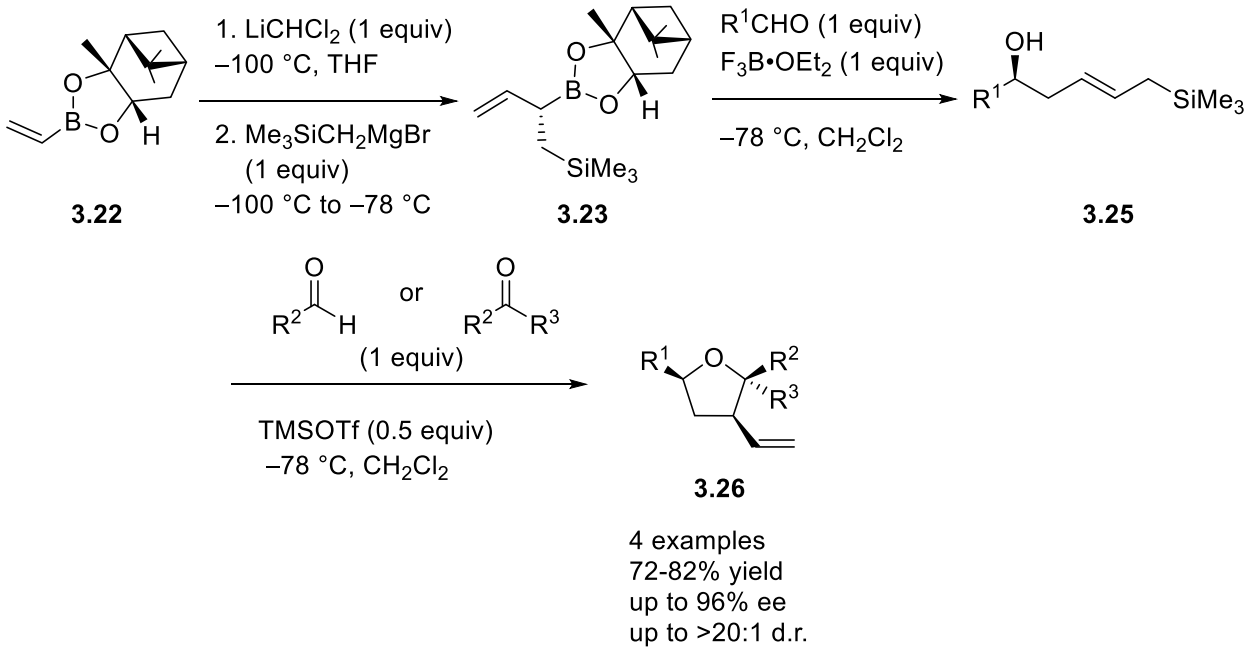

Scheme 3-9: Synthesis of substituted tetrahydrofuran via allylation by Hall and co-workers.

Lastly, in 2015 Spilling and co-workers published their efforts towards intramolecular trapping of hemiacetals with a palladium π-allyl complex (Scheme 3-10).[17] Unfortunately, this report describes a rather unimpressive transfer of chirality from an enantioenriched starting material to the cyclic product and with only a slight diastereoselective control of the transformation (*ee* of the product is not reported and the best example of diastereoselectivity is a 3:1 d.r.). This account does

illustrate the difficulties and challenges in enantioselectively synthesizing substituted tetrahydrofuran cores.

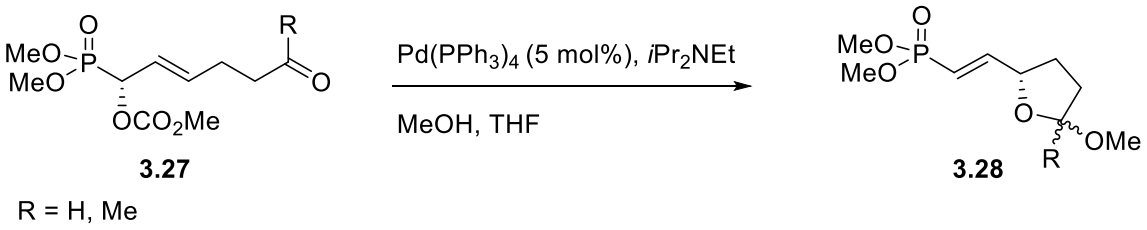

Scheme 3-10: Synthesis of substituted tetrahydrofurans by intramolecular trapping hemiacetals by Spilling and co-workers.

3.4 Synthetic Strategies Towards Pyrrolidinyl- Scaffolds

The chemistry commonly used for the synthesis of substituted pyrrolidines shares some similarities to the synthetic strategies used to access substituted tetrahydrofurans; however, the two heterocycles are characteristically different because of the nature of the heteroatom. This section will summarize a small collection of recent reports for the synthesis of substituted pyrrolidines, again, with an effort to highlight the various synthetic strategies that have been used. The synthesis of pyrrolidines has been achieved through electrocyclic cycloaddition, radical cyclization, Lewis acid catalyzed and transition metal-catalyzed cyclization.

In a similar fashion to the three-component cycloaddition reported by Fox in 2009, the Aron group published their work to achieve a diastereo- and enantio- selective three-component coupling to highly substituted pyrrolidines (Scheme 3-11).[18] This system uses catalytic amounts of Cu(II) salts complexed with chiral 1,2-diamines and racemic or achiral amino acid ester **3.29**, aryl aldehyde **3.30** and alkenyl starting materials. The mechanism of this transformation presumably occurs *via*

in situ formation of the imine, subsequent formation of the azomethine ylide with the aid of the chiral Cu(II)-ligand complex leads to a [3+2] cycloaddition with alkenyl dipolarophiles. Highly substituted pyrrolidine were obtained with good enantio- and diastereo- selectivity, however the substituents and thus the substrate scope was quite limited.

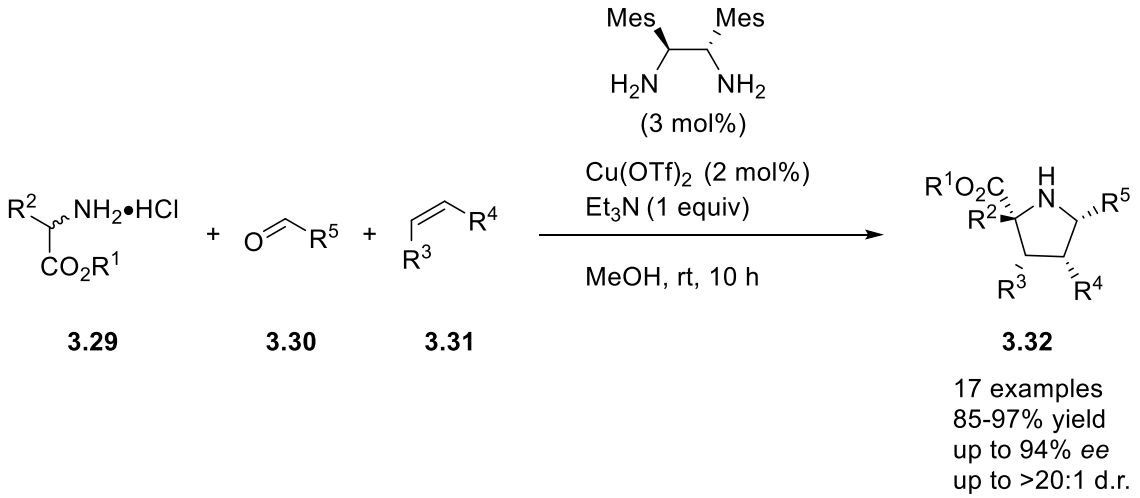

Scheme 3-11: Synthesis of substituted pyrrolidines by three component coupling by Aron and co-workers. Mes = mesityl

In contrast, Renaud and co-workers developed a three-component system to access pyrrolidines *via* a radical carboazidation with subsequent reductive amination sequence (Scheme 3-12).[19] Although this process is moderately efficient (yields between 52%-99%) and atom economical, it is neither catalytic nor enantioselective and only provided moderate diastereoselectivity (only two examples were reported with 72% *dr* and 88% *dr*).

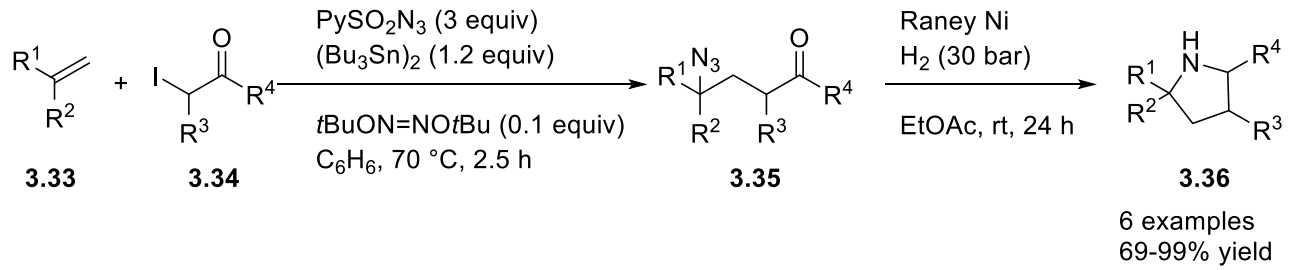

Scheme 3-12: Synthesis of substituted pyrrolidines via a radical carboazidation by Renaud and co-workers.

Furthermore, the Toste Group reported a method to access optically enriched 3,4-disubstituted pyrrolidines (Scheme 3-13).[20] With the use of a Lewis acidic gold catalyst and depending on the chiral ligand, the transformation of the allenene substrate can effectively undergo two distinct pathways. One optimized pathway accesses γ-lactams in good yield and *ee*; in contrast, the alternative pathway would provide chiral 3,4-disubstituted pyrrolidines.

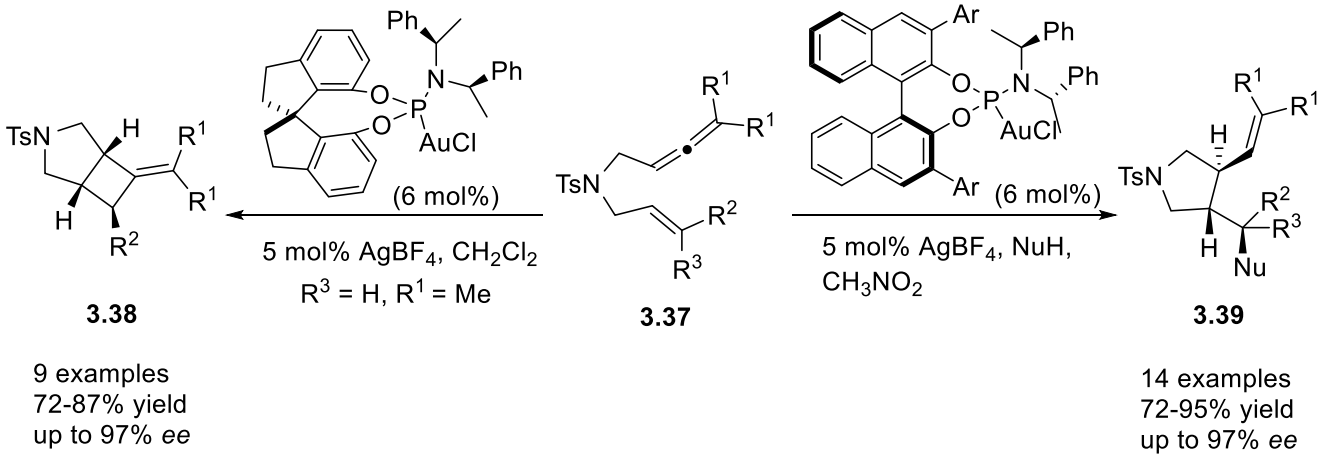

Scheme 3-13: Synthesis of substituted pyrrolidines using a gold catalyst by Toste and co-workers.

Lastly, in 2012 Trost and Silverman published a protocol for the enantioselective palladium-catalyzed [3+2] cycloaddition of trimethylenemethane with imines (Scheme 3-14).[21] To summarize their efforts, *N*-aryl imines, and *N*-Boc imines with various aryl and heteroaryl substituents was well tolerated (23 examples). Expanding the substrate scope of the trimethylenemethane coupling partner **3.41**, a cyano-substituted partner was also investigated. With the cyano moiety, more electron rich imines were also suited to this transformation to afford products of type **3.42** as the major isomer.

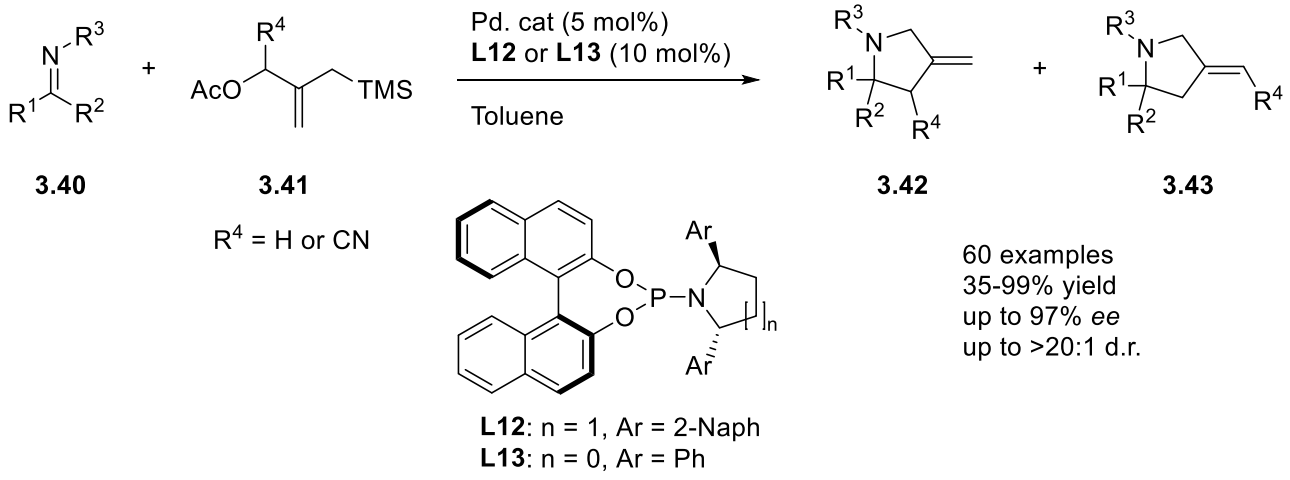

Scheme 3-14: Synthesis of substituted pyrrolidines by a palladium catalyzed [3+2] cycloaddition by Trost and co-workers.

In summary, there are a variety of processes to access substituted tetrahydrofuryl- and pyrrolidinyl-scaffolds. All of the above synthetic strategies are focused on the formation, or cyclization, of the five-membered heterocycle. Thus, stereochemical -control would ultimately be dependent on harnessing the ring closing event. This significantly limits the ability of any of the aforementioned methods to be applied to a wide range of substrates to achieve the desired transformation.

3.5 Expanding the Scope of the Catalytic Enantioselective Borylative Transformation Towards the Tetrahydrofuryl- and Pyrrolidinyl- Scaffolds

Taking into consideration the above synthetic strategies to access the tetrahydrofuryl- and pyrrolidinyl- scaffolds, there is a paucity of methods in an organic chemist's toolbox for a general method that can catalytically and asymmetrically provide substituted five-membered heterocycles. Specifically, for the selected examples of tetrahydrofuryl and pyrrolidinyl scaffold synthesis, the underlying strategy is to control the stereochemistry of the molecule during the formation of the heterocyclic ring. This strategy is severely limited in that either the acyclic substrate must contain stereogenic centres or, if the stereoschemistry is induced intermolecularily by a chiral ligand or catalyst system, the substrate needs to be tailored for the reaction parameters. Additionally, the substitution pattern around the heterocycle is pre-determined by the substrates.

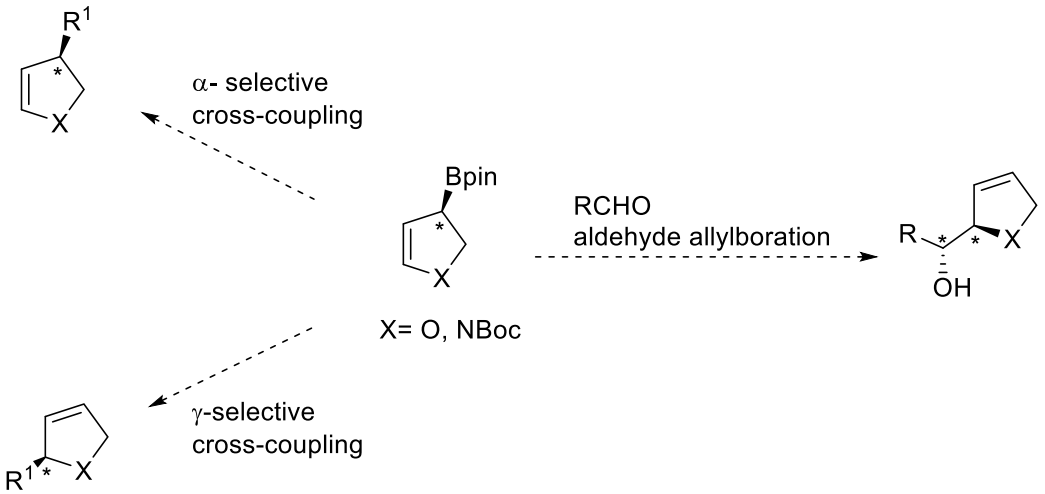

Scheme 3-15: Potential synthetic applications of pyrrolidinyl- and tetrahydrofuryl-allylic boronates prepared by catalytic enantioselective borylative migration.

A recent literature search failed to reveal any facile synthetic routes to access enantio-enriched tetrahydrofuryl- and pyrrolidinyl- allylic boronates and as such these methods are under developed. Considering the synthetic utility of the piperidinyl- and pyranyl- allylic boronate intermediates, it is worthwhile to explore this area of research. This method could provide a highly efficient and enantioselective route to substituted tetrahydrofurans and pyrrolidines.

3.6 Synthesis of Starting Material

The pyranyl and piperidinyl triflate have been synthesized using *N*-phenyl-bis(trifluoromethanesulfonimide) as illustrated in Scheme 3-16. Of note, the product is acid-sensitive and purification via flash column chromatography must be performed with silica gel neutralized by triethylamine in the eluent system. Moreover, the triflating by-product unexpectedly complicated the purification of the alkenyl triflate because of a difficult separation.

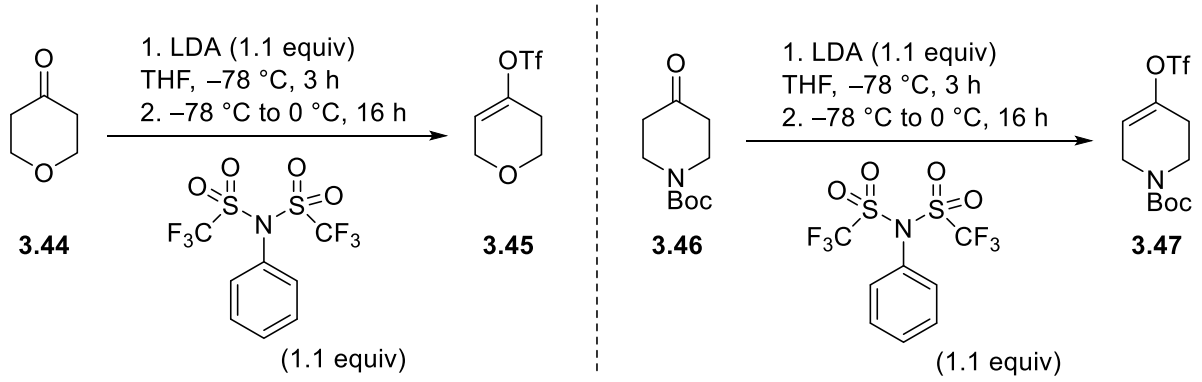

Scheme 3-16: Synthesis of alkenyl triflate substrates.

Unlike the pyranyl and piperidinyl substrates, the five-membered heterocycles present an additional problem of chemo- and regio- selectivity (illustrated by Scheme 3-17). With the six-membered heterocycles, it is immediately apparent that the symmetry of the molecule simplifies

the generation of the prerequisite alkenyl triflate or alkenyl nonaflate starting material. However, dihydrofuran-3-one and *N*-boc-3-pyrrolidinone features two distinctive types of α-methylene protons (in relation to the ketone moiety). Presumably, the desired alkenyl triflate **3.53** would be preferentially formed for the *N*-boc-3-pyrrolidinone substrate if a bulky kinetic base was used. With regard to the dihydrofuran-3-one substrate, the slight difference in acidity between the two sets of α- methylene protons could be sufficient to provide, with careful addition and selection of base, selective deprotonation and subsequent enolate formation (**3.50**).

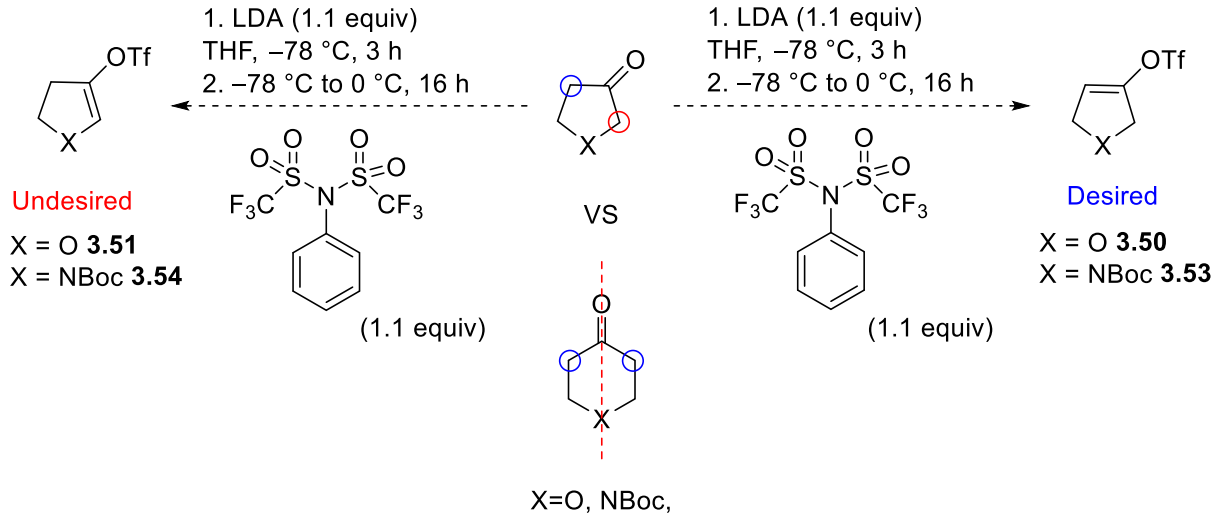

Scheme 3-17: Potential regio- and chemo-selectivity issues with the five-membered heterocyclic substrates.

Although **3.49** is commercially available, its preparation was achieved as illustrated in Scheme 3-18 via the oxidation of **3.48**. Care must be taken upon removal of organic solvent because the product is highly volatile.

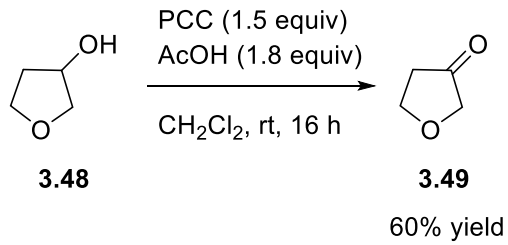

Scheme 3-18: Synthesis of dihydro-3(2H)-furanone precursor **3.45**.

Attempts to selectively deprotonate the carbonyl α-protons and trap the corresponding enolate with *N*-phenyl-bis(trifluoromethanesulfonimide) to provide **3.50** proved unsuccessful (Scheme 3-18). Monitoring the reaction by thin layer chromatography (TLC) showed complete consumption of the starting material, however attempts to isolate **3.50** only provided trace yields. Running a 2D TLC that was pre-neutralized with triethylamine showed that the product decomposes upon treatment with silica. Great effort was spent in trying to obtain **3.50** efficiently and in good yield. To summarize, some of the parameters that were explored include temperature, concentration of the solution of reagents for addition and equivalents of the base employed. Ultimately, the compound was not suitable for the requisite work-up and purification conditions.

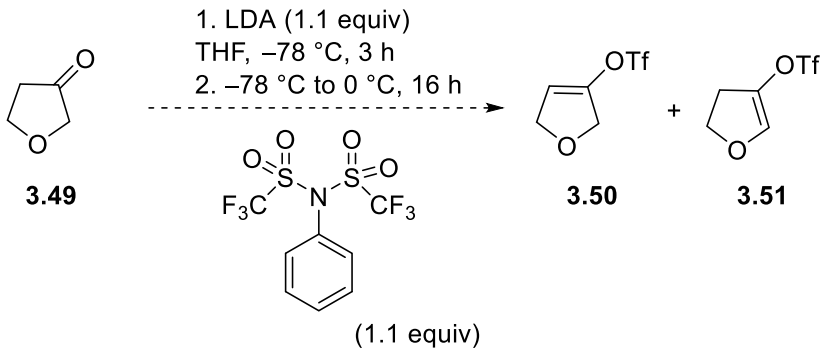

Scheme 3-19: Synthesis of tetrahydrofuran alkenyl triflate substrate **3.50**.

Concurrently, efforts to transform *N*-boc-3-pyrrolidinone, adapted from a protocol described by Venier and co-workers (Scheme 3-20),[22] to the corresponding alkenyl triflate provided a mixture of **3.53** and **3.54**. Several attempts to purify and separate the two isomers were unsuccessful. Correspondence with the authors revealed that the isomers are evidently inseparable.

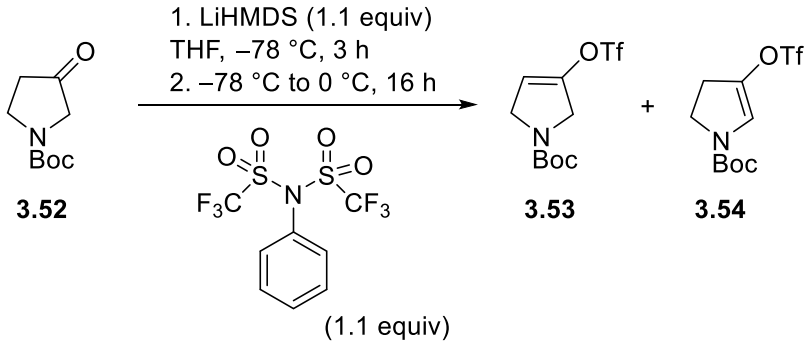

Scheme 3-20: Synthesis of pyrrolidine alkenyl triflate substrate **3.53** and **3.54**.

Fortuitously, the piperidinyl alkenyl nonaflate **3.55** was recently described in our group to be an excellent substrate for the borylative migration transformation.[23] Synthesis of **3.55** has proven to be more facile than **3.47**, as compound **3.55** is a more stable compound and thus is easier to handle

and purify. Optimistically, the hope was that this chemistry would be more readily transferrable to **3.52** than the above described triflation conditions. Additionally, the triflating agent is more expensive than perfluorobutanesulfonyl fluoride (NfF) and therefore the use of NfF is preferable.

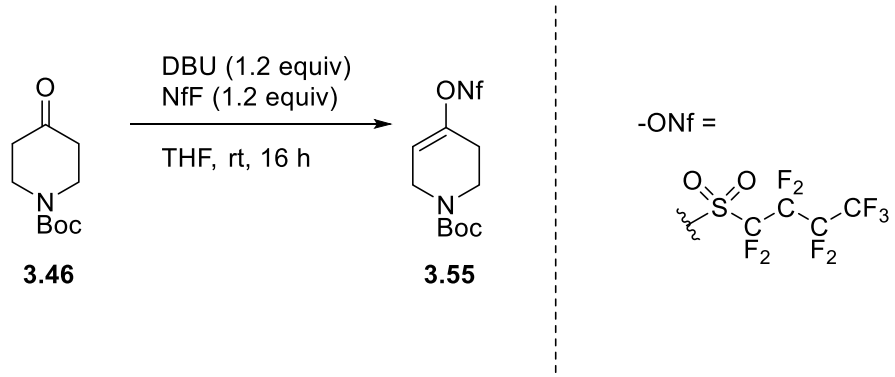

Scheme 3-21: Synthesis of piperidine alkenyl nonaflate substrate **3.55**.

Transformation of *N*-boc-3-pyrrolidinone into the more viable alkenyl nonaflate substrate was achieved with minimal optimization. Illustrated in Scheme 3-22, **3.56** was obtained in good yield and on gram scale (3.5 g). This substrate is also easily purified via flash column chromatography.

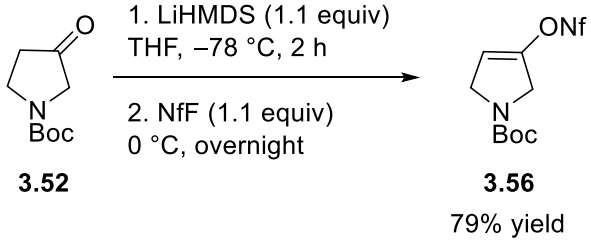

Scheme 3-22: Synthesis of pyrrolidine alkenyl nonaflate substrate **3.56**.

3.7 Application of the Borylative Migration to Access Pyrrolidinyl- Allyl Boronate

With the alkenyl- nonaflate in hand, **3.56** was subjected to the borylative migration conditions. Under previously optimized racemic conditions[5] for the borylative migration and subsequent

aldehyde allylboration, compound **3.59** was obtained in good yield over two steps (Scheme 3-23). Of note, formation of **3.58** was not observed.

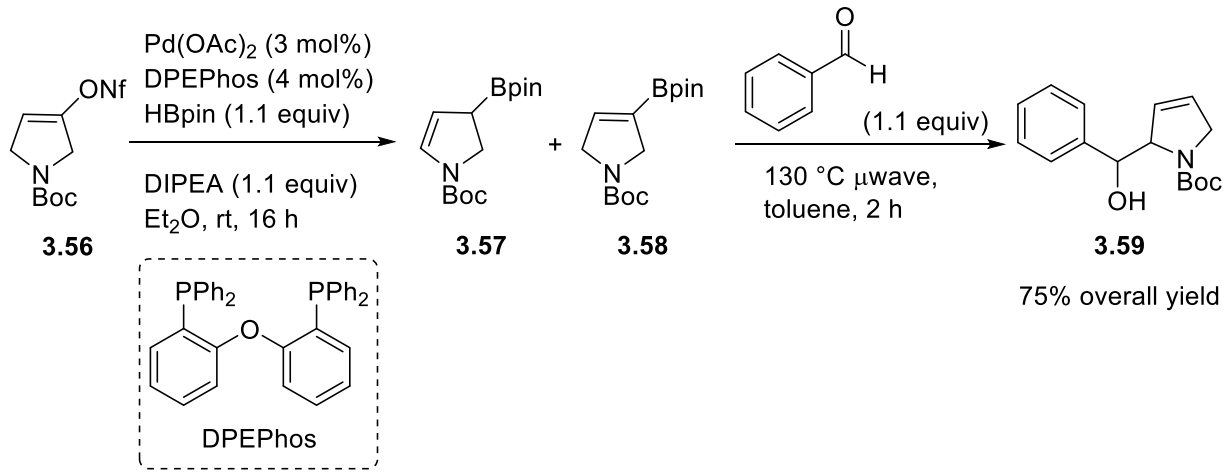

Scheme 3-23: Racemic borylative migration of the pyrrolidinyl substrate **3.56**.

Next, subjecting **3.56** to the previously optimized asymmetric conditions[5] resulted in a complete shut-down of the transformation. Only starting material **3.52** was recovered with no observed conversion to **3.57** or **3.58**. Several trials were performed to confirm this negative outcome.

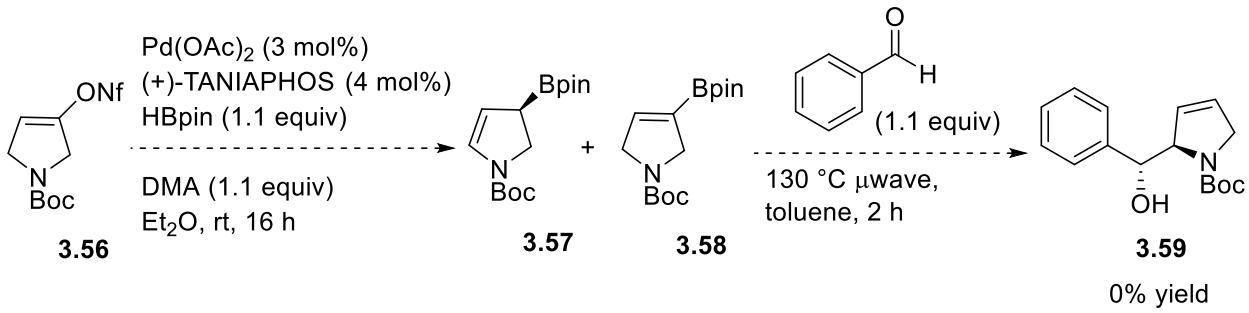

Scheme 3-24: Initial attempt for the enantioselective borylative migration of the pyrrolidinyl substrate **3.56**.

There are several parameters worth exploring for the development of the enantioselective transformation. Previous studies have shown that this chemistry is strongly influenced by the amine base used, the chiral ligand and the solvent. Considering the success of the racemic conditions, a small screening of chiral ligands was explored to establish a starting point for the optimization of a catalytic enantioselective borylative migration reaction.

3.7.1 Exploration of the Ligand Employed in the Catalytic Enantioselective Borylative Migration

The following preliminary results were determined by ^{1}H NMR of the crude reaction mixture after filtering through a short silica plug. It should be noted that the ratio of **3.56** to **3.57** was determined in the absence of an internal standard. The initial ligand screening was conducted using Hunig's base and it is evident that this transformation can occur in the presence of a chiral ligand as illustrated by the, albeit very modest, 7% conversion of **3.56** to **3.57** when TANIAPHOS was employed (Figure 3-2). Of note, for the asymmetric conditions employing the six-membered heterocyclic substrates the optimal base is DMA. The ligand screening was not performed using DMA because the fortuitous outcome of the racemic conditions using Hunig's base (and the subsequent results illustrated in Figure 3-3) suggested that Hunig's base is a more optimal base. The ratio of **3.56** to **3.57**, was improved to 44% and 40% conversion using ligands **III** and **VI** respectively. It would appear that the amine functional group present in TANIAPHOS may hinder the asymmetric variant of this transformation. Additionally, aromatic substituted phosphine groups may be essential as suggested by the negative outcome when ligand **V** was employed. However, further studies are required before a firm conclusion can be made.

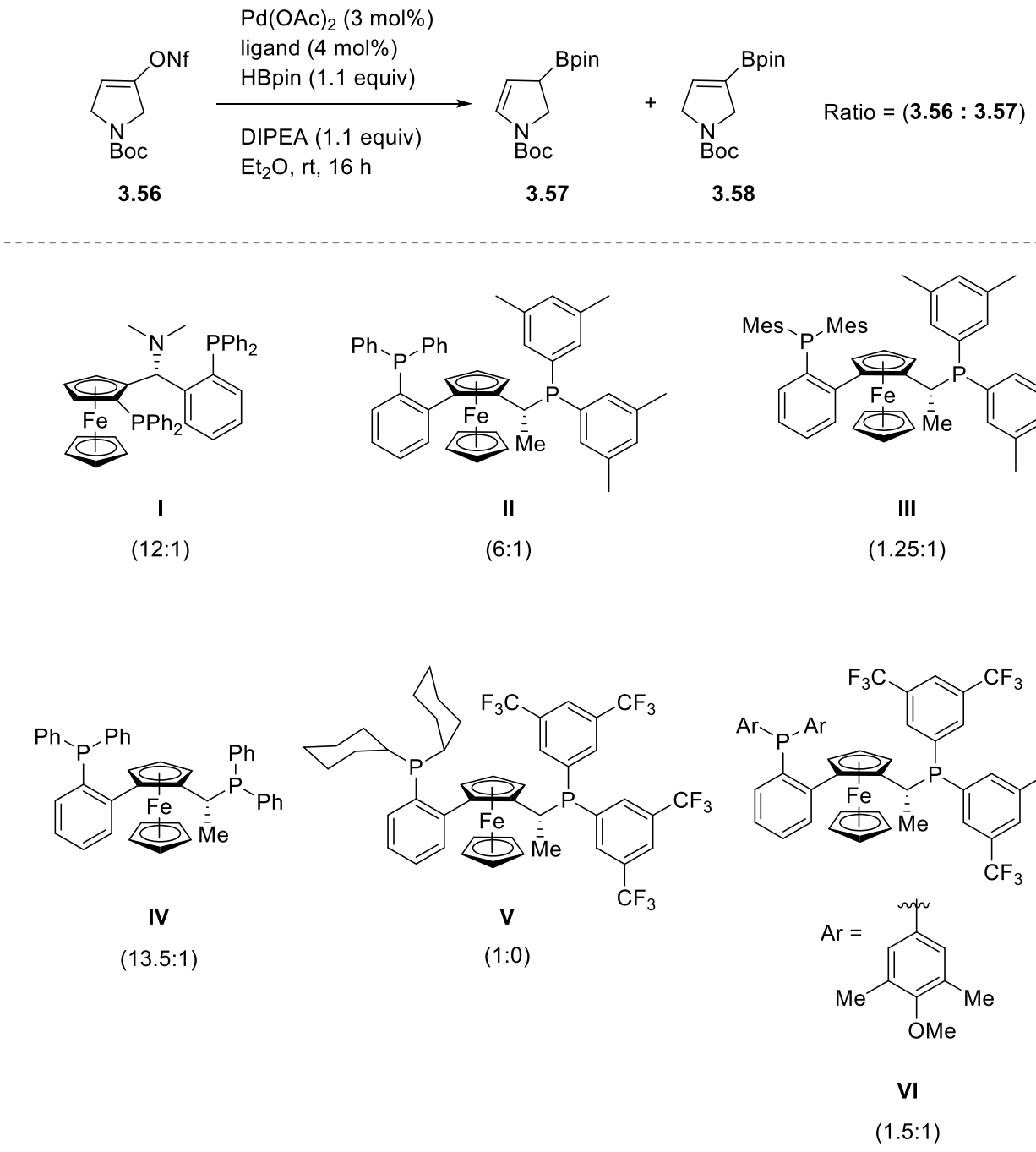

Figure 3-2: Preliminary screening of the chiral ligand for the enantioselective borylative migration of pyrrolidine substrate **3.56**.

3.7.2 Exploration of the Base Employed in the Catalytic Enantioselecitve Borylative Migration

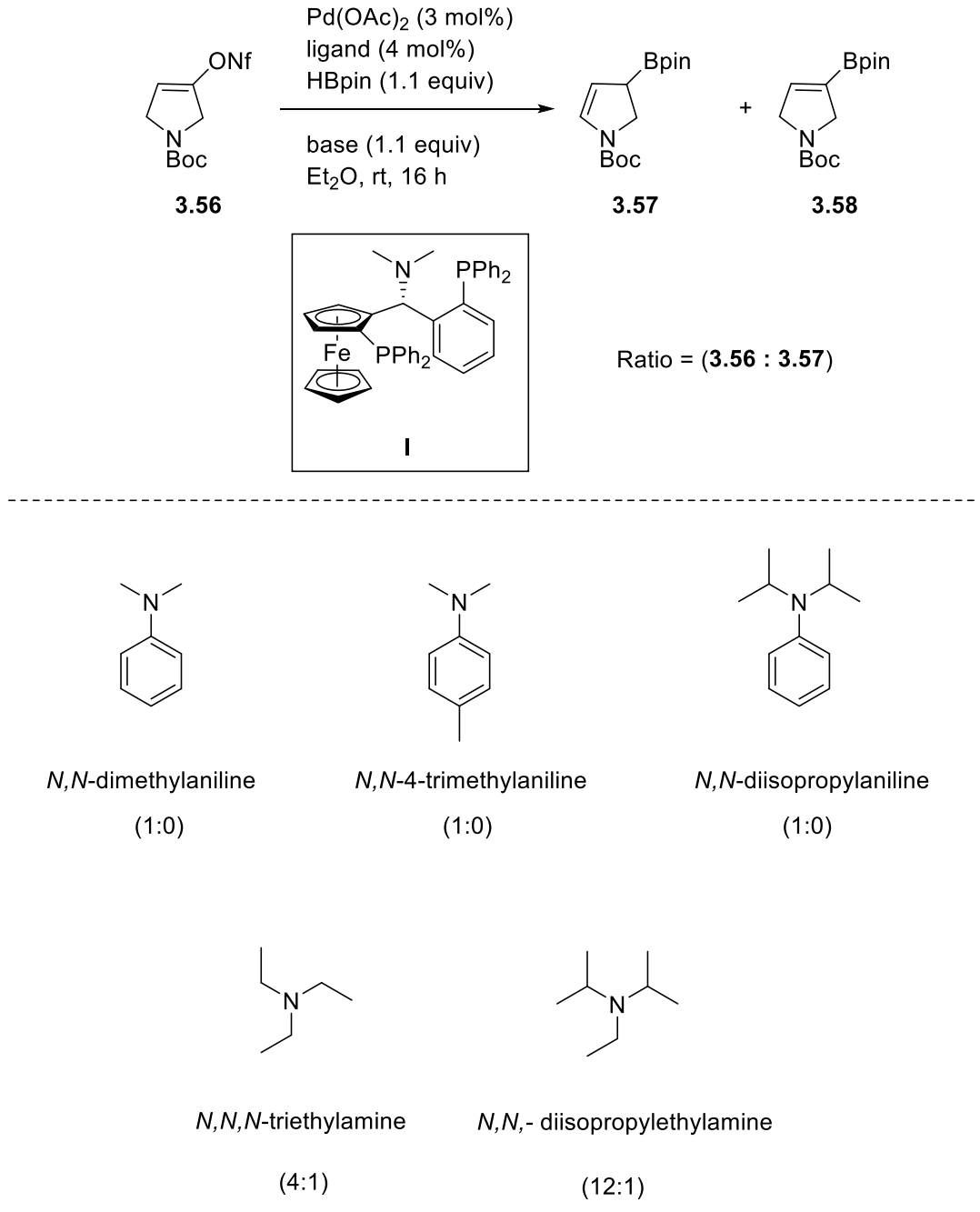

Figure 3-3: Preliminary screening of the amine base for the catalytic enantioselective borylative migration of the pyrrolidine substrate **3.56**.

Next, the amine base was briefly explored. As illustrated in Figure 3-3, it is evident that aniline based amines are detrimental to this reaction when TANIAPHOS is employed. The use of triethylamine improved the conversion of **3.56** to 20%, from the initial screening which afforded a 7% conversion when Hunig's base was employed. It would appear that trialkylamine bases could provide the desired outcome. With this in mind, a second cursory screening of trialkylamine bases employing the more optimal ligands **VI** and **III** was conducted. Summarized in Figure 3-4, the best conversion thus far is 50%. Overall, the small trialkylamine bases performed well. With the relatively few examples it would appear that the reaction is tolerant of bulkier trialkylamines. Although these results are not yet of practical use, the progress towards improving the conversion of **3.56** to **3.57** shows great potential to develop a catalytic asymmetric variant of the borylative migration to access enantioenriched pyrrolidinyl-allyl boronates. Interestingly, throughout these preliminary studies, formation of alkenylboronate **3.58** was not observed.

It is worthy to note that there are other classes of amines that may prove more fruitful. One such class are the pyridine based amines. The pyridine bases did not perform well with the six-membered heterocyclic substrates. However, they are worthwhile to examine considering a proposed hypothesis that π-π interactions may be an influencing factor in enantioselective induction. Another class of amines that may be worth exploring are the secondary amines or dialkylamines. For the initial screening they were not assayed considering the lack of precedence with the six-membered heterocyclic system. Moreover, the inorganic bases such as phosphates, carbonates and hydroxide bases could be another venue to explore. Nonetheless, a comprehensive study will require the consideration of different amine base classes.

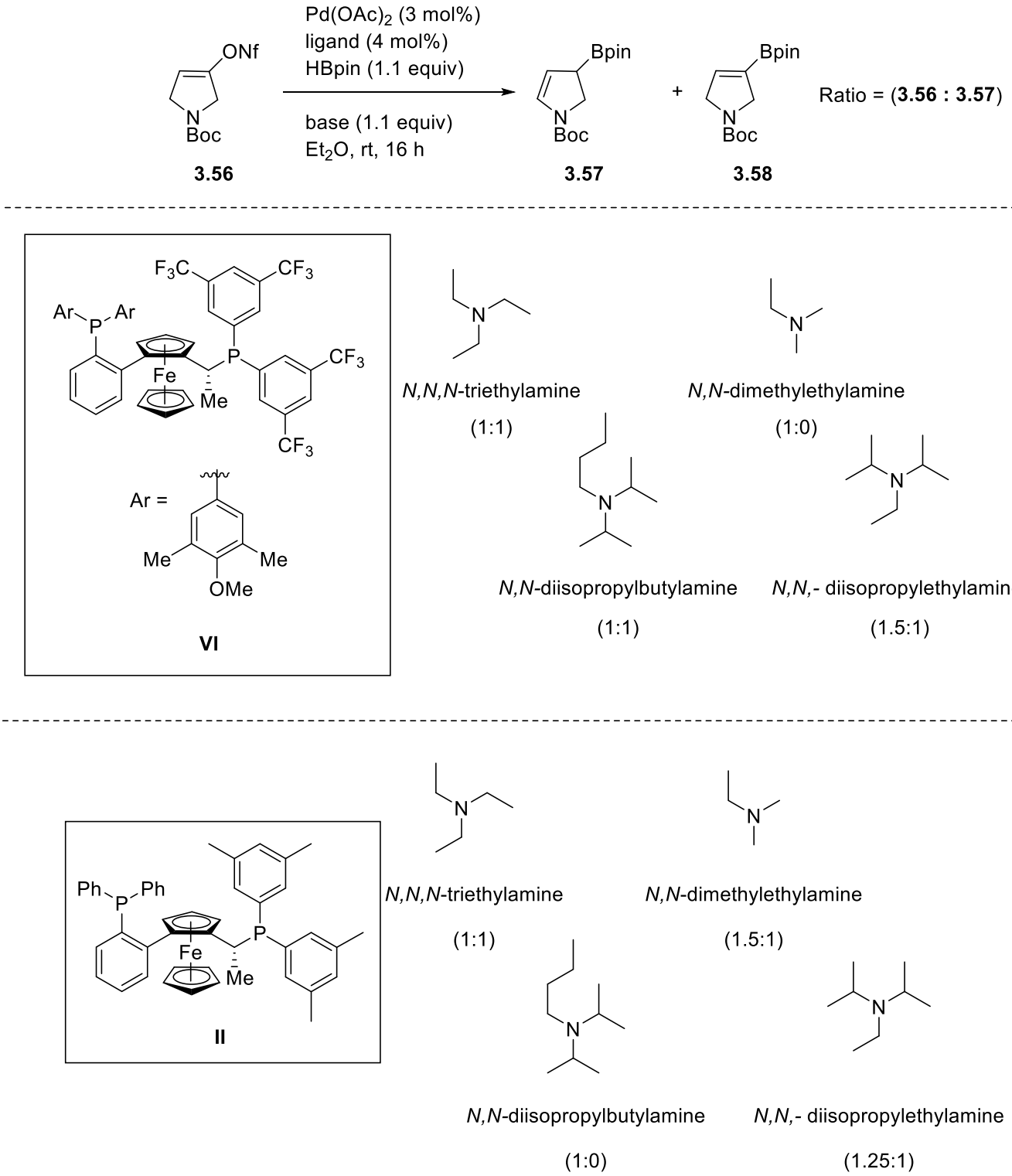

Figure 3-4: Preliminary screening of the amine base for the catalytic enantioselective borylative migration of pyrrolidine substrate **3.56**.

3.7.3 Brief Exploration of the Temperature and Solvent Employed in the Borylative Migration Transformation

Parameters established for the piperidinyl and/or pyranyl substrates were investigated to determine whether the conditions are transferrable to smaller ring substrates. Entry 1 from Table 3-1 is one of the initial conditions employed during the study of the synthesis of the pyranyl allylic boronate.[6] These conditions were detrimental for the reaction of substrate **3.56**. A preliminary solvent screening (entries 2-4) established that the previously optimal solvent dioxane[6] is deleterious to this system. In contrast, the ethereal solvents CPME (cyclopentyl methyl ether) and MTBE (methyl *tert*-butyl ether) afforded a moderate conversion. Heating the reaction to 40 °C noticeably impeded the reaction, even when the more optimal base triethylamine was employed. Preliminary results employing a higher catalyst loading of 5% and chiral ligand of 5.5% provided complete conversion of the starting material **3.56** (Scheme 3-25).

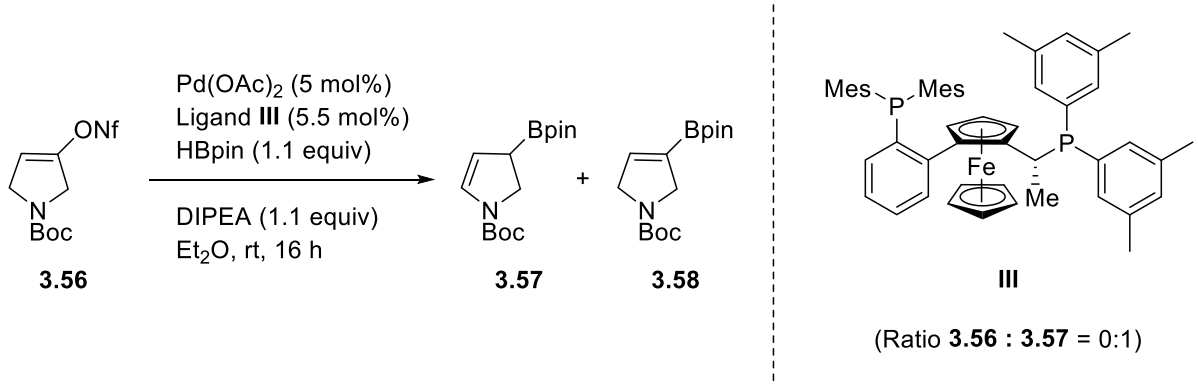

Scheme 3-25: Preliminary screening of the catalyst and ligand loading for the catalytic enantioselective borylative migration of pyrrolidine substrate **3.56**.

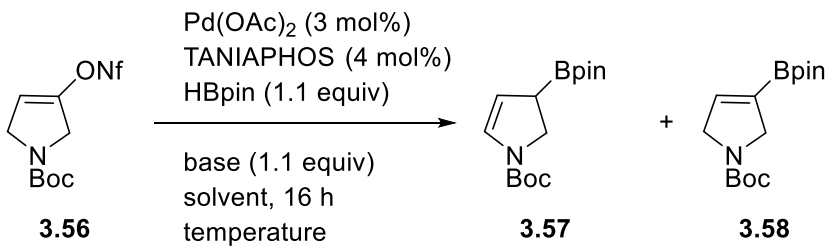

Table 3-1: Summary of conditions tested for the catalytic enantioselective borylative migration of pyrrolidinyl substrate **3.56**.

Trial	Base	Solvent	Temperature	Result Ratio of **3.56** : **3.57**
1*	*N,N*- dimethylaniline	Toluene	rt	1:0
2	*N,N*-diisopropylethylamine	Dioxane	rt	1:0
3	*N,N*-diisopropylethylamine	CPME	rt	9:1
4	*N,N*-diisopropylethylamine	MTBE	rt	7:1
5	triethylamine	CPME	40 °C	1:0
6	triethylamine	MTBE	40 °C	17:1

*Preliminary screened conditions for the synthesis of the pyranyl allylic boronate[6]

3.8 Additional Investigations to Expand the Substrate Scope

With an established method to access alkenyl nonaflate substrates, experiments to determine if the chemistry could be applied to larger ring substrates were conducted. Surprisingly, subjecting *N*-Boc-hexahydro-1H-azepin-4-one (**3.60**) to the conditions illustrated in Scheme 3-26 afforded **3.61** as a single isomer in good yield.

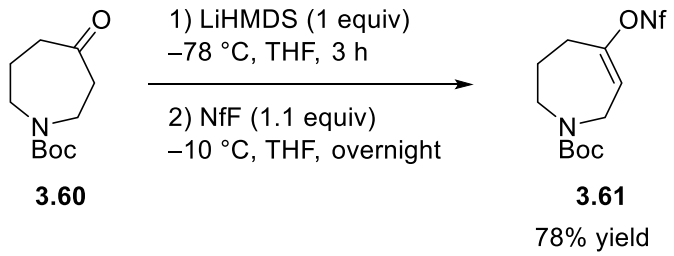

Scheme 3-26: Synthesis of the azepane alkenyl nonaflate substrate **3.61**.

Subjecting **3.61** to the racemic borylative migration conditions and subsequent aldehyde allylboration led to **3.64** in good yield (Scheme 3-27). Investigations into rendering this transformation enantioselective are underway.

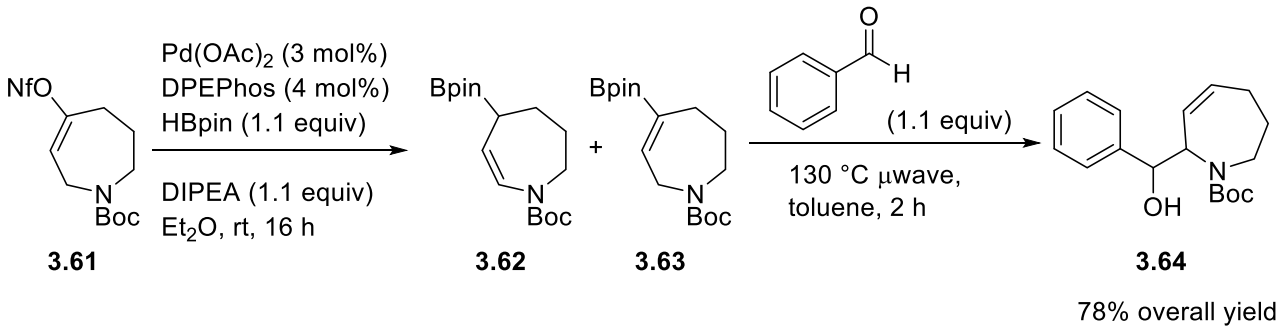

Scheme 3-27: Racemic borylative migration of the azepane substrate **3.61**.

It is evident that the borylative migration of enol perfluorosulfonates is not limited to six-membered heterocyclic substrates. Albeit under racemic conditions, the success with the pyrrolidine and azepane alkenyl nonaflate substrates demonstrates the tremendous potential of this chemistry. Determining the conditions to provide an asymmetric variant is not a trivial task. However, there is great promise for the development of the enantioselective conditions considering the positive result with a higher catalyst and ligand loading (Scheme 3-25).

3.9 Brief Investigation Towards the Feasibility of Other 6-membered Heterocycles

Lastly, additional efforts into studying the expansion of substrates that are suitable to the borylative migration chemistry will be briefly summarize. One of the first substrates that were examined was tetrahydro-4*H*-thiopyran-4-one **3.65**.

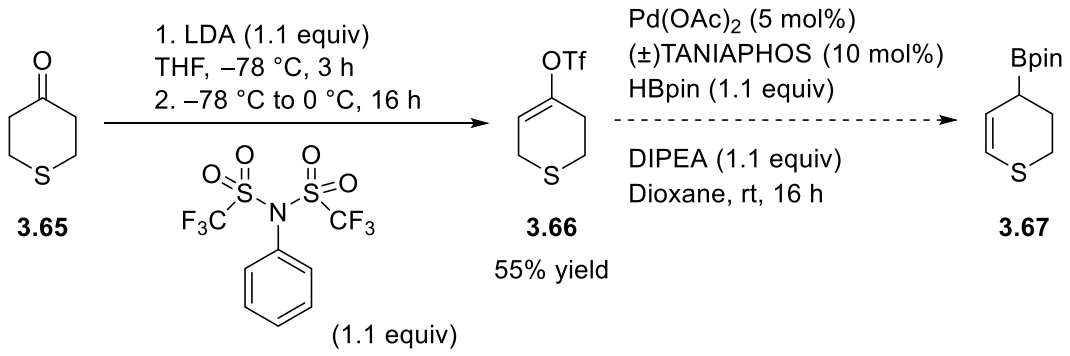

Scheme 3-28: Attempted synthesis of the thiopyranyl allylic boronate **3.67**.

Employing the reaction conditions illustrated in Scheme 3-28 afforded **3.66** in moderate yield. Subjecting this substrate to the catalytic borylative migration conditions resulted in the recovery of starting material. This trial was conducted in triplicate to affirm the observed result. The sulfur heteroatom incurs a detrimental effect to the reaction, presumably by inhibiting the Pd catalyst.

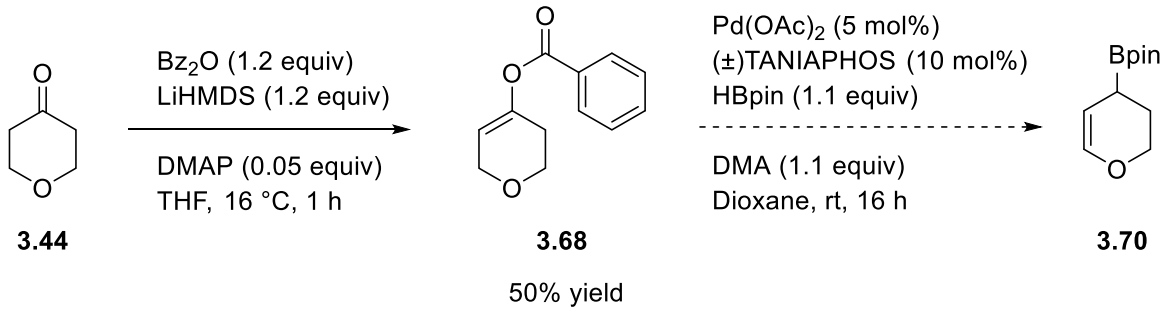

Scheme 3-29: Synthesis of alkenyl benzoate substrate **3.68**.

Second, preliminary investigations into the viability of different leaving groups was performed. As illustrated in Scheme 3-29 and 3-30, substrates with a benzoate or a trimethylsilyl leaving group were synthesized. Unfortunately, in both cases only the starting material was isolated after subjecting these substrates to the borylative migration conditions. It would appear that the triflate and nonaflate leaving groups are essential to this unique transformation.

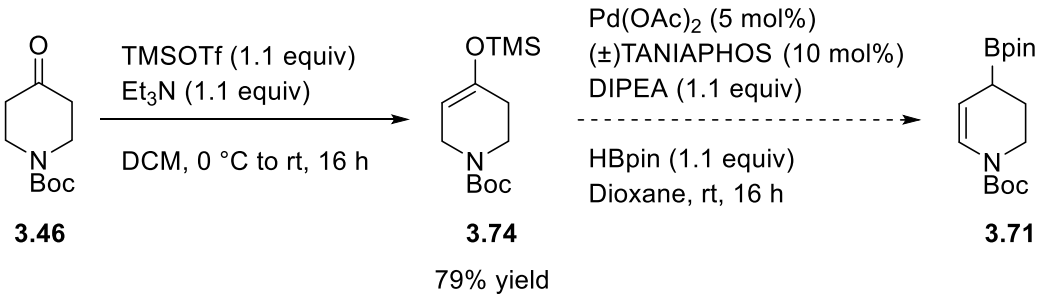

Scheme 3-30: Synthesis of alkenyl trimethylsilyl substrate.

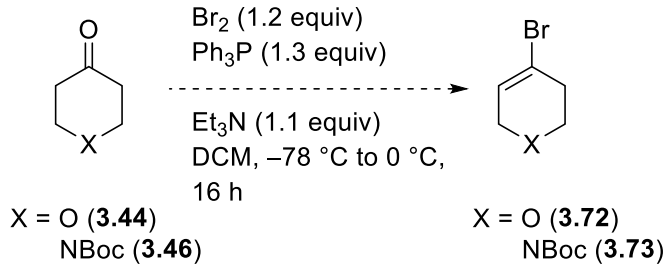

Scheme 3-31: Attempted synthesis of vinyl bromide substrates.

Finally, since triflate is often considered a pseudo-halide it would be interesting to determine if this reactivity was transferrable to the borylative migration reaction of an alkenyl halide substrate. Unfortunately, ongoing attempts to isolate **3.72** and **3.73** after purification were unsuccessful. The lack of success is presumably due to the highly sensitive nature of **3.72** and **3.73** towards temperature.

3.10 Summary

In summary, although tremendous effort was spent in synthesizing the five-membered heterocyclic alkenyl triflate substrate; the success in accessing the pyrrolidinyl- alkenyl nonaflate establishes an exciting point of expansion for the unique borylative migration chemistry. The efforts reported herein illustrate the potential of this chemistry to access an enantioenriched, synthetically useful intermediate. However, significant optimization is still required; specifically, an investigation into the ligand, the base and solvent employed. Furthermore, initial results with the azepane substrate indicate that the chemistry is transferrable to larger ring systems. Expanding the borylative migration transformation opens a whole new and exciting realm of synthetic possibility. Lastly, a brief investigation into the nature of the leaving group reveals that the triflate or nonaflate is essential for the borylation migration to occur.

3.11 Experimental

3.11.1 General Information

Unless otherwise indicated, all reactions were performed under a nitrogen atmosphere using glassware that was washed thoroughly with water and acetone and flame-dried *in vacuo* prior to use. Toluene, tetrahydrofuran and dichloromethane were used directly from a mBraun Solvent Purification System. Diethyl ether was distilled over sodium/benzophenone ketyl. *N,N*-Dimethylaniline, *N,N*- 4-trimethylaniline, *N,N*- diisopropylaniline, triethylamine, *N,N*-diisopropylethylamine, *N,N*-dimethylethylamine and *N,N*-diisopropylbutylamine were purchased from Sigma Aldrich and distilled over sodium hydroxide prior to use. *N*-butyl lithium solution (2.5 M in hexanes) was purchased from Sigma Aldrich. 1-Boc-piperidone (reagent grade, 98%), tetrahydro-3-furanol (reagent grade, 98%), *N*-boc-3-pyrrolidinone (reagent grade, 98%), *N*-boc-hexahydro-1H-azepin-4-one (reagent grade, 97%), perfluorobutanesulfonyl fluoride (reagent grade, 96%) and *N*-phenyl-bis(trifluoromethanesulfonimide) (reagent grade, 98%) were purchased from Combi-Blocks Inc.; and used without further purification. Palladium (II) acetate (reagent grade, >99%), (+) and (-)- TANIAPHOS (reagent grade, >97%), (oxydi-2,1-phenylene)bis(diphenylphosphine) (reagent grade, 98%) and Solvias Walphos Ligand Kit (reagent grade, >97%) were purchased from Strem Chemical Inc.; and used without further purification. Pinacolborane (reagent grade, >97%) was purchased from Oakwood Chemicals and was purified by distillation. Flash chromatography was performed on ultra pure silica gel 230-400 mesh. Nuclear magnetic resonance (NMR) spectra were recorded on Agilent/Varian DD2-400, INOVA-400, INOVA-500 or VNMRS-500 MHz instruments. ^{1}H NMR data are presented as follows: chemical shift in ppm downfield from tetramethylsilane (multiplicity, coupling constant, integration). High resolution mass spectra were recorded by the University of Alberta Mass

Spectrometry Services Laboratory using either electron impact (EI) or electrospray (ESI) ionization techniques. Infrared spectra (performed on a Nicolet Magna-IR 750 instrument equipped with a Nic-Plan microscope) and optical rotations (performed using a Perkin-Elmer 241 polarimeter) were recorded by the University of Alberta Analytical and Instrumentation Laboratory. The enantiomeric excess for chiral compounds were determined using a HPLC Agilent instrument with a Chiralcel-OD column.

3.11.2 Procedure and Spectral Data for Five-membered Heterocycle Precursors

Dihydro-3(2*H*)-Furanone (3.45):

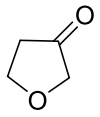

Pyridinium chlorochromate (6.5 g, 30 mmol, 1.5 equiv) was dissolved in 100 ml DCM at rt. Tetrahydro-3-furanol (1.6 ml, 20 mmol, 1 equiv) was added dropwise. 4 Å molecular sieves (16 g) and glacial acetic acid (2 ml) were respectively added. The reaction mixture was stirred at rt overnight. A generous amount of Celite ® 545 was added and the solvent was removed by reduced pressure. The residue was then passed through a Celite ® 545 plug (10% dichloromethane/diethyl ether) and the solvent was removed *in vacuo*. The residue was then purified by flash column chromatography (10% dichloromethane/diethyl ether) to afford **3.45** (60% yield). Spectral data correspond to that reported.[24] ^{1}H NMR (400 MHz, $CDCl_3$): δ 4.24 (t, J = 7.3 Hz, 2 H), 3.86 (s, 2 H), 2.48 (t, J = 7.3 Hz, 2 H).

1*H*-Pyrrole-1-carboxylic acid, 2,5-dihydro-3-[[(trifluoromethyl)sulfonyl]oxy]-,1,1-dimethylethyl ester (3.49, desired isomer) and 1*H*-Pyrrole-1-carboxylic acid, 2,3-dihydro-4-[[(trifluoromethyl)sulfonyl]oxy]-, 1,1-dimethylethyl ester (3.50, undesired isomer):

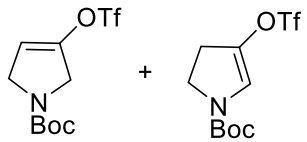

N-Boc-3-pyrrolidinone (0.50 g, 2.7 mmol, 1.0 equiv) was dissolved in 10 ml of THF in a pre-dried 50 mL round bottom flask under a nitrogen atmosphere. The solution was cooled to −78 °C. A solution of 1 M lithium bis(trimethylsilyl)amide (3.0 ml, 3.0 mmol, 1.1 equiv) in THF was added dropwise at − 78 °C. The reaction mixture was allowed to stir for 3 h. *N*-phenyl-

bis(trifluoromethanesulfonimide) (0.97 g, 3.0 mmol, 1.1 equiv) dissolved in 10 ml THF was added dropwise to the reaction mixture which was allowed to warm to 0 °C after the addition. The reaction was stirred overnight at 0 °C. The reaction was quenched with a saturated aqueous solution of sodium bicarbonate and the aqueous layer was extracted three times with dichloromethane. The combined organic layer was washed with citric acid (1N), sodium hydroxide, (1M), water, brine, dried (Na_2SO_4), filtered, then the solvent was removed under reduced pressure. The residue was then purified by flash column chromatography (10% dichloromethane/diethyl ether) to afford a mixture of approximately 1:3 (**3.49**:**3.50**). Spectral data correspond to that reported.[22] ^{1}H NMR (400 MHz, $CDCl_3$) rotomers are present: δ 6.75 (m, 1 H), 5.75 (m, 0.33 H), 4.33 – 4.15 (m, 0.66 H), 3.87 (t, *J* = 9.5 Hz, 2 H), 2.98 – 2.91 (m, 2 H).

3.11.3 Procedure and Spectral Data for the Alkenyl Nonaflate Substrate

1*H*-Pyrrole-1-carboxylic acid, 2,5-dihydro-3-[nonafluorobutylsulfonyloxy]-, 1,1-dimethylethyl ester (3.52):

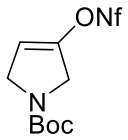

N-Boc-3-pyrrolidinone (3.5 g, 19 mmol, 1.0 equiv) was dissolved in 70 ml THF in a pre-dried 250 mL round bottom flask under a nitrogen atmosphere. The solution was cooled to −78 °C. A solution of 1 M lithium bis(trimethylsilyl)amide (21 ml, 21 mmol, 1.1 equiv) in THF was added dropwise at −78 °C. The reaction was allowed to stir for 3 h. Perfluorobutanesulfonyl fluoride (3.8 ml, 21 mmol, 1.1 equiv) was added dropwise to the reaction mixture which was allowed to warm to 0 °C

after the addition. The reaction was stirred overnight at 0 °C. The reaction was quenched with a saturated aqueous solution of sodium bicarbonate and the aqueous layer was extracted three times with dichloromethane. The combined organic layer was washed with water, brine, dried (Na_2SO_4), filtered, then the solvent was removed under reduced pressure. The residue was purified by flash column chromatography (20% ethyl acetate/pentanes) to afford **3.52** as a dark yellow oil (7.0 g, 79% yield). ^{1}H NMR (500 MHz, $CDCl_3$) rotomers are present: δ 5.83 – 5.66 (m, 1 H), 4.32 – 4.13 (m, 4 H), 1.50 (s, 9 H). ^{19}F NMR (376 MHz, $CDCl_3$) δ -80.6 (t, J = 9.5 Hz, 3 F), -108.9 – -109.0 (m, 2 H), -120.8 – -121.2 (m, 2 F), -125.8 (t, J = 13.9 Hz, 2 F). ^{13}C NMR (100 MHz, $CDCl_3$, ^{19}F and ^{1}H decoupled) rotomers are present: δ 153.7, 153.6, 143.3, 142.9, 117.0, 114.7, 112.8, 112.7, 109.8, 108.4, 80.6, 80.5, 50.4, 50.1, 50.0, 49.8, 28.4. IR ($CHCl_3$ cast film, cm^{-1}): 2980, 1712, 1671, 1408, 1241, 1144, 793. HRMS (ESI) for $(M+Na)^+$ $C_{13}H_{14}F_9NNaO_5S$: calcd. 490.0341; found 490.0342.

1*H*-Azepine-1-carboxylic acid, 2,3,4,7-tetrahydro-5-[nonafluorobutylsulfonyloxy]-,1,1-dimethylethyl ester (3.57):

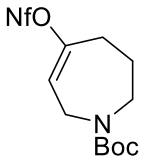

N-Boc-hexahydro-1H-azepin-4-one (1.0 g, 4.7 mmol, 1.0 equiv) was dissolved in 20 ml THF in a pre-dried 50 mL round bottom flask under a nitrogen atmosphere. The solution was cooled to −78 °C. A solution of 1 M lithium bis(trimethylsilyl)amide (5.2 ml, 5.2 mmol, 1.1 equiv) in THF was added dropwise at −78 °C. The reaction was allowed to stir for 3 h. Perfluorobutanesulfonyl fluoride (1.0 ml, 5.2 mmol, 1.1 equiv) was added dropwise to the reaction mixture which was

allowed to warm to −10 °C after the addition. The reaction was stirred overnight at −10 °C. The reaction was quenched with a saturated aqueous solution of sodium bicarbonate and the aqueous layer was extracted three times with dichloromethane. The combined organic layer was washed with water, brine, dried (Na_2SO_4), filtered, then the solvent was removed under reduced pressure. The residue was purified by flash column chromatography (20% ethyl acetate/pentanes) to afford **3.57** as a yellow oil (1.8 g, 78% yield). ^{1}H NMR (498 MHz, $CDCl_3$) rotomers are present: δ 5.99 – 5.87 (m, 1 H), 4.03 – 3.93 (m, 2 H), 3.67 – 3.50 (m, 2 H), 2.65 – 2.53 (m, 2 H), 2.04 – 1.90 (m, 2 H), 1.48 (s, 9 H). ^{19}F NMR (376 MHz, $CDCl_3$) δ -80.66 (t, J = 9.8 Hz, 3 F), -109.74 – -109.87 (m, 2 F), -120.98 (app. s, 2 F), -125.90 (t, J = 12.8 Hz, 2 H). ^{13}C NMR (100 MHz, $CDCl_3$, ^{19}F and ^{1}H decoupled) rotomers are present: δ 155.0, 152.7, 151.7, 121.0, 117.0, 114.2, 109.8, 108.4, 80.2, 52.1, 47.3, 46.6, 41.6, 41.4, 31.2, 30.9, 28.3, 28.1, 24.6. IR ($CHCl_3$ cast film, cm^{-1}): 2980, 1698, 1418, 1240, 1172, 1010, 794. HRMS (ESI) for $(M+Na)^+$ $C_{15}H_{18}F_9NNaO_5S$: calcd. 518.0654; found 518.0659.

3.11.4 General Procedure for the Synthesis of α-hydroxyalkyl dehydropyrrolidine and α-hydroxyalkyl dehydroazepane

A flame dried round bottom flask was charged with palladium (II) acetate (1.4 mg, 6.2 μmol, 0.03 equiv) and ligand (8.3 μmol, 0.04 equiv). The flask was evacuated and backfilled with argon three times. The catalyst and ligand were dissolved in 2 ml of freshly distilled ether and allowed to stir at room temperature for one hour. Amine base (0.23 mmol, 1.1 equiv), pinacolborane (35 μl, 0.23 mmol, 1.1 equiv) and the alkenyl nonaflate (100 mg, 0.20 mmol, 1 equiv) were added respectively. The resulting reaction mixture was allowed to stir for 16 hours at room temperature. The solvent was removed by reduced pressure and the resulting residue was quickly filtered through a silica

plug (100% ether). Once again the solvent was removed by reduced pressure and the crude allyl boronate was dissolved in 2 mL toluene. Aldehyde (30 µl, 0.23 mmol, 1.1 equiv) was added and the reaction was heated at 130°C for 2 hours in a Biotage™ microwave oven. The reaction mixture was cooled to rt and the solvent was removed by reduced pressure and purified as described below.

1*H*-Pyrrole-1-carboxylic acid, 2,5-dihydro-2-(hydroxyphenylmethyl)-,1,1-dimethylethyl ester (3.55):

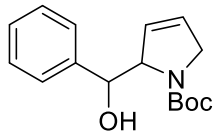

The residue was purified by flash column chromatography (gradient 10% to 20% ethyl acetate/pentanes) to afford **3.57** as a yellow oil (44 mg, 75% yield). Spectral data correspond to that reported.[25] ^{1}H NMR (400 MHz, $CDCl_3$) rotomers are present: δ 7.39 – 7.28 (m, 5 H), 6.13 (s, 1 H), 5.73 – 5.71 (m, 1 H), 5.16 – 5.08 (m, 1 H), 4.82 – 4.78 (m, 1 H), 4.61 (d, J = 8.2 Hz, 1 H), 4.30 – 4.19 (m, 1 H), 4.09 – 3.99 (m, 1 H), 1.54 (s, 9 H). HRMS (ESI) for $(M+Na)^+$ $C_{16}H_{21}NNaO_3$: calcd. 298.1414; found 298.1409.

1*H*-Azepine-1-carboxylic acid, 2,5-dihydro-2-(hydroxyphenylmethyl)-,1,1-dimethylethyl ester (3.56):

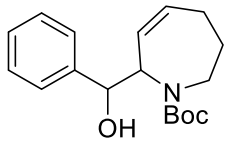

The residue was purified by flash column chromatography (gradient 10% to 20% ethyl acetate/pentanes) to afford **3.57** as a yellow oil (48 mg, 78% yield). ^{1}H NMR (400 MHz, $CDCl_3$)

rotomers are present: δ 7.44 – 7.29 (m, 5 H), 5.61 (d, J = 65.0 Hz, 1 H), 5.28 – 5.18 (m, 1 H), 5.10 – 4.85 (m, 1 H), 4.70 (d, J = 30.2 Hz, 1 H), 3.83 (d, J = 41.7 Hz, 1 H), 3.64 (d, J = 14.4 Hz, 1 H), 3.60 – 3.40 (m, 1 H), 3.29 – 3.17 (m, 1 H), 2.35 – 2.13 (m, 1 H), 2.01 (d, J = 38.8 Hz, 1 H), 1.49 – 1.45 (m, 9 H). ^{13}C NMR (126 MHz, $CDCl_3$) rotomers are present: δ 157.7, 155.6, 141.7, 129.6, 128.4, 127.9, 127.4, 127.2, 80.3, 79.1, 62.9, 48.5, 45.5, 45.1, 43.0, 28.6, 25.7, 23.8. IR ($CHCl_3$ cast film, cm^{-1}): 3439, 2929, 1692, 1455, 1415, 1167, 703. HRMS (ESI) for $(M+Na)^+$ $C_{18}H_{25}NNaO_3$: calcd. 326.1727; found 326.1726.

3.11.5 Procedure and Spectral Data for Other Potential Six-membered Heterocycle Substrates

4-Benzoate- 3,6-dihydro-, 2*H*-pyran-4-ol (3.64):

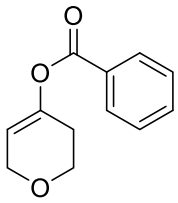

Benzoic anhydride (1.36 g, 6.0 mmol, 1.2 equiv), 1-(dimethylamino)pyridine (31 mg, 2.1 mmol, 0.050 equiv) and tetrahydro-4*H*-pyran-4-one (0.50 g, 5.0 mmol, 1 equiv) were dissolved in 15 ml THF. The reaction mixture was cooled to 16 °C with stirring. A solution of 1 M lithium bis(trimethylsilyl)amide (9.0 ml, 6 mmol, 1.2 equiv) in THF was added dropwise at 16 °C. The reaction was stirred for 1 h. After the reaction time, the mixture was quenched with a saturated aqueous solution of sodium bicarbonate and the aqueous layer was extracted with ethyl acetate three times. The organic layers were combined and washed with brine, dried (Na_2SO_4), filtered,

then the solvent was removed under reduced pressure. The residue was purified by flash column chromatography (20% ethyl acetate/hexanes) to afford **3.64** as a yellow oil (510 mg, 50% yield). Spectral data correspond to that reported.[26] ^{1}H NMR (400 MHz, $CDCl_3$): δ 8.13 – 8.03 (m, 2 H), 7.62 – 7.58 (m, 1 H), 7.51 – 7.44 (m, 2 H), 5.61 – 5.59 (m, 1 H), 4.30 (dt, *J* = 2.6, 2.7 Hz, 2 H), 3.95 (t, *J* = 5.5 Hz, 2 H), 2.45 – 2.41 (m, 2 H).

***tert*-Butyl 4-[(trimethylsilyl)oxy]-1,2,5,6-tetrahydropyridine-1-carboxylate (3.70):**

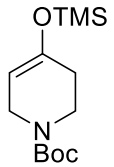

1-Boc-4-piperidone (0.50 g, 2.5 mmol, 1 equiv) was dissolved in 20 ml DCM and cooled to 0 °C with stirring. Triethylamine (0.40 ml, 2.8 mmol, 1.1 equiv) was added dropwise followed by the dropwise addition of trimethylsilyl trifluoromethanesulfonate (0.50 ml, 2.8 mmol, 1.1 equiv) at 0 °C. The reaction was allowed to warm to rt with stirring overnight. The reaction mixture was quenched with a saturated aqueous solution of sodium bicarbonate and the aqueous layer was extracted with dichloromethane three times. The organic layers were combined and washed with water, brine, dried (Na_2SO_4), filtered, then the solvent was removed under reduced pressure. The residue was purified by flash column chromatography (10% ethyl acetate/hexanes) to afford **3.70** as a colourless oil (540 mg, 79% yield). Spectral data correspond to that reported.[27] ^{1}H NMR (400 MHz, $CDCl_3$): δ 4.79 (s, 1 H), 3.92 – 3.79 (m, 2 H), 3.52 (t, *J* = 5.7 Hz, 2 H), 2.10 (app s, 2 H), 1.46 (s, 9 H), 0.19 (s, 9 H).

Methanesulfonic acid, 1,1,1-trifluoro-,3,6-dihydro-2*H*-thiopyran-4-yl ester (3.62):

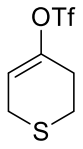

Diiopropylamine (0.70 ml, 4.7 mmol, 1.1 equiv) was diluted in 15 ml THF and cooled to −78 °C. A solution of 2.5 M *n*butyllithium (0.50 ml, 4.7 mmol, 1.1 equiv) in hexanes was added dropwise at −78 °C. The reaction mixture was stirred for 30 min. After the reaction time, an 80 mM solution of tetrahydro-4H-thiopyran-4-one (0.50 g, 4.3 mmol, 1 equiv) was added dropwise and the reaction mixture was allowed to stir for an additional 3 h at−78 °C. After the reaction time a 90 mM solution of *N*-phenyl-bis(trifluoromethanesulfonimide) (1.7 g, 4.7 mmol, 1.1 equiv) was added dropwise. The reaction was gradually warmed to 0 °C with stirring for 16 h. The reaction was quenched with the slow addition of water and extracted three times with diethyl ether. The organic layers were combined and washed with water, brine, dried (Na_2SO_4), filtered, then the solvent was removed under reduced pressure. The residue was purified by flash column chromatography (10% ethyl acetate/hexanes) to afford **3.62** as a yellow oil (590 mg, 55% yield). Spectral data correspond to that reported.[28] ^{1}H NMR (400 MHz, $CDCl_3$): δ 6.01 (app. s, 1 H), 3,31 – 3.29 (m, 2 H), 2.88 – 2.85 (m, 2 H), 2.64 – 2.60 (m, 2 H).

3.12 References

(1) Gilman, E.F., Watson, D. G. *Asimina triloba*; 1993.

(2) McLaughlin, J. L. *J. Nat. Prod.* **2008**, *71*, 1311–1321.

(3) Avedissian, H.; Sinha, S. C.; Yazbak, A.; Sinha, A.; Neogi, P.; Sinha, S. C.; Keinan, E. *J. Org. Chem.* **2000**, *65*, 6035–6051.

(4) Sinha, S. C.; Sinha, A.; Yazbak, A.; Keinan, E. *J. Org. Chem.* **1996**, *6*, 7640–7641.

(5) Kim, Y.-R.; Hall, D. G. *Org. Biomol. Chem.* **2016**, *14*, 4739–4748.

(6) Lessard, S.; Peng, F.; Hall, D. G. *J. Am. Chem. Soc.* **2009**, *131*, 9612–9613.

(7) Ding, J.; Hall, D. G. *Angew. Chem. Int. Ed.* **2013**, *52*, 8069–8073.

(8) Ding, J.; Rybak, T.; Hall, D. G. *Nat. Commun.* **2014**, *5*, 1–9.

(9) Lawson, A. P.; Klang, J. A. *Synth. Commun.* **1993**, *23*, 3205–3210.

(10) Chen, Z.; Sun, J. *Angew. Chem. Int. Ed.* **2013**, *52*, 13593–13596.

(11) Deangelis, A.; Taylor, M. T.; Fox, J. M. *J. Am. Chem. Soc.* **2009**, *131*, 1101–1105.

(12) Yuan, X.; Lin, L.; Chen, W.; Wu, W.; Liu, X.; Feng, X. *J. Org. Chem.* **2015**, 4–10.

(13) Grandjean, J. M. M.; Nicewicz, D. A. *Angew. Chem. Int. Ed.* **2013**, *52*, 3967–3971.

(14) Loh, T. P.; Hu, Q. Y.; Tan, K. T.; Cheng, H. S. *Org. Lett.* **2001**, *3*, 2669–2672.

(15) Gogoi, P.; Das, V. K.; Saikia, A. K. *J. Org. Chem.* **2014**, *79*, 8592–8598.

(16) Peng, F.; Hall, D. G. *J. Am. Chem. Soc.* **2007**, *129*, 3070–3071.

(17) Sutivisedsak, N.; Dawadi, S.; Spilling, C. D. *Tetrahedron Lett.* **2015**, *56*, 3534–3537.

(18) Chaulagain, M. R.; Felten, A. E.; Gilbert, K.; Aron, Z. D. *J. Org. Chem.* **2013**, *78*, 9471–9476.

(19) Lapointe, G.; Schenk, K.; Renaud, P. *Chem. - A Eur. J.* **2011**, *17*, 3207–3212.

(20) González, A. Z.; Benitez, D.; Tkatchouk, E.; Goddard, W. A.; Toste, F. D. *J. Am. Chem.*

Soc. **2011**, *133*, 5500–5507.

(21) Trost, B. M.; Silverman, S. M. *J. Am. Chem. Soc.* **2012**, *134*, 4941–4954.

(22) Venier, O.; Pascal, C.; Braun, A.; Namane, C.; Mougenot, P.; Crespin, O.; Pacquet, F.; Mougenot, C.; Monseau, C.; Onofri, B.; Dadji-Faïhun, R.; Leger, C.; Ben-Hassine, M.; Van-Pham, T.; Ragot, J. L.; Philippo, C.; Güssregen, S.; Engel, C.; Farjot, G.; Noah, L.; Maniani, K.; Nicolaï, E. *Bioorg. Med. Chem. Lett.* **2011**, *21*, 2244–2251.

(23) Kim, Y.-R.; Hall, D. G. *Org. Biomol. Chem.* **2016**, *14*, 4739–4748.

(24) Avi, M.; Fechter, M. H.; Gruber, K.; Belaj, F.; Pöchlauer, P.; Griengl, H. *Tetrahedron* **2004**, *60*, 10411–10418.

(25) Lindsay, K. B.; Tang, M.; Pyne, S. G. *Synlett* **2002**, *5*, 731–734.

(26) Butora, G., Guiadeen, D., Kothandaraman, S., Maccoss, M., Mills, S., Yang, L. Aminocyclopentyl pyridopyrazinone modulators of chemokine receptor activity. WO 2005/072361 A2, 2004.

(27) Budzik, B.; Garzya, V.; Shi, D.; Walker, G.; Lauchart, Y.; Lucas, A. J.; Rivero, R. A.; Langmead, C. J.; Watson, J.; Wu, Z.; Forbes, I. T.; Jin, J. *Bioorg. Med. Chem. Lett.* **2010**, *20*, 3545–3549.

(28) Richardson, T. I.; Frank, S. A.; Wang, M.; Clarke, C. A.; Jones, S. A.; Ying, B. P.; Kohlman, D. T.; Wallace, O. B.; Shepherd, T. A.; Dally, R. D.; Palkowitz, A. D.; Geiser, A. G.; Bryant, H. U.; Henck, J. W.; Cohen, I. R.; Rudmann, D. G.; McCann, D. J.; Coutant, D. E.; Oldham, S. W.; Hummel, C. W.; Fong, K. C.; Hinklin, R.; Lewis, G.; Tian, H.; Dodge, J. A. *Bioorg. Med. Chem. Lett.* **2007**, *17*, 3544–3549.

Chapter 4. Thesis Conclusions

This thesis described the application of a unique borylative migration of heterocyclic enol perfluorosulfonates towards the synthesis of all four enantioenriched stereoisomers of Vacquinol-1. This approach and synthetic strategy facilitates the access to a whole new class of analogs in an enantioselective manner. Motivated by the success of the six-membered heterocyclic substrates, an extension of this chemistry was explored to five- and seven-membered heterocycles. Although the results are still preliminary, the borylative migration transformation has been achieved with the pyrrolidine and azepane substrates.

Identified in 2014, the vacquinol compounds were determined to be effective against the brain cancer, glioblastoma multiforme. Namely, Vacquinol-1 exhibited the best balance between efficacy and selectivity, while Vacquinol-15 exhibited the highest potency. However, a complex mixture of stereoisomers was tested and there is no indication from the initial account that further investigation of each enantioenriched stereoisomer would be studied independently. For the development of potential therapeutics, a thorough study of the biological activity of each stereoisomer must be conducted. A synthetic strategy has been applied, with great success, towards the synthesis of all four stereoisomers of mefloquine. Application of this strategy towards the synthesis of Vacquinol-1 is described. Synthesis of all four stereoisomers of Vacquinol-1 was achieved in good overall yield and enantiomeric excess. Notably, hydrogenation of the endocyclic alkene, a residual functional group present after the aldehyde allylboration, required significant optimization.

In collaboration with Dr. Roseline Godbout at the Cross Cancer Institute investigation of the efficacy the synthesized compounds to induce cancerous cell death was explored. Biological results employing all four enantioenriched stereoisomers of Vacquinol-1 and a corresponding set of unsaturated Vacquinol-1 analogs revealed that saturation of the endocyclic alkene is preferred. However, one stereoisomer of the Vacquinol-1 analog is an exception. The study revealed the identity of the most effective stereoisomer, hence fulfilling a major shortcoming from the original report. Moreover, the synthetic strategy has two key points for divergence that can be employed for the synthesis of more optimal analogs.

First, the residual endocyclic alkene can be used as a synthetic handle to install different functional groups or substituents around the piperidine moiety. Since the mechanism of action is unknown and considering the biological results obtained, examining the landscape of the piperidine motif may provide insight to the interactions these small molecules have with GBM cells. Second, the synthesis of the aldehyde partner provides a strategic point of divergence. Installing different substituents around the aryl ring can be achieved by using commercially available acetophenone derivatives. As a proof of concept, a set of optically enriched enantiomers with four different aryl substituents was synthesized to provide a total of eight analogs of Vacquinol-1 in good overall yield and enantiomeric excess. Likewise, the derivation of the quinoline moiety could be achieved depending on the substituents of the isatin starting material.

Although the synthetic utility of the borylative migraton transformation to access all four enantioenriched stereoisomers of Vacquinol-1 has been demonstrated, this project still has several areas for further study. Identification of the more effective stereoisomer will facilitate a more

focused effort towards identifying and synthesizing a more optimal Vacquinol-1 analog and therefore, a potentially viable therapeutic agent for the treatment of glioblastoma multiforme.

Next, this thesis described the efforts to expanding the borylative migration transformation to five- and seven- membered heterocyclic substrates. To our delight, the racemic conditions transferred well to the two new substrates, however employing the asymmetric conditions with TANIAPHOS as the ligand essentially shut down the transformation. Preliminary optimization parameters that were explored include the solvent, the amine base and chiral ligand. From these results, it can be surmised that diethyl ether is still the optimal solvent while the chiral ligand TANIAPHOS hinders the transformation of the five-membered heterocyclic substrate. Furthermore, aniline based amines hinder this reaction while tri-alkylamines appear to be better suited to improve the conversion. Overall, further optimization is required to render the asymmetric five- and seven-membered transformation synthetically useful.

In future, one can imagine expanding the borylative migration to larger heterocyclic ring to explore the limits of this chemistry. The eight-membered heterocyclic substrates could provide mechanistic insight as to whether Pd-“chain” walking occurs with our system. Moreover, examining the borylative migration employing acyclic substrates could be a novel method to selectively access mono-protected chiral diols or aminols after aldehyde allylboration with the chiral acyclic allylic boronate intermediate.

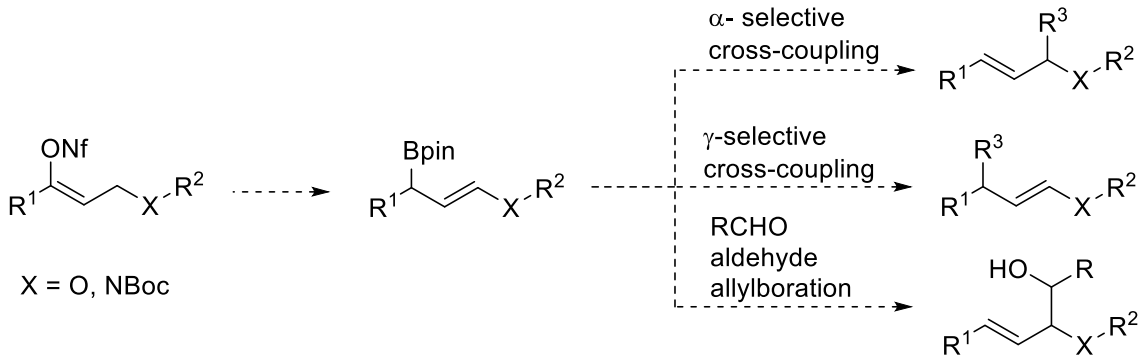

Scheme 4-1: Potential application of the borylative migration of acyclic enol perfluorosulfonates

4.1 Bibliography

(1) Hartwig, J. *Organotransition Metal Chemistry: From Bonding to Catalysis*; University Science Books, **2009**.

(2) All Nobel Prizes in Chemistry http://www.nobelprize.org/nobel_prizes/chemistry/laureates/.

(3) Dougherty, D. A., Anslyn, E. V. In *Modern Physical Organic Chemistry*; University Science Books, **2004**; pp 333–340.

(4) Pirkle, W.H., Pochapsky, T. C. *Chem. Rev.* **1989**, *89*, 347–362.

(5) Itsuno, S. *Prog. Polym. Sci* **2005**, *30*, 540–558.

(6) Vargesson, N. *Birth Defects Res. (Part C)* **2015**, *105*, 140–156.

(7) Candy, M.; Audran, G.; Bienaymé, H.; Bressy, C.; Pons, J.-M. *Org. Lett.* **2009**, *11* (21), 4950–4953.

(8) Patel, R. N. *ACS Catal.* **2011**, *1* (9), 1056–1074.

(9) Lachance, H.; Hall, D. G. *Allylboration of Carbonyl Compounds*; John Wiley & Sons, Inc., **2009**.

(10) Chausset-Boissarie, L.; Ghozati, K.; LaBine, E.; Chen, J. L.-Y.; Aggarwal, V. K.; Crudden, C. M. *Chem. – A Eur. J.* **2013**, *19* (52), 17698–17701.

(11) Raducan, M.; Alam, R.; Szabó, K. J. *Angew. Chem. Int. Ed.* **2012**, *51*, 13050–13053.

(12) Yamamoto, Y.; Takada, S.; Miyaura, N. *Chem. Lett.* **2006**, *35* (7), 704–705.

(13) Yamamoto, Y.; Takada, S.; Miyaura, N. *Chem. Lett.* **2006**, *35* (7), 1368–1369.

(14) Sebelius, S.; Olsson, V. J.; Wallner, O. A.; Szabó, K. J. *J. Am. Chem. Soc.* **2006**, *128* (25), 8150–8151.

(15) Farmer, J. L.; Hunter, H. N.; Organ, M. G. *J. Am. Chem. Soc.* **2012**, *134* (42), 17470–17473.

(16) Elford, T. G.; Hall, D. G. *Boronic Acids*; Wiley-VCH Verlag GmbH & Co. KGaA, **2011**; *73*, 393–425.

(17) Herold, T.; Hoffmann, R. W. *Angew. Chem. Int. Ed.* **1978**, *17* (10), 768–769.

(18) Corey, E. J.; Yu, C. M.; Kim, S. S. *J. Am. Chem. Soc.* **1989**, *111* (14), 5495–5496.

(19) Brown, H. C.; Jadhav, P. K.; Bhat, K. S. *J. Am. Chem. Soc.* **1985**, *107* (8), 2564–2565.

(20) Roush, W. R.; Walts, A. E.; Hoong, L. K. *J. Am. Chem. Soc.* **1985**, *107* (26), 8186–8190.

(21) Rauniyar, V.; Hall, D. G. *Angew. Chem. Int. Ed.* **2006**, *45* (15), 2426–2428.

(22) Carosi, L.; Lachance, H.; Hall, D. G. *Tetrahedron Lett.* **2005**, *46* (52), 8981–8985.

(23) Peng, F.; Hall, D. G. *J. Am. Chem. Soc.* **2007**, *129* (11), 3070–3071.

(24) Brown, H. C.; Jadhav, P. K. *J. Am. Chem. Soc.* **1985**, *10*, 2564–2565.

(25) Brown, H.C., Bhat, K.S., Jadhav, P. K. *J. Chem. Soc. Transac* **1991**, *11*, 2633–2638.

(26) Atkins, W. J.; Burkhardt, E. R.; Matos, K. *Org. Process Res. Dev.* **2006**, *10* (6), 1292–1295.

(27) Renard, P.-Y., Lallemand, J.-Y. *Tetrahedron: Asymmetry* **1996**, *7* (9), 2523–2524.

(28) Hoffmann, R. W.; Dresely, S. *Angew. Chem. Int. Ed.* **1986**, *25* (2), 189.

(29) Hoffmann, R. W.; Dresely, S.; Hoffmann, R. W.; Dresely, S. *Chem. Ber.* **1989**, *122*, 903–909.

(30) Hoffmann, R.W., Landmann, B. *Tetrahedron Lett.* **1983**, *24* (31), 3209–3212.

(31) Hoffmann, R. W.; Landmann, B. *Chem. Ber.* **1986**, *119* (3), 1039–1053.

(32) Suginome, M.; Ito, Y. *J. Organomet. Chem.* **2003**, *680* (1-2), 43–50.

(33) Durieux, G.; Gerdin, M.; Moberg, C.; Jutand, A. *Eur. J. Inorg. Chem.* **2008**, *27*, 4236–4241.

(34) Gerdin, M.; Penhoat, M.; Zalubovskis, R.; Pétermann, C.; Moberg, C. *J. Organomet. Chem.* **2008**, *693* (23), 3519–3526.

(35) Tailor, J.; Hall, D. G. *Org. Lett.* **2000**, *2* (23), 3715–3718.

(36) Deligny, M.; Carreaux, F.; Carboni, B. *Synlett* **2005**, *9*, 1462–1464.

(37) Gademann, K.; Chavez, D. E.; Jacobsen, E. N. *Angew. Chem. Int. Ed.* **2002**, *41* (16), 3059–3061.

(38) Gao, X.; Hall, D. G. *J. Am. Chem. Soc.* **2005**, *127* (6), 1628–1629.

(39) Lessard, S.; Peng, F.; Hall, D. G. *J. Am. Chem. Soc.* **2009**, *131* (28), 9612–9613.

(40) Murata, M.; Oyama, T.; Watanabe, S.; Masuda, Y. *Synthesis.* **2000**, *6*, 778–780.

(41) Kim, Y.-R.; Hall, D. G. *Org. Biomol. Chem.* **2016**, *14*, 4739–4748.

(42) Ding, J.; Rybak, T.; Hall, D. G. *Nat. Commun.* **2014**, *5*, 1–9.

(43) Beng, T. K.; Gawley, R. E. *Org. Lett.* **2011**, *8*, 11–14.

(44) Amat, M.; Bosch, J.; Hidalgo, J.; Cantó, M.; Perez, M.; Llor, N.; Molins, E.; Miravitlles, C.; Orozco, M.; Luque, J. *J. Org. Chem.* **2000**, *65* (10), 3074–3084.

(45) Matos, K.; Soderquist, J. A. *J. Org. Chem.* **1998**, *63*, 461–470.

(46) Ridgway, B. H.; Woerpel, K. A. *J. Org. Chem.* **1998**, *63* (3), 458–460.

(47) Ding, J.; Hall, D. G. *Angew. Chem. Int. Ed.* **2013**, *52* (31), 8069–8073.

(48) Karle, J. M., Olmeda, R., Gerena, L., Milhous, W. K. *Exp. Parasitol.* **1993**, *76*, 345–351.

(49) Roche, F.H.-L., Brober, E., Hofneinz, W., Meili, A. Eur. Pat. 553778, 1993.

(50) Xie, Z.X., Zhang, L.Z., Ren, X.J., Tang, S.Y., Li, Y. *Chinese J. Chem.* **2008**, *26*, 1272–1276.

(51) Knight, J. D.; Sauer, S. J.; Coltart, D. M. *Org. Lett.* **2011**, *13* (12), 3118–3121.

(52) Kitambi, S. S.; Toledo, E. M.; Usoskin, D.; Wee, S.; Harisankar, A.; Svensson, R.; Sigmundsson, K.; Kalderén, C.; Niklasson, M.; Kundu, S.; Aranda, S.; Westermark, B.; Uhrbom, L.; Andäng, M.; Damberg, P.; Nelander, S.; Arenas, E.; Artursson, P.; Walfridsson, J.; Forsberg Nilsson, K.; Hammarström, L. G. J.; Ernfors, P. *Cell* **2014**, *157* (2), 313–328.

(53) Galluzzi, L.; Zamzami, N.; La, T. De; Rouge, M.; Lemaire, C.; Brenner, C.; Kroemer, G. *Apoptosis* **2007**, *12*, 803–813.

(54) Tsujimoto, Y.; Shimizu, S. *Cell Death Differ.* **2005**, *12*, 1528–1534.

(55) Brain Tumor Statistics http://www.abta.org/about-us/news/brain-tumor-statistics/ (accessed Apr 21, 2016).

(56) Kitambi, S. S.; Toledo, E. M.; Usoskin, D.; Wee, S.; Harisankar, A.; Svensson, R.; Sigmundsson, K.; Kalderén, C.; Niklasson, M.; Kundu, S.; Aranda, S.; Westermark, B.; Uhrbom, L.; Andäng, M.; Damberg, P.; Nelander, S.; Arenas, E.; Artursson, P.; Walfridsson, J.; Forsberg Nilsson, K.; Hammarström, L. G. J.; Ernfors, P. *Cell* **2014**, *157*, 313–328.

(57) Karim, R.; Palazzo, C.; Evrard, B.; Piel, G. *J. Control. Release* **2016**, *227*, 23–37.

(58) Hawkins, B. T.; Davis, T. P. *Pharmacol. Rev.* **2005**, *57*, 173–185.

(59) Prados, M. D.; Byron, S. A.; Tran, N. L.; Phillips, J. J.; Molinaro, A. M.; Ligon, K. L.; Wen, P. Y.; Kuhn, J. G.; Mellinghoff, I. K.; De Groot, J. F.; Colman, H.; Cloughesy, T. F.; Chang, S. M.; Ryken, T. C.; Tembe, W. D.; Kiefer, J. A.; Berens, M. E.; Craig, D. W.; Carpten, J. D.; Trent, J. M. *Neuro. Oncol.* **2015**, *17*, 1051–1063.

(60) Stavrovskaya, A. A.; Shushanov, S. S.; Rybalkina, E. Y. *Biochem.* **2016**, *81*, 91-100.

(61) Eguchi, Y.; Srinivasan, A.; Tomaselli, K. J.; Shimizu, S.; Tsujimoto, Y. *Cancer Res.* **1999**, *59*, 2174–2181.

(62) Galluzzi, L.; Zamzami, N.; La, T. De; Rouge, M.; Lemaire, C.; Brenner, C.; Kroemer, G. *Apoptosis* **2007**, *13*, 803–813.

(63) Orrenius, S.; Zhivotovsky, B.; Nicotera, P. *Nat. Rev. Mol. Cell Biol.* **2003**, *4*, 552–565.

(64) Mizushima, N. *Genes Dev.* **2007**, *21*, 2861–2873.

(65) Cuenda, A. *Int. J. Biochem. Cell Biol.* **2000**, *32*, 581–587.

(66) Ding, J.; Hall, D. G. *Angew. Chem. Int. Ed.* **2013**, *52*, 8069–8073.

(67) Kim, Y.-R.; Hall, D. G. *Org. Biomol. Chem.* **2016**, *14*, 4739–4748.

(68) Calaway, P.K., Henze, H. R. *J. Am. Chem. Soc.* **1939**, *61*, 1355–1358.

(69) Buu-Hoï N.P., Royer R., Xuong, N. D. *J. Org. Chem* **1953**, *18*, 1209–1224.

(70) Hegedus, L. S. *Transition metals in the synthesis of complex organic molecules*, 3rd ed.; Söderberg, B. C. G., Ed.; University Science Books: Sausalito, Calif., **2010**.

(71) Duan, Z.; Li, X.; Huang, H.; Yuan, W.; Zheng, S.-L.; Liu, X.; Zhang, Z.; Choy, E.; Harmon, D.; Mankin, H.; Hornicek, F. *J. Med. Chem.* **2012**, *55*, 3113–3121.

(72) Staehelin, A. *Comptes rendus Hebd. des séances l ' Académie des Sci. Série B* **1972**, *275*, 262–264.

(73) Cassebaum, H.; Modest, J.; Bergmann, F.; Smuszkovicz, J. *Dehydrasemodelle auf Chinon- und Isatin-Basis,* **1957**, *4207*, 138–139.

(74) Garalene, V.N., Stakyavichus, A.P., Mazhilis, L. Yu., Sapragonene, M.S., Risyalis, S.P., Terentyev, P.B., Rotchka, V.-S. M. In *Search of New Medecines*; 1986; pp 1305–1308.

(75) Karpenko, A. S.; Shibinskaya, M. O.; Zholobak, N. M.; Olevinskaya, Z. M.; Lyakhov, S. A.; Litvinova, L. A.; Spivak, M. Y.; Andronati, S. A. *Pharm. Chem. J.* **2006**, *40*, 595–602.

(76) Chang, D.; Gu, Y.; Shen, Q. *Chem. Eur. J.* **2015**, *21*, 6074–6078.

(77) Holla, B. S.; Poojary, K. N.; Poojary, B.; Bhat, K. S.; Kumari, N. S. *Indian J. Chem., Sec B,* **2005**, *44*, 2114–2119.

(78) Qin, J.; Li, F.; Xue, L.; Lei, N.; Ren, Q.; Wang, D.; Zhu, H. *Acta. Chim. Slov.* **2014**, 170–176.

(79) Wang, L. M.; Hu, L.; Chen, H. J.; Sui, Y. Y.; Shen, W. *J. Fluor. Chem.* **2009**, *130*, 406–409.

(80) Molina, P., Alajarin, M., Sanchez-Andrada, P. *Synthesis (Stuttg).* **1993**, 225–228.

(81) Klein, L. L.; Tufano, M. D. *Tetrahedron Lett.* **2013**, *54*, 1008–1011.

(82) Gilman, E.F., Watson, D. G. *Asimina triloba*; 1993.

(83) McLaughlin, J. L. *J. Nat. Prod.* **2008**, *71*, 1311–1321.

(84) Avedissian, H.; Sinha, S. C.; Yazbak, A.; Sinha, A.; Neogi, P.; Sinha, S. C.; Keinan, E. *J. Org. Chem.* **2000**, *65*, 6035–6051.

(85) Sinha, S. C.; Sinha, A.; Yazbak, A.; Keinan, E. *J. Org. Chem.* **1996**, *6*, 7640–7641.

(86) Kim, Y.-R.; Hall, D. G. *Org. Biomol. Chem.* **2016**, *14*, 4739–4748.

(87) Lessard, S.; Peng, F.; Hall, D. G. *J. Am. Chem. Soc.* **2009**, *131*, 9612–9613.

(88) Ding, J.; Hall, D. G. *Angew. Chem. Int. Ed.* **2013**, *52*, 8069–8073.

(89) Ding, J.; Rybak, T.; Hall, D. G. *Nat. Commun.* **2014**, *5*, 1–9.

(90) Lawson, A. P.; Klang, J. A. *Synth. Commun.* **1993**, *23*, 3205–3210.

(91) Chen, Z.; Sun, J. *Angew. Chem. Int. Ed.* **2013**, *52*, 13593–13596.

(92) Deangelis, A.; Taylor, M. T.; Fox, J. M. *J. Am. Chem. Soc.* **2009**, *131*, 1101–1105.

(93) Yuan, X.; Lin, L.; Chen, W.; Wu, W.; Liu, X.; Feng, X. *J. Org. Chem.* **2015**, 4–10.

(94) Grandjean, J. M. M.; Nicewicz, D. A. *Angew. Chem. Int. Ed.* **2013**, *52*, 3967–3971.

(95) Loh, T. P.; Hu, Q. Y.; Tan, K. T.; Cheng, H. S. *Org. Lett.* **2001**, *3*, 2669–2672.

(96) Gogoi, P.; Das, V. K.; Saikia, A. K. *J. Org. Chem.* **2014**, *79*, 8592–8598.

(97) Peng, F.; Hall, D. G. *J. Am. Chem. Soc.* **2007**, *129*, 3070–3071.

(98) Sutivisedsak, N.; Dawadi, S.; Spilling, C. D. *Tetrahedron Lett.* **2015**, *56*, 3534–3537.

(99) Chaulagain, M. R.; Felten, A. E.; Gilbert, K.; Aron, Z. D. *J. Org. Chem.* **2013**, *78*, 9471–9476.

(100) Lapointe, G.; Schenk, K.; Renaud, P. *Chem. - A Eur. J.* **2011**, *17*, 3207–3212.

(101) González, A. Z.; Benitez, D.; Tkatchouk, E.; Goddard, W. A.; Toste, F. D. *J. Am. Chem. Soc.* **2011**, *133*, 5500–5507.

(102) Trost, B. M.; Silverman, S. M. *J. Am. Chem. Soc.* **2012**, *134*, 4941–4954.

(103) Venier, O.; Pascal, C.; Braun, A.; Namane, C.; Mougenot, P.; Crespin, O.; Pacquet, F.; Mougenot, C.; Monseau, C.; Onofri, B.; Dadji-Faïhun, R.; Leger, C.; Ben-Hassine, M.; Van-Pham, T.; Ragot, J. L.; Philippo, C.; Güssregen, S.; Engel, C.; Farjot, G.; Noah, L.; Maniani, K.; Nicolaï, E. *Bioorg. Med. Chem. Lett.* **2011**, *21*, 2244–2251.

(104) Kim, Y.-R.; Hall, D. G. *Org. Biomol. Chem.* **2016**, *14*, 4739–4748.

(105) Avi, M.; Fechter, M. H.; Gruber, K.; Belaj, F.; Pöchlauer, P.; Griengl, H. *Tetrahedron* **2004**, *60*, 10411–10418.

(106) Lindsay, K. B.; Tang, M.; Pyne, S. G. *Synlett* **2002**, *5*, 731–734.

(107) Butora, G., Guiadeen, D., Kothandaraman, S., Maccoss, M., Mills, S., Yang, L. Aminocyclopentyl pyridopyrazinone modulators of chemokine receptor activity. WO 2005/072361 A2, 2004.

(108) Budzik, B.; Garzya, V.; Shi, D.; Walker, G.; Lauchart, Y.; Lucas, A. J.; Rivero, R. A.; Langmead, C. J.; Watson, J.; Wu, Z.; Forbes, I. T.; Jin, J. *Bioorg. Med. Chem. Lett.* **2010**, *20*, 3545–3549.

(109) Richardson, T. I.; Frank, S. A.; Wang, M.; Clarke, C. A.; Jones, S. A.; Ying, B. P.; Kohlman, D. T.; Wallace, O. B.; Shepherd, T. A.; Dally, R. D.; Palkowitz, A. D.; Geiser, A. G.; Bryant, H. U.; Henck, J. W.; Cohen, I. R.; Rudmann, D. G.; McCann, D. J.; Coutant, D. E.; Oldham, S. W.; Hummel, C. W.; Fong, K. C.; Hinklin, R.; Lewis, G.; Tian, H.; Dodge, J. A. *Bioorg. Med. Chem. Lett.* **2007**, *17*, 3544–3549.

Appendix: Reproductions of Important NMR Spectra and Selected Chromatograms for Enantiomeric Excess Measurements

See experimental sections for conditions

2-(4-Chlorophenyl)-α-(2*R*)-2-piperidinyl-, (α*R*)- 4-quinolinemethanol (2.1):

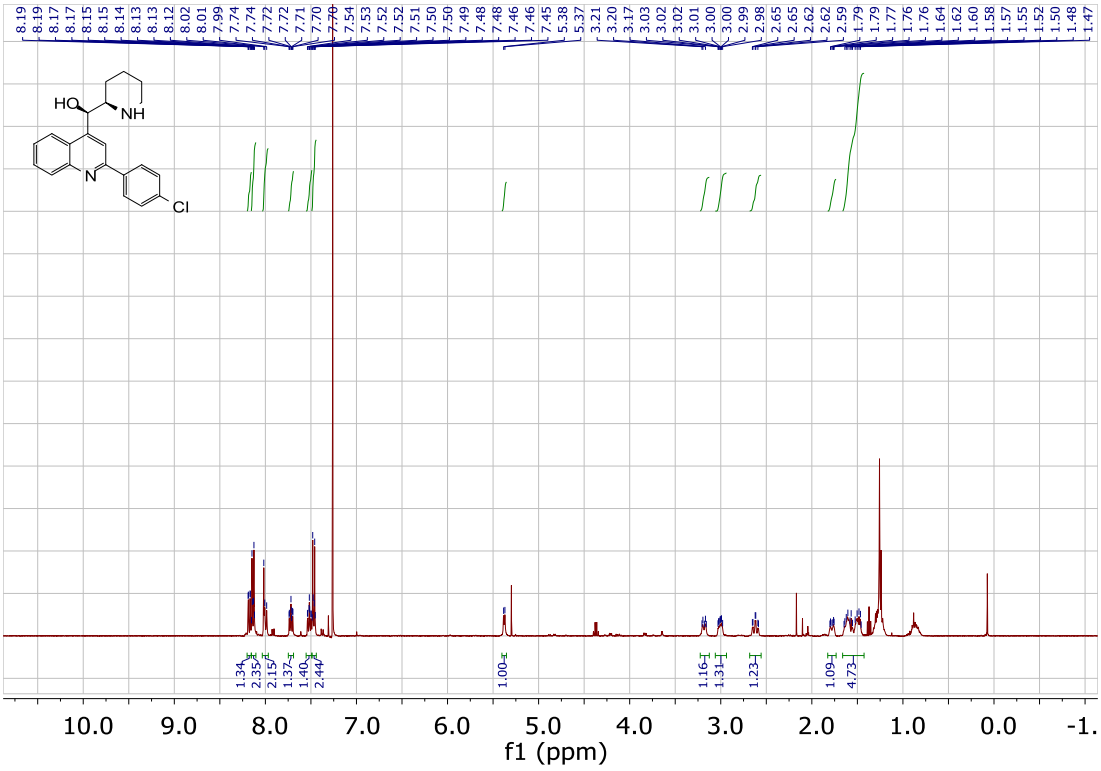

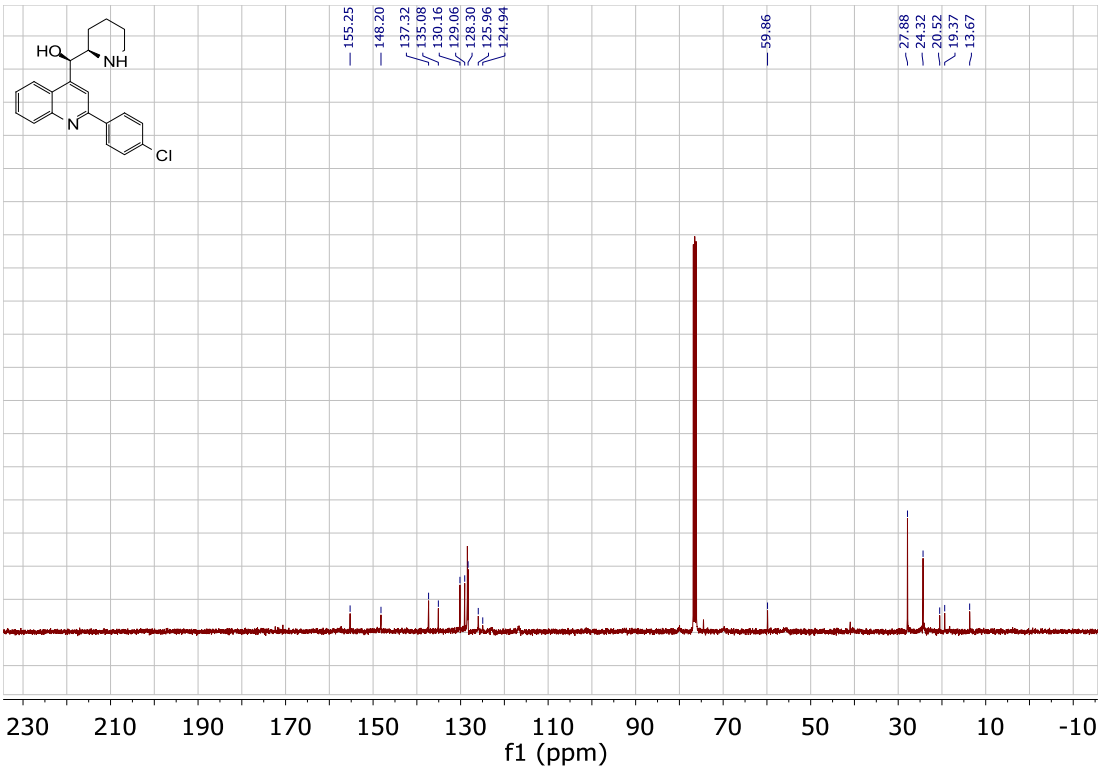

2-(4-Chlorophenyl)-α-(2*S*)-2-piperidinyl-, (α*S*)- 4-quinolinemethanol (2.3):

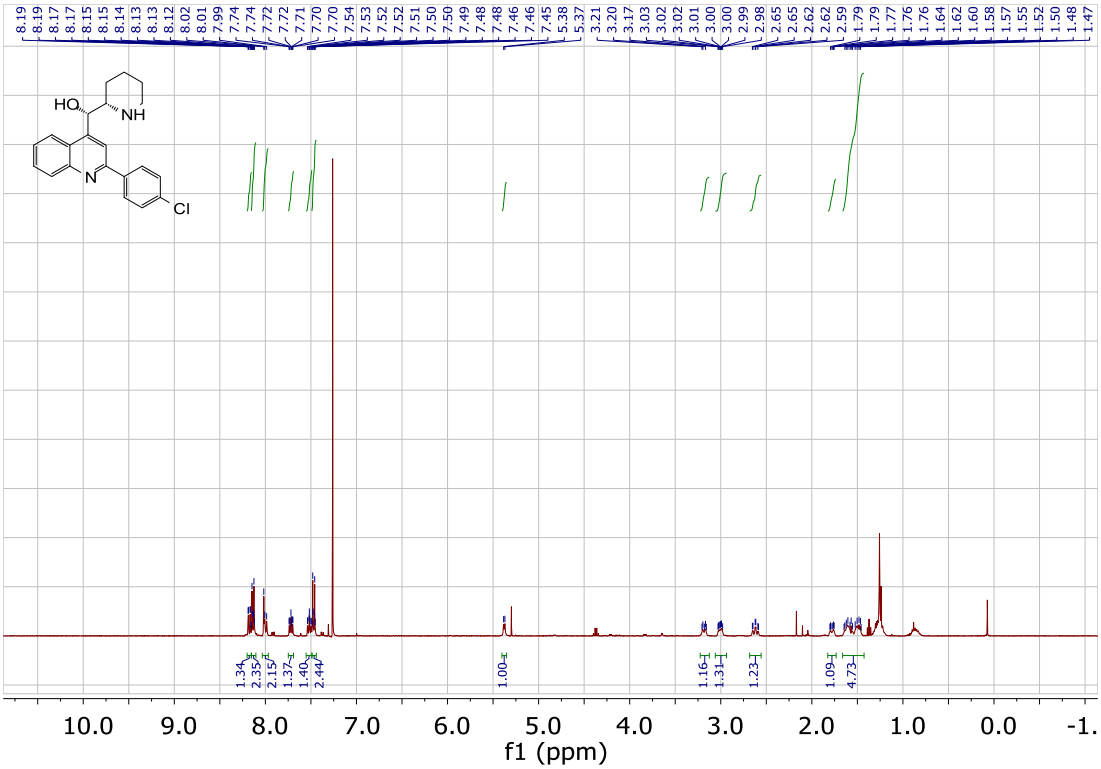

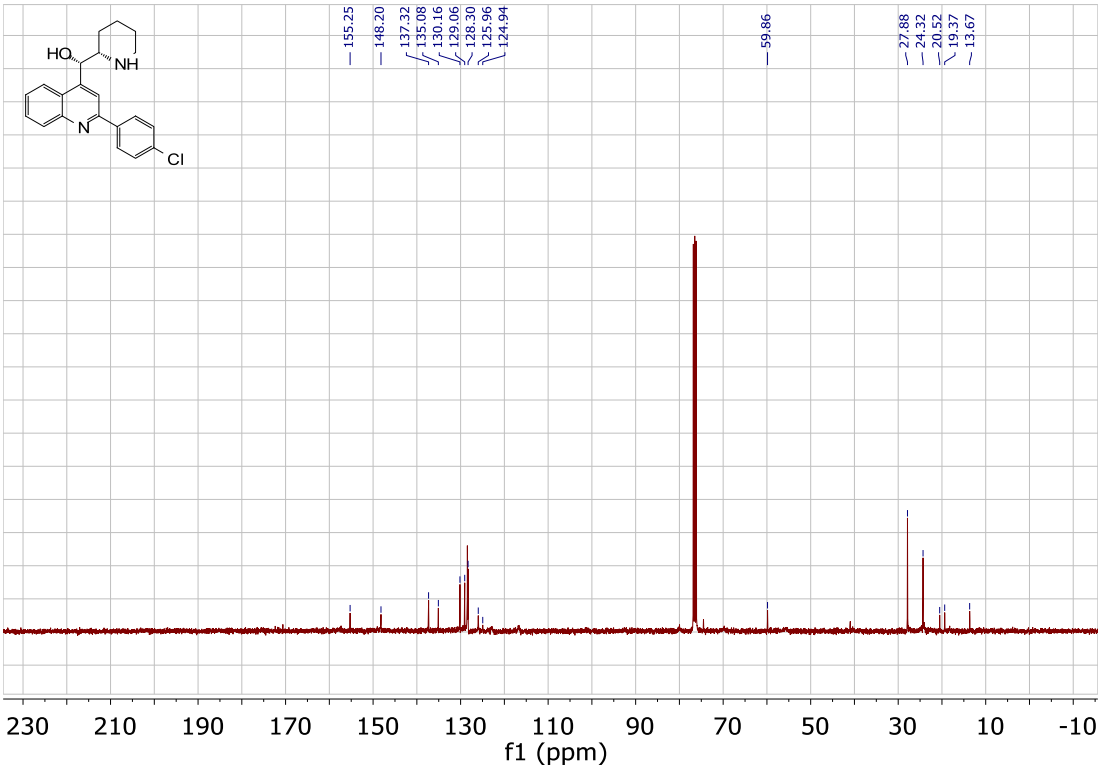

2-(4-Chlorophenyl)-α-(2*R*)-2-5,6-dihydropyridinyl-, (α*R*)- 4-quinolinemethanol:

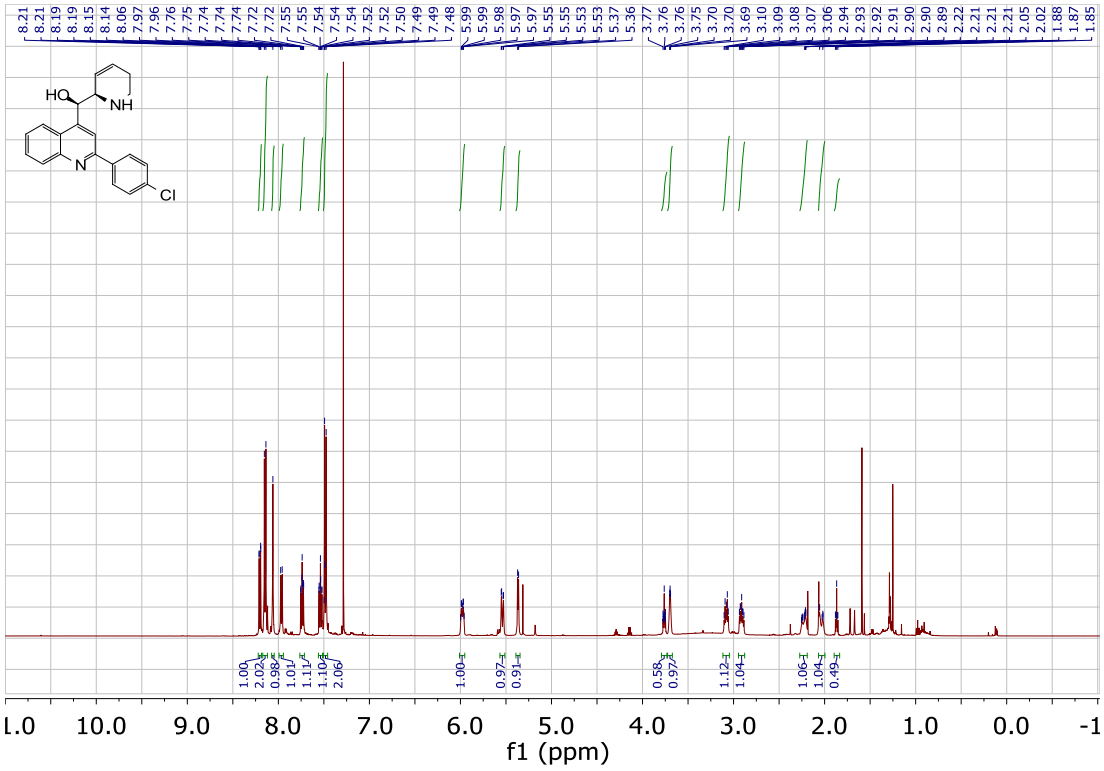

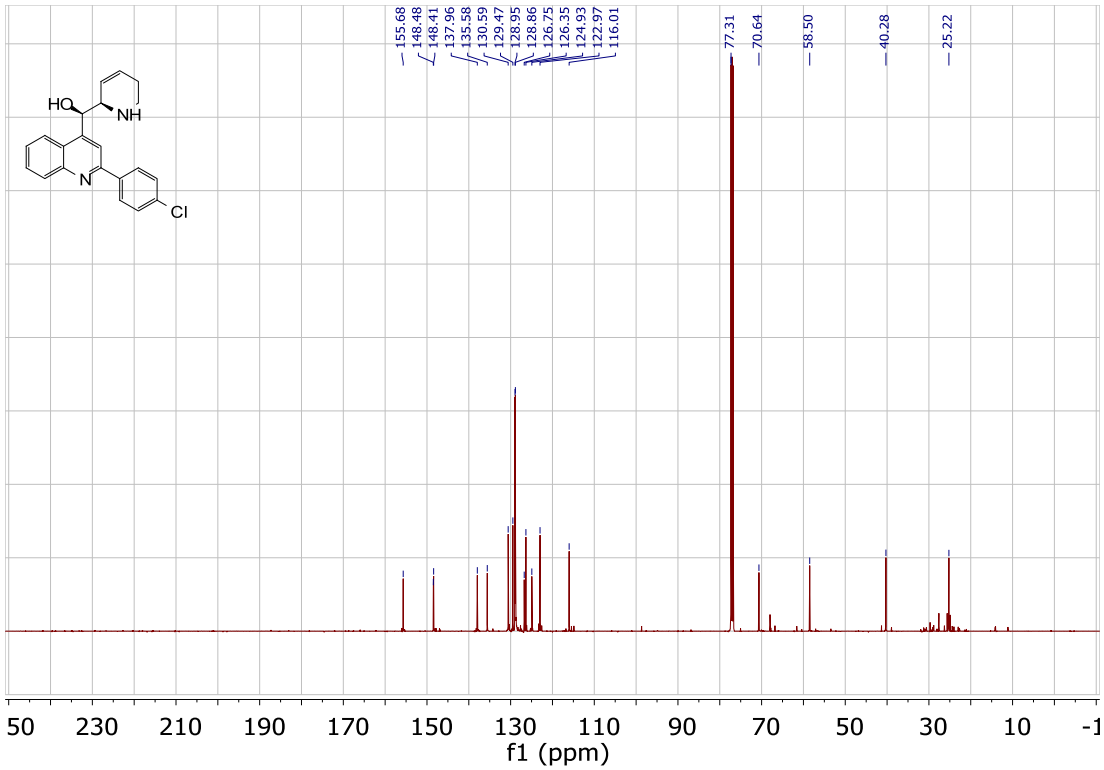

2-(4-Chlorophenyl)-α-(2*S*)-2-5,6-dihydropyridinyl-, (α*S*)- 4-quinolinemethanol:

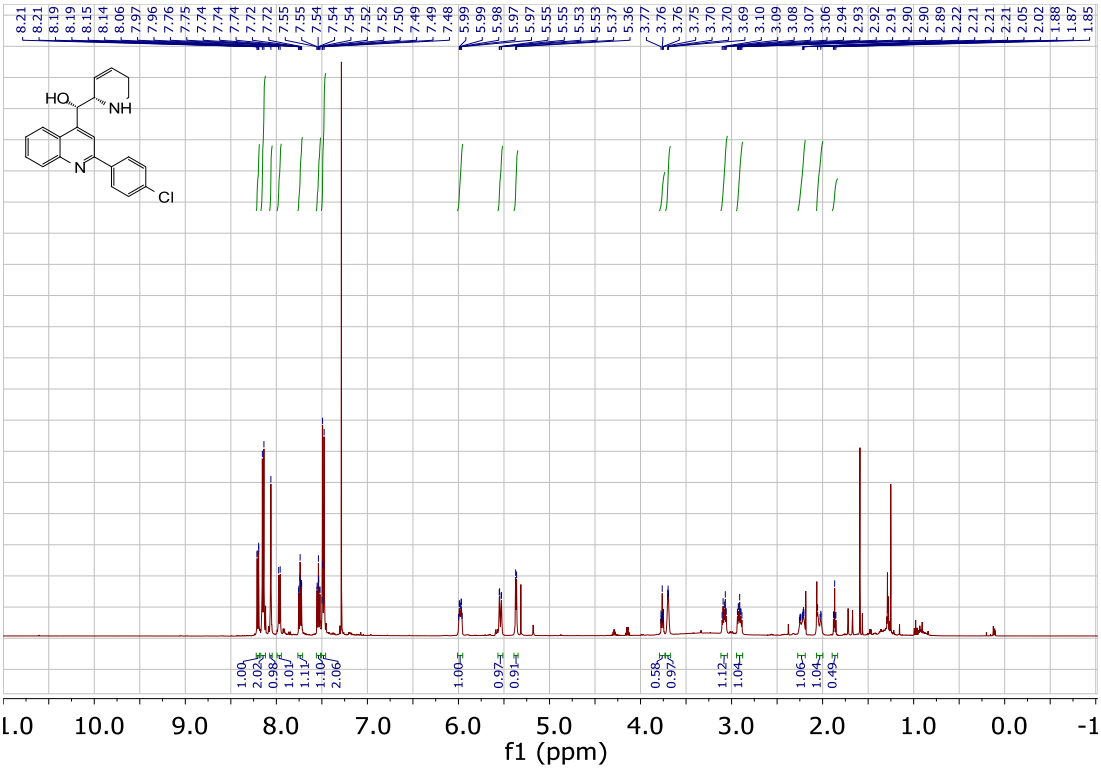

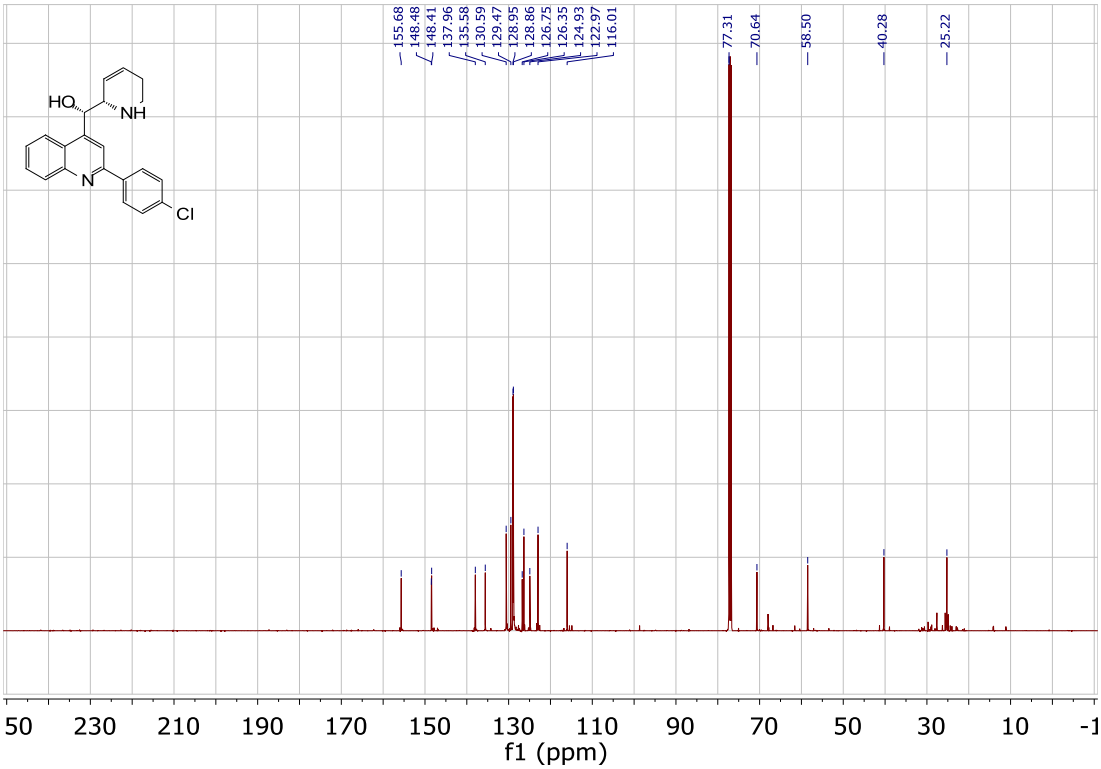

2-(4-Chlorophenyl)-α-(2*R*)-2-5,6-dihydropyridinyl-, (α*S*)- 4-quinolinemethanol:

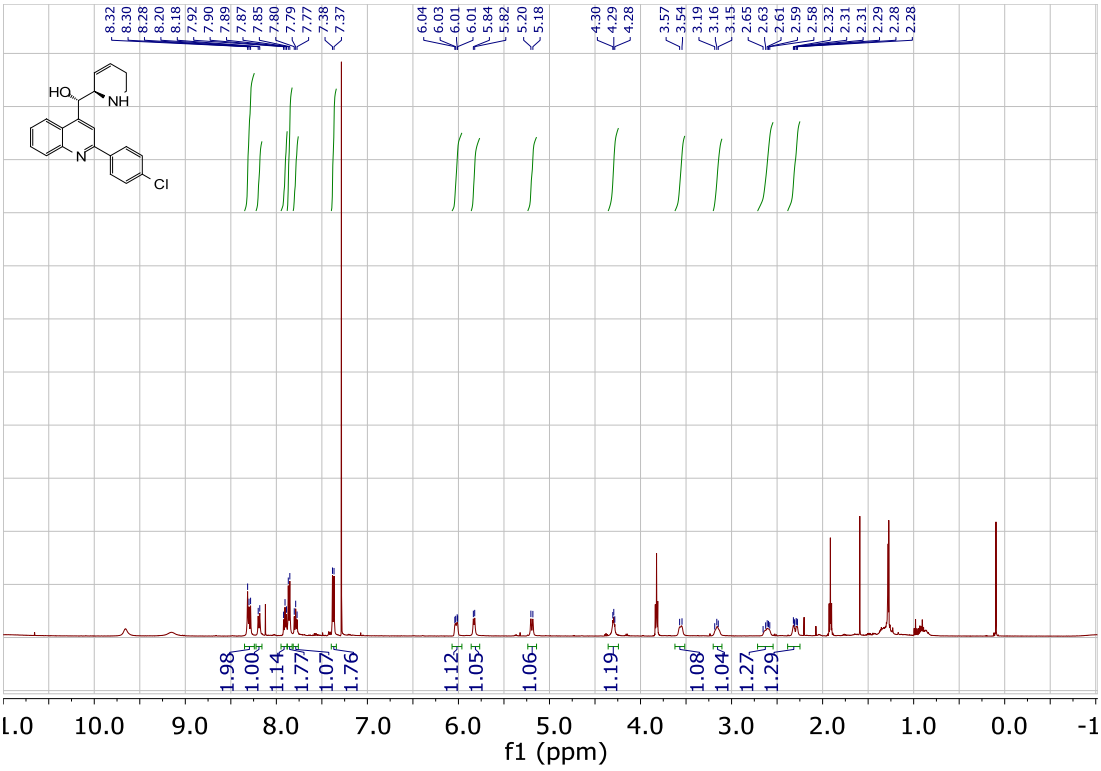

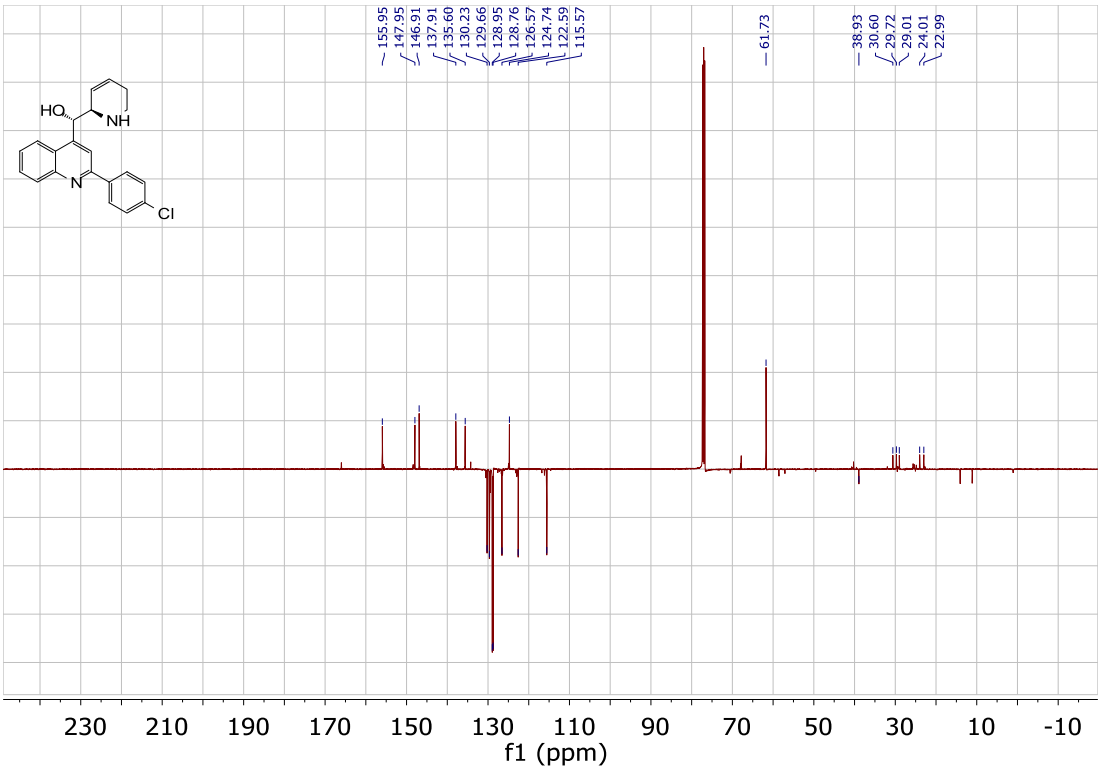

2-(4-Chlorophenyl)-α-(2*S*)-2-5,6-dihydropyridinyl-, (α*R*)- 4-quinolinemethanol:

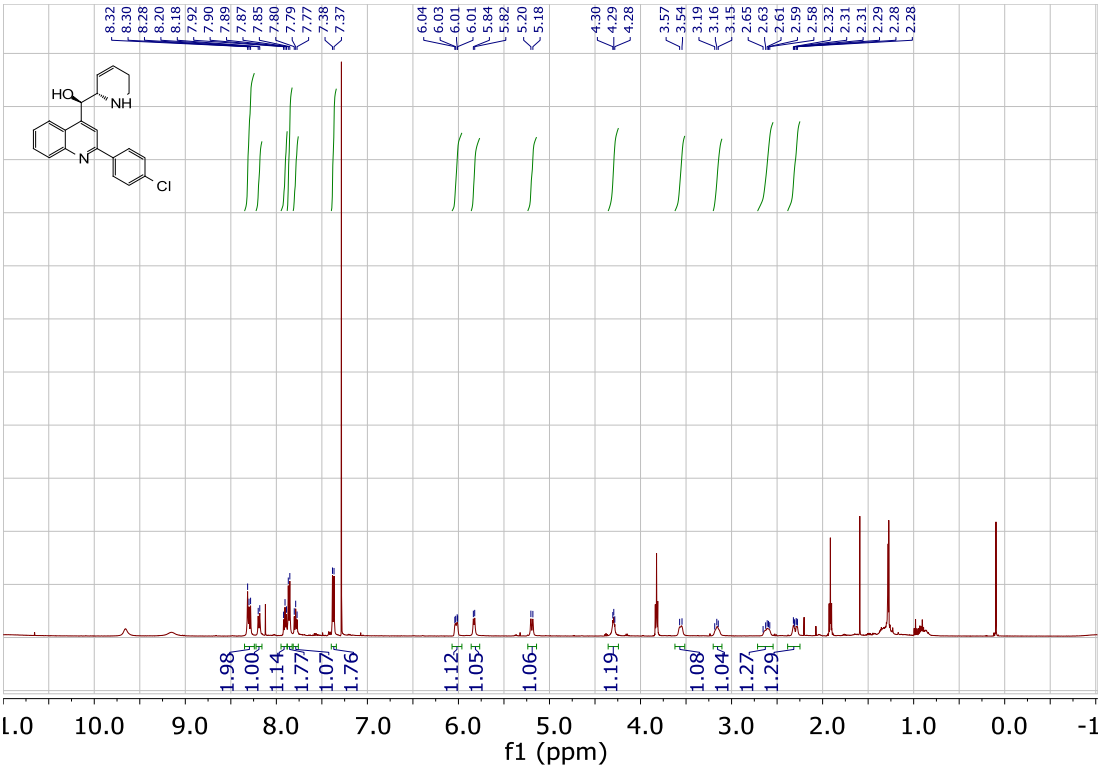

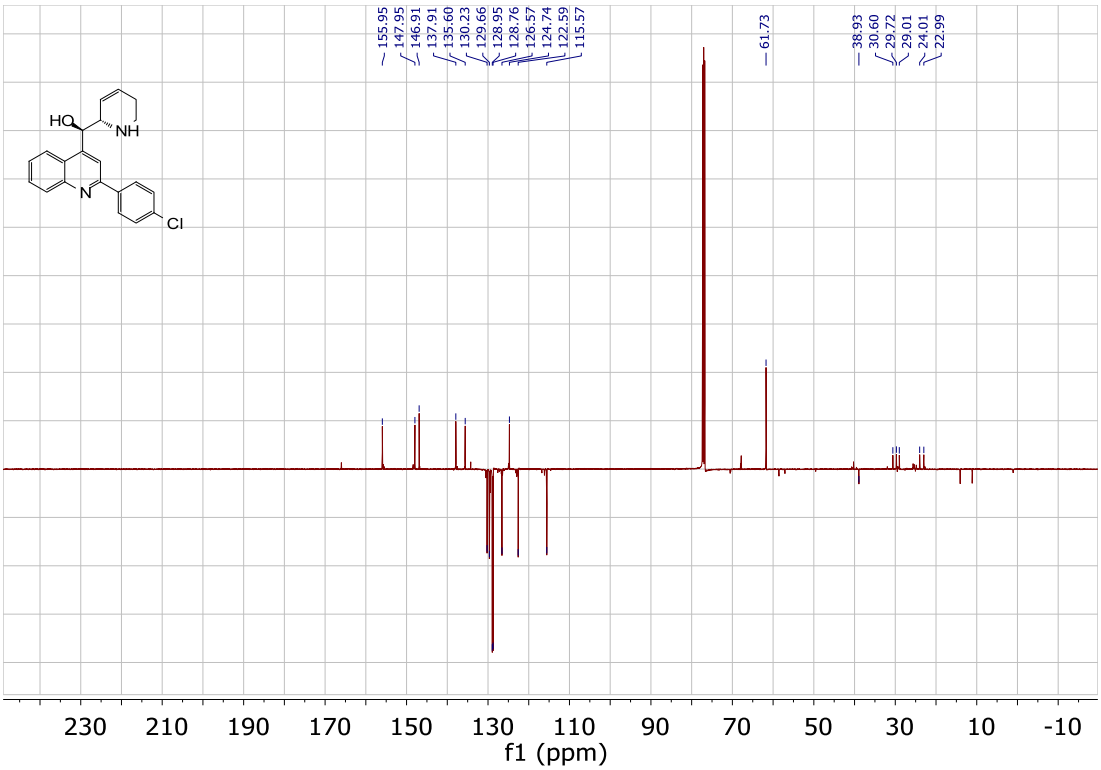

2-(4-Chlorophenyl)-α-(2*S*)-2-piperidinyl-, (α*R*)- 4-quinolinemethanol (2.4):

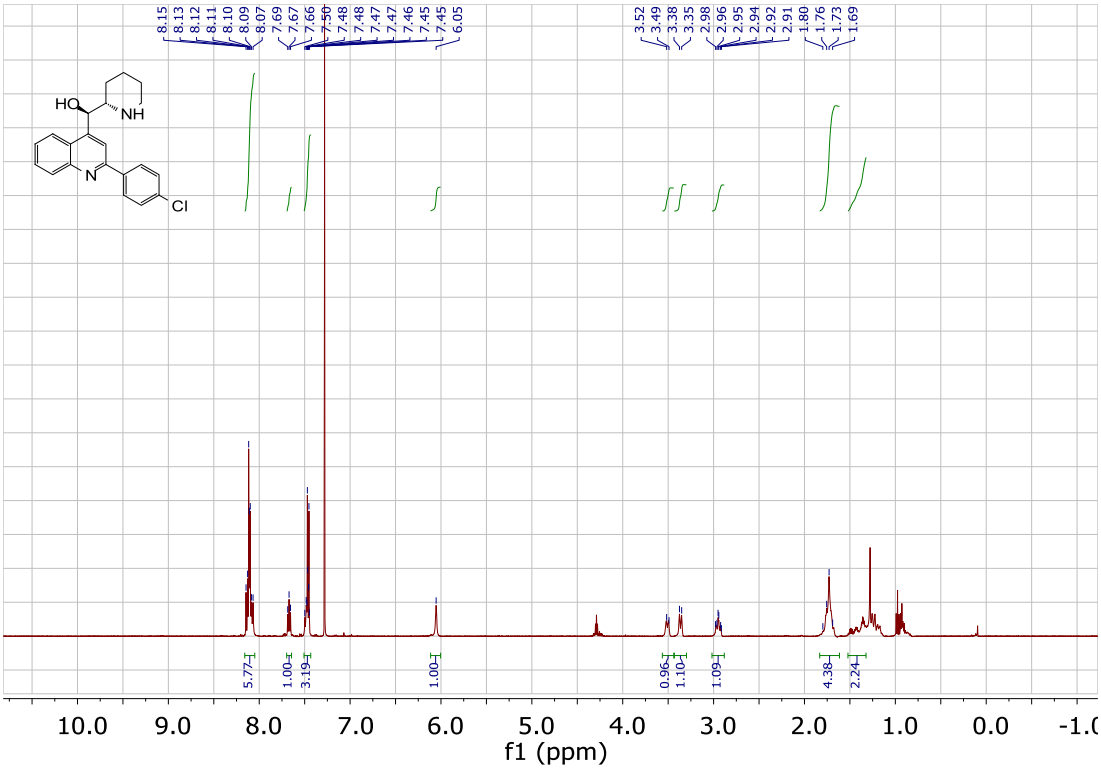

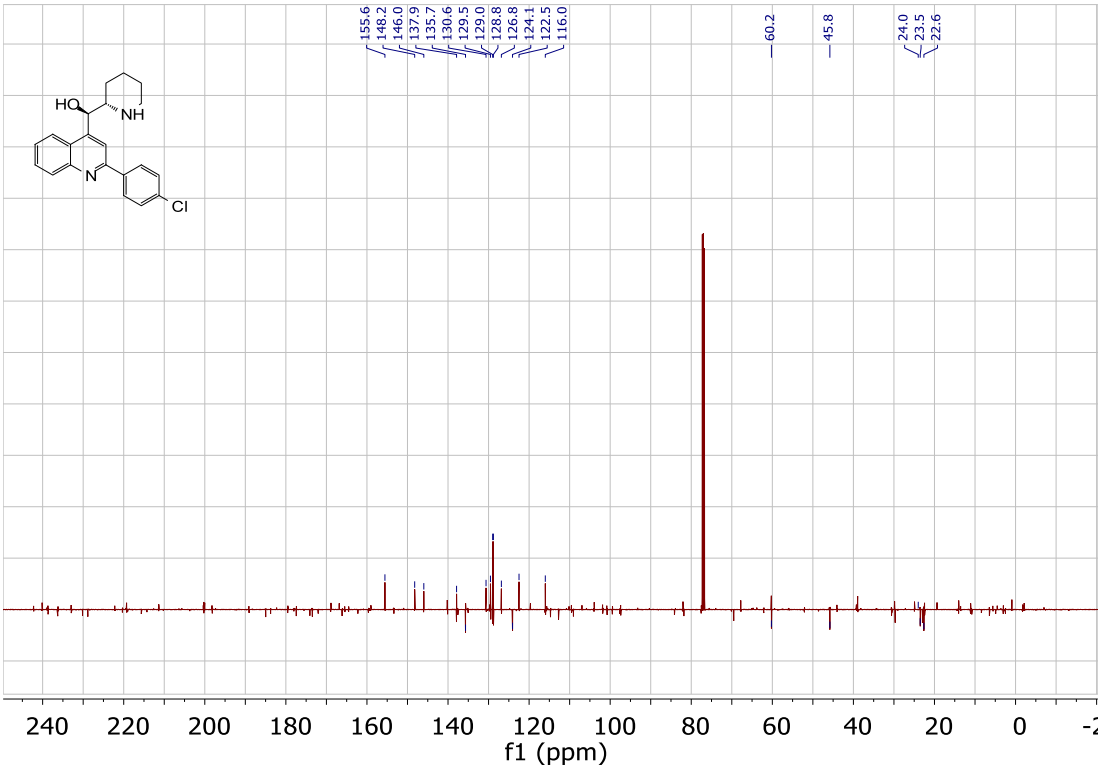

2-(4-Chlorophenyl)-α-(2*R*)-2-piperidinyl-, (α*S*)- 4-quinolinemethanol (2.2):

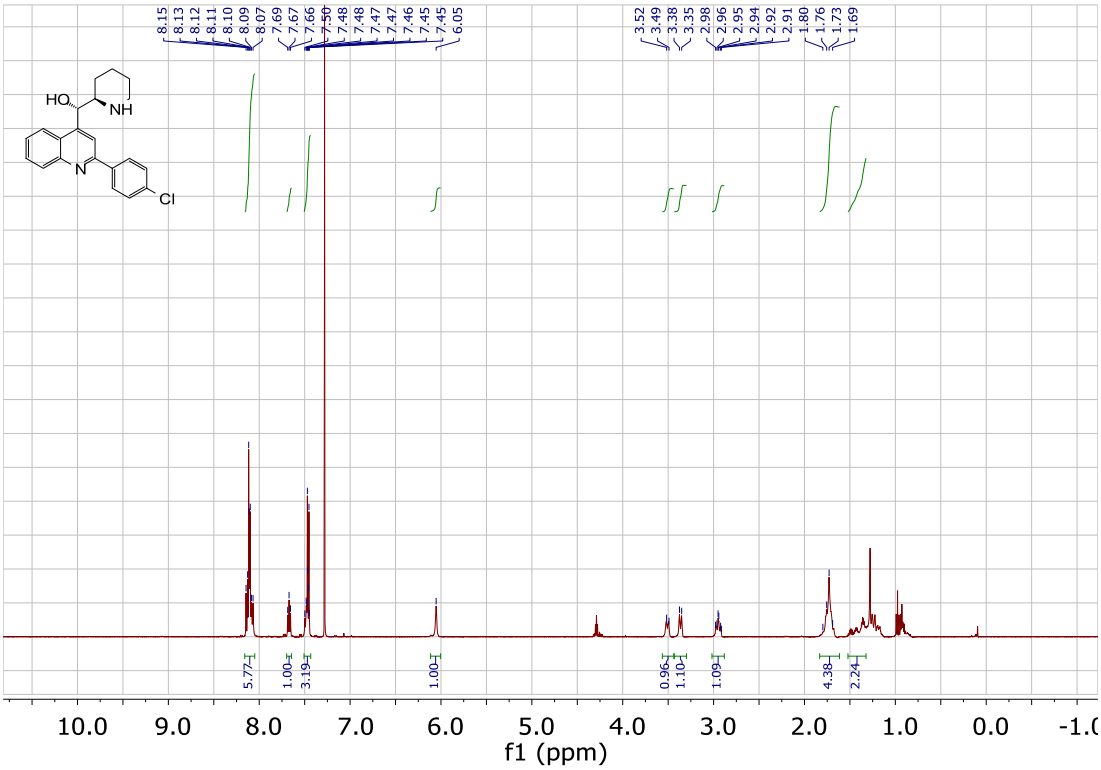

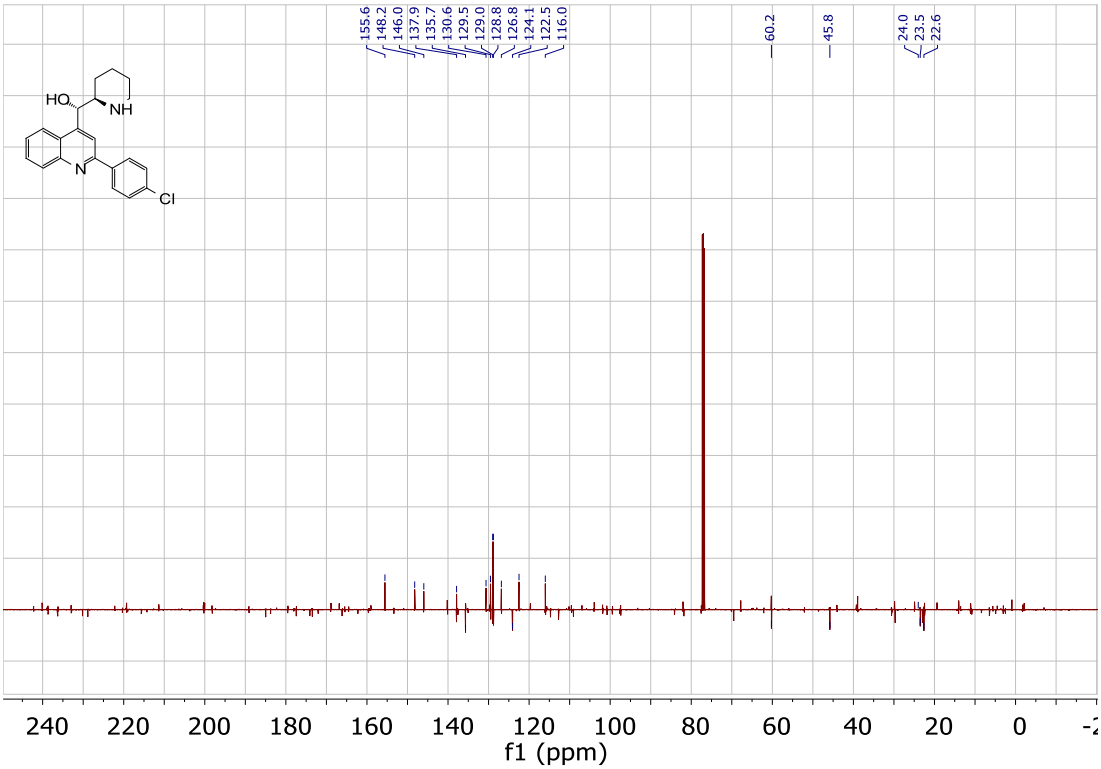

2-(Phenyl)-α-(2*R*)-2-piperidinyl-, (α*R*)- 4-quinolinemethanol:

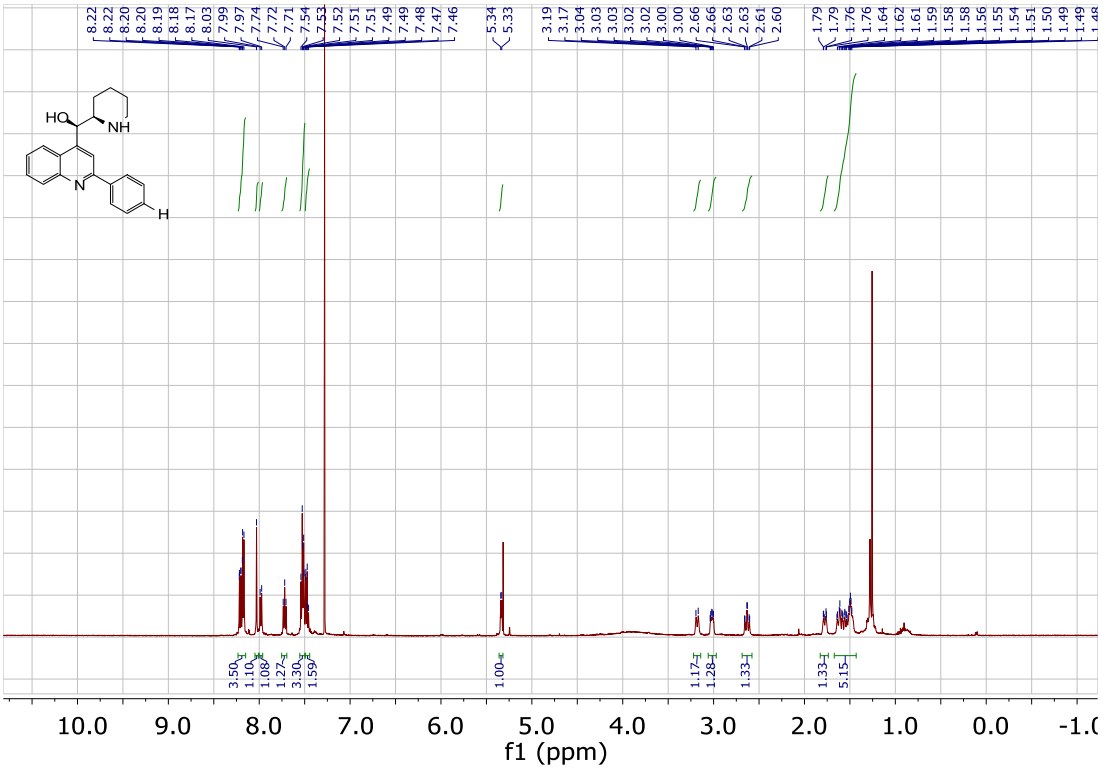

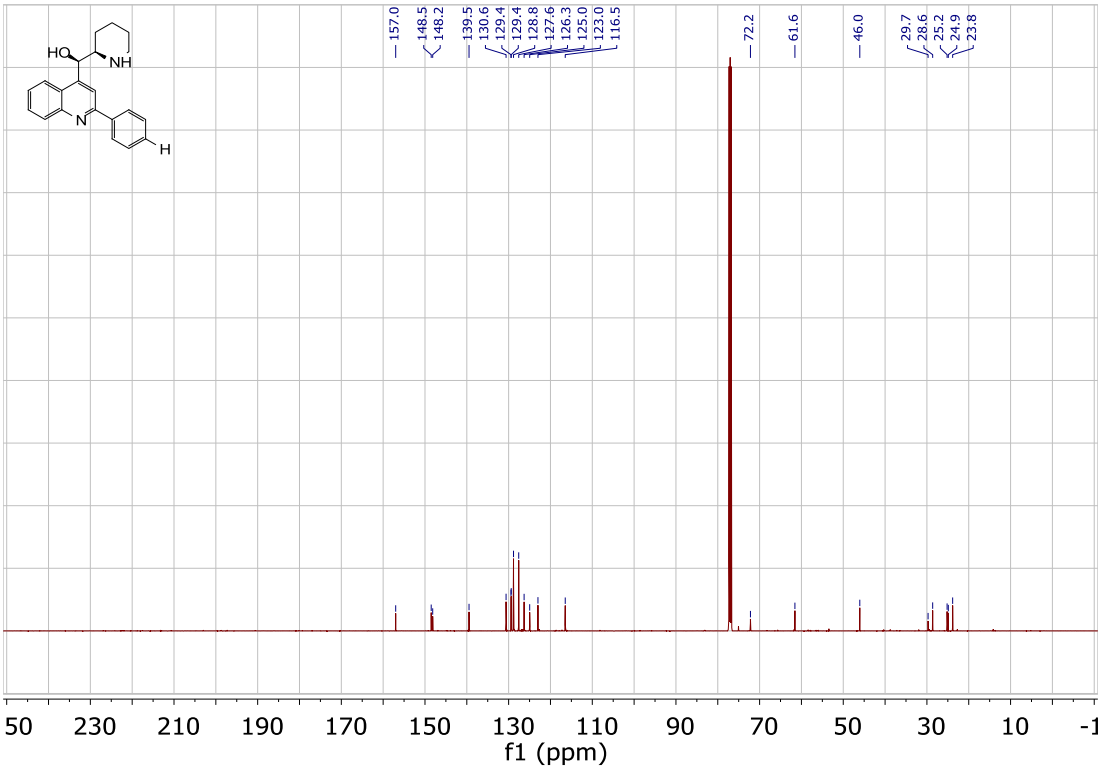

2-(4-Bromophenyl)-α-(2*R*)-2-piperidinyl-, (α*R*)- 4-quinolinemethanol:

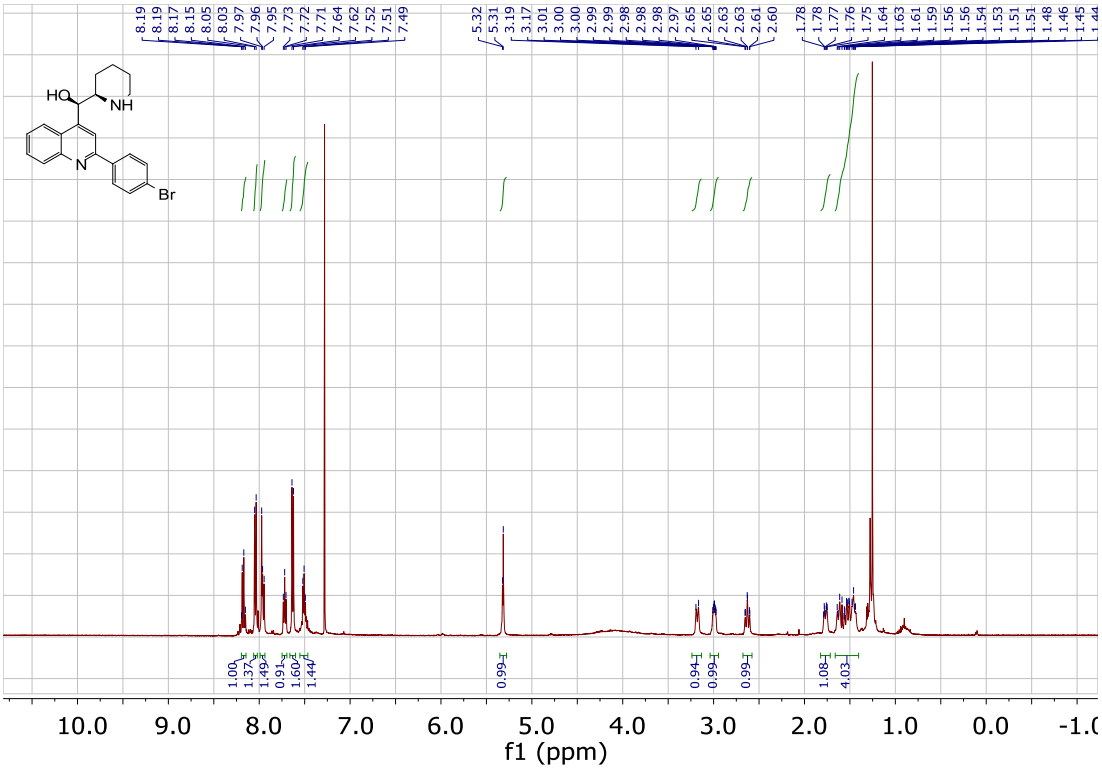

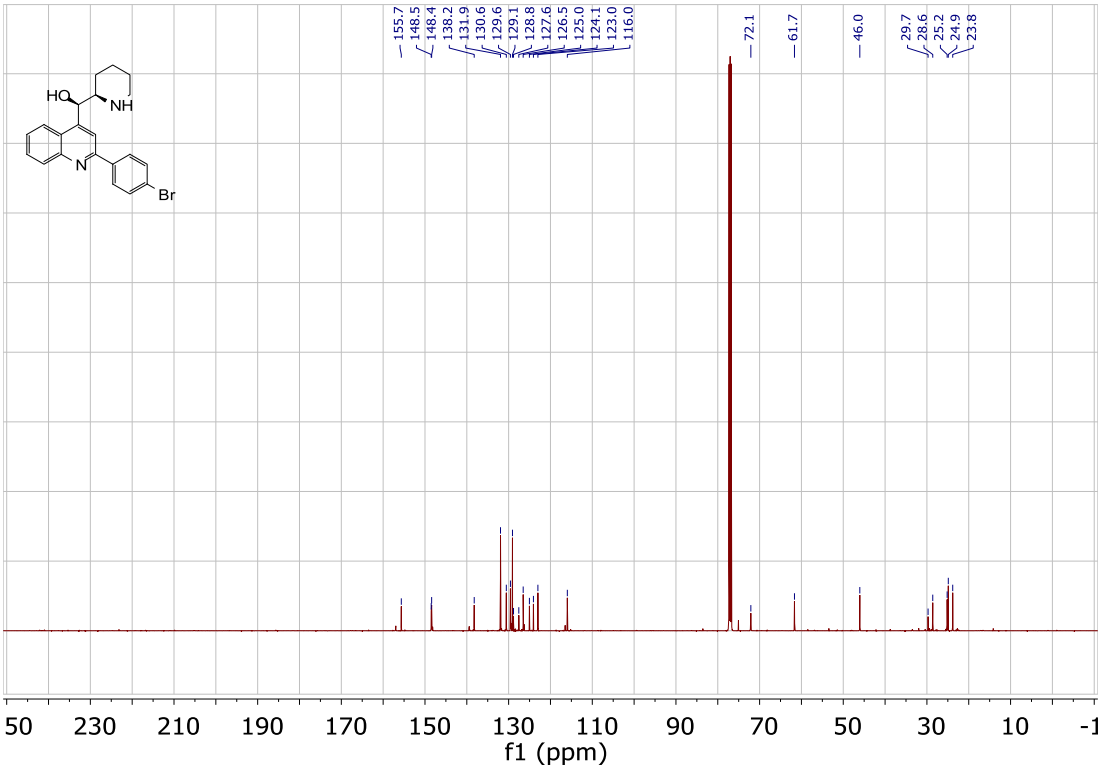

2-(4-Methoxyphenyl)-α-(2*R*)-2-piperidinyl-, (α*R*)- 4-quinolinemethanol:

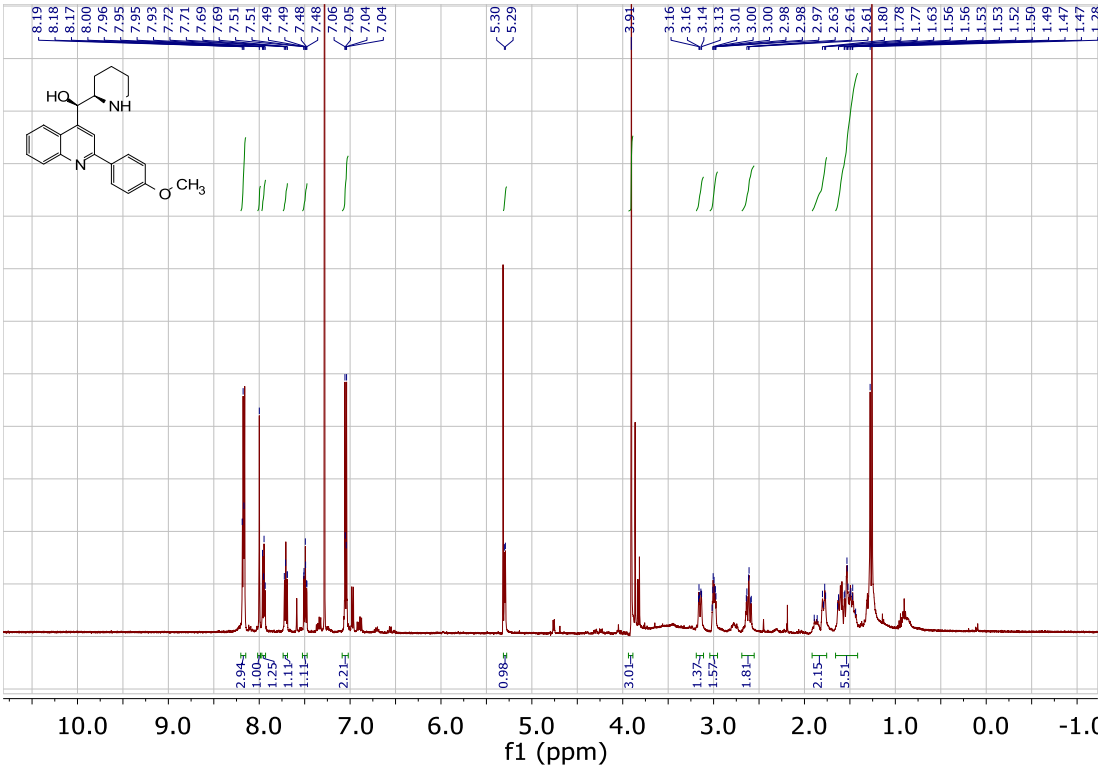

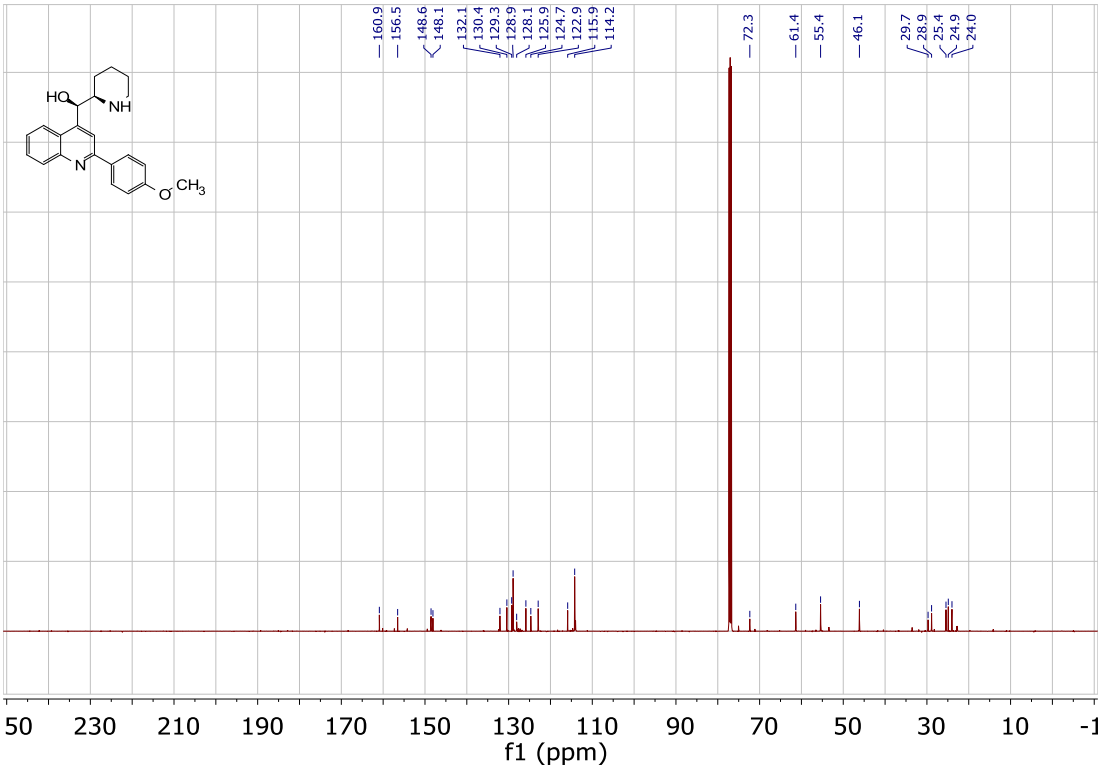

2-(4-Methylphenyl)-α-(2*R*)-2-piperidinyl-, (α*R*)- 4-quinolinemethanol:

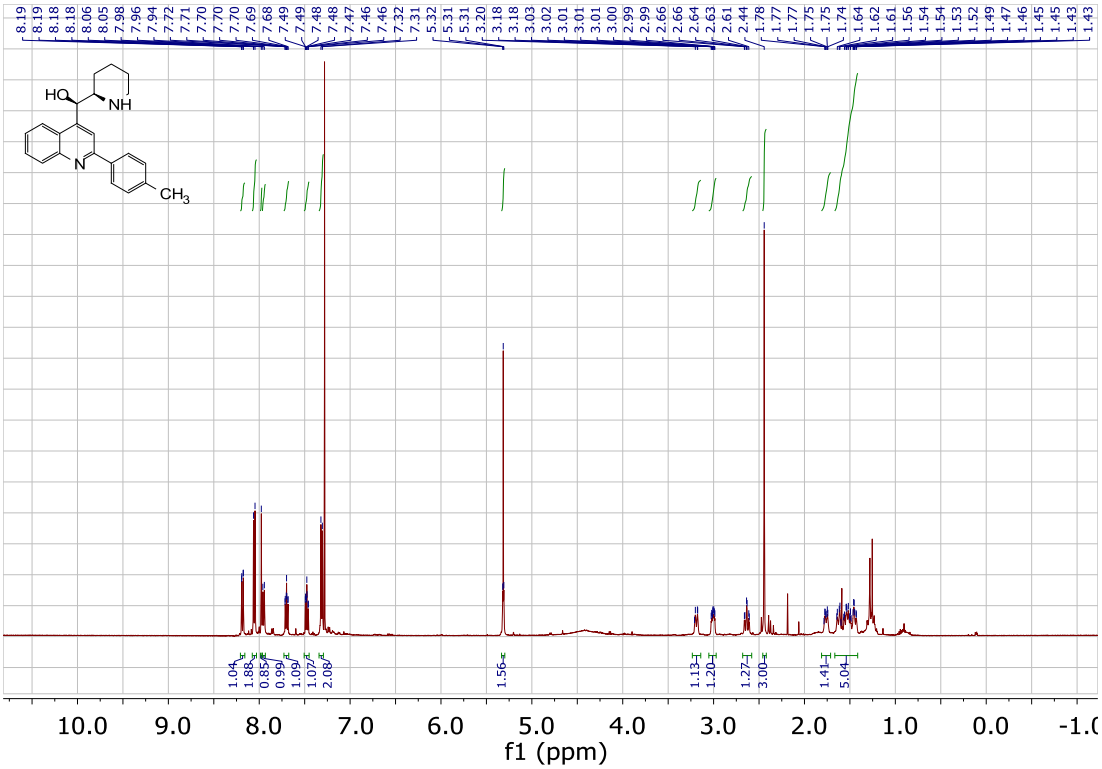

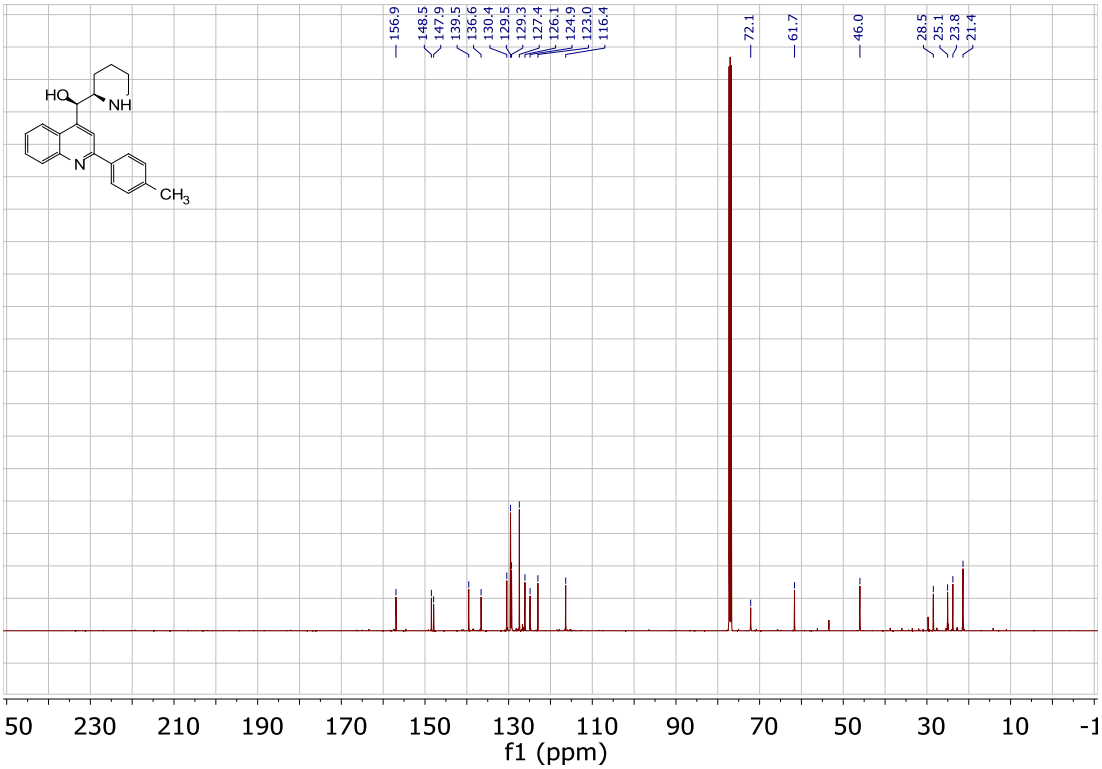

2-(Phenyl)-α-(2*S*)-2-piperidinyl-, (α*S*)- 4-quinolinemethanol:

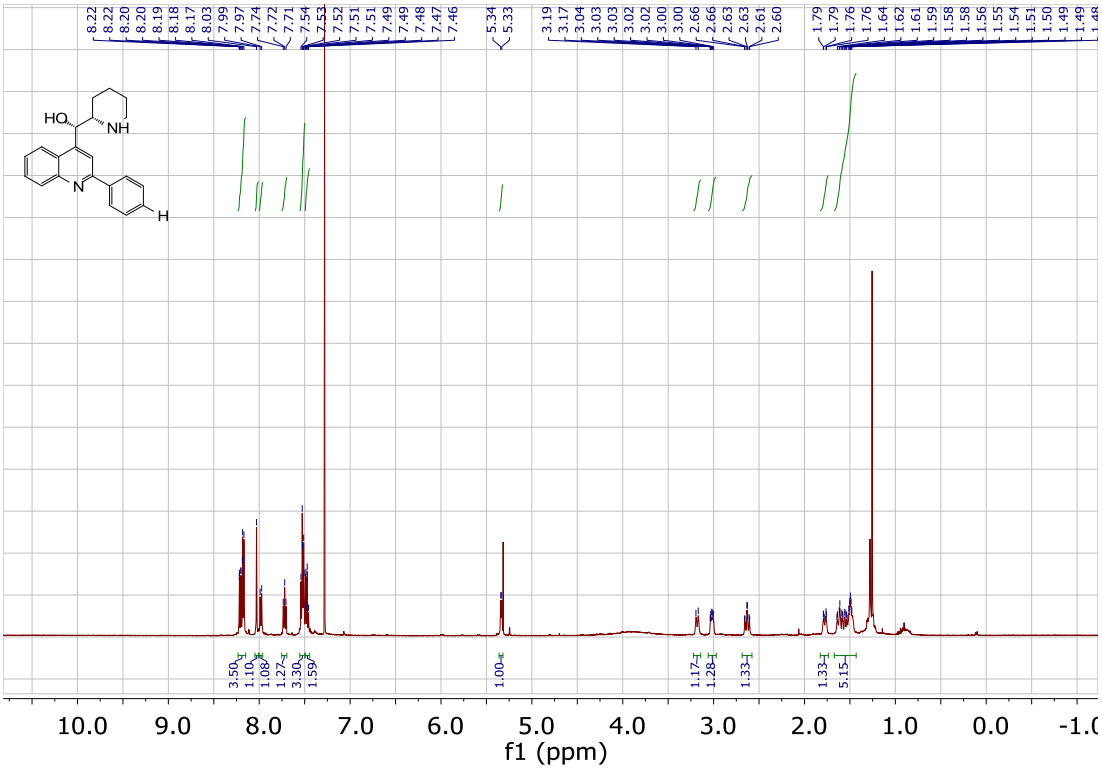

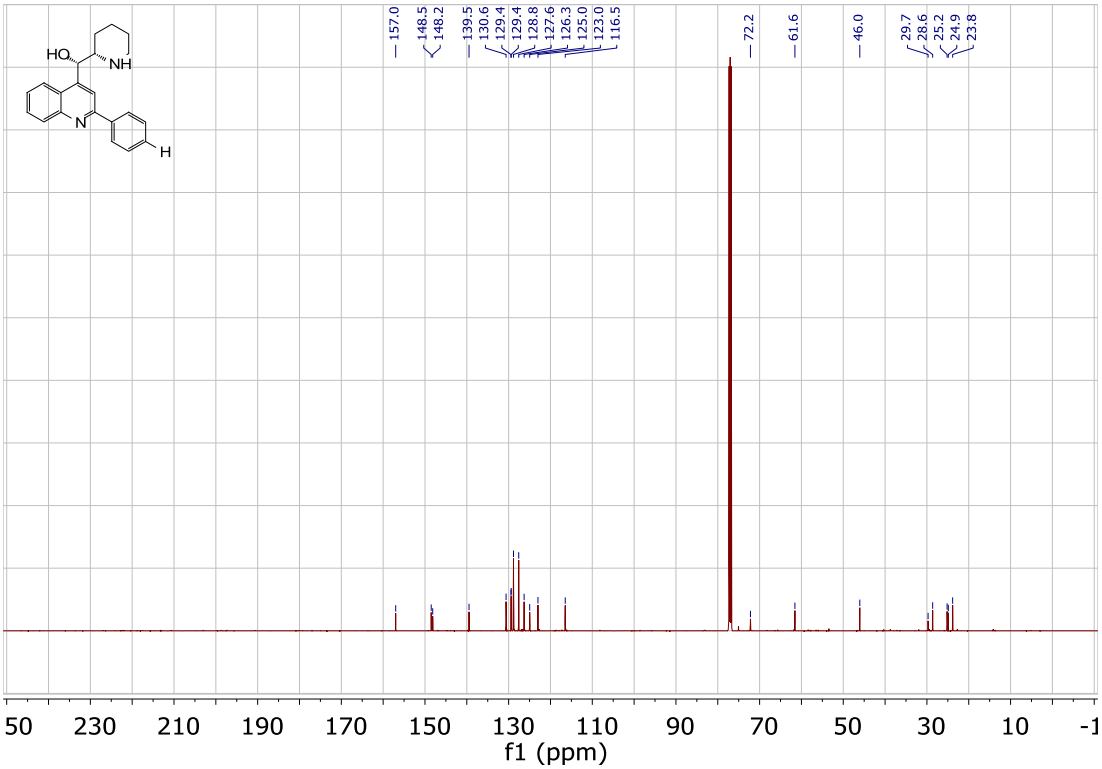

2-(4-Bromophenyl)-α-(2*S*)-2-piperidinyl-, (α*S*)- 4-quinolinemethanol:

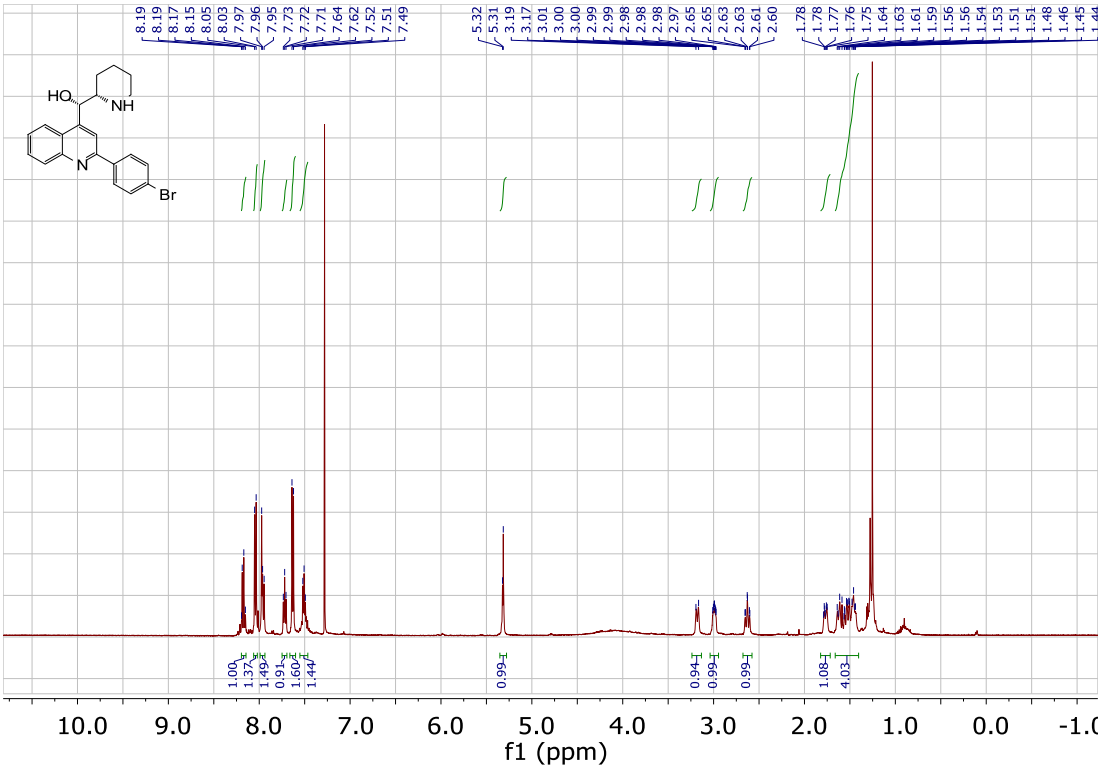

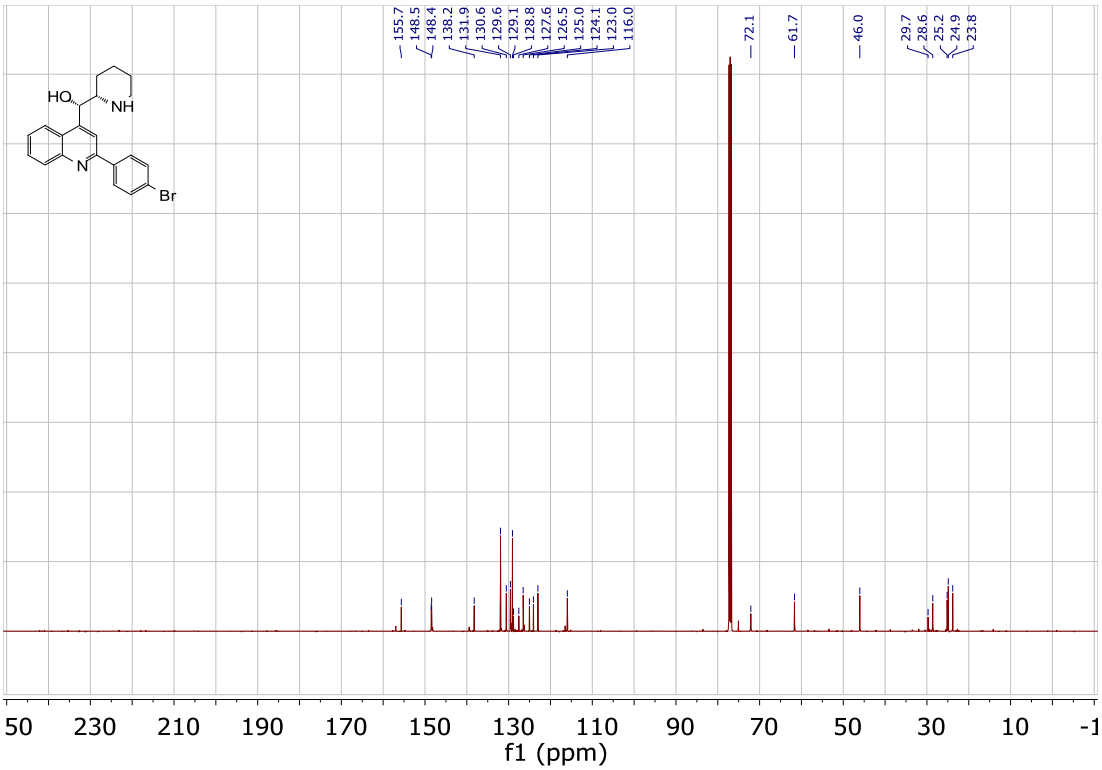

2-(4-Methoxyphenyl)-α-(2*S*)-2-piperidinyl-, (α*S*)- 4-quinolinemethanol:

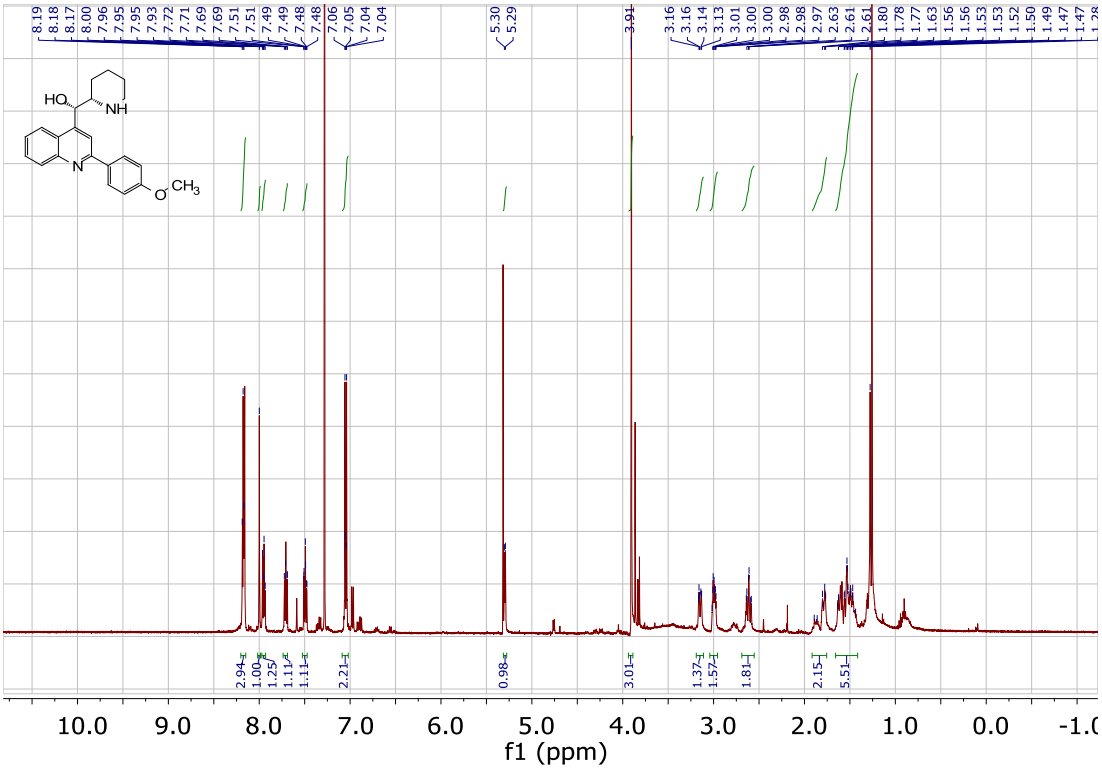

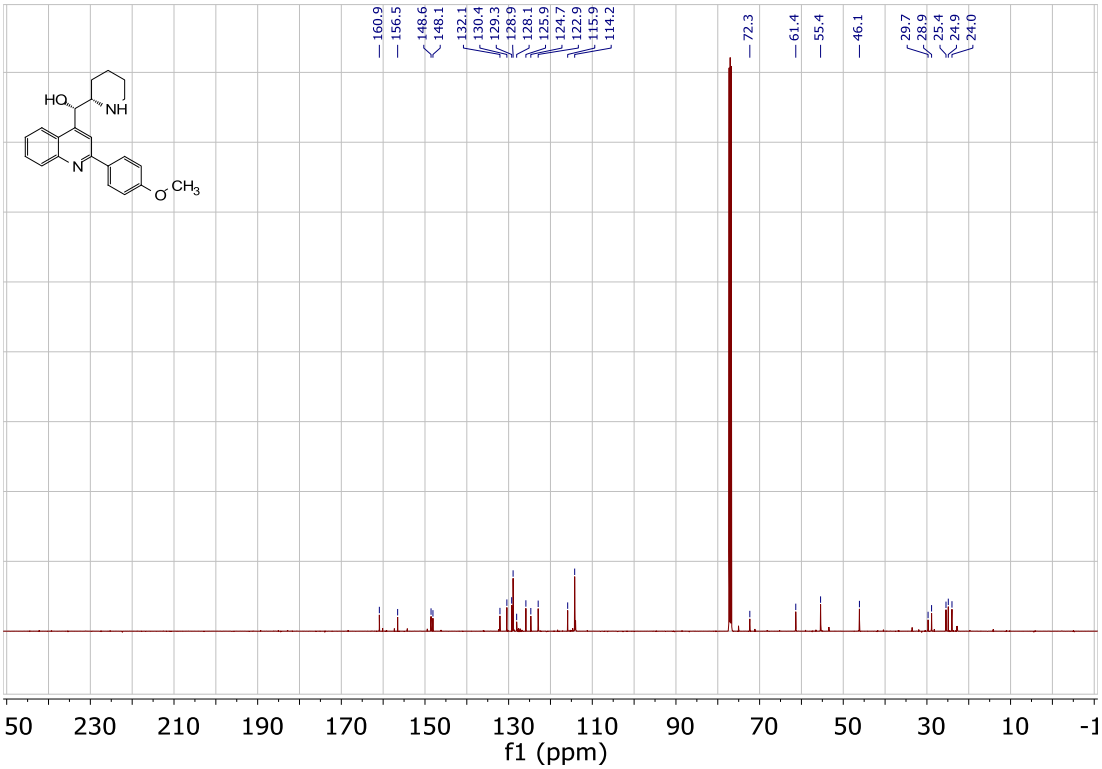

2-(4-Methylphenyl)-α-(2*S*)-2-piperidinyl-, (α*S*)- 4-quinolinemethanol:

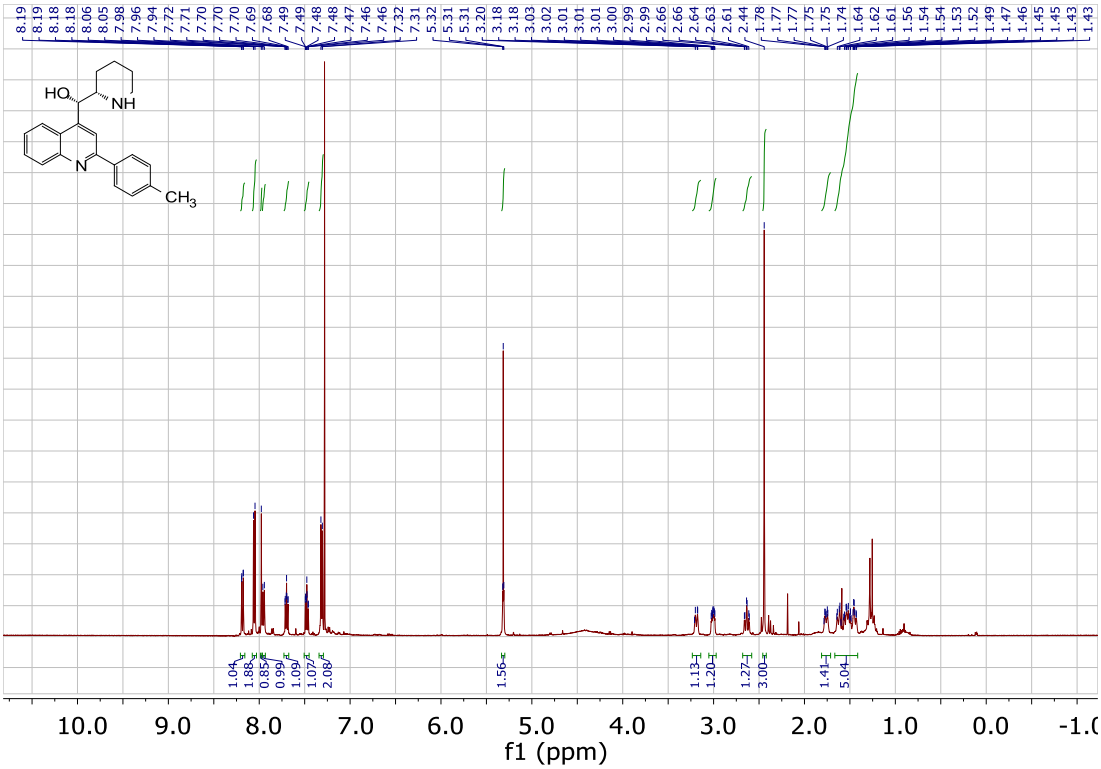

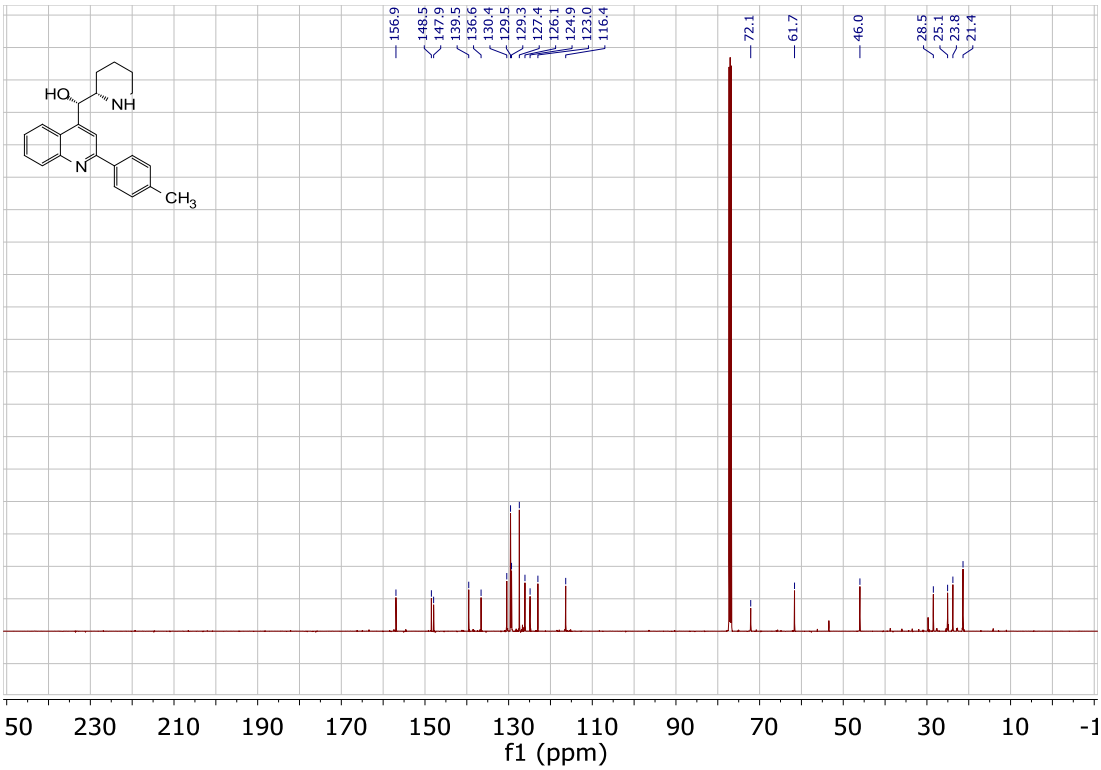

***tert*-Butyl 2-(4-chlorophenyl)-α-(2*S*)-2-piperinyl-, (α*S*)- 4-quinolinemethanol- 1(2H)-carboxylate:**

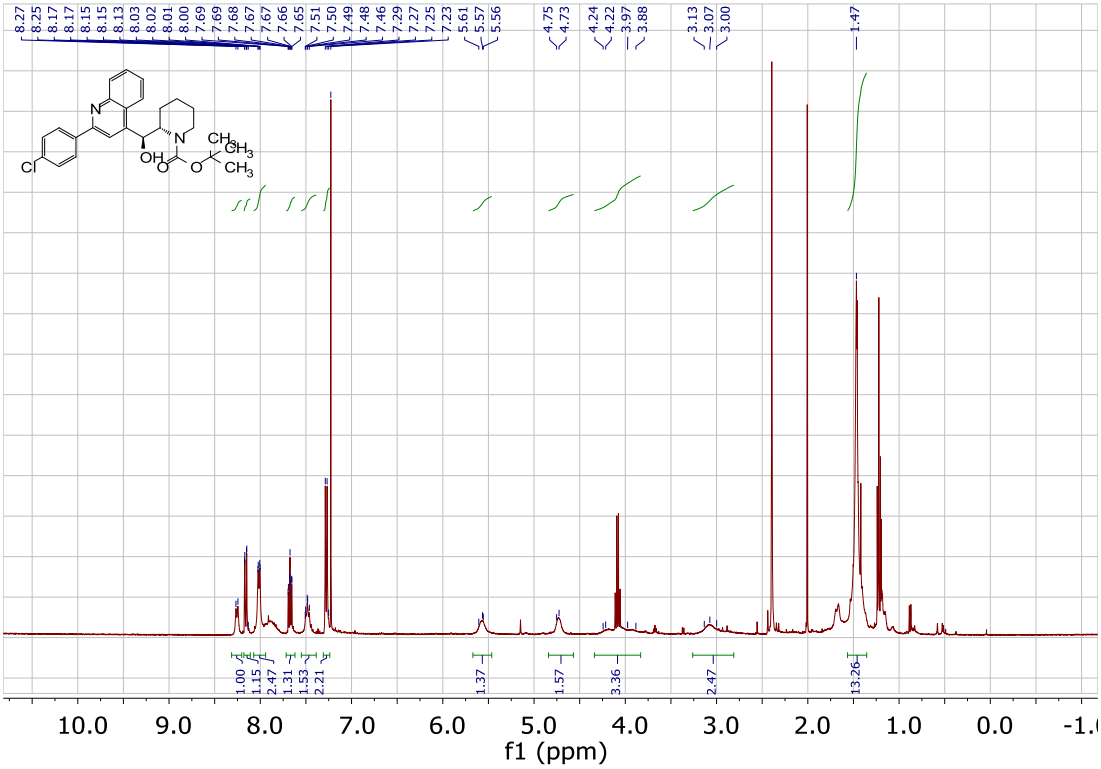

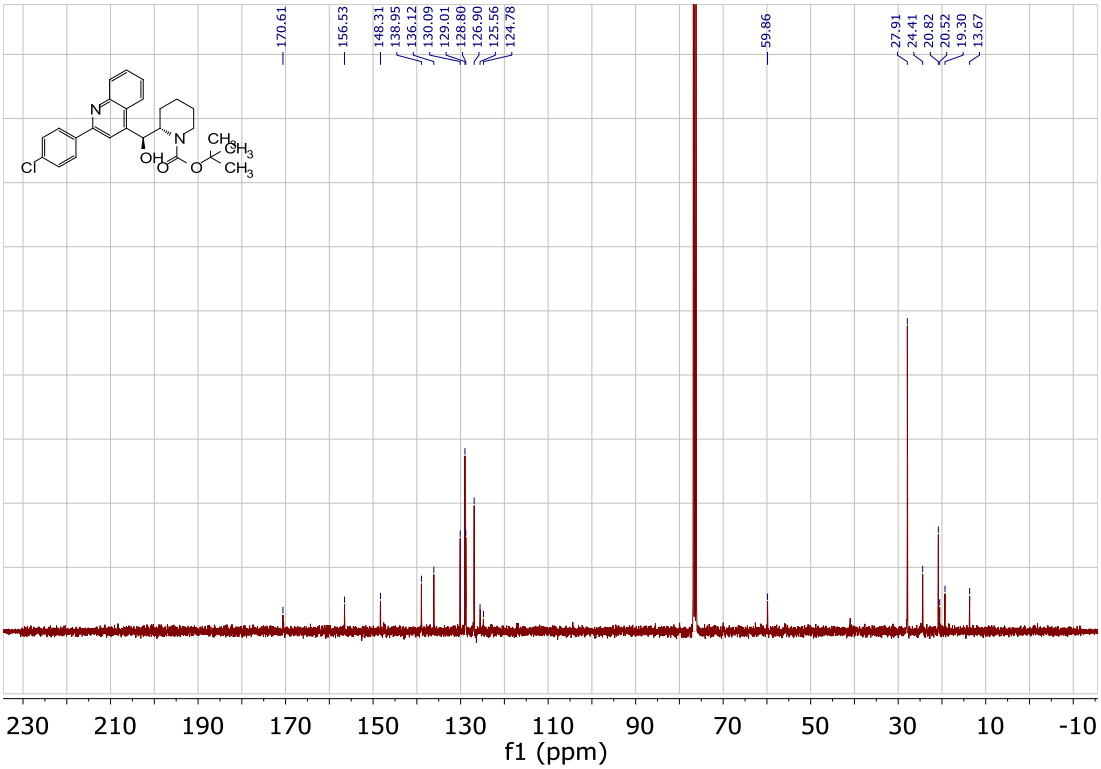

***tert*-Butyl 2-(4-chlorophenyl)-α-(2*R*)-2-piperinyl-, (α*R*)- 4-quinolinemethanol- 1(2H)-carboxylate:**

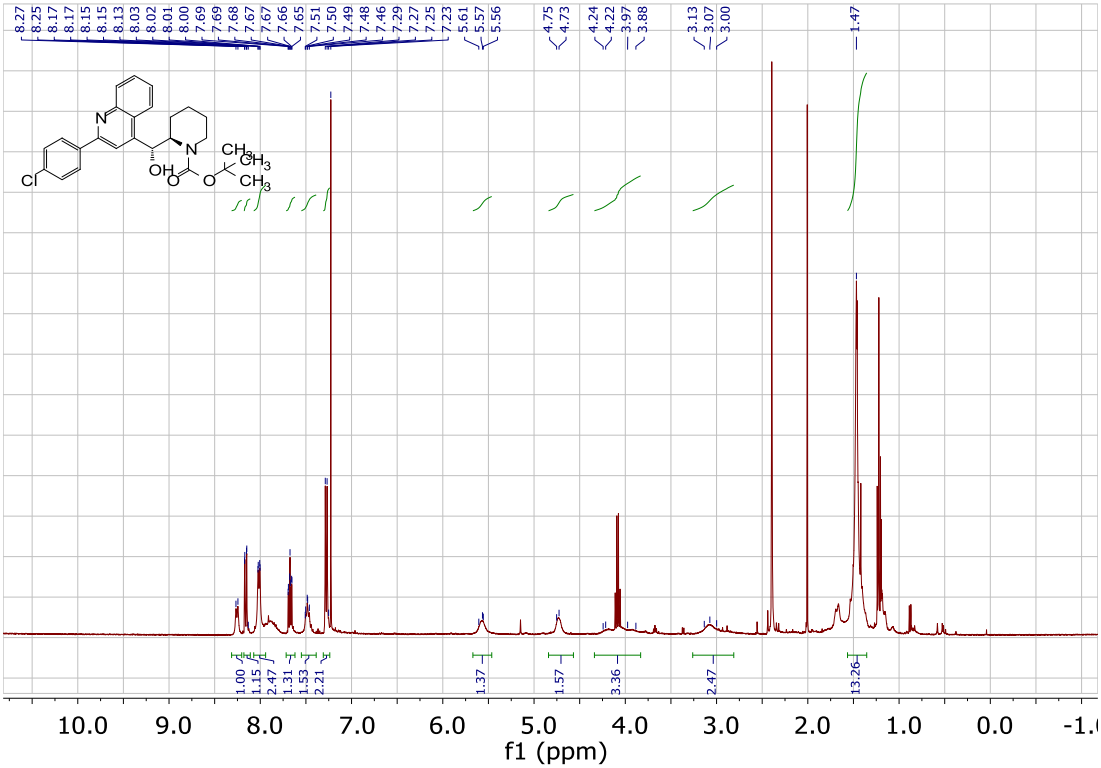

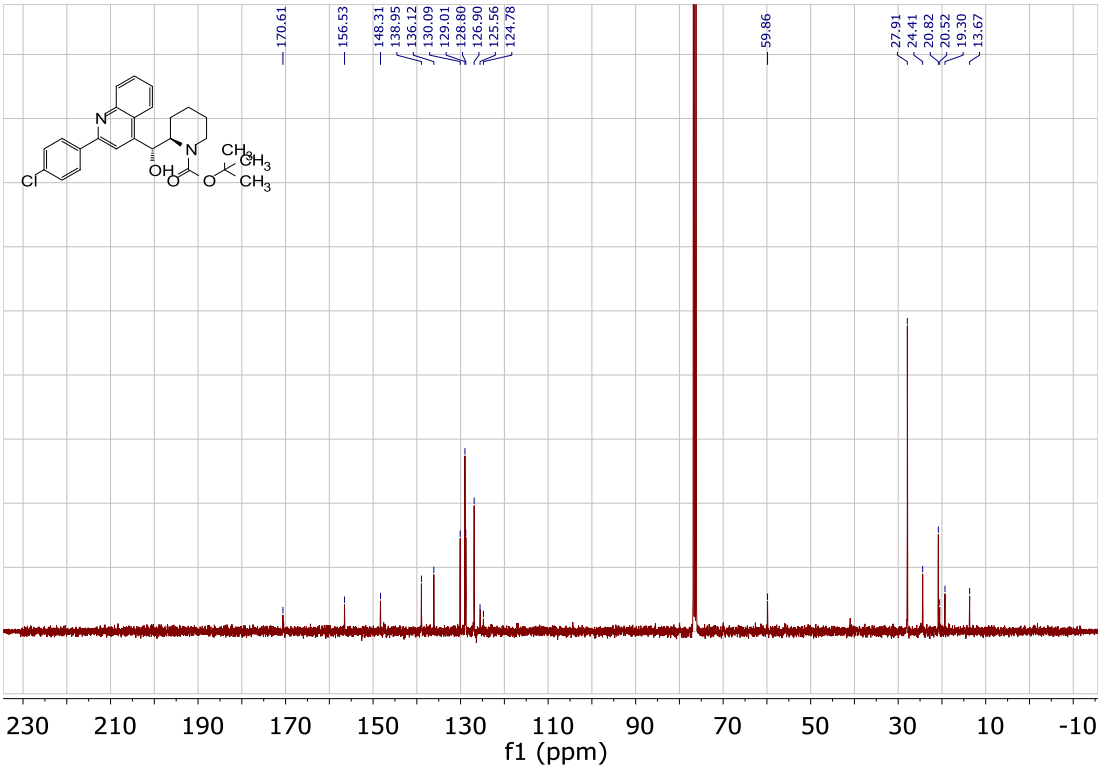

***tert*-Butyl 2-(4-chlorophenyl)-α-(2*R*)-2-5,6-dihydropyridinyl-, (α*S*)- 4-quinolinemethanol-1(2H)-carboxylate (2.24):**

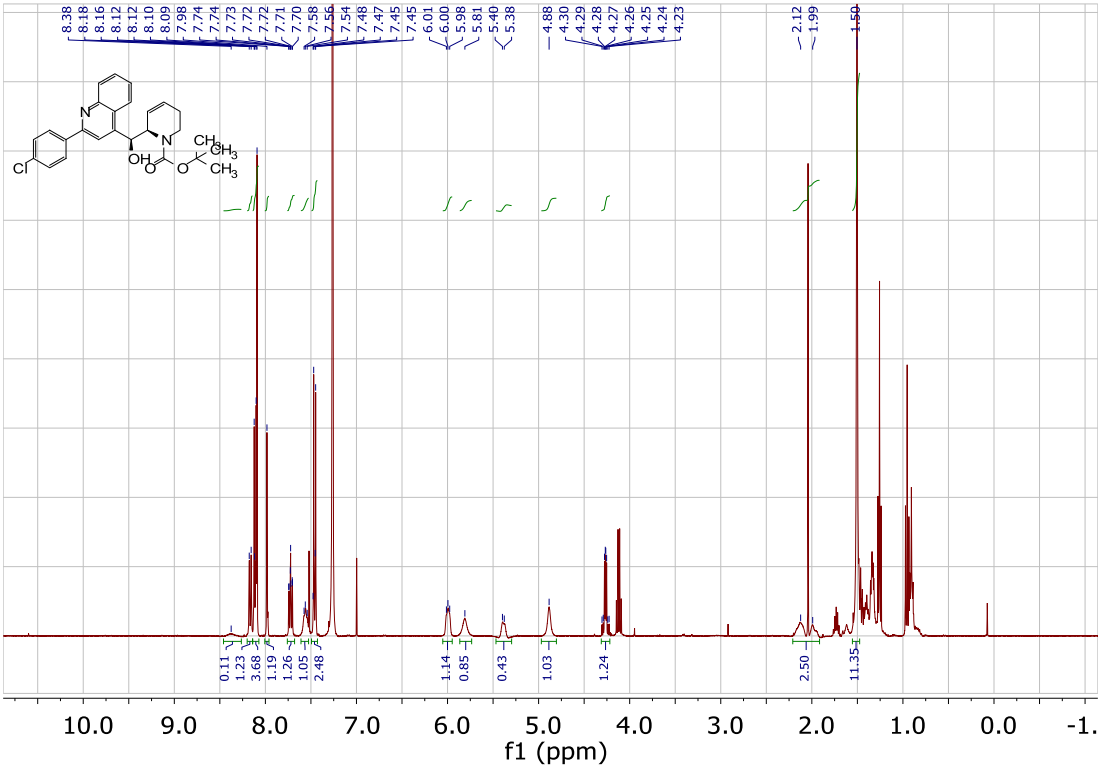

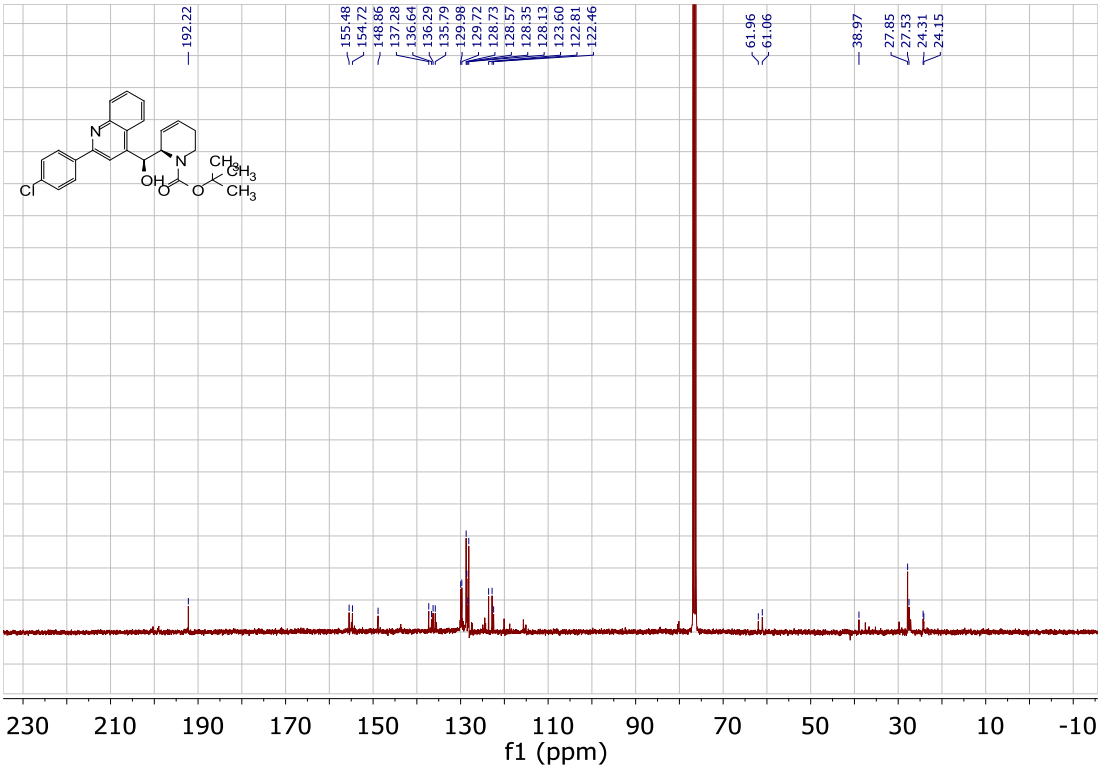

***tert*-Butyl 2-(4-chlorophenyl)-α-(2*S*)-2-5,6-dihydropyridinyl-, (α*R*)- 4-quinolinemethanol-1(2H)-carboxylate (2.26):**

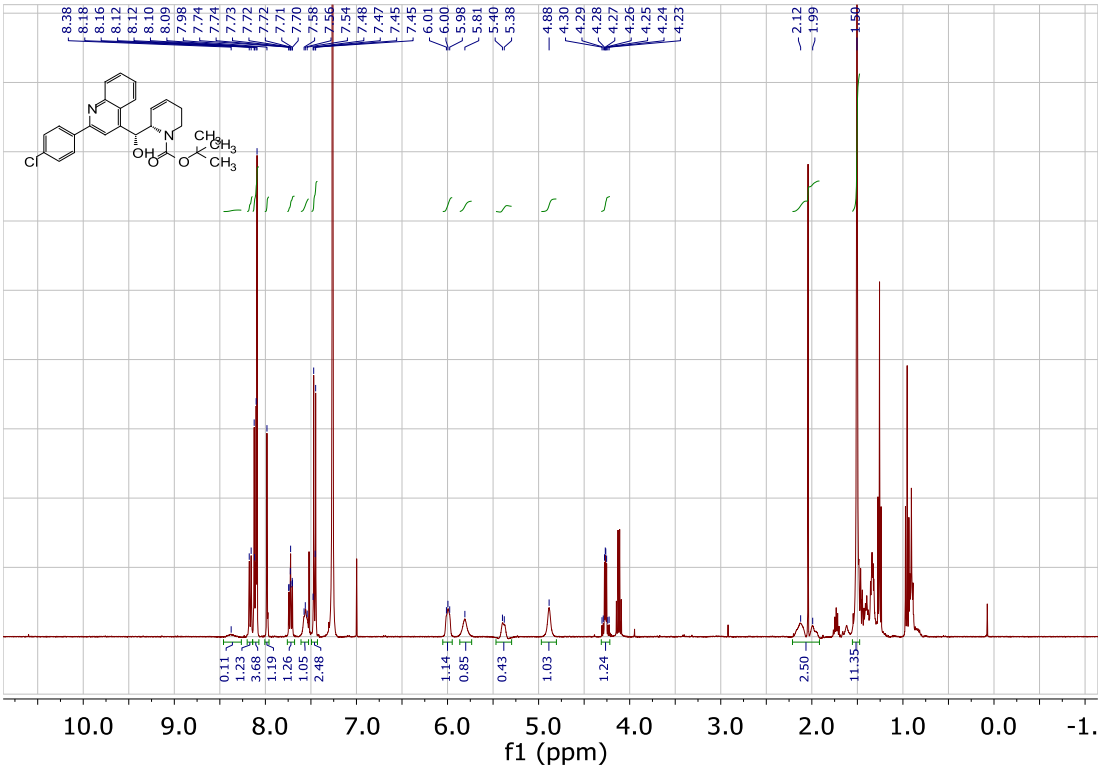

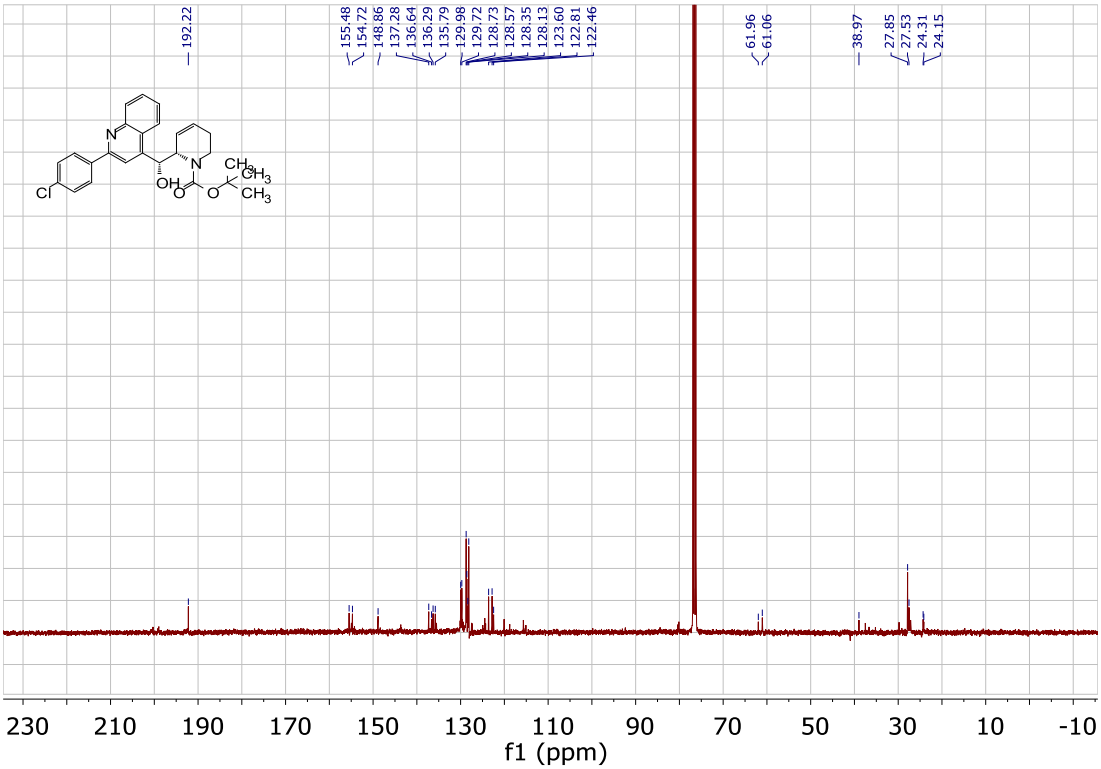

***tert*-Butyl 2-(4-chlorophenyl)-α-(2*R*)-2-5,6-dihydropyridinyl-, (α*R*)- 4-quinolinemethanol-1(2H)-carboxylate (2.5):**

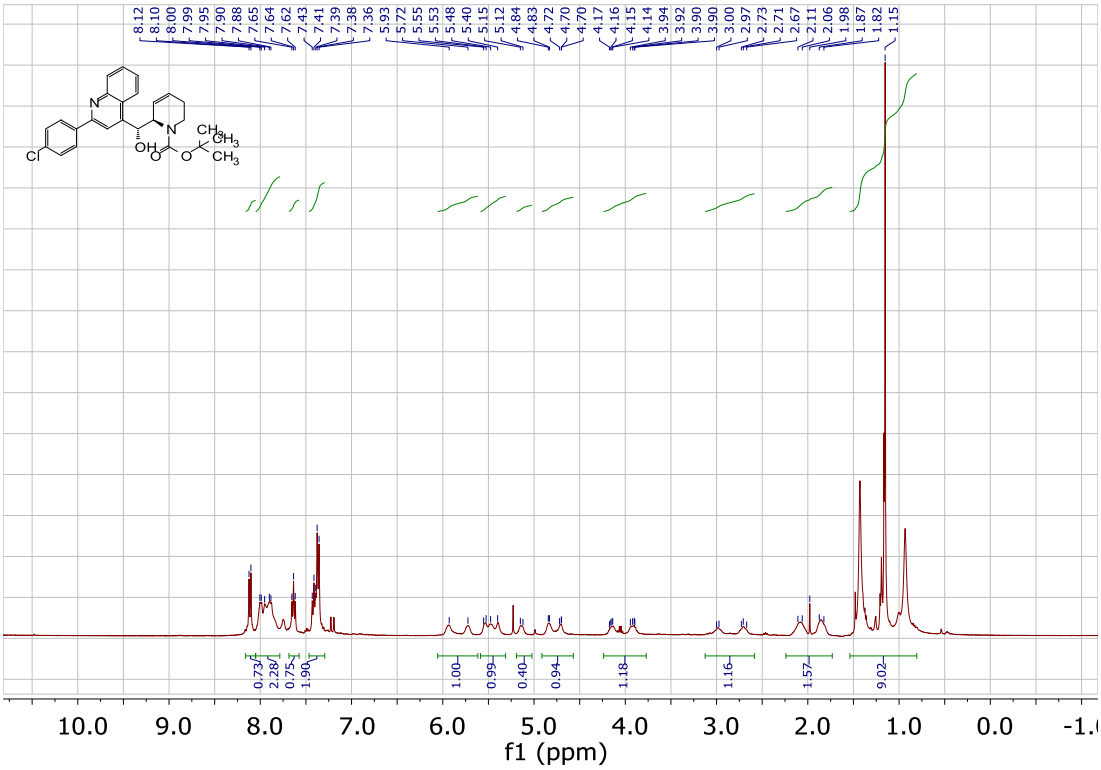

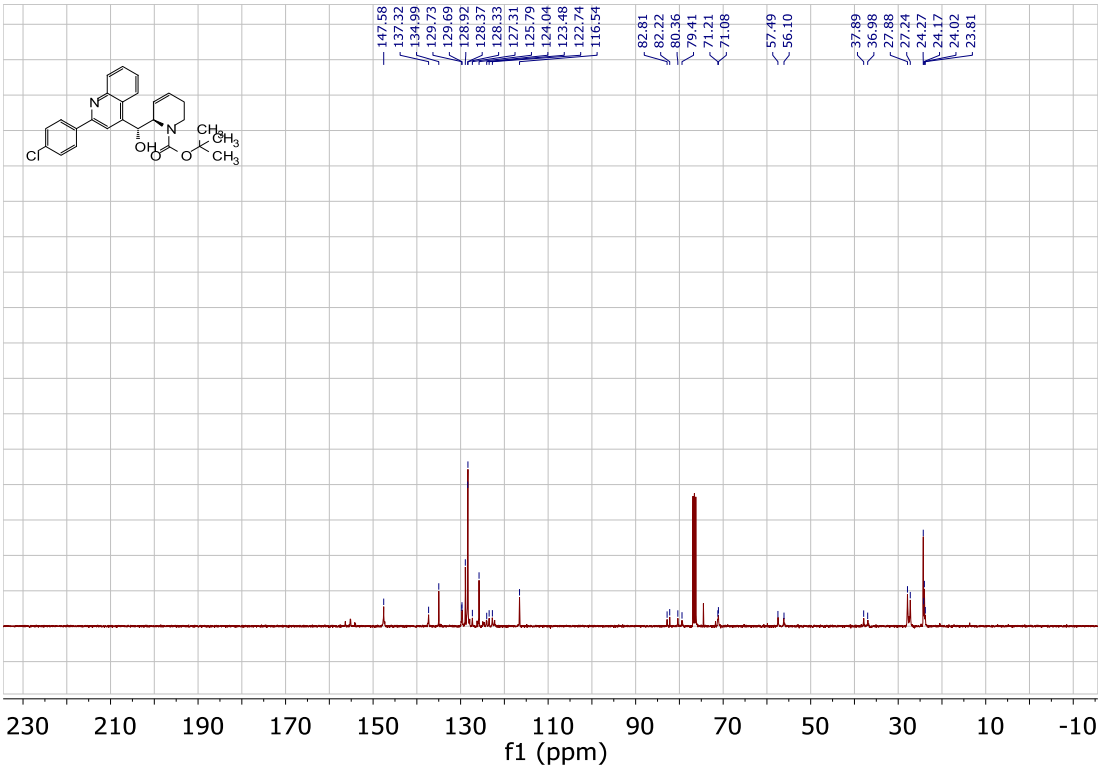

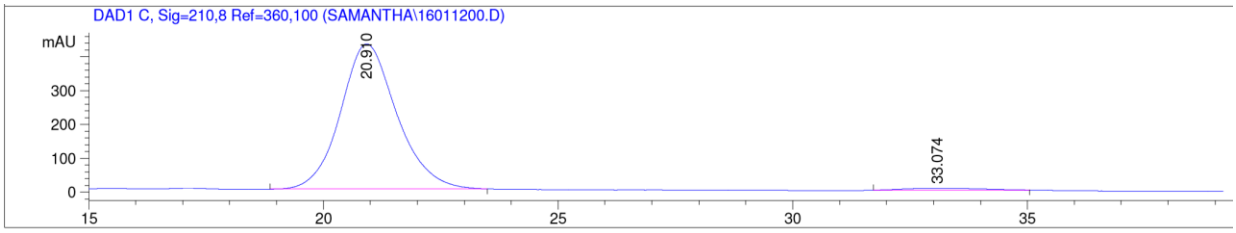

Signal 3: DAD1 C, Sig=210,8 Ref=360,100

Peak #	RetTime [min]	Type	Width [min]	Area [mAU*s]	Height [mAU]	Area %
1	20.910	BB	1.1829	3.58494e4	429.02133	97.7285
2	33.074	BB	1.4393	833.23474	6.81077	2.2715

tert-Butyl 2-(4-chlorophenyl)-α-(2*S*)-2-5,6-dihydropyridinyl-, (α*S*)- 4-quinolinemethanol-1(2H)-carboxylate (2.6):

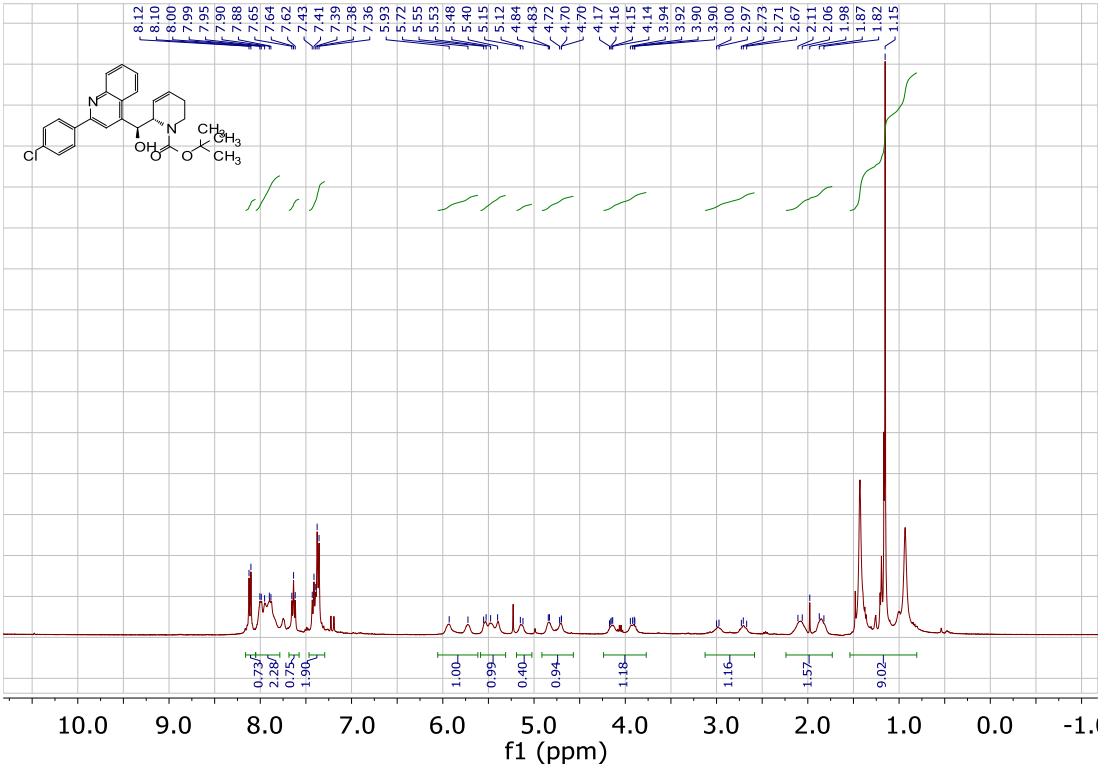

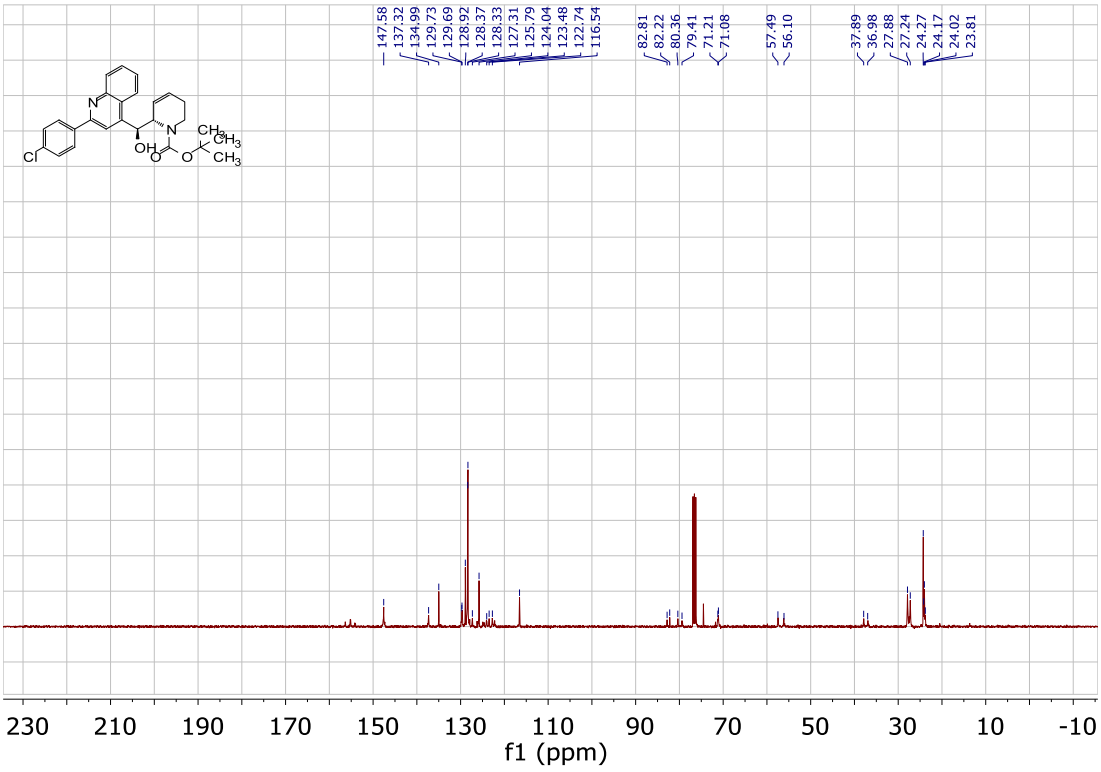

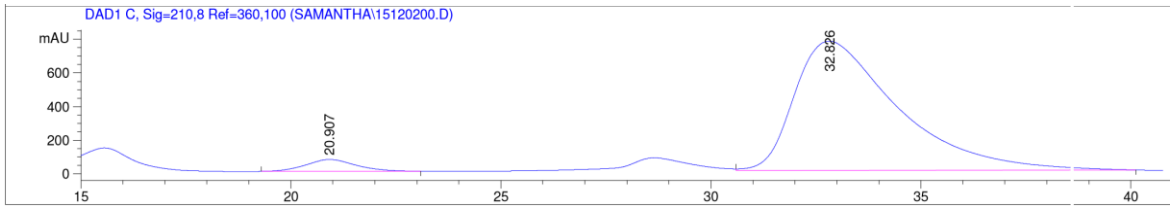

Signal 3: DAD1 C, Sig=210,8 Ref=360,100

Peak #	RetTime [min]	Type	Width [min]	Area [mAU*s]	Height [mAU]	Area %
1	20.907	BB	0.9816	5906.73730	70.92416	4.2749
2	32.826	VB	2.0254	1.32265e5	769.48413	95.7251

***tert*-Butyl 2-(-phenyl)-α-(2*S*)-2-5,6-dihydropyridinyl-, (α*S*)- 4-quinolinemethanol- 1(2H)-carboxylate:**

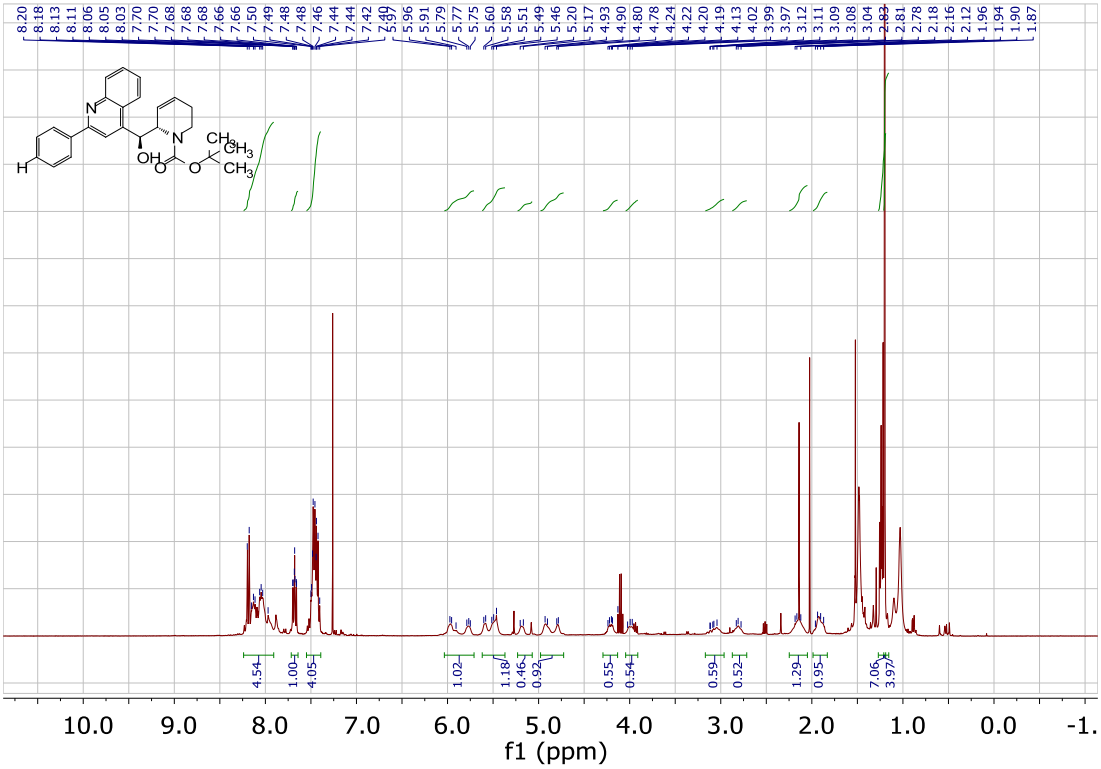

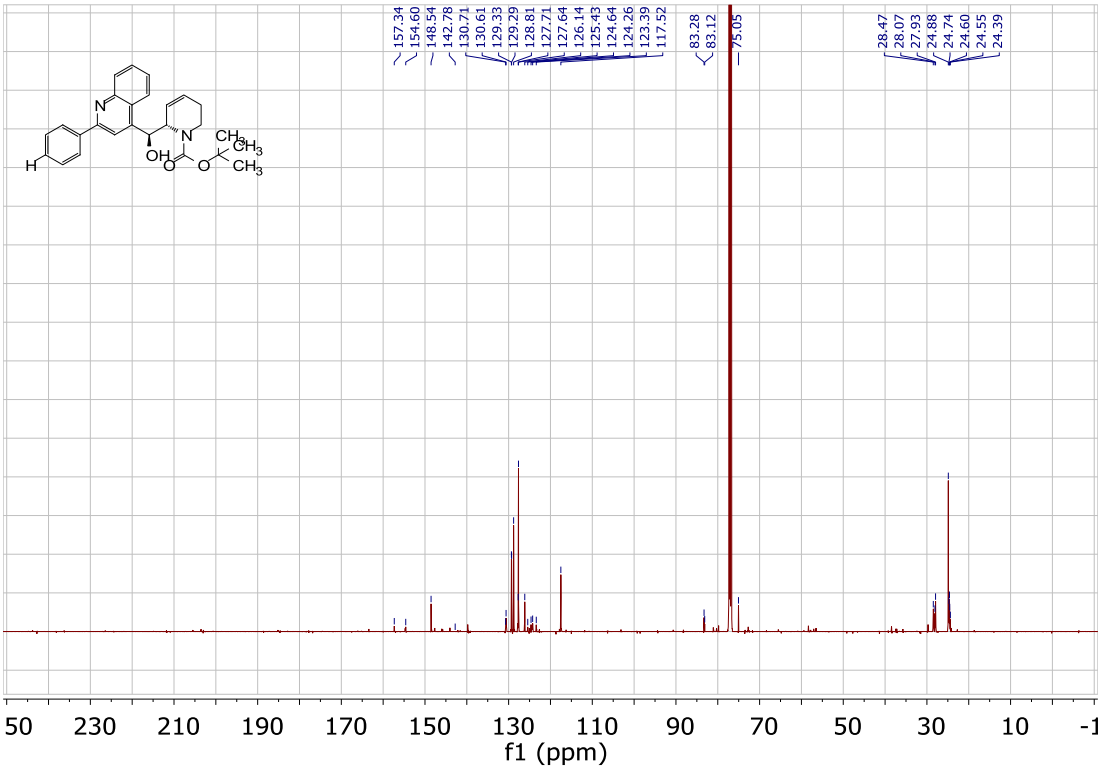

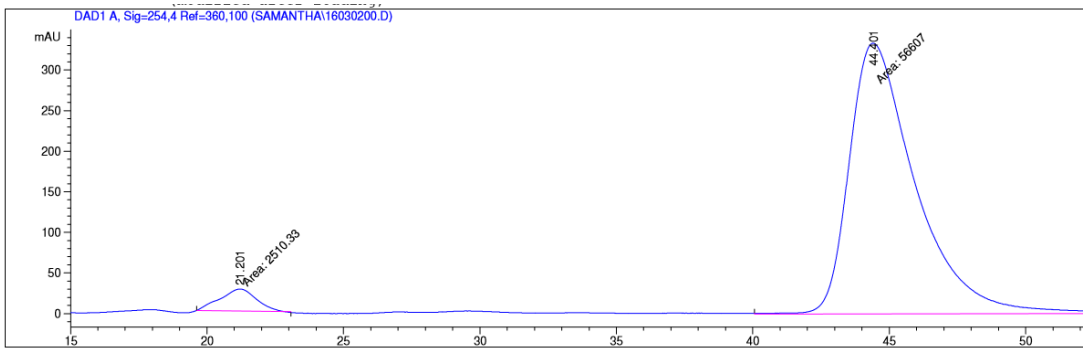

Signal 1: DAD1 A, Sig=254,4 Ref=360,100

Peak #	RetTime [min]	Type	Width [min]	Area [mAU*s]	Height [mAU]	Area %
1	21.201	MM	1.5409	2510.32886	27.15197	4.2464
2	44.401	MM	2.8272	5.66070e4	333.70627	95.7536

tert-Butyl 2-(4-bromophenyl)-α-(2*S*)-2-5,6-dihydropyridinyl-, (α*S*)- 4-quinolinemethanol-1(2H)-carboxylate:

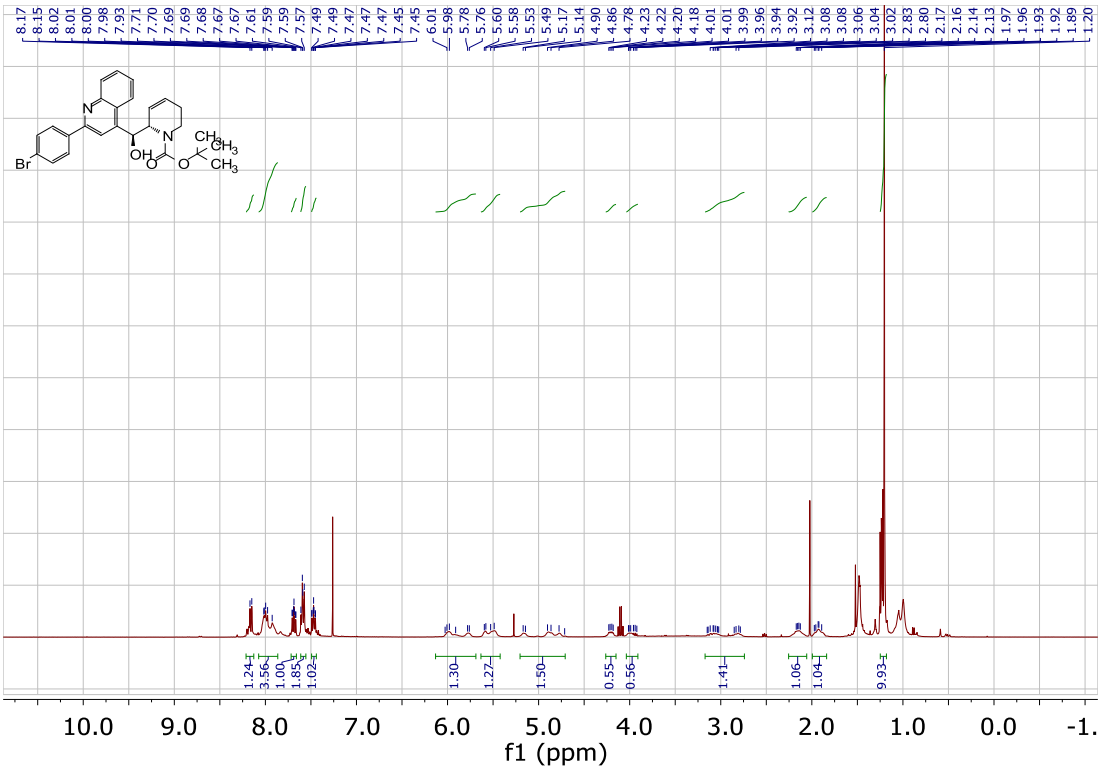

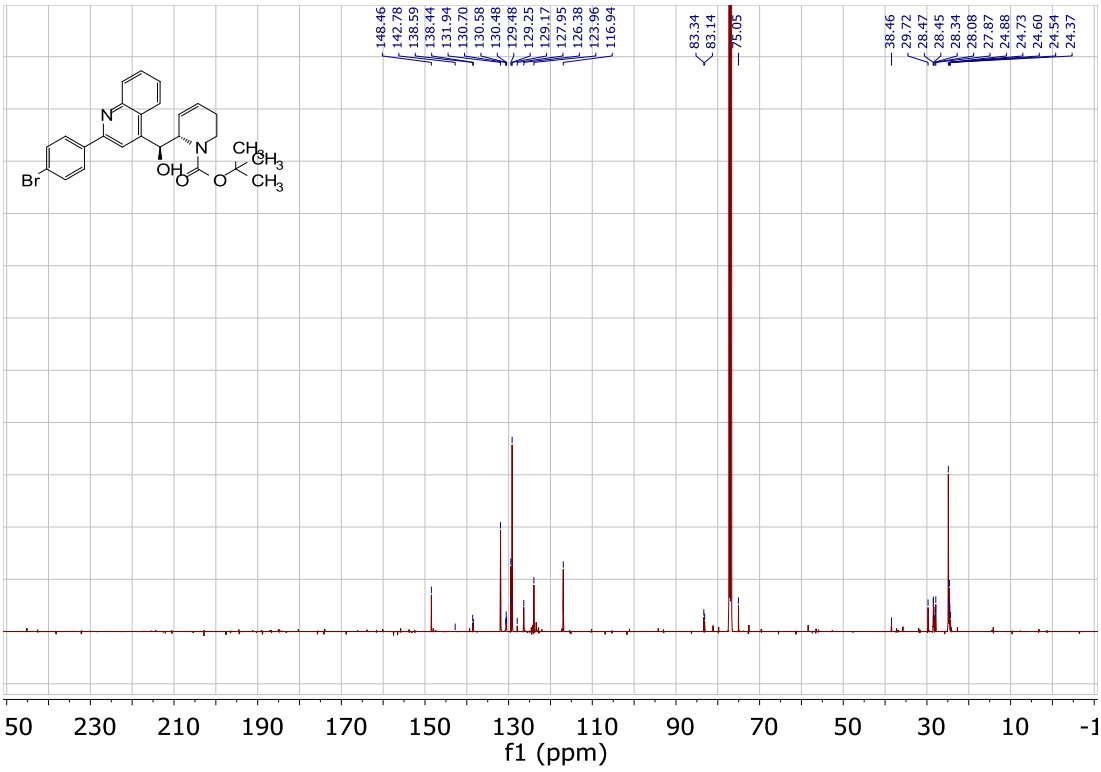

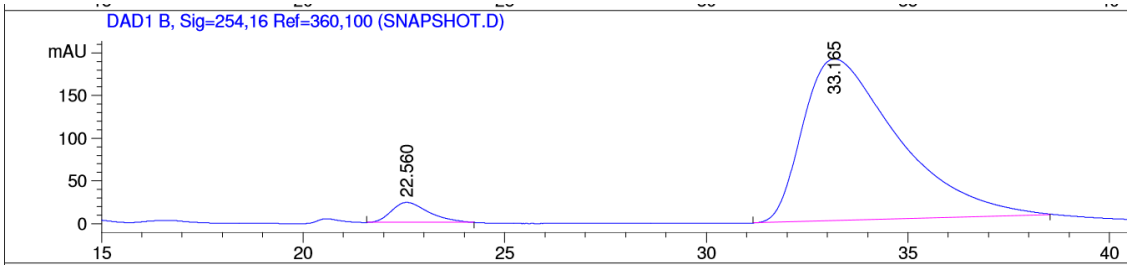

Signal 2: DAD1 B, Sig=254,16 Ref=360,100

Peak #	RetTime [min]	Type	Width [min]	Area [mAU*s]	Height [mAU]	Area %
1	22.560	PB	0.8481	1526.31970	23.49060	4.6717
2	33.165	BB	2.2014	3.11453e4	189.30707	95.3283

***tert*-Butyl 2-(4-methoxyphenyl)-α-(2*S*)-2-5,6-dihydropyridinyl-, (α*S*)- 4-quinolinemethanol-1(2H)-carboxylate:**

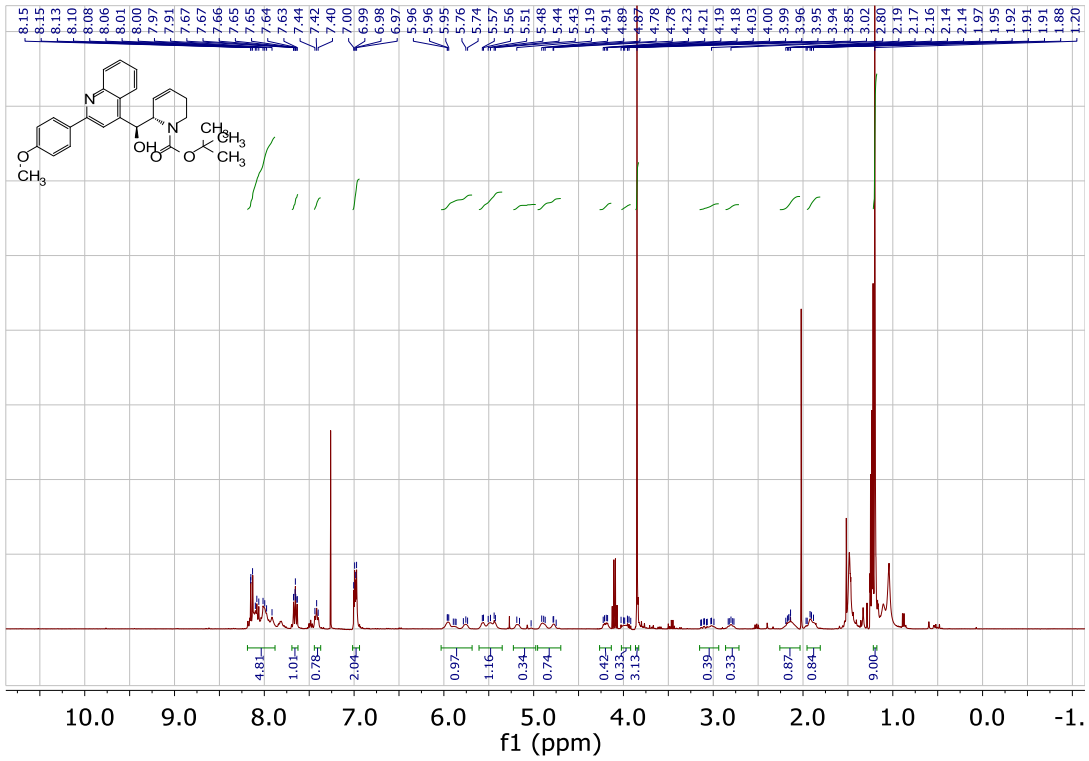

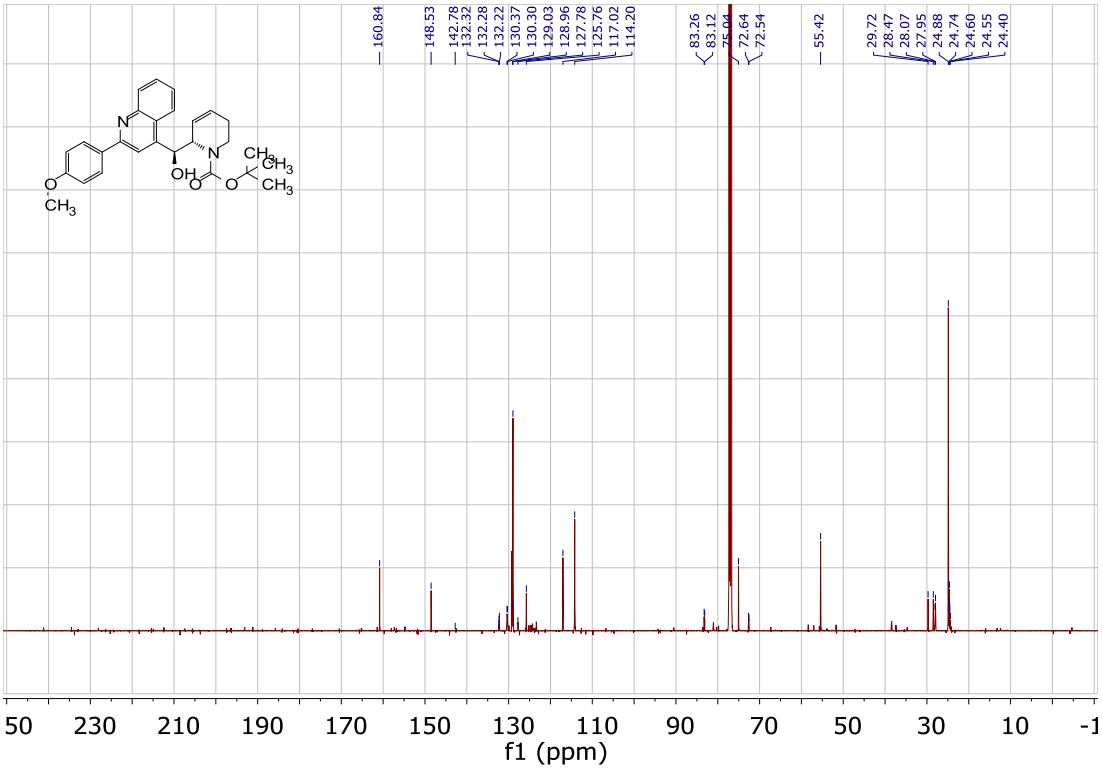

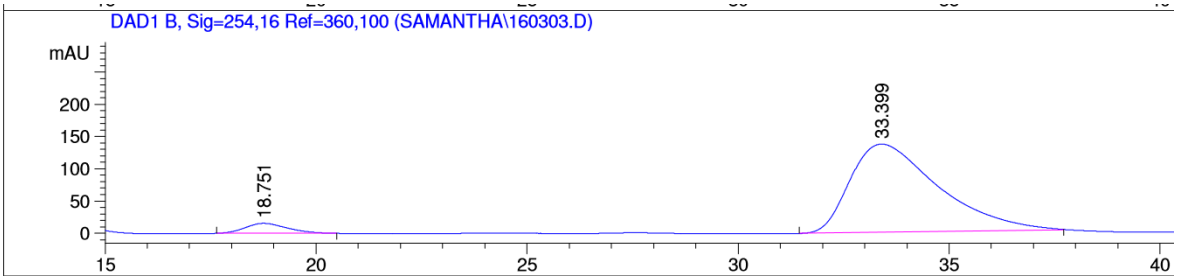

Signal 2: DAD1 B, Sig=254,16 Ref=360,100

Peak #	RetTime [min]	Type	Width [min]	Area [mAU*s]	Height [mAU]	Area %
1	18.751	BB	0.8341	1104.80090	15.71772	5.2441
2	33.399	BB	1.9734	1.99625e4	137.04651	94.7559

tert-Butyl 2-(4-methylphenyl)-α-(2*S*)-2-5,6-dihydropyridinyl-, (α*S*)- 4-quinolinemethanol-1(2H)-carboxylate:

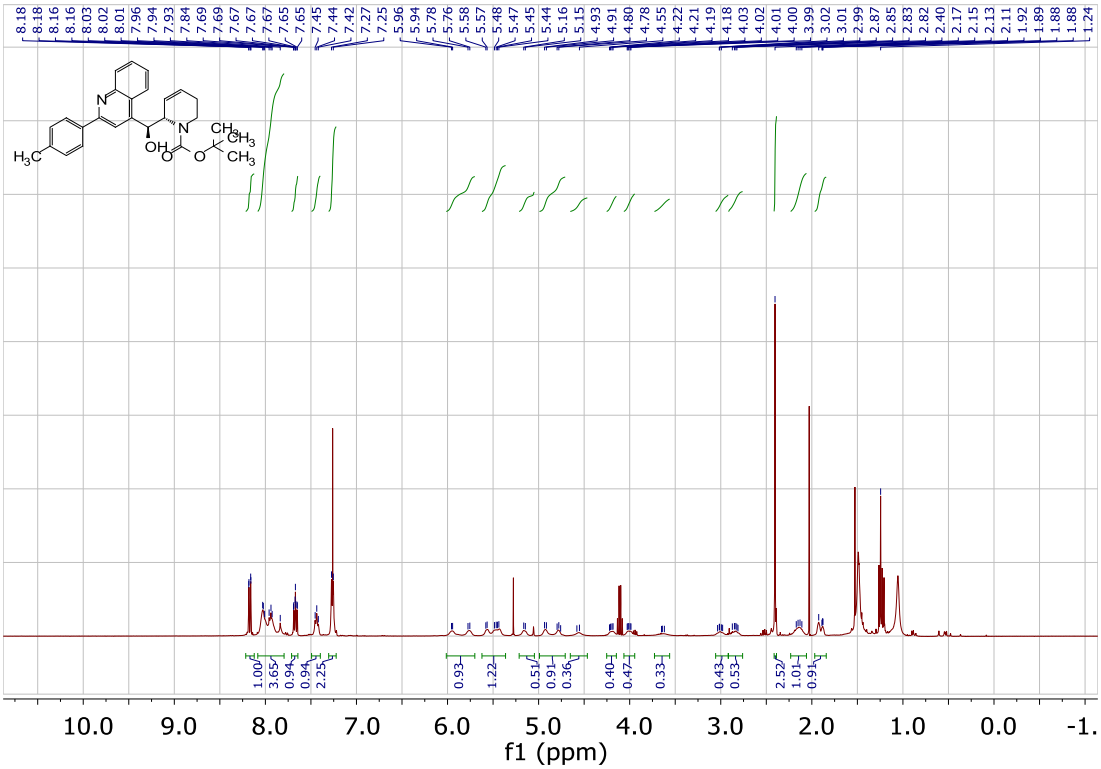

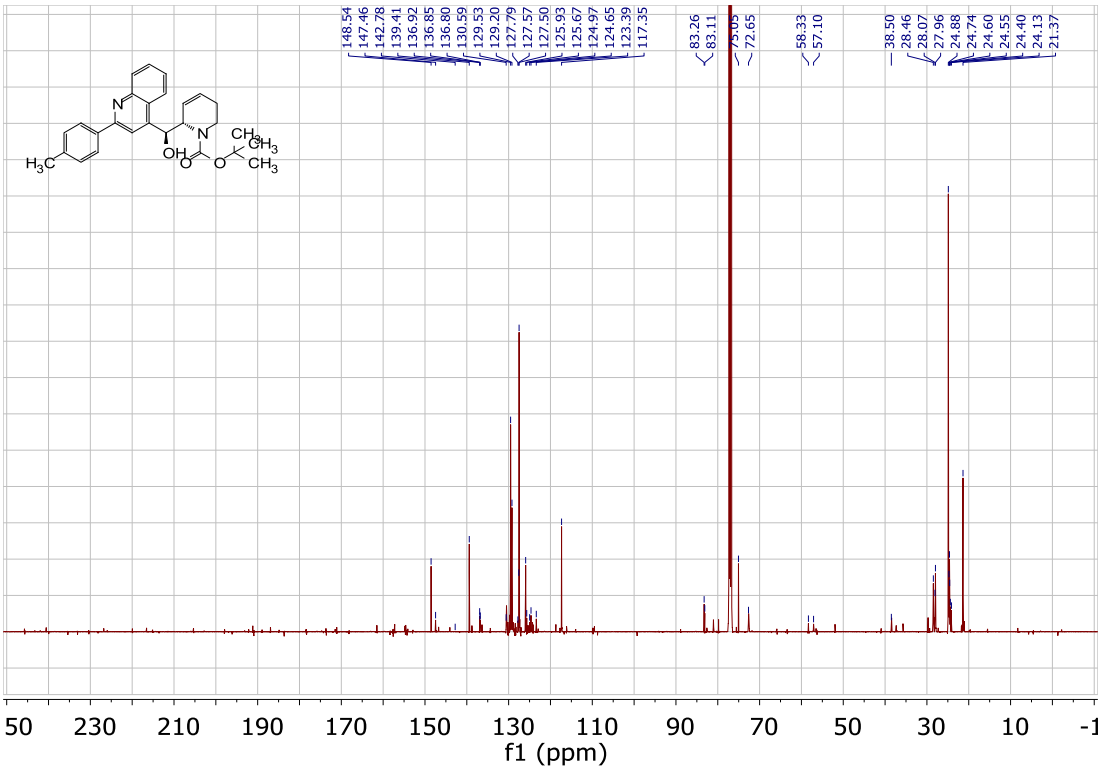

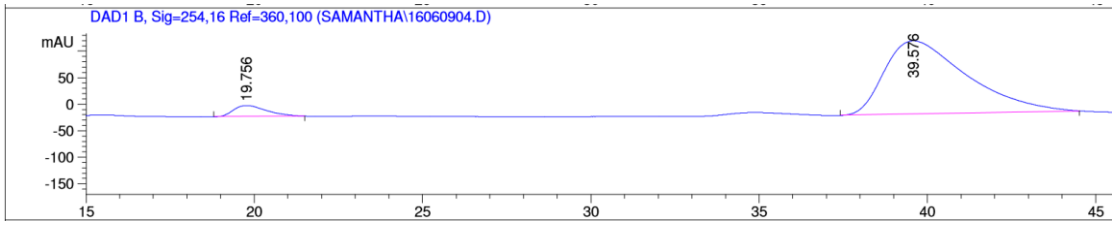

Signal 2: DAD1 B, Sig=254,16 Ref=360,100

Peak #	RetTime [min]	Type	Width [min]	Area [mAU*s]	Height [mAU]	Area %
1	19.756	BB	0.8695	1465.05420	21.11441	5.8437
2	39.576	BB	2.0368	2.36056e4	138.33781	94.1563

***tert*-Butyl 2-(-phenyl)-α-(2*R*)-2-5,6-dihydropyridinyl-, (α*R*)- 4-quinolinemethanol- 1(2H)-carboxylate:**

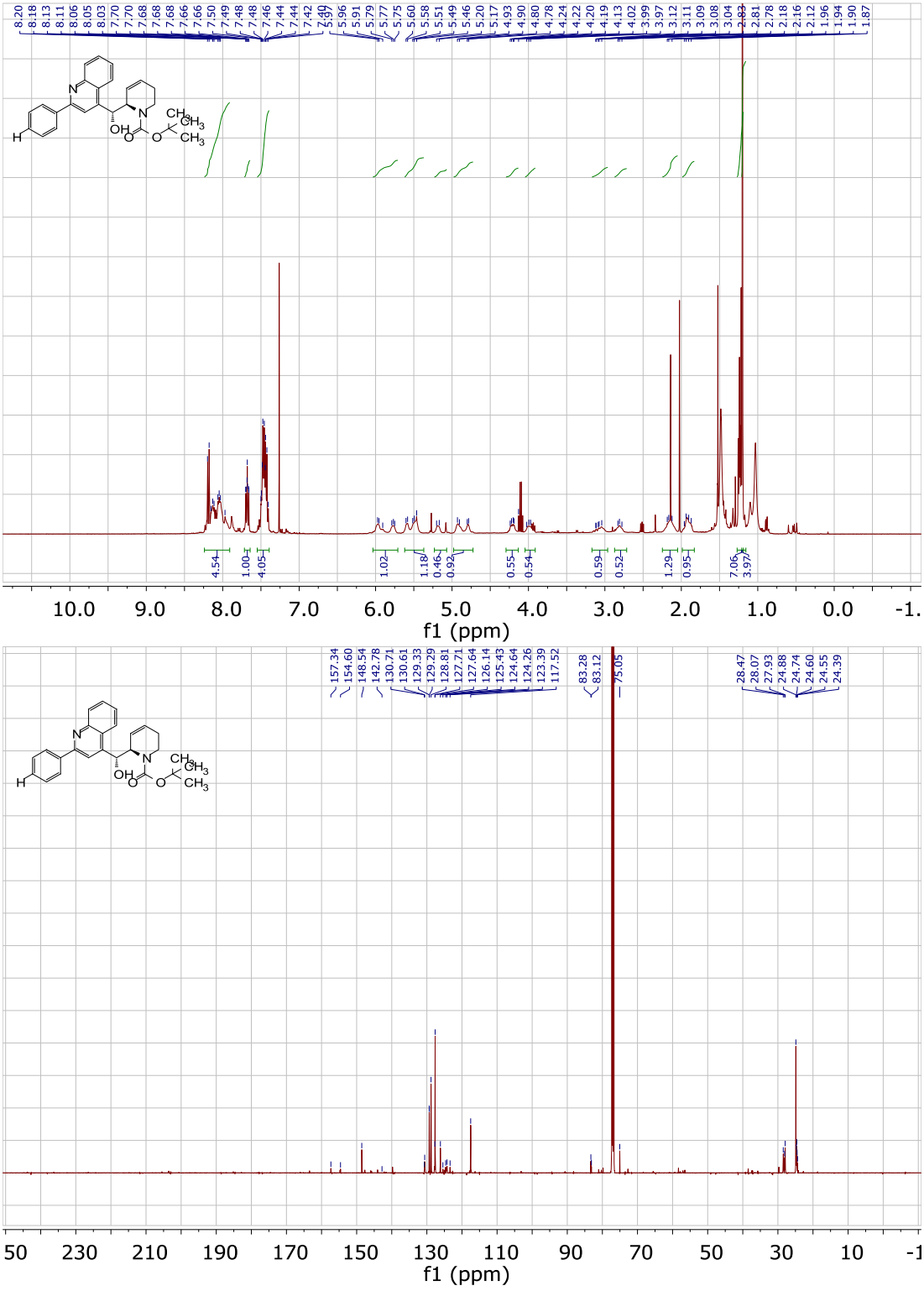

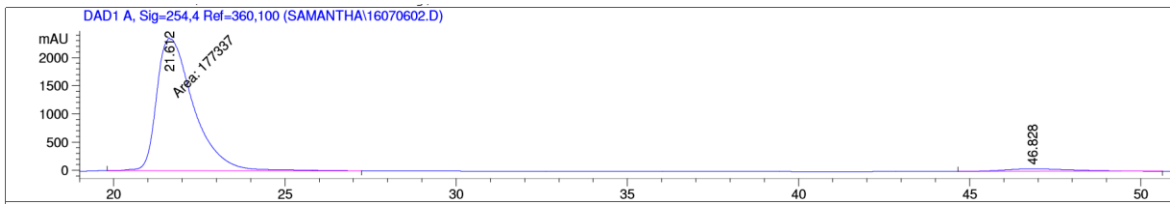

Signal 1: DAD1 A, Sig=254,4 Ref=360,100

Peak #	RetTime [min]	Type	Width [min]	Area [mAU*s]	Height [mAU]	Area %
1	21.612	MM	1.2511	1.77337e5	2362.47388	96.1850
2	46.828	BB	1.7495	7033.68652	47.28320	3.8150

***tert*-Butyl 2-(4-bromophenyl)-α-(2*R*)-2-5,6-dihydropyridinyl-, (α*R*)- 4-quinolinemethanol-1(2H)-carboxylate:**

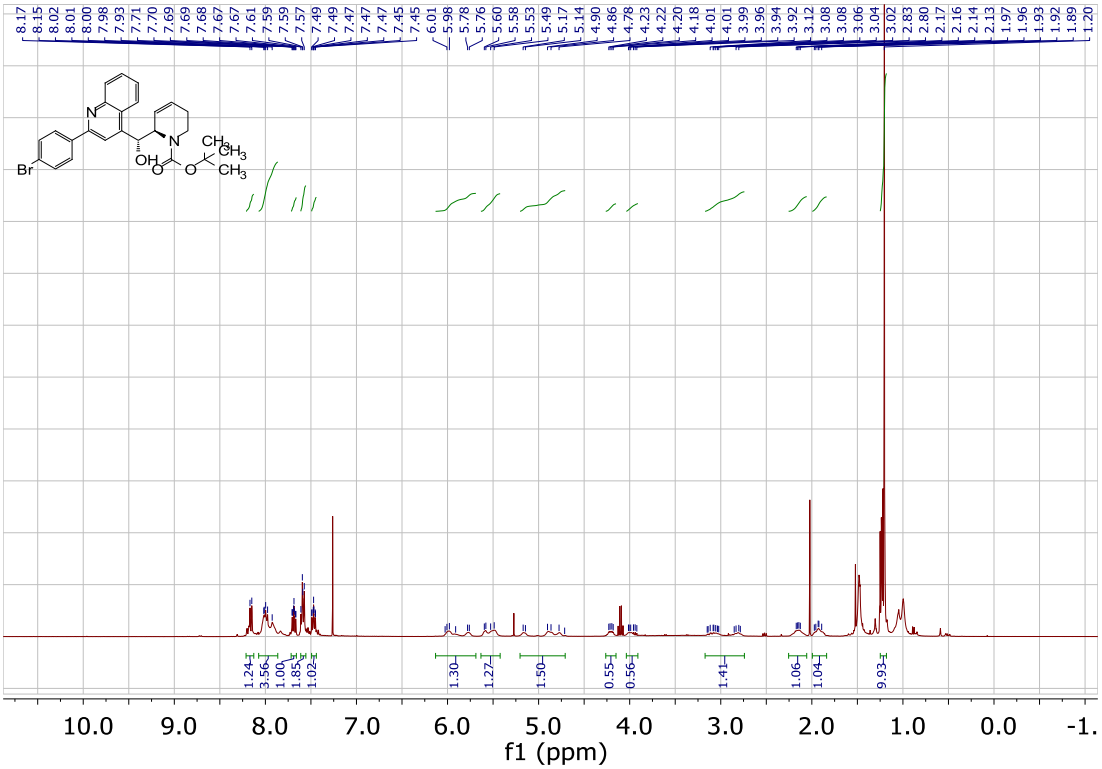

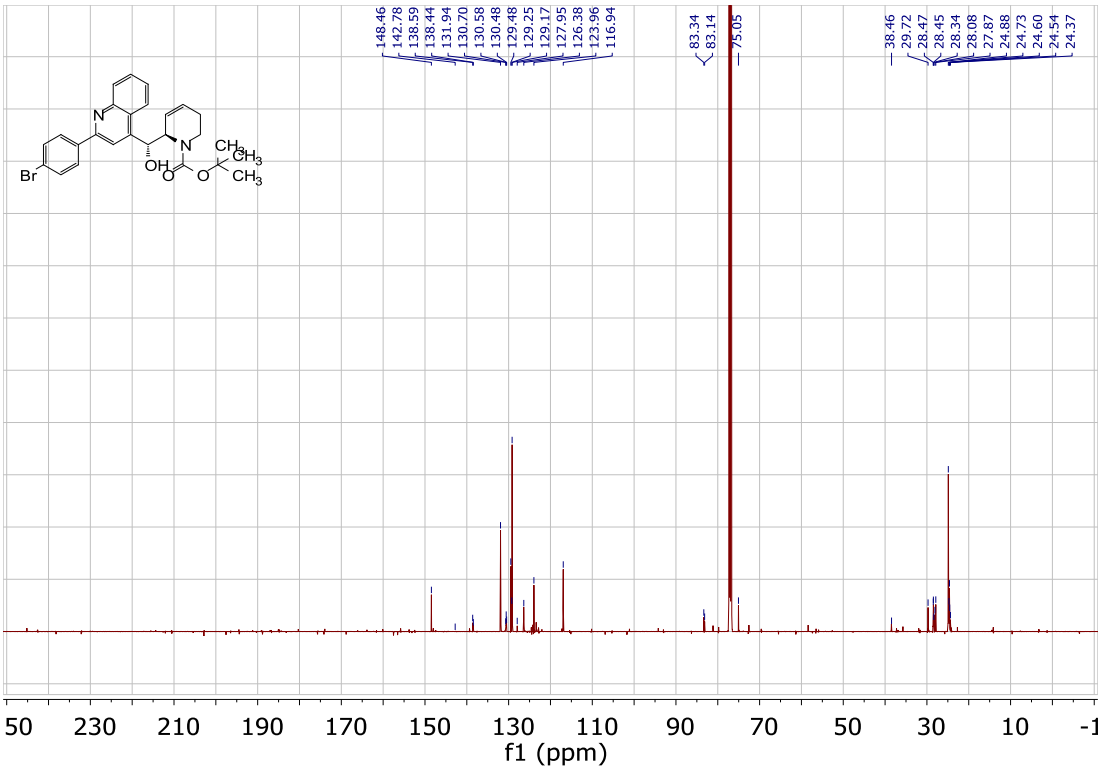

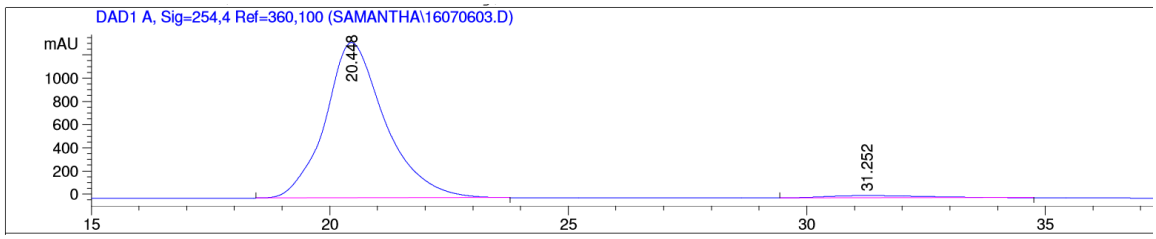

Signal 1: DAD1 A, Sig=254,4 Ref=360,100

Peak #	RetTime [min]	Type	Width [min]	Area [mAU*s]	Height [mAU]	Area %
1	20.448	BB	1.1931	1.16728e5	1338.87659	97.4079
2	31.252	BB	1.7972	3106.21191	20.23139	2.5921

***tert*-Butyl 2-(4-methoxyphenyl)-α-(2*R*)-2-5,6-dihydropyridinyl-, (α*R*)- 4-quinolinemethanol-1(2H)-carboxylate:**

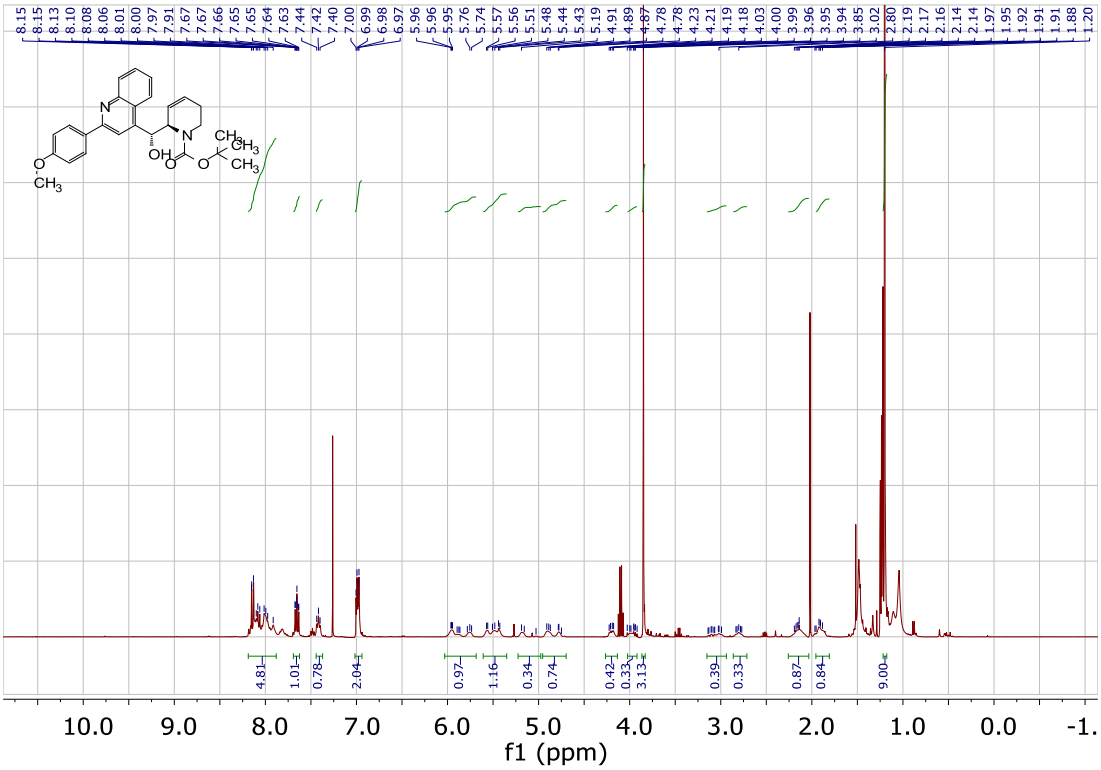

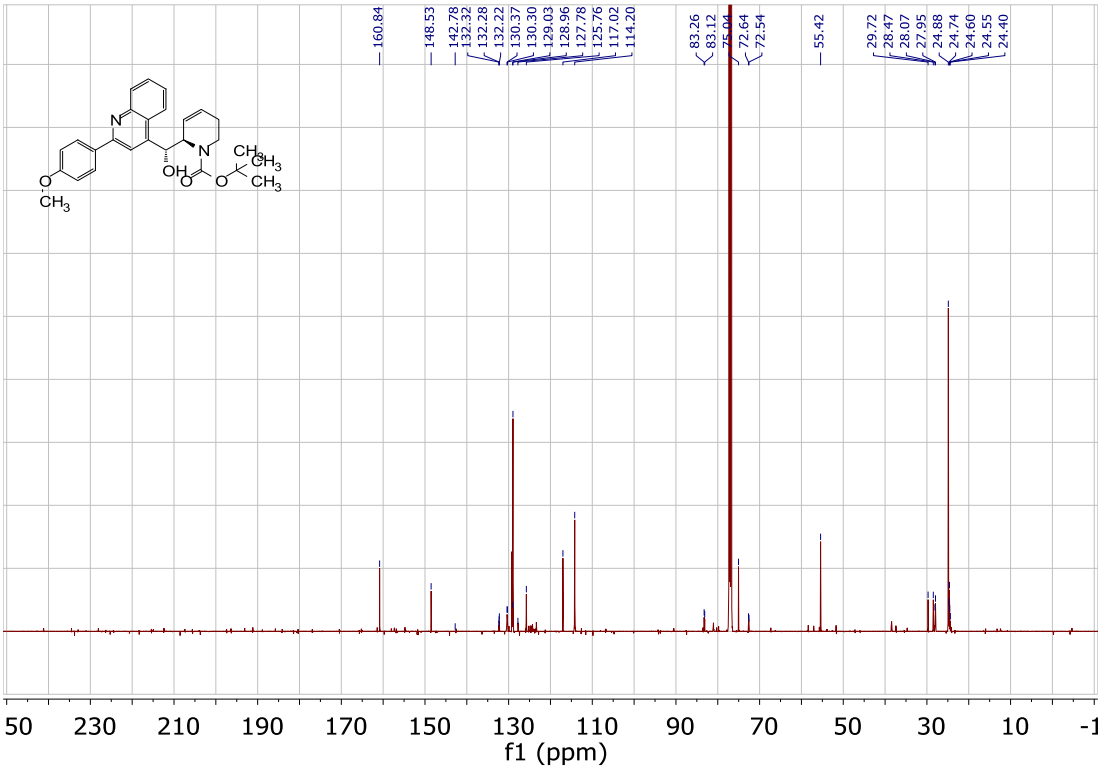

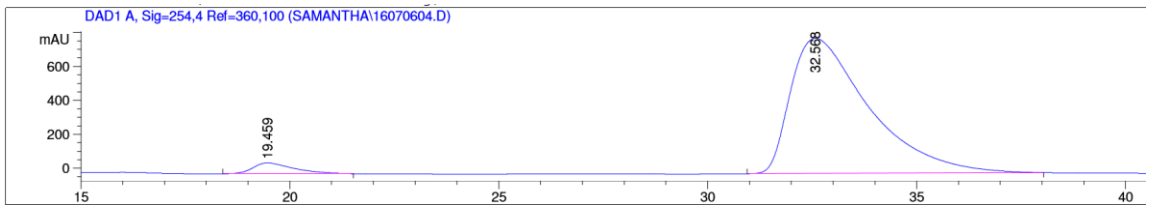

Signal 1: DAD1 A, Sig=254,4 Ref=360,100

Peak #	RetTime [min]	Type	Width [min]	Area [mAU*s]	Height [mAU]	Area %
1	19.459	BB	0.9320	4406.54443	64.09938	4.0754
2	32.568	BB	1.7188	1.03719e5	796.69720	95.9246

***tert*-Butyl 2-(4-methylphenyl)-α-(2*R*)-2-5,6-dihydropyridinyl-, (α*R*)- 4-quinolinemethanol-1(2H)-carboxylate:**

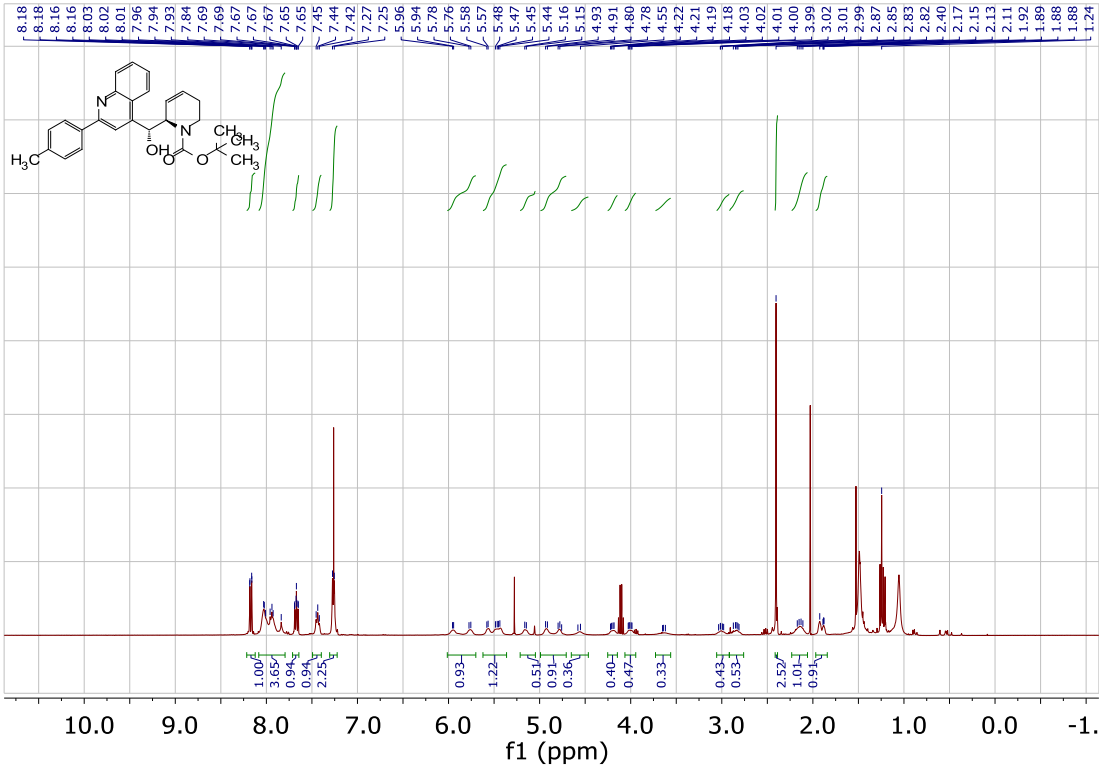

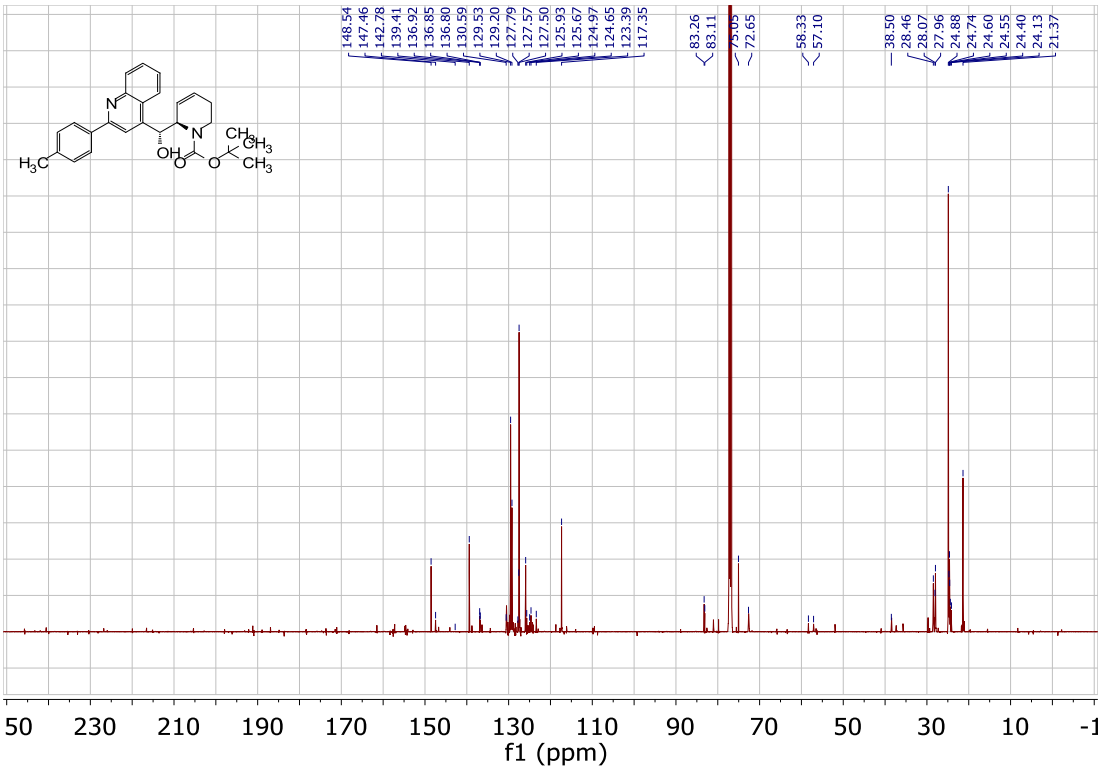

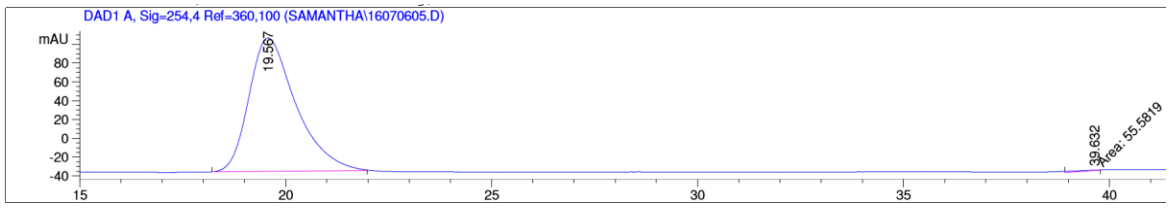

Signal 1: DAD1 A, Sig=254,4 Ref=360,100

Peak #	RetTime [min]	Type	Width [min]	Area [mAU*s]	Height [mAU]	Area %
1	19.567	BB	1.1263	1.12612e4	142.13339	99.5089
2	39.632	MM	1.0459	55.58185	7.29068e-1	0.4911

2-(Phenyl)-4-quinolinecarboxylic acid:

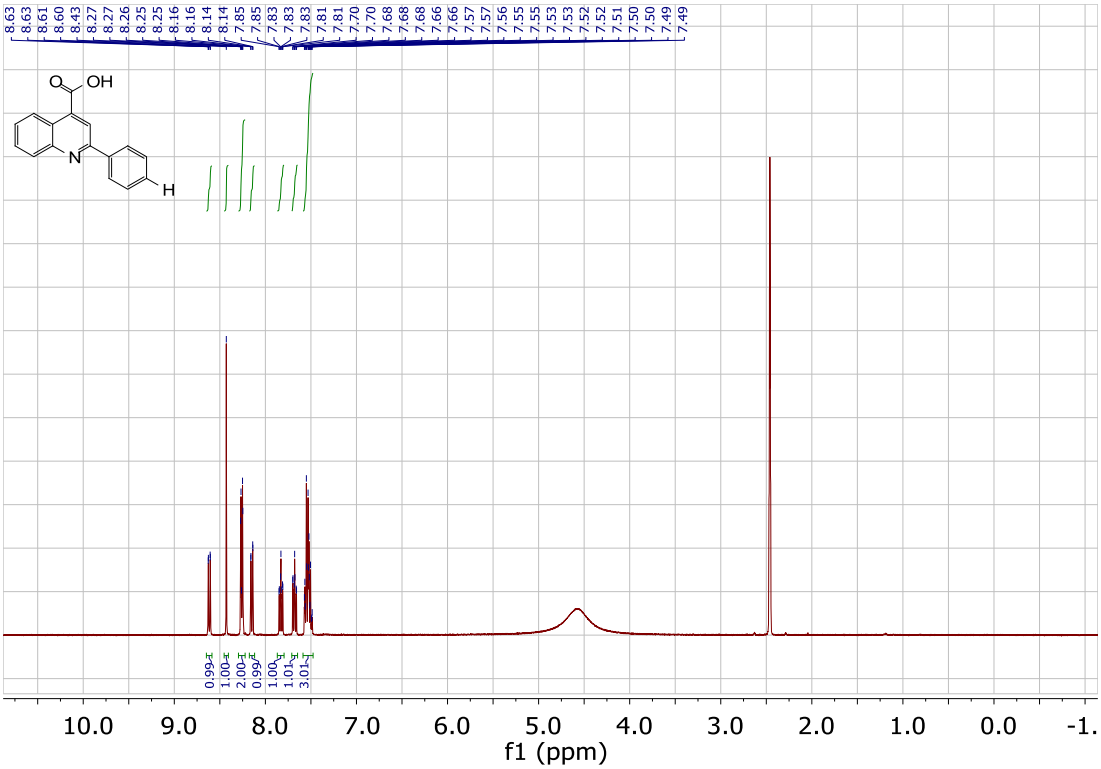

2-(4-Bromophenyl)-4-quinolinecarboxylic acid:

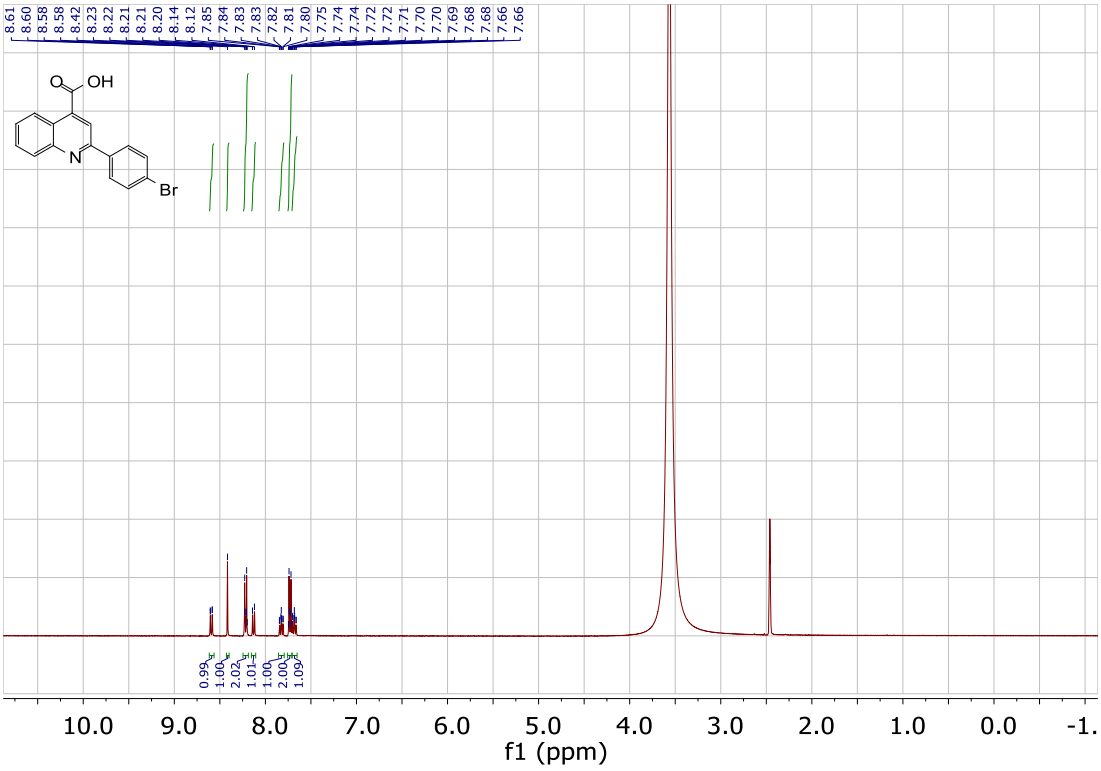

2-(4-Methoxyphenyl)-4-quinolinecarboxylic acid:

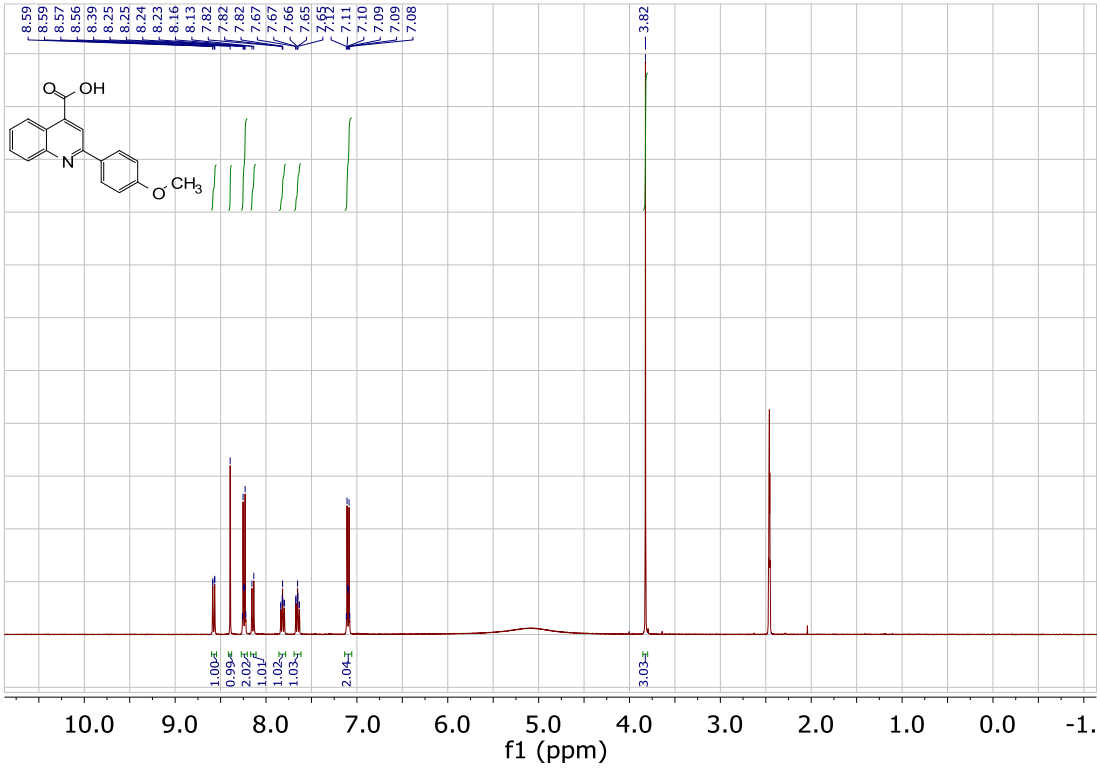

2-(4-Methylphenyl)-4-quinolinecarboxylic acid:

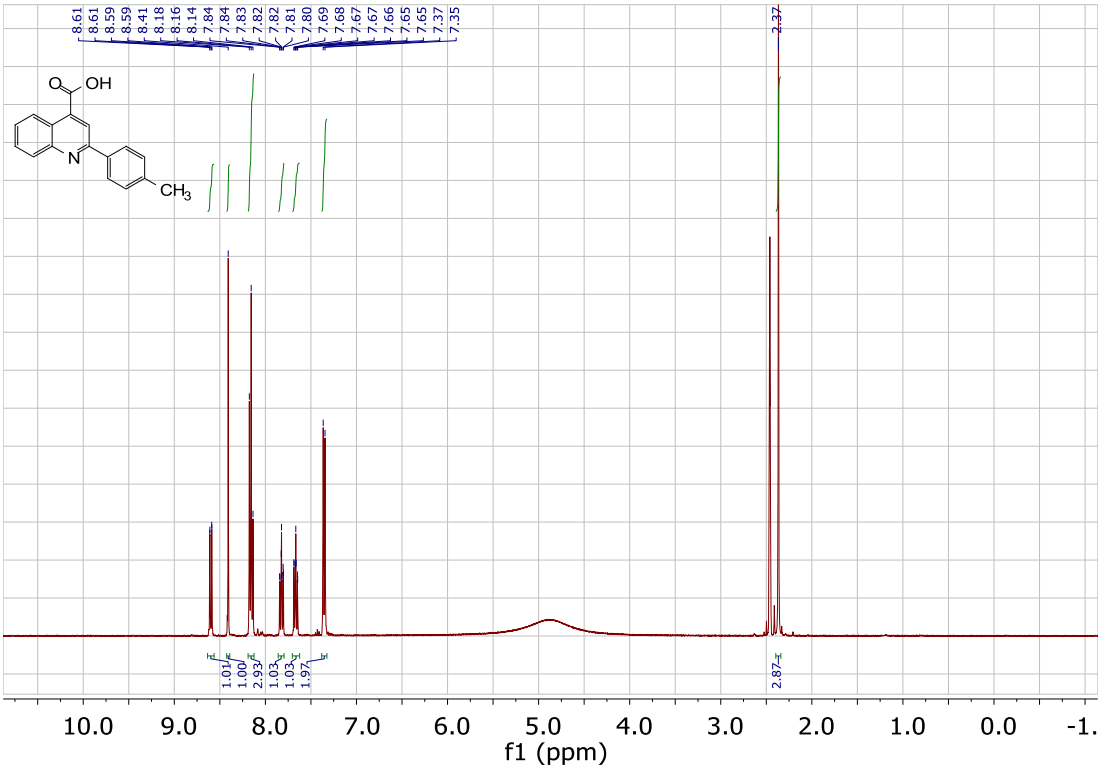

2-phenyl-4-Quinolinecarboxaldehyde (2.27):

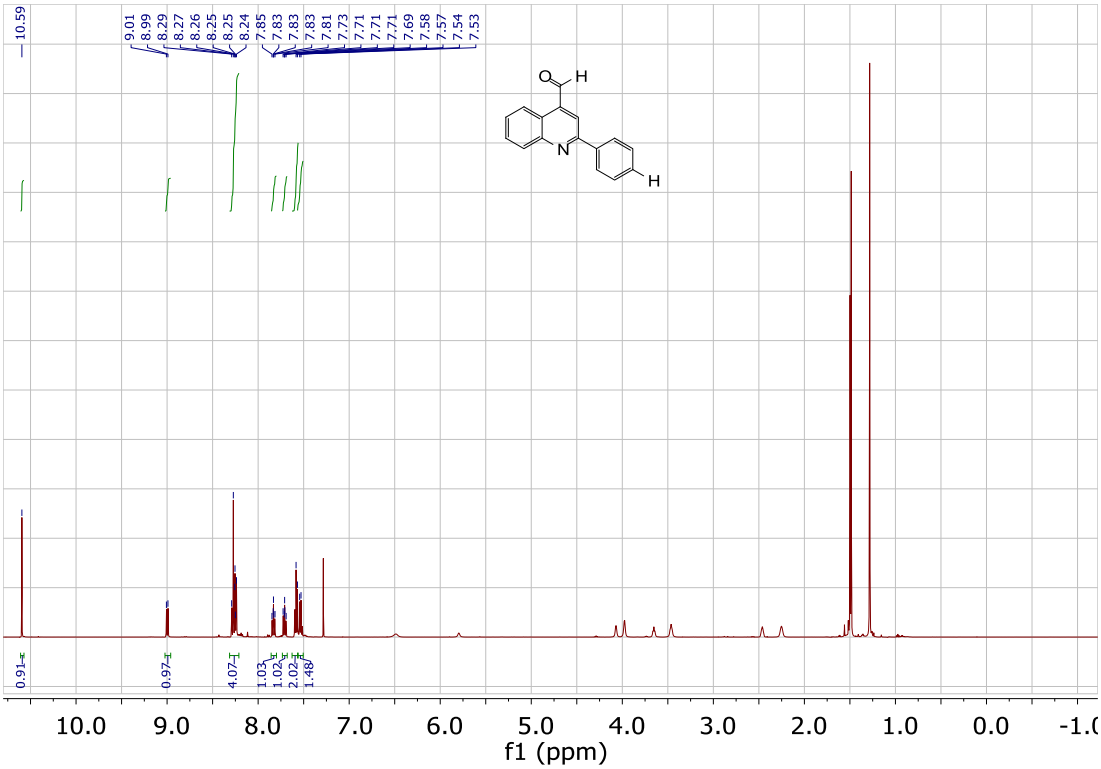

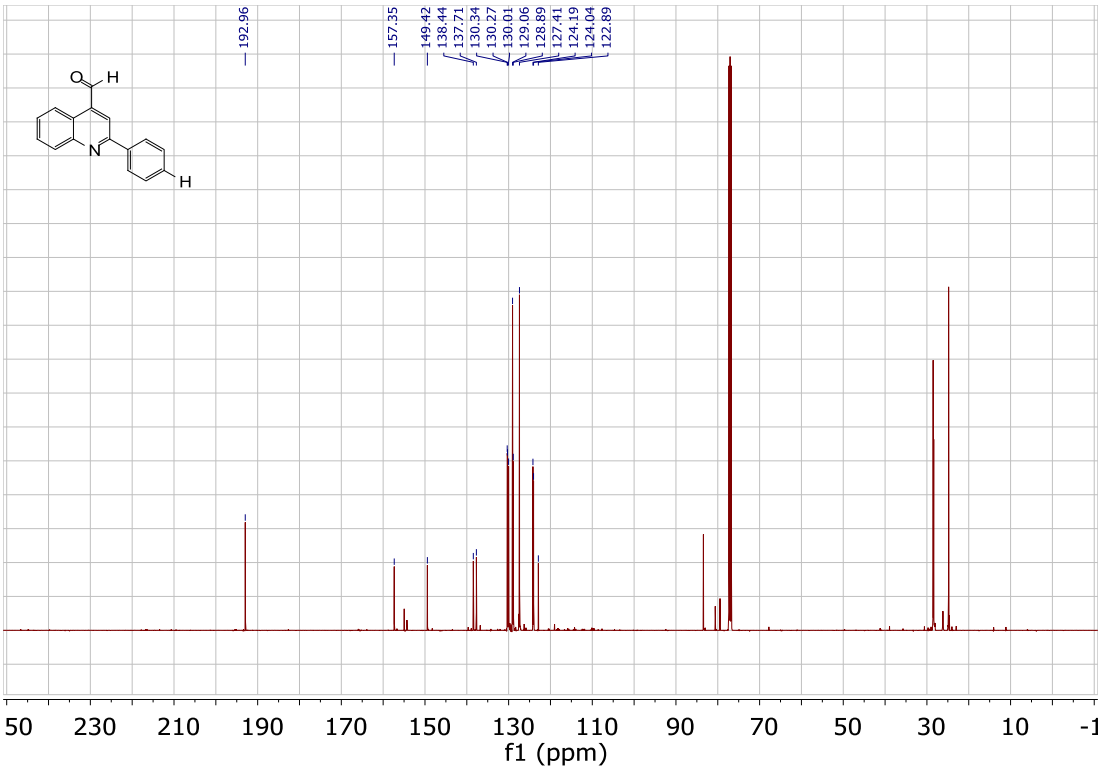

2-(4-bromophenyl)-4-Quinolinecarboxaldehyde (2.28):

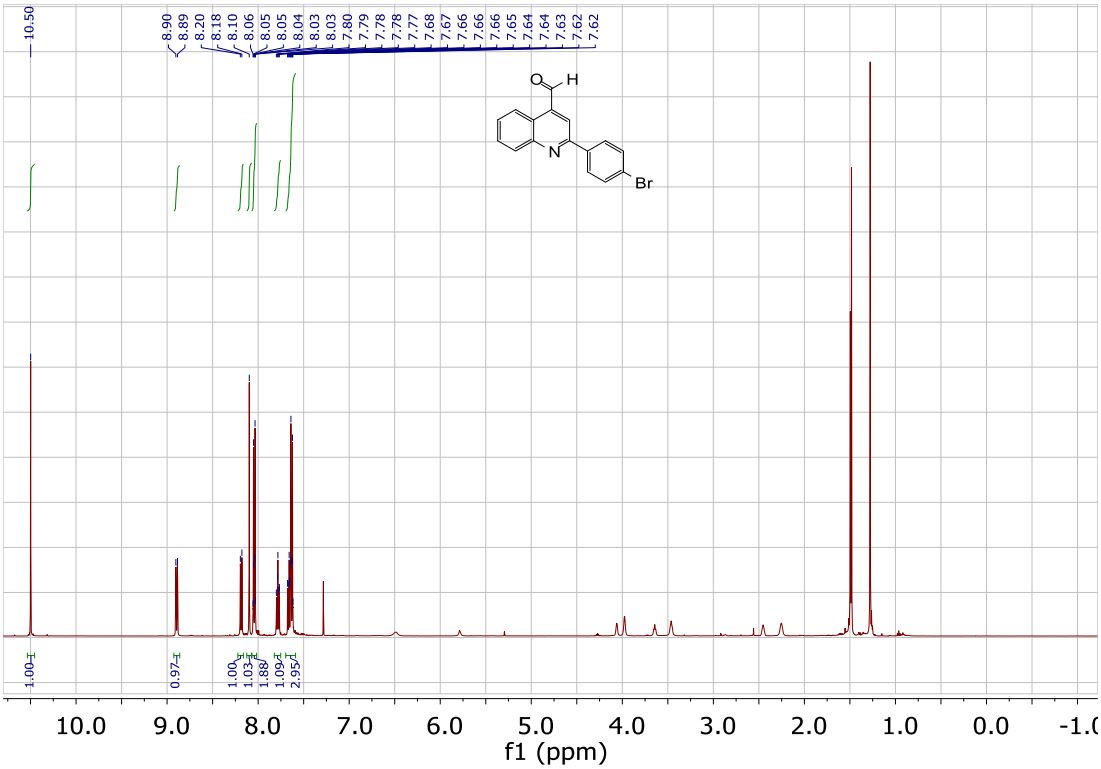

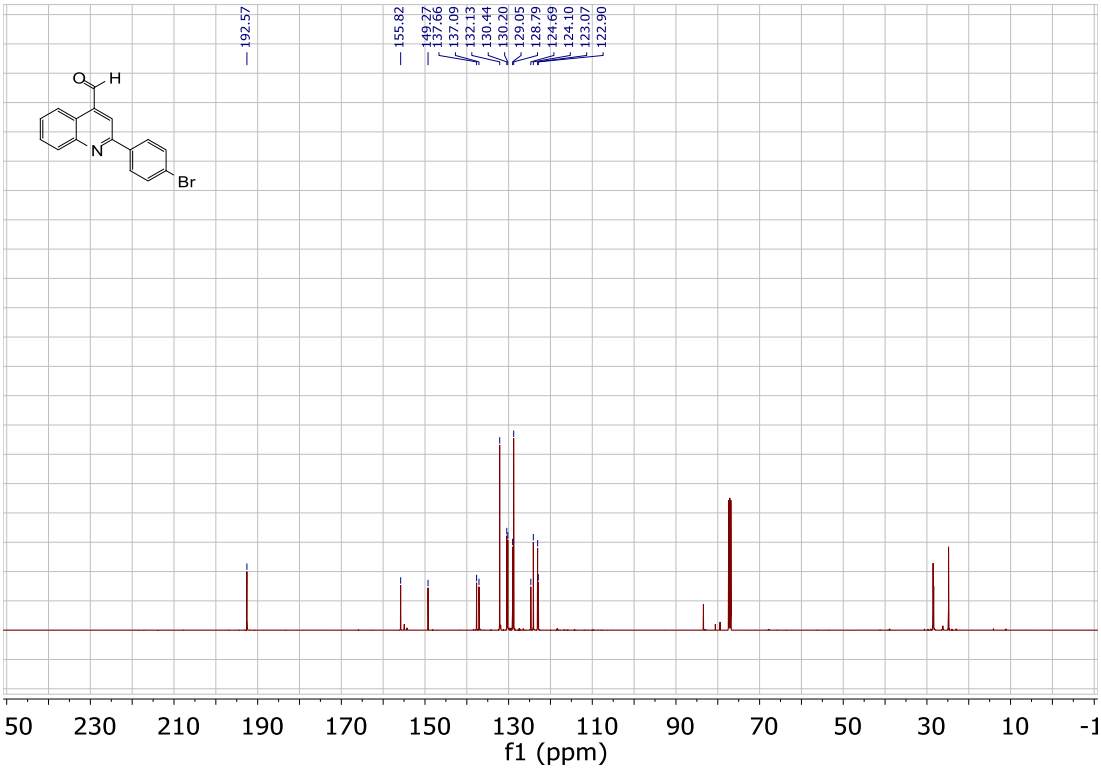

2-(4-methylphenyl)-4-Quinolinecarboxaldehyde (2.30):

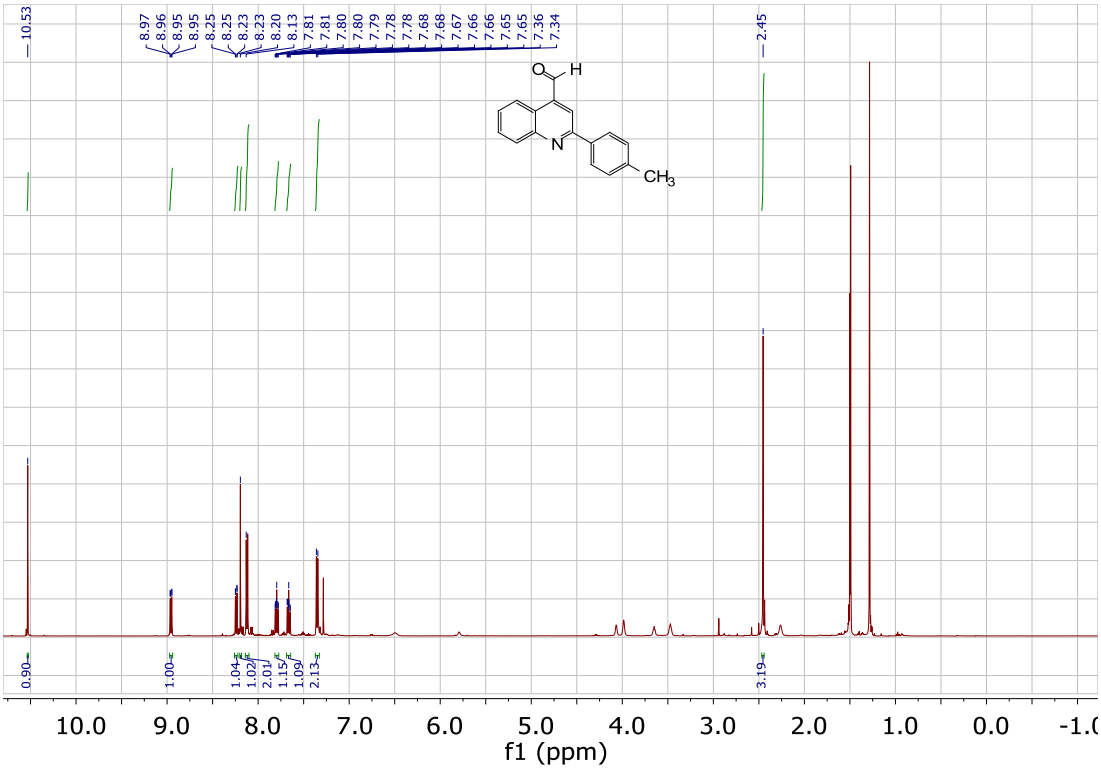

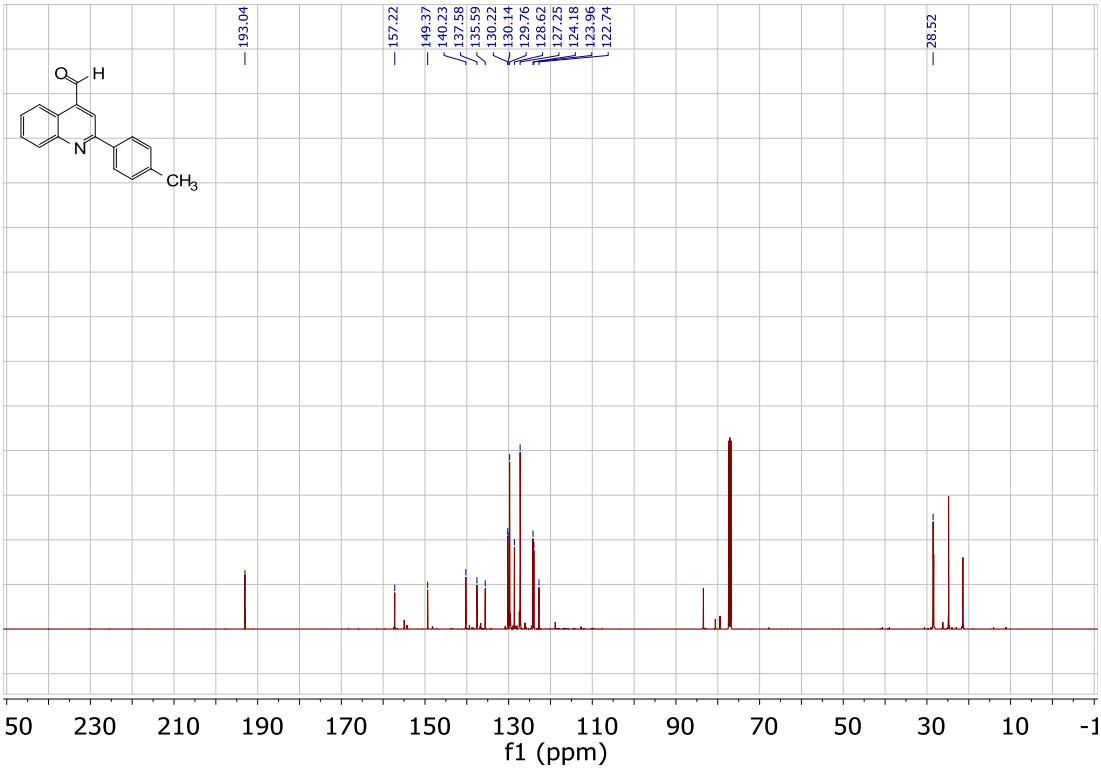

2-(4-methoxyphenyl)-4-Quinolinecarboxaldehyde (2.29):

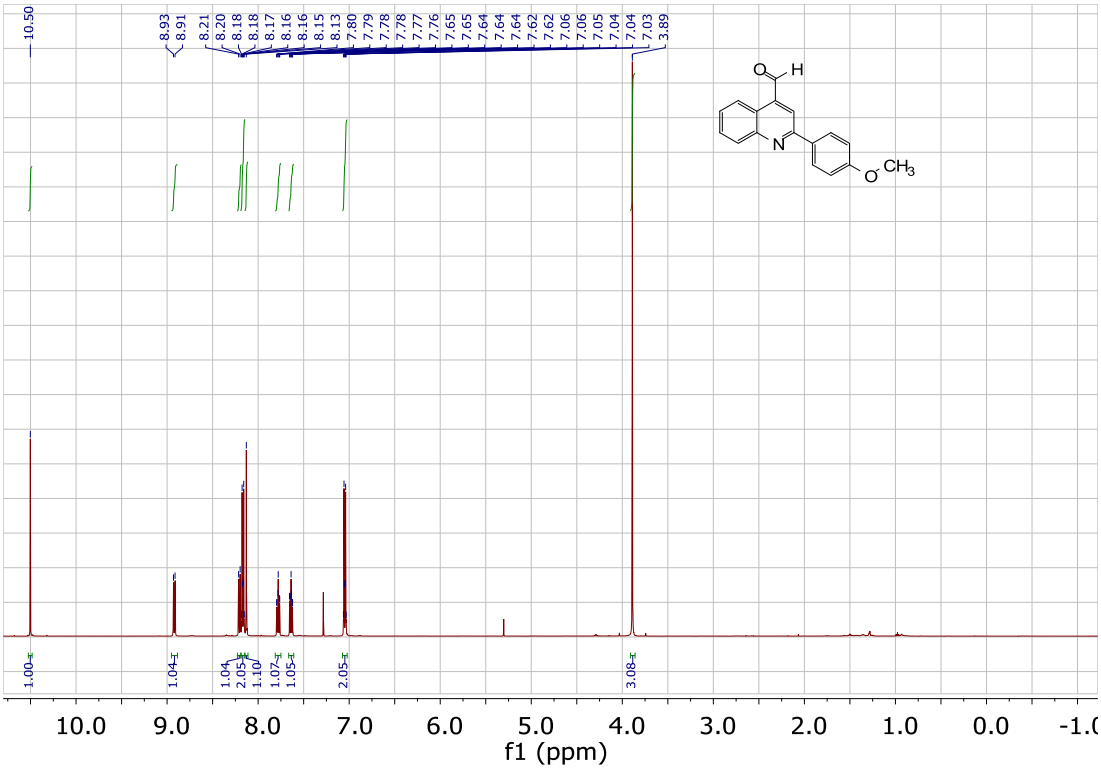

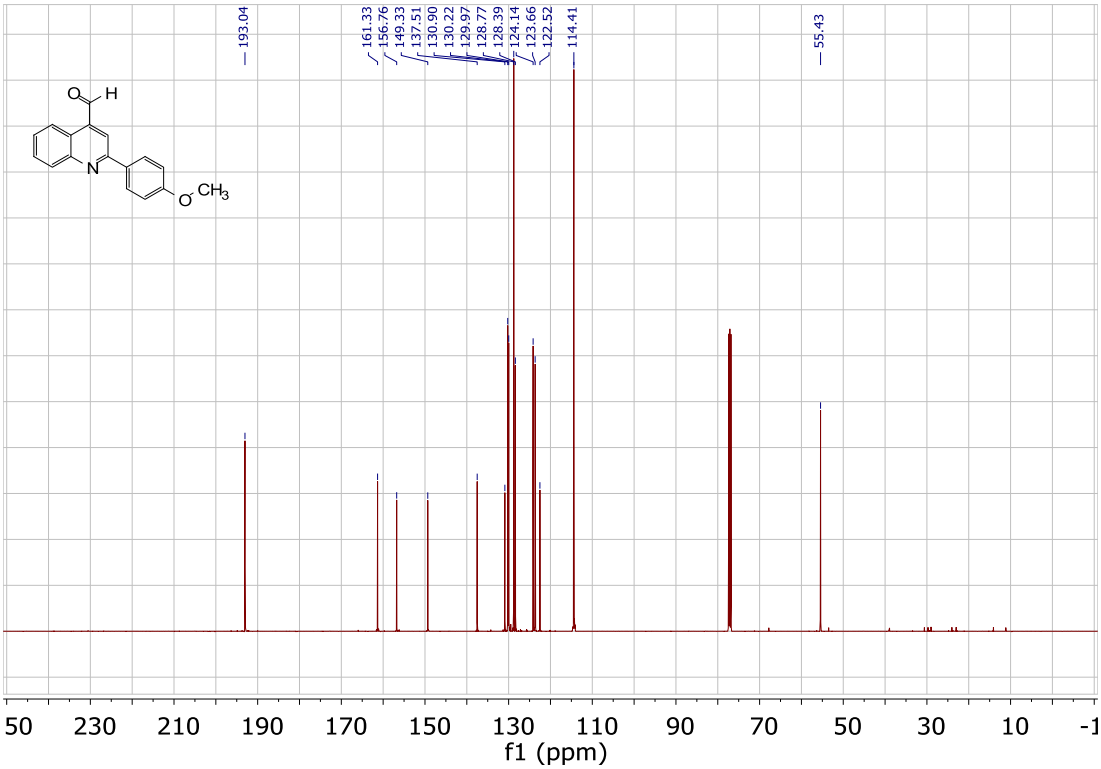

2-[(phenylmethoxy)imino]-Acetic acid (2.33):

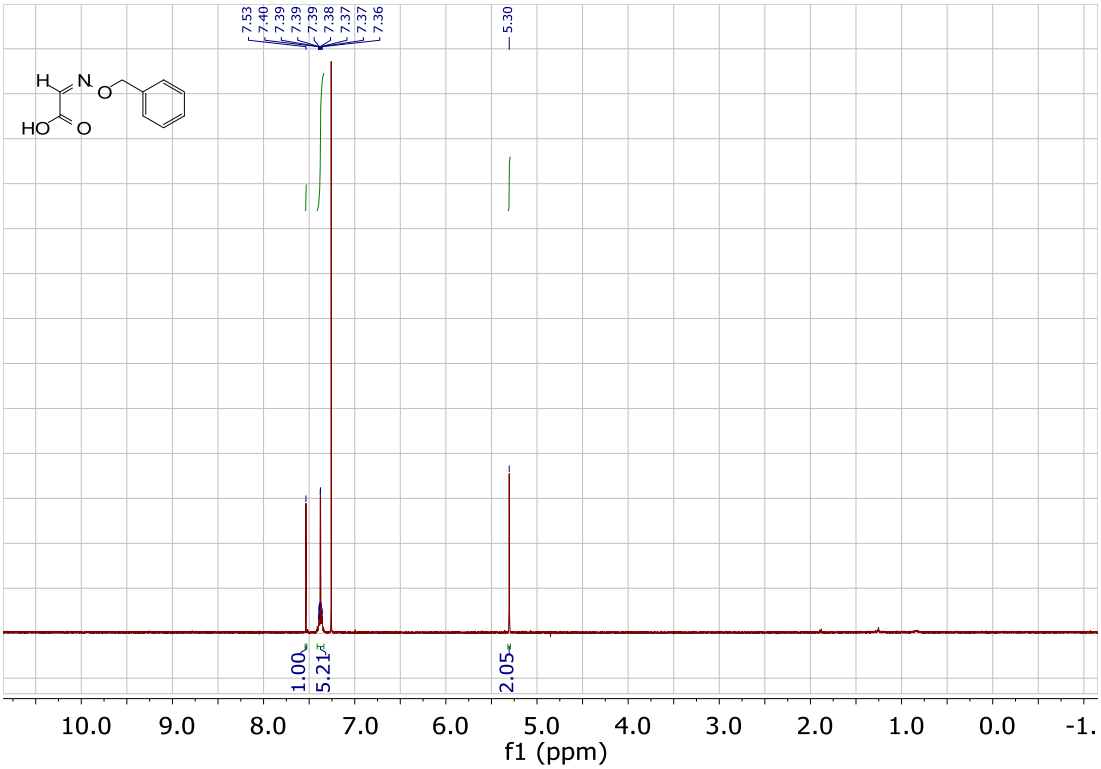

2-[(Benzyloxy)imino]-acetyl chloride (2.34):

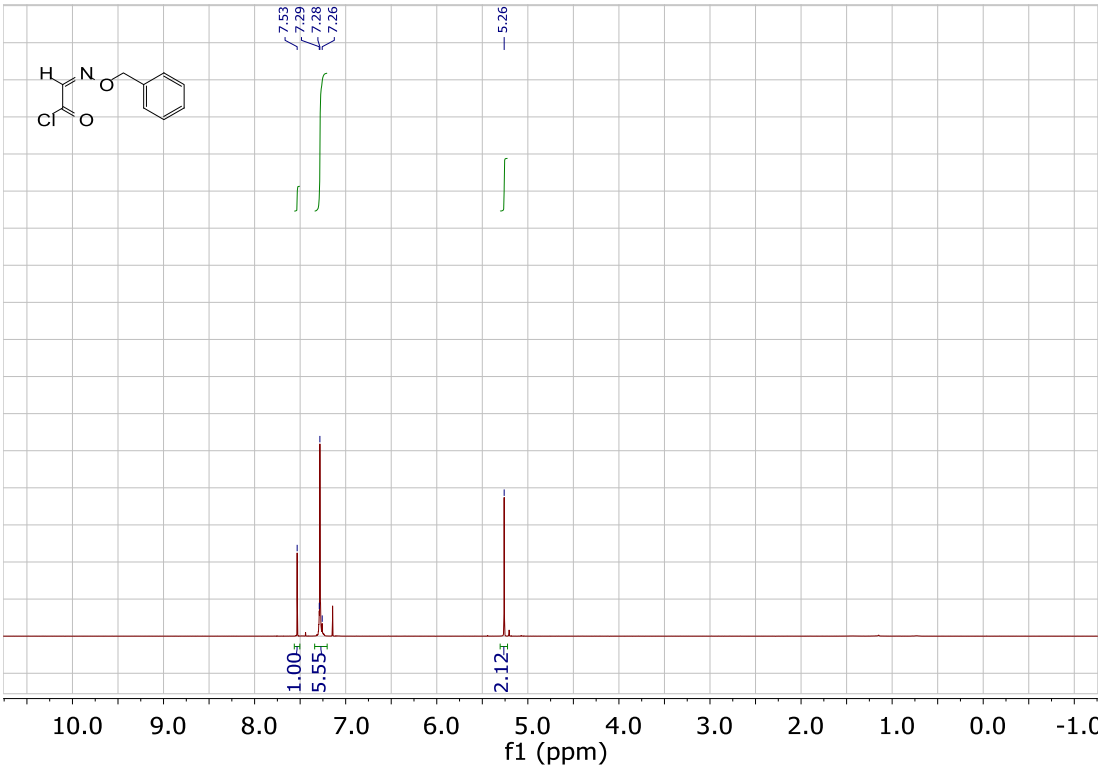

***N*-2-Napthyl-2-[(phenylmethoxy)imino]- acetamide (2.36):**

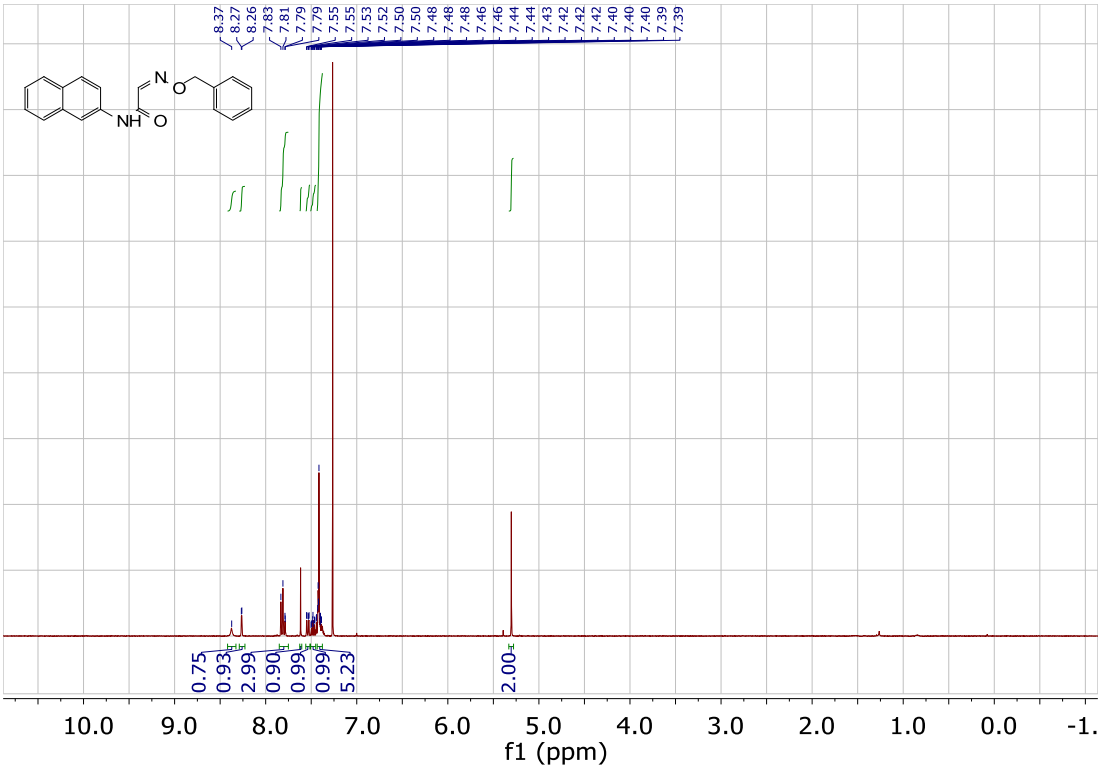

1*H*-Benz[*e*]indole-1,2(3*H*)-dione (2.39):

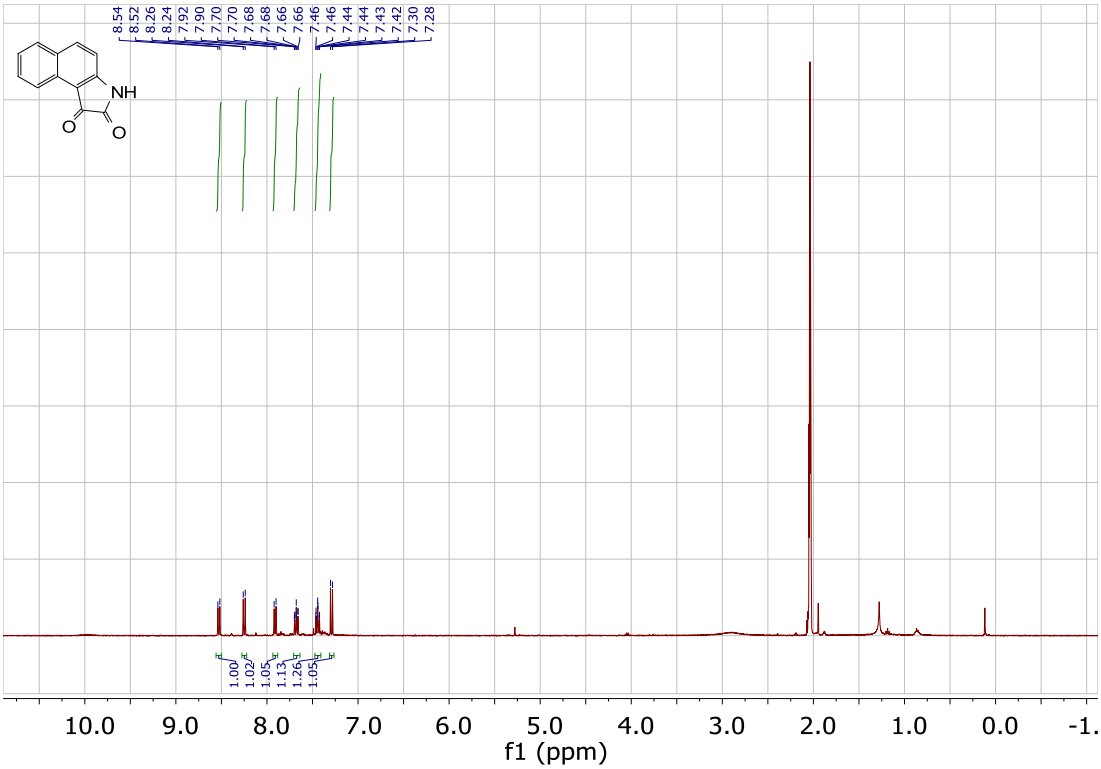

Zoom in of aromatic region of 1*H*-Benz[*e*]indole-1,2(3*H*)-dione (2.39):

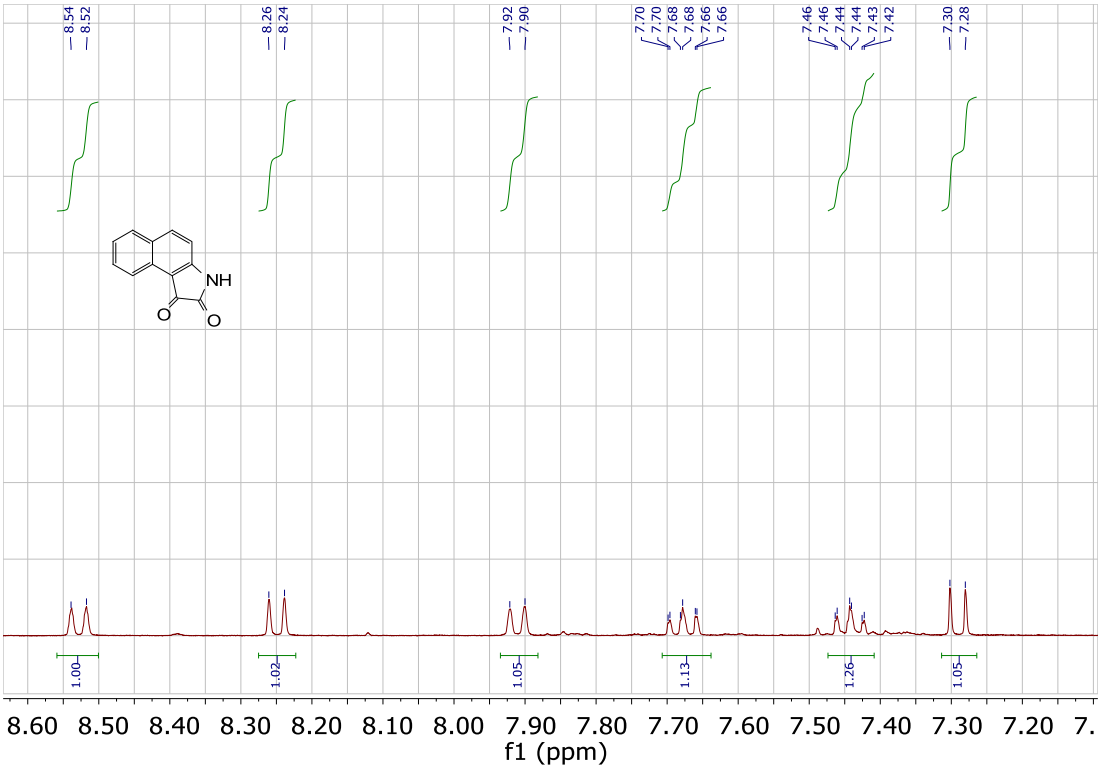

Dihydro-3(2*H*)-Furanone (3.45):

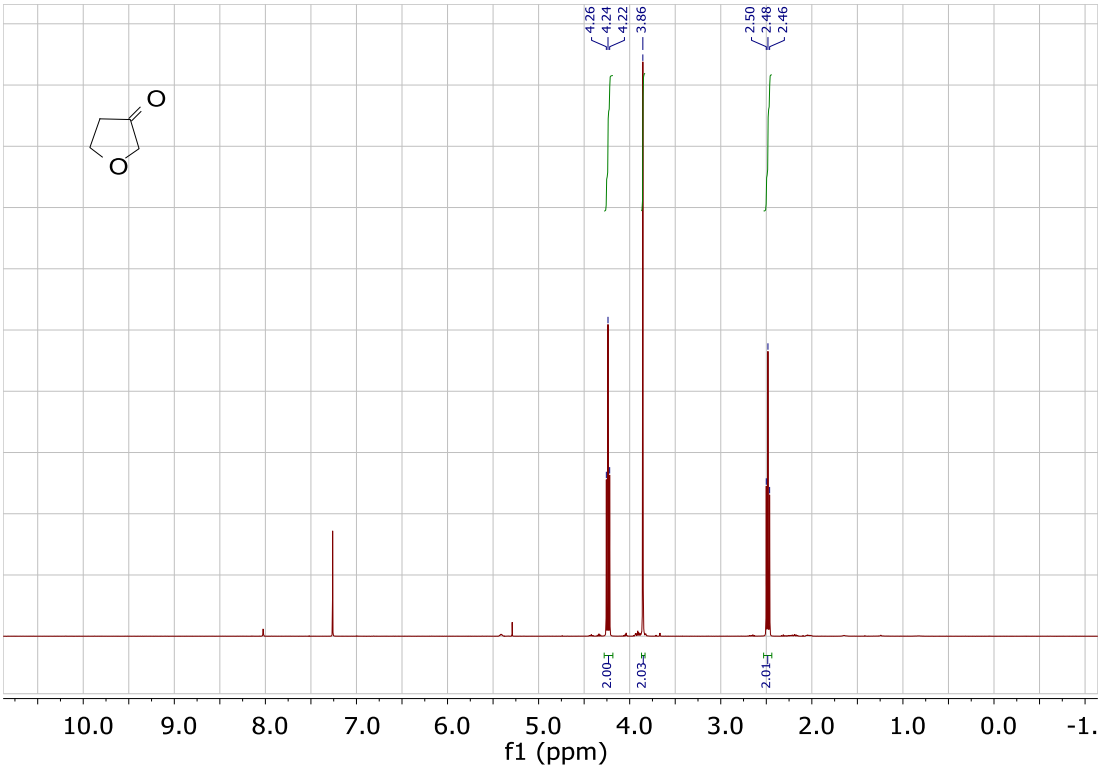

1*H*-Pyrrole-1-carboxylic acid, 2,5-dihydro-3-[[(trifluoromethyl)sulfonyl]oxy]-,1,1-dimethylethyl ester (3.49, desired isomer) and 1*H*-Pyrrole-1-carboxylic acid, 2,3-dihydro-4-[[(trifluoromethyl)sulfonyl]oxy]-,1,1-dimethylethyl ester (3.50, undesired isomer):

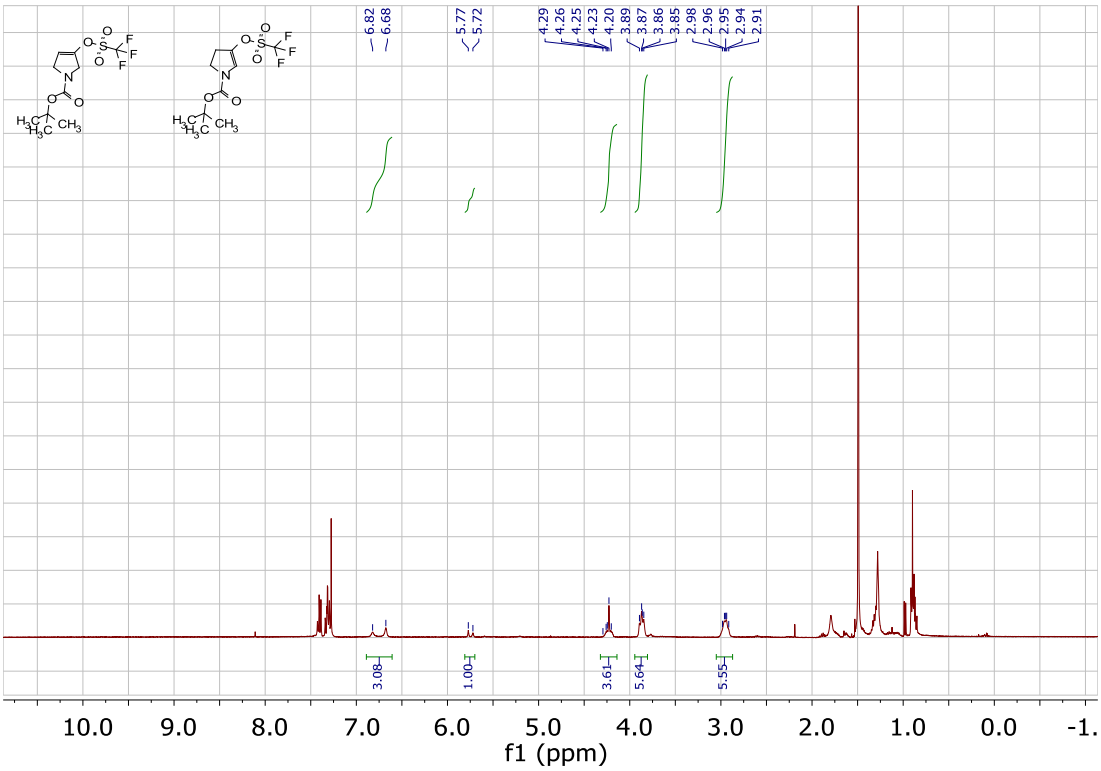

1*H*-Pyrrole-1-carboxylic acid, 2,5-dihydro-3-[nonafluorobutylsulfonyloxy]-, 1,1-dimethylethyl ester (3.52):

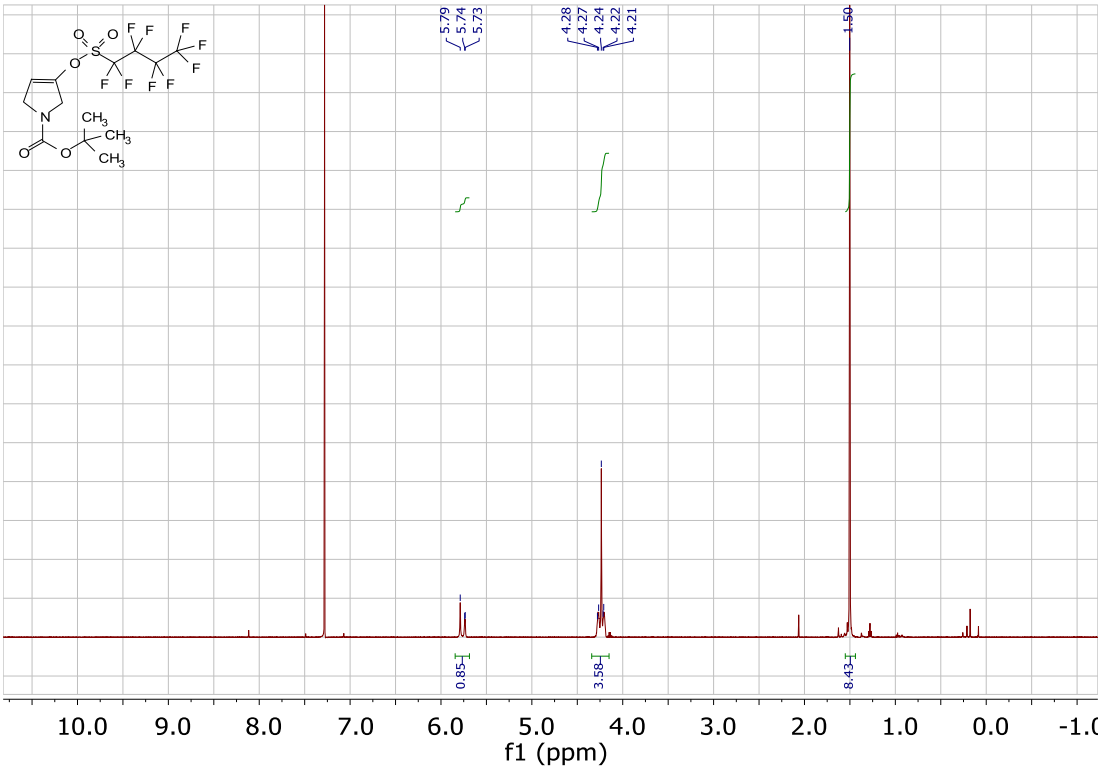

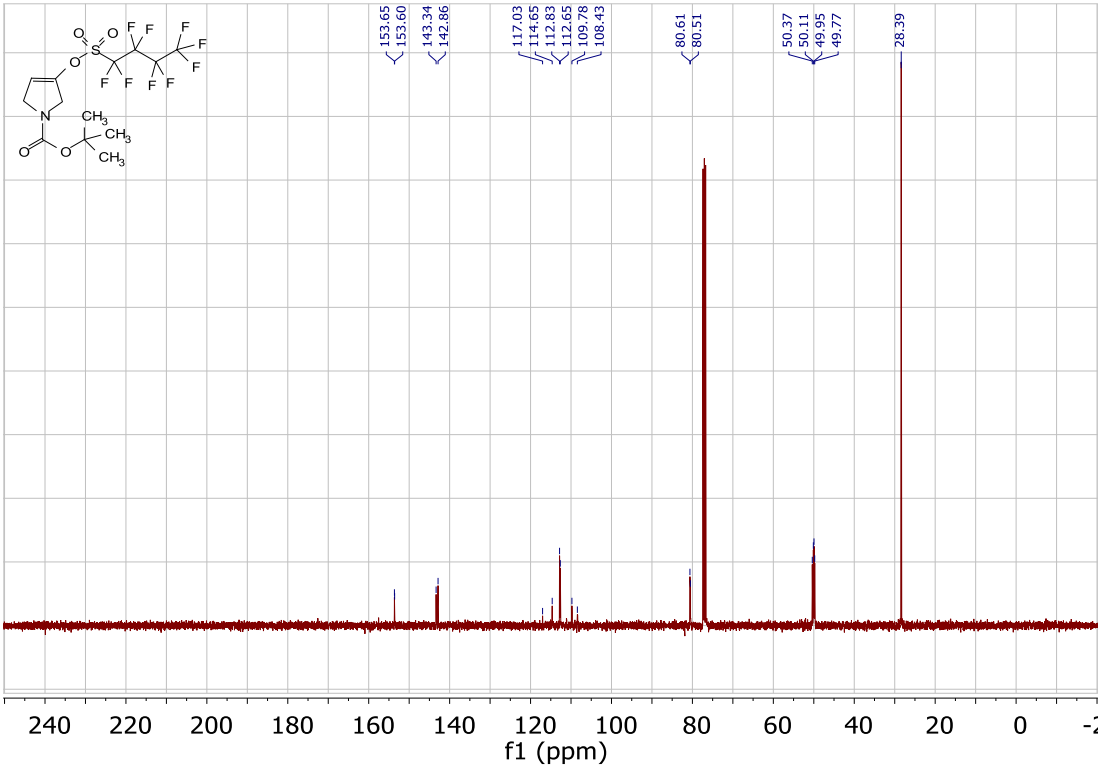

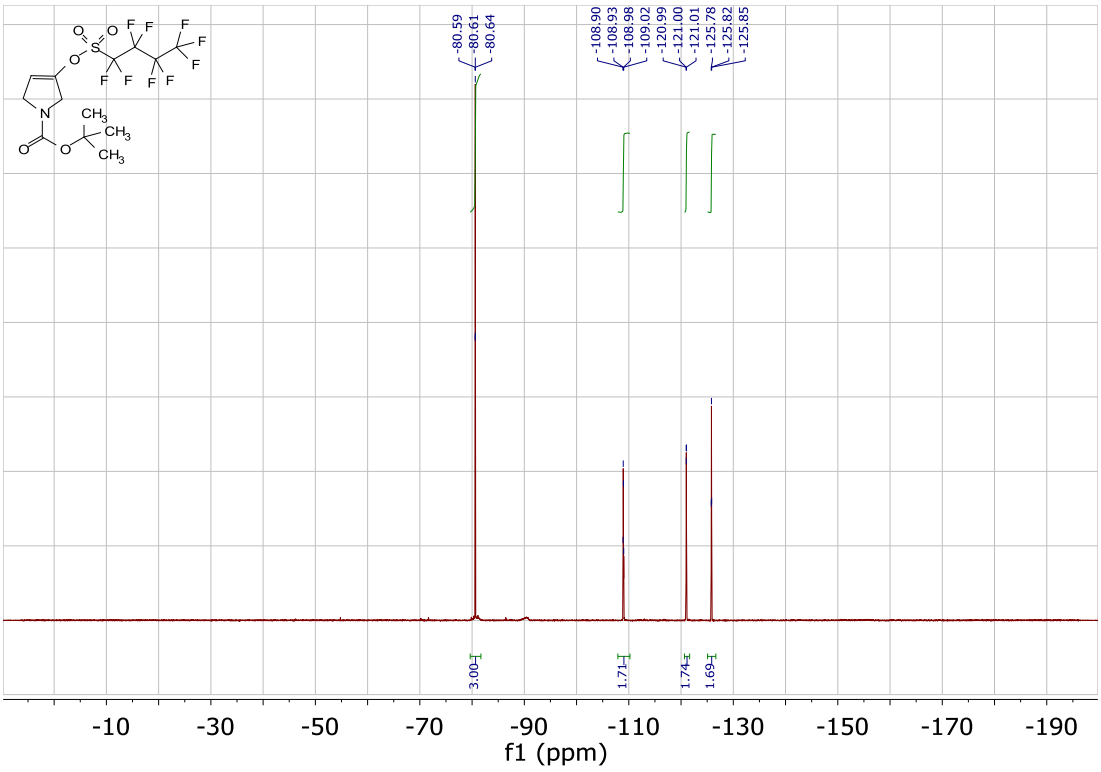

1*H*-Azepine-1-carboxylic acid, 2,3,4,7-tetrahydro-5-[nonafluorobutylsulfonyloxy]-,1,1-dimethylethyl ester (3.57):

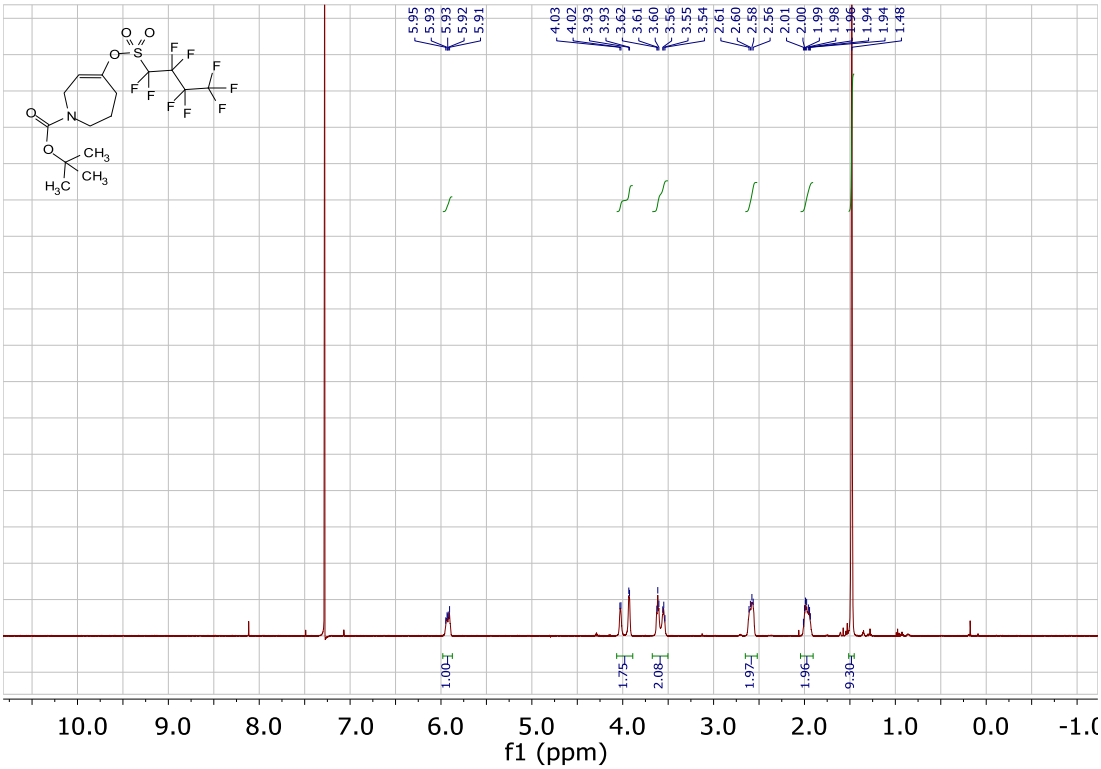

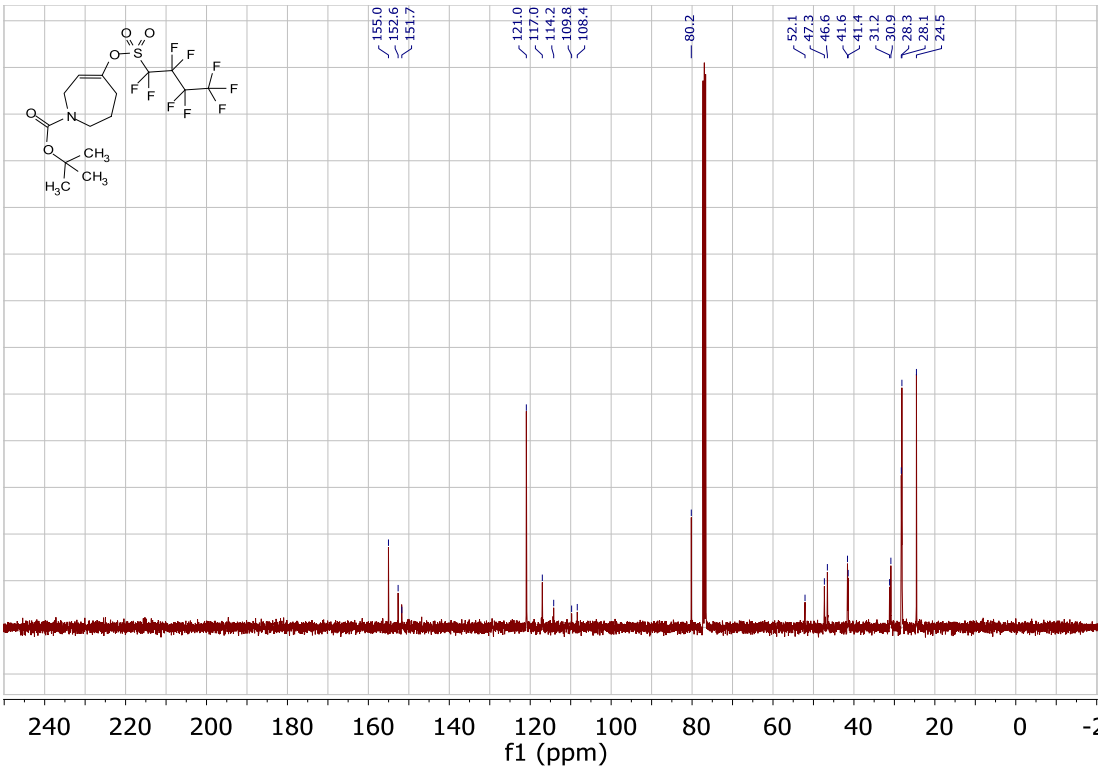
155.0
152.6
151.7
121.0
117.0
114.2
109.8
108.4
80.2
52.1
47.3
46.6
41.6
41.4
31.2
30.9
28.3
28.1
24.5
240 220 200 180 160 140 120 100 80 60 40 20 0
f1 (ppm)

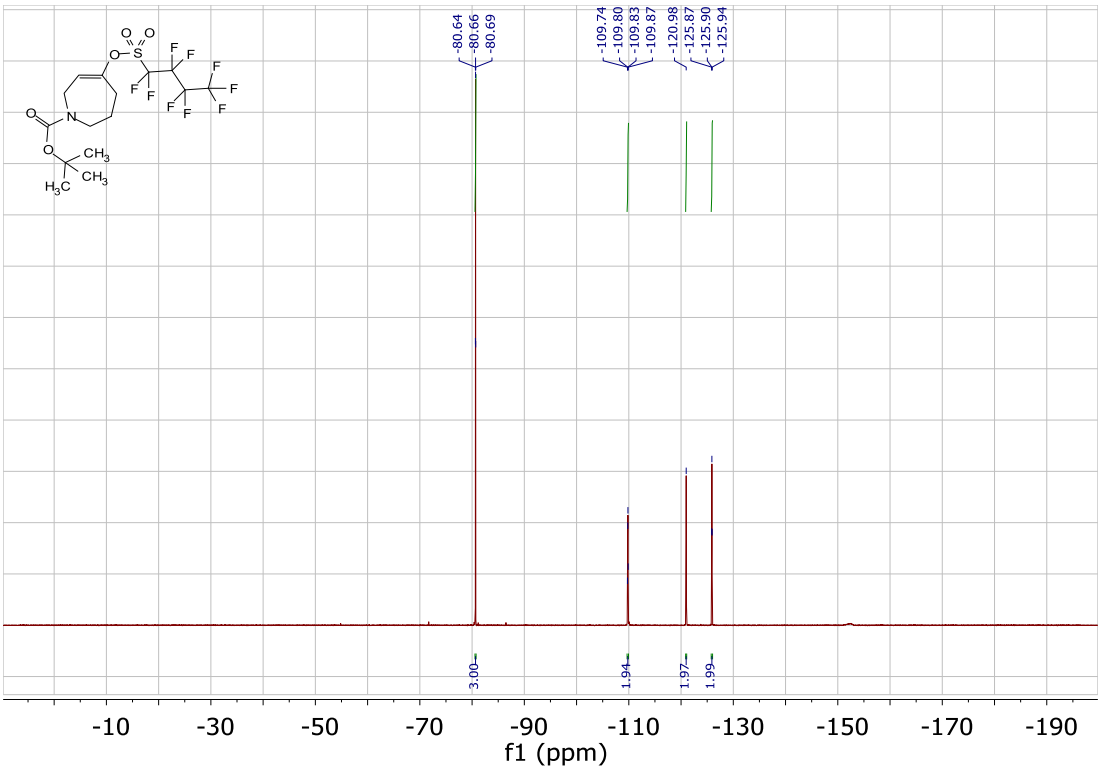
-80.64
-80.66
-80.69
-109.74
-109.80
-109.83
-109.87
-120.98
-125.87
-125.90
-125.94
3.00
1.94
1.97
1.99
-10 -30 -50 -70 -90 -110 -130 -150 -170 -190
f1 (ppm)

1*H*-Pyrrole-1-carboxylic acid, 2,5-dihydro-2-(hydroxyphenylmethyl)-,1,1-dimethylethyl ester (3.55):

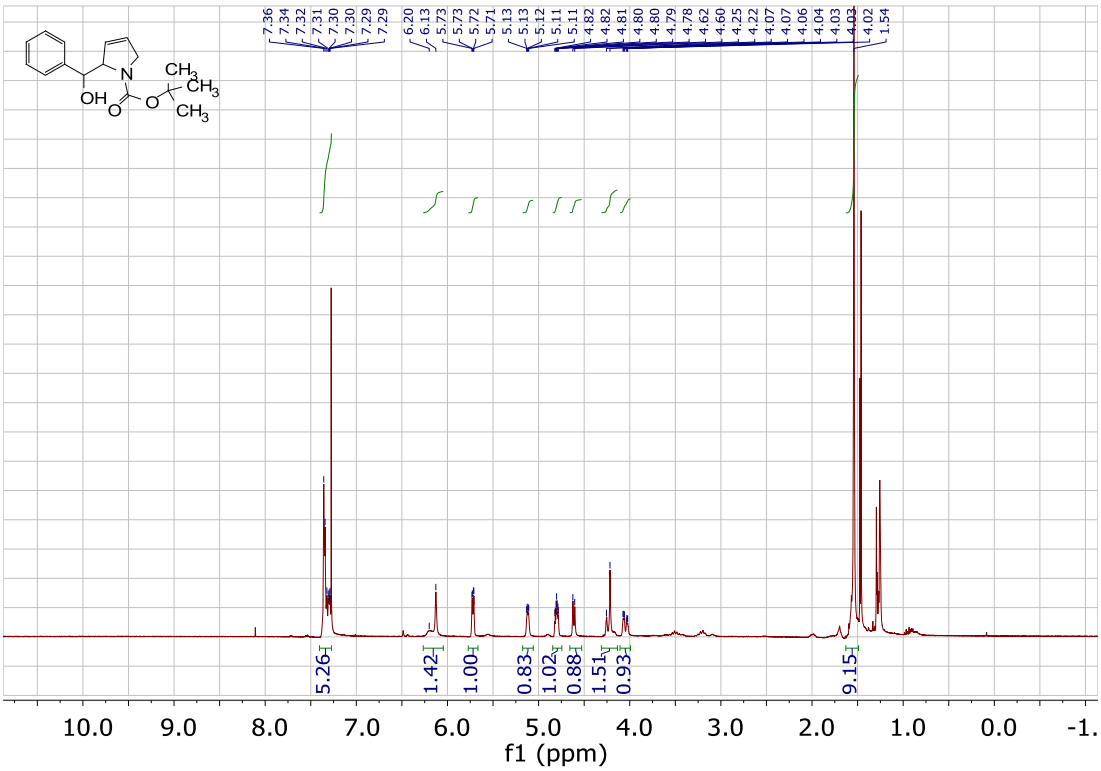

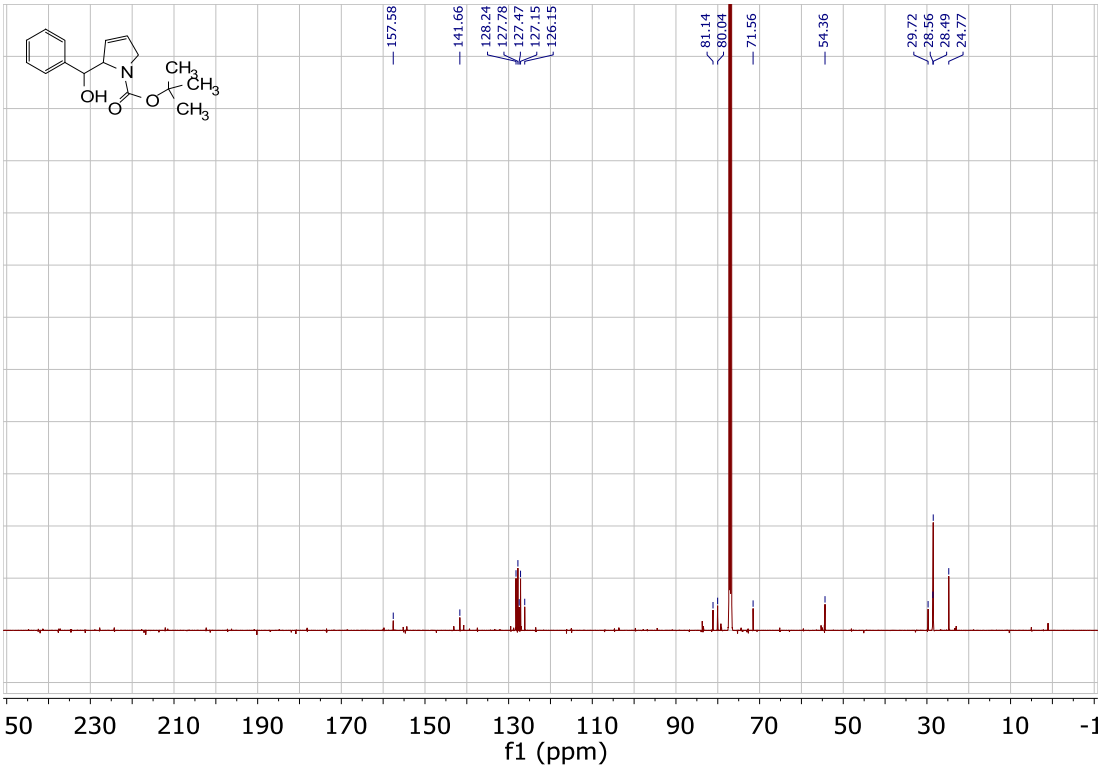

1*H*-Azepine-1-carboxylic acid, 2,5-dihydro-2-(hydroxyphenylmethyl)-,1,1-dimethylethyl ester (3.56):

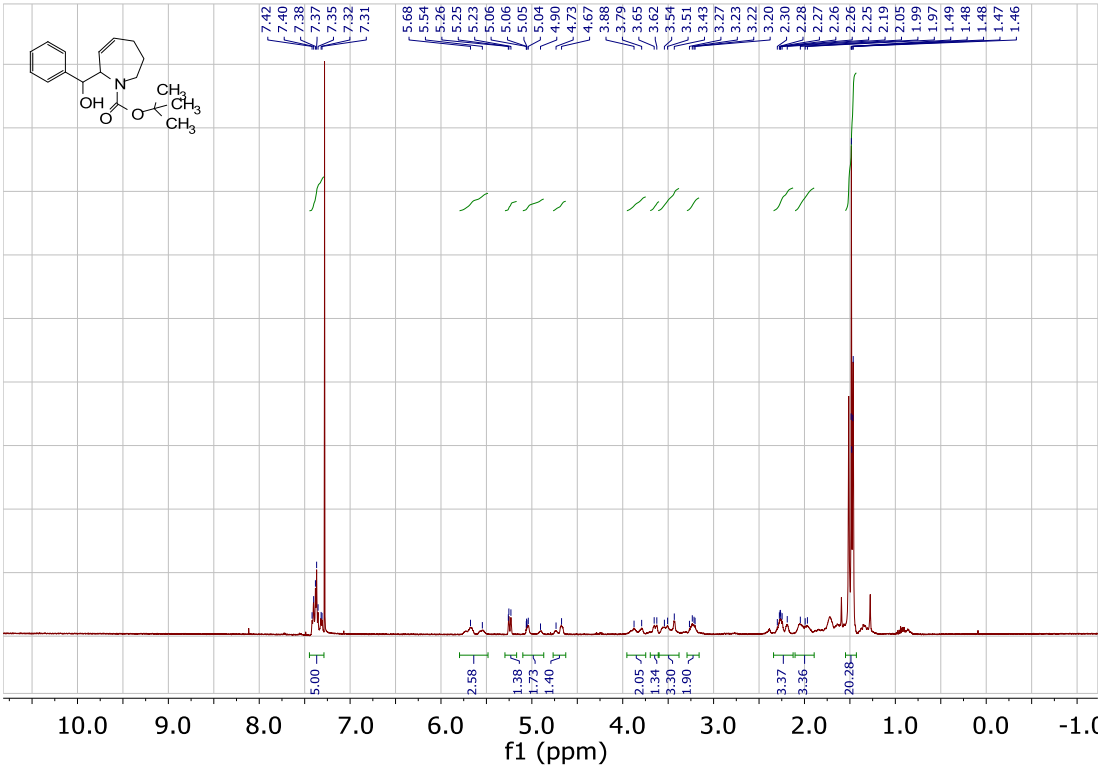

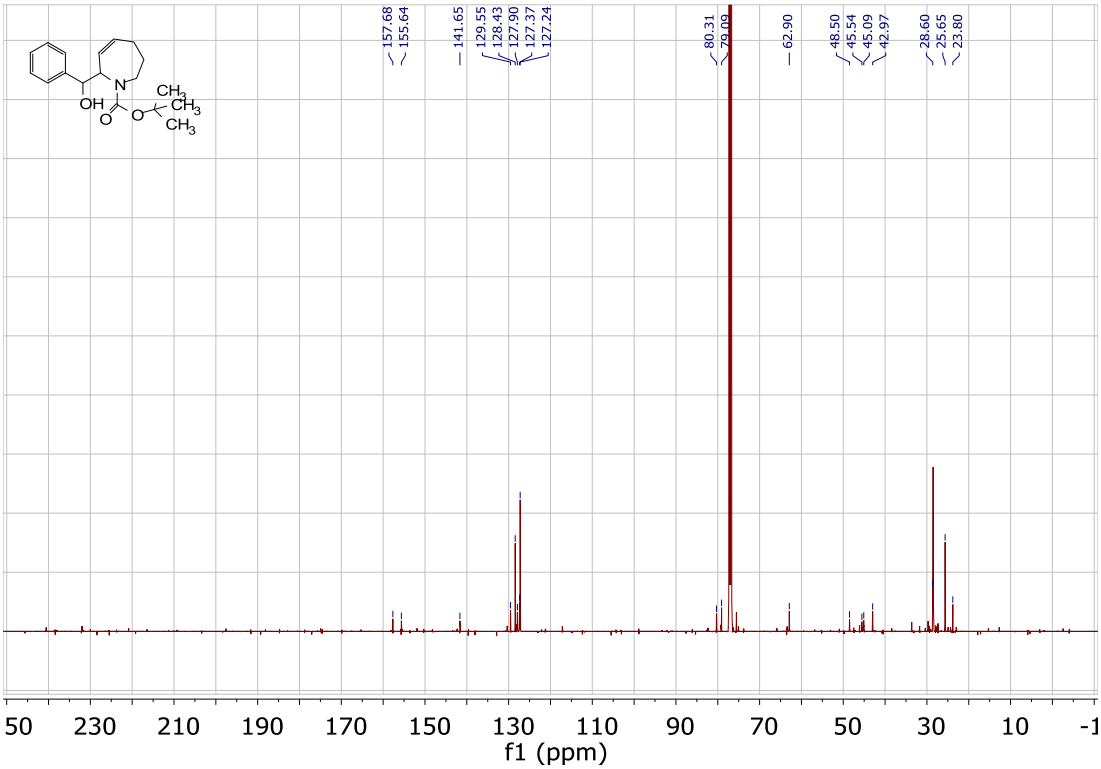

***tert*-Butyl 4-[(trimethylsilyl)oxy]-1,2,5,6-tetrahydropyridine-1-carboxylate (3.70):**

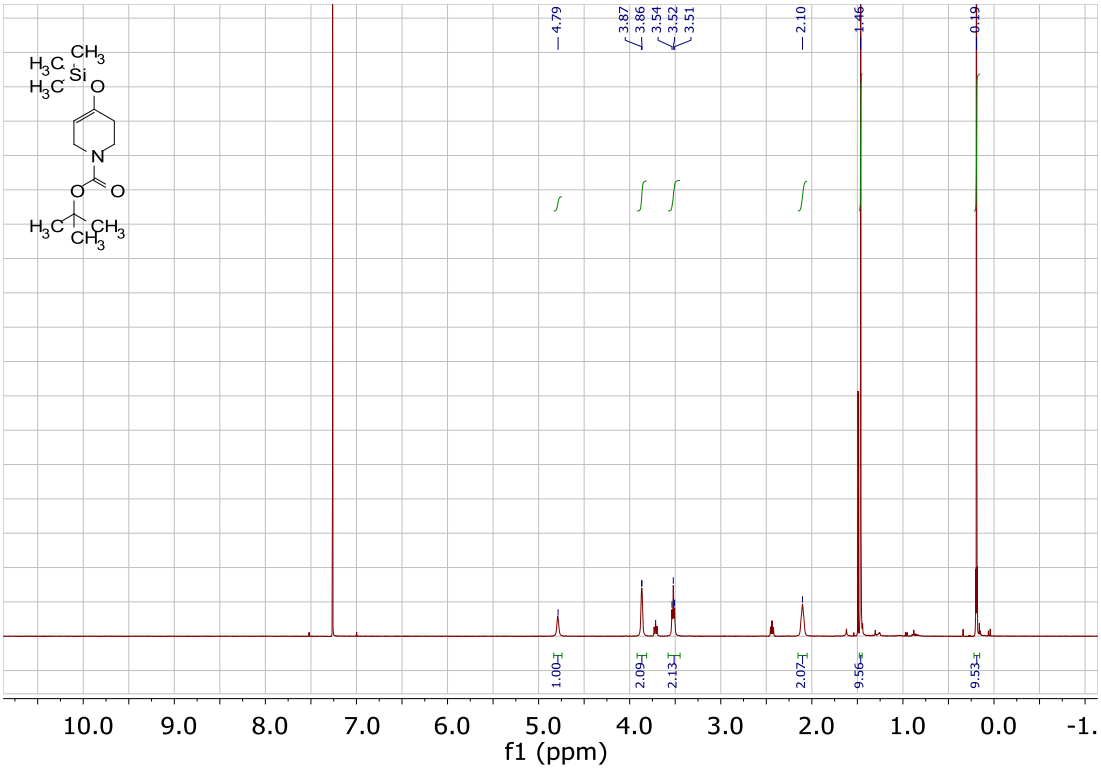

4-benzoate- 3,6-dihydro-, 2*H*-Pyran-4-ol (3.64):

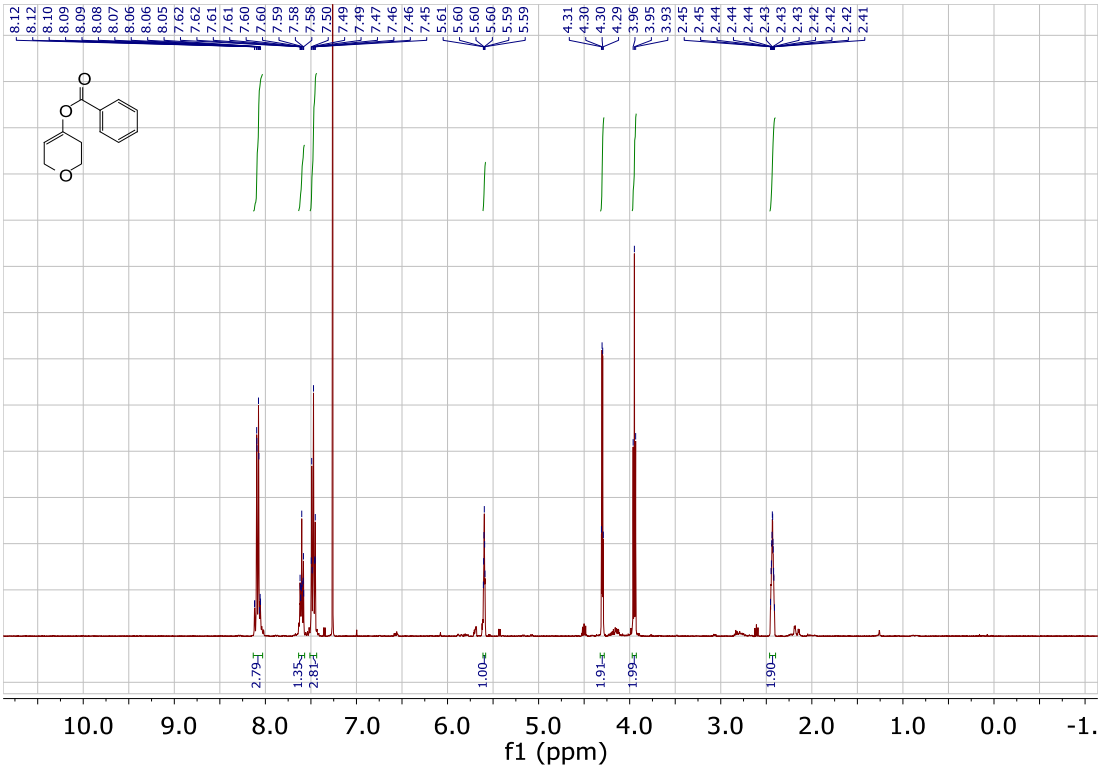

Methanesulfonic acid, 1,1,1-trifluoro-,3,6-dihydro-2*H*-thiopyran-4-yl ester (3.62):